Universitat de Girona

PARTIAL NITRITATION OF LANDFILL LEACHATE IN A SBR PRIOR TO AN ANAMMOX REACTOR : OPERATION AND MODELLING

Ramon **GANIGUÉ PAGÈS**

Universitat de Girona

PhD THESIS

PARTIAL NITRITATION OF LANDFILL LEACHATE IN A SBR PRIOR TO AN ANAMMOX REACTOR: OPERATION AND MODELLING

RAMON GANIGUÉ PAGÈS

2009

PROGRAMA DE DOCTORAT DE MEDI AMBIENT

DIRIGIDA PER: DR. JESÚS COLPRIM GALCERAN I DRA. MARIA DOLORS BALAGUER CONDOM

Memòria presentada per optar al títol de doctor per la Universitat de Girona

MARIA DOLORS BALAGUER CONDOM I JESÚS COLPRIM GALCERAN,
Professors del Departament d'Enginyeria Química, Agrària i Tecnologia
Agroalimentària de la Universitat de Girona

CERTIFIQUEN

Que el llicenciat Ramon Ganigué Pagès ha dut a terme, sota la seva direcció, el treball que, amb el títol ***Partial nitritation of landfill leachate in a SBR prior to an anammox reactor: operation and modelling***, es presenta en aquesta memòria, la qual constitueix la seva Tesi per optar al Grau de Doctor per la Universitat de Girona, i que compleix els requeriments per poder optar a Menció Europea.

I perquè en prengueu coneixement i tingui els efectes que correspongui, presentem davant la Facultat de Ciències de la Universitat de Girona l'esmentada Tesi, signant aquesta certificació a

Girona, 4 de Desembre del 2009

Maria Dolors Balaguer Condom   Jesús Colprim Galceran

Resum

La deposició en abocadors és la solució més emprada per al tractament de residus sòlids urbans. En aquest sentit, el problema ambiental més important derivat d'aquestes instal·lacions són els lixiviats d'abocador, aigües residuals molt contaminades. Aquests lixiviats d'abocador es caracteritzen per tenir concentracions molt elevades d'amoni i un baix contingut de matèria orgànica biodegradable. Degut a això, el tractament d'aquests lixiviats a través dels processos convencionals de nitrificació-desnitrificació té un cost econòmic molt gran pels elevats requeriments d'aeració i a les necessitats de dosificació d'una font de carboni externa. Durant aquests últims anys, s'ha demostrat la viabilitat del procés combinat de nitritació parcial i anammox per al tractament d'aigües residuals amb una baixa relació C:N, alternativa que resulta molt prometedora enfront dels processos convencionals. Entre les diferents experiències descrites, la majoria s'han centrat en el tractament d'efluents de digestors anaerobis. No obstant l'aplicació d'aquest procés autotròfic per al tractament de lixiviats d'abocador és encara molt limitat.

Prèviament al procés anammox, l'amoni present en els lixiviats ha de ser parcialment oxidat a nitrit pels organismes oxidadors d'amoni (AOB). La posterior oxidació de nitrit a nitrat, duta a terme pels organismes nitrit oxidants (NOB) ha de ser evitada per tal de permetre una eliminació òptima del nitrogen per part dels bacteris anammox. A més a més, la matèria orgànica present en el lixiviat ha de ser també eliminada per evitar possibles efectes adversos en el procés anammox. Aquesta tesis tracta sobre el tractament de lixiviats d'abocador urbà a través de la tecnologia SBR, com a pas previ al tractament amb un procés anammox.

Primerament els estudis es van centrar en l'avaluació de la viabilitat d'aquesta configuració per tal d'assolir una nitritació parcial. Aquests estudis es van dur a terme a escala de laboratori, cosa que va permetre demostrar la viabilitat del procés. Durant aquests estudis es van analitzar les condicions d'operació adequades i l'estratègia d'alimentació òptima, i es van obtenir els millors resultats per l'estratègia "step-feed" basada en múltiples alimentacions al llarg d'un cicle. A més a més, es va estudiar la inhibició dels organismes AOB a causa de les elevades concentracions d'amoníac i àcid nitrós, així com la reducció del seu creixement per la limitació en el bicarbonat. Finalment, el procés va ser avaluat amb vista a ser escalat a planta industrial, tot usant diferents indicadors. Així, la relació molar bicarbonat:amoni a l'influent va resultar un paràmetre clau per controlar la conversió del procés. Per altra banda, la quantitat d'oxigen consumida diàriament va ser identificada com un bon paràmetre per al seguiment en línia del procés.

Quan es tracta amb aigües residuals amb un contingut d'amoni molt elevat, com seria el cas dels lixiviats d'abocador, les altes concentracions d'amoni i nitrit a l'interior del reactor poden

produir una important inhibició de l'activitat AOB. Aquesta inhibició pot ser un punt crític ja que els lixiviats poden arribar a presentar concentracions d'amoni de fins a 6,000 mg N-NH$_4^+$·L$^-$[1]. En aquest sentit, qualsevol reducció de la quantitat de nitrogen total a l'interior del reactor ha de ser entesa com una oportunitat per reduir aquests efectes inhibitoris. Així, malgrat el baix contingut de matèria orgànica biodegradable, la inclusió de fases anòxiques durant les alimentacions pot ajudar a la reducció del contingut de nitrogen a través de la desnitrificació heterotròfica via nitrit, fet que disminueix la inhibició sobre els organismes amoni oxidants. En aquest sentit, els estudis es van realitzar a nivell de planta industrial com a pas intermedi en l'escalat a planta real. Aquest experiments van servir, doncs, per demostrar la viabilitat d'aquesta tecnologia per produir un efluent adequat i estable, així com per posar de manifest la seva estabilitat a llarg termini. Aquest estudi ha demostrat també que la matèria orgànica present en els lixiviats pot ser utilitzada per a la desnitrificació heterotròfica. A més a més, la població bacteriana d'AOB i NOB s'ha caracteritzat a través d'assajos cinètics i tècniques moleculars, fet que ha permès tenir-ne un grau de comprensió més elevat.

A través dels experiments de laboratori i planta pilot, s'ha demostrat la viabilitat de la tecnologia SBR per tal d'aconseguir una nitritació parcial d'afluents amb una alta càrrega de nitrogen. No obstant això, malgrat l'experiència adquirida, la resposta del reactor a canvis en les condicions d'operació i/o característiques de l'influent no sempre és fàcil de predir, a causa de la complexitat del sistema (interaccions entre l'aeració, l'"stripping" del CO$_2$, el pH, les inhibicions i les velocitats de nitrificació, entre altres). Els models matemàtics poden ser una bona eina per incrementar el coneixement sobre el procés, i ajudar a una major comprensió dels processos biològics, físics i químics que tenen lloc en el reactor SBR de nitritació parcial. El modelatge matemàtic ha assumit tradicionalment la nitrificació i desnitrificació com dos processos compostos d'un sol pas. Tanmateix, quan es modela un sistema de nitritació parcial, el nitrit s'ha de tenir en compte com un intermediari d'ambdós processos. Avui en dia hi ha diferents models biològics capaços de descriure l'acumulació de nitrit. Alguns d'aquests models fan referència al tractament d'afluents amb una elevada càrrega amoniacal i poden ser usats com a base per al desenvolupament de models d'aplicacions específiques. No obstant, és clar que aquest models preexistents han de ser modificats i/o estesos per incloure els processos biològics i fisicoquímics més rellevants. A més a més, el model necessita ser calibrat per un influent i per a paràmetres concrets. Això s'ha estudiat a l'última part de la tesis, on s'ha desenvolupat, calibrat i validat un model matemàtic del procés de nitritació parcial per al tractament de lixiviats, posant un èmfasi especial en l'adquisició de coneixement i centrant l'estudi en les dinàmiques de cicle. Finalment, un cop desenvolupada, aquesta eina s'ha aplicat a un problema específic: l'avaluació de la producció de nitrit en diferents influents i condicions d'operació.

Resumen

La deposición en vertederos es la solución más utilizada para el tratamiento de residuos sólidos urbanos. La mayor problemática ambiental derivada de estas instalaciones es la producción de lixiviados de vertedero, aguas residuales altamente contaminadas con un amplio rango de contaminantes químicos. Entre todos ellos, los lixiviados urbanos se caracterizan habitualmente por elevadas concentraciones de amonio y bajos contenidos en materia orgánica biodegradable. Por esa razón, el tratamiento de los lixiviados aplicando el proceso convencional de nitrificación-desnitrificación resulta económicamente inviable debido a la elevada demanda de oxígeno y al requerimiento de la adición externa de materia orgánica. Durante los últimos años se ha demostrado la viabilidad del proceso combinado de nitritación parcial-anammox para el tratamiento de afluentes con elevadas cargas de nitrógeno y relaciones bajas de C:N, siendo esta aplicación una prometedora alternativa a los sistemas convencionales de nitrificación/desnitrificación. Entre todas las experiencias descritas referentes a esta nueva tecnología, la mayoría de ellas se han centrado en el tratamiento de efluentes de digestión de fangos. No obstante, son pocas las experiencias del tratamiento de lixiviados urbanos a través de procesos totalmente autotróficos como el sistema de nitritación parcial-anammox.

Previamente al proceso anammox, el amonio presente en el agua residual debe ser parcialmente oxidado a nitrito a través de bacterias oxidantes de amonio (AOB). Una posterior nitratación a nitrato, llevada a cabo por bacterias oxidantes de nitrito (NOB), debe ser evitada para alcanzar una óptima eliminación de nitrógeno gracias a la bacteria Anammox. Además, la materia orgánica biodegradable presente en el lixiviado debe ser eliminada del sistema para evitar los efectos negativos en el sub-siguiente proceso anammox. Así pues, esta tesis aborda el tratamiento de los lixiviados urbanos de vertedero aplicando la tecnología de reactor discontinuo secuencial (SBR) como paso previo a un reactor anammox.

Primeramente, los estudios se centraron en la evaluación de la viabilidad de la configuración SBR para la obtención de la nitritación parcial. Estos experimentos se realizaron a escala de laboratorio, permitiendo demostrar la viabilidad del proceso. Además, se han investigado las condiciones de operación y la estrategia de alimentación más apropiadas para el proceso, obteniendo mejores resultados con una alimentación escalada (step-feed strategy), basada en alimentaciones cortas a través del ciclo. Por otro lado, la inhibicion de las bacterias AOB provocadas por amoníaco y ácido nitroso libre, así como la reducción de su actividad debido a una limitación en el bicarbonato disponible han sido estudiadas. Finalmente, el proceso fue evaluado a escala de laboratorio usando diferentes indicadores. Así pues, la relación de bicarbonato y amonio en el influente resultó ser el factor clave para el control de la reacción, mientras que el oxígeno consumido por día fue utilizado como un buen parámetro para la evaluación en línea del proceso.

Cuando se tratan aguas residuales con un contenido de amonio muy elevado, como sería el caso de los lixiviados de vertedero, las elevadas concentraciones de amonio y nitrito en el interior del

reactor pueden producir una importante inhibición de la actividad AOB. Así, esta inhibición puede ser un punto crítico ya que los lixiviados pueden llegar a presentar concentraciones de amonio de hasta 6,000 mgN-NH4+·L-1. En este sentido, cualquier reducción de la cantidad de nitrógeno total en el interior del reactor tiene que ser entendida como una oportunidad para disminuir estos efectos inhibitorios. Así, a pesar del bajo contenido de materia orgánica biodegradable, la inclusión de fases anóxicas durante las alimentaciones puede ayudar a la reducción del contenido de nitrógeno a través de la desnitrificación heterotrófica vía nitrito, permitiendo disminuir la inhibición sobre los organismos AOB. En este sentido, los estudios se realizaron a nivel de planta industrial como paso intermedio en el escalado a planta real. Estos experimentos sirvieron para demostrar la viabilidad de esta tecnología para producir un efluente adecuado, así como también poner de manifiesto su estabilidad a largo plazo. Los estudios han demostrado además que la materia orgánica presente en los lixiviados puede ser utilizada para la desnitrificación heterotrófica. Finalmente, la población bacteriana de AOB y NOB se ha caracterizado a través de ensayos cinéticos y técnicas moleculares, permitiendo un mayor grado de comprensión sobre ésta.

A través de los experimentos de laboratorio y planta piloto, se ha demostrado la viabilidad de la tecnología SBR con el fin de conseguir una nitritació parcial de afluentes con una alta carga de nitrógeno. No obstante, a pesar de la experiencia adquirida, la respuesta del reactor a cambios en las condiciones de operación y/o características del influente no siempre es fácil de predecir, dada la complejidad del sistema (interacciones entre la aireación, el "stripping" del CO2, el pH, las inhibiciones y las velocidades de nitrificación, entre otros). Los modelos matemáticos pueden ser una buena herramienta para incrementar el conocimiento sobre el sistema, ayudando a una mayor comprensión de los procesos biológicos, físicos y químicos que tienen lugar en el reactor SBR de nitritación parcial. Tradicionalmente, el modelado matemático de procesos biológicos ha asumido la nitrificación y desnitrificación como dos procesos compuestos de un solo paso. No obstante, cuando se modela un sistema de nitritación parcial, el nitrito ha de ser tenido en cuenta como un intermediario de ambos procesos. Hoy en día hay diferentes modelos biológicos capaces de describir la acumulación de nitrito. Algunos de estos modelos hacen referencia al tratamiento de afluentes con una elevada carga amoniacal y pueden ser usados como base por el desarrollo de modelos de aplicaciones específicas. No obstante, estos modelos preexistentes tienen que ser modificados y/o extendidos para incluir todos los procesos biológicos y fisicoquímicos más relevantes. Además, el modelo necesita ser calibrado para uno influente y parámetros concretos. Eso se ha estudiado en la última parte de la tesis, dónde se ha desarrollado, calibrado y validado un modelo matemático del proceso de nitritació parcial para el tratamiento de lixiviados, haciendo especial énfasis en la adquisición de conocimiento, y centrando el estudio en las dinámicas de ciclo. Finalmente, una vez desarrollada esta herramienta, se ha aplicado a un problema específico: la evaluación de la producción de nitrito para diferentes afluentes y condiciones de operación.

iv

Summary

Landfilling is the most widespread technology for the treatment of urban solid wastes. The main environmental concern which arises from its management centres on urban landfill leachate, highly contaminated wastewater with a wide range of chemical contaminants, usually characterised by high ammonium concentrations and low biodegradable organic matter content. Treating leachate through conventional nitrification-denitrification processes is expensive due to its high oxygen demand and the requirement of a supplementary external carbon source. In recent years, the feasibility of treating highly nitrogen loaded streams with a low C:N ratio by a combined partial nitritation-anammox process has been demonstrated, and shown itself to be a promising alternative to conventional nitrification/denitrification systems. However, the majority of reported experiences have focused on the treatment of sludge digester supernatant, while experiences with a fully autotrophic partial nitritation-anammox process for the treatment of urban landfill leachate have been very limited in number.

Prior to the anammox process, the ammonium present in wastewater must be partially oxidised to nitrite by ammonium oxidising bacteria (AOB). Further nitrification to nitrate, carried out by nitrite oxidising bacteria (NOB) has to be avoided in order to allow optimal N-removal by anammox bacteria. In addition, biodegradable organic matter needs to be removed to prevent it having negative effects on the subsequent anammox process. This thesis deals with the treatment of urban landfill leachate by partial nitritation SBR technology as a preparative step for an anammox reactor.

Firstly, experiments performed with a lab-scale reactor focused on the assessment of the feasibility of this configuration for achieving partial nitritation. In addition, proper operational conditions and a suitable feeding strategy were investigated, and optimal results were obtained for a step-feed strategy, based on short feeding events through the cycle. Inhibition of AOB by free ammonia (FA) and free nitrous acid (FNA), were screened, together with possible bicarbonate substrate limitation. Finally, the process was assessed with a view to scale-up, using different indicators. Here, the bicarbonate to ammonium influent molar ratio revealed itself to be the key factor in the control of the process conversion, while the amount of oxygen consumed per day was identified as a good parameter for on-line process evaluation.

The aim of a partial nitritation system is to oxidise about half of the influent ammonium to nitrite. In the particular case of highly ammonium-loaded wastewater such as landfill leachate, the ammonium and nitrite concentrations inside a partial nitritation reactor can be very high, and inhibit AOB activity. Inhibition can be a critical issue when dealing with landfill leachate, with concentrations of up to 6,000 mg $N\text{-}NH_4^+ \cdot L^{-1}$ being present. In light of this, any reduction in total nitrogen concentration inside the partial nitritation reactor could be seen as an opportunity

to reduce the inhibition factors. Despite the low levels of biodegradable organic matter available in the leachate, the inclusion of anoxic phases during the feeding events may help to reduce the nitrogen content by heterotrophic denitrification via nitrite, diminishing the inhibition over AOB. Studies were carried out at pilot-scale with a view to future full-scale application, and experiments served to achieve stable production of a suitable mixture of ammonium and nitrite, as well as demonstrate the viability of long-term nitrite build-up in a biomass retention system. It was also shown that low levels of available biodegradable organic matter present in leachate could be used for denitrification purposes. Furthermore, the characterisation by DNA-based molecular techniques and kinetic batch studies of microbial populations involved in the aerobic processes of N-compound oxidation (AOB and NOB) has provided a better understanding of the partial nitritation process, the bacterial community and kinetics.

By means of lab and pilot-scale experiments, the feasibility of partial nitritation in sequencing batch reactor (SBR) technology for the treatment of highly nitrogen-loaded streams was demonstrated. However, despite the experience gained, the reactor's response to changes in operational conditions and influent characteristics was not always easy to understand or predict, given the complexity of the way the system relies on interactions between oxygen supply, CO_2 stripping, alkalinity, pH, inhibition effects and nitrification kinetics, among other factors. Mathematical models can be useful tools to increase process knowledge and help to better understand the biological processes and the physical phenomena taking place in a partial nitritation-sequencing batch reactor (PN-SBR). Traditional modelling has assumed nitrification and denitrification as single-step processes. However, when modelling a partial nitrification system it is necessary to consider nitrite as an intermediary step in nitrification and denitrification. Nowadays there are several biological models describing nitrite build-up. Some of these focus on the treatment of high nitrogen-loaded streams and can be used as a basis for modelling specific processes. Nevertheless, it is clear that existing models may need to be modified or extended to include all relevant physical-chemical processes and biochemical transformations for a given application. Besides, the model needs to be calibrated for influent and process specific parameters. This is illustrated in the last part of this thesis, where a mathematical model of the process is developed, calibrated and validated, with the aim of increasing process knowledge and focusing on short-term dynamics (cycle basis). This work also addresses the question of the usefulness of a systematic calibration guideline and its refinement. Finally, once it has been developed, the tool is applied to a specific problem, the assessment of nitrite build-up under different influent and operational conditions.

NOTATION AND ABBREVIATIONS

η: Anoxic reduction factor

f_{BOD}: Correction factor for BOD estimation

ρ_i: Reaction rate of reaction i [mg·L^{-1}·d^{-1}]

ρK: Determinant value

f_{ns}: Non-settable fraction of the sludge

fx_I: Production of X_I in endogenous respiration [gCOD·gCOD^{-1}]

μ_{max}^{AOB}: Maximum growth rate for AOB [d^{-1}]

μ_{max}^{H}: Maximum growth rate for heterotrophic bacteria [d^{-1}]

μ_{max}^{NOB}: Maximum growth rate for NOB [d^{-1}]

a: Sigmoidal kinetic constant

AC: ACclimated sludge

ANAMMOX: ANaerobic AMMonium OXidation

AOB: Ammonium Oxidising Bacteria

ARD: Average Relative Deviation

ASM: Activated Sludge Models

b_{AOB}: Aerobic endogenous respiration rate for AOB [d^{-1}]

BCOD: Biodegradable Chemical Oxygen Demand [mgO$_2$·L^{-1}]

b_H: Aerobic endogenous respiration rate for heterotrophic bacteria [d^{-1}]

b_{NOB}: Aerobic endogenous respiration rate for NOB [d^{-1}]

BOD: Biochemical Oxygen Demand [mgO$_2$·L^{-1}]

BOD$_u$: Ultimate Biochemical Oxygen Demand [mgO$_2$·L^{-1}]

CANON: Completely Autotrophic N-removal Over Nitrite

$C_{L,i}^{*}$: Saturation concentration of component i [mg·L^{-1}]

$C_{L,i}$: Concentration of component i [mg·L^{-1}]

$C_{L,i}^{in}$: Concentration of component i in the influent [mg·L^{-1}]

$C_{L,i}^{out}$: Concentration of component i in the effluent [mg·L^{-1}]

$C_{L,i}^{reactor}$: Concentration of component i in the reactor [mg·L^{-1}]

CO$_3^{2-}$: Carbonate [mgC-CO$_3^{2-}$·L^{-1}]

COD: Chemical Oxygen Demand [mgO$_2$·L^{-1}]

D_i: Diffusion coefficient of i (i as O$_2$, CO$_2$, N$_2$ or NH$_3$) [m·s^{-2}]

DN/PN: Denitrification/Partial Nitrition

DO$^{(T)}$: Dissolved oxygen concentration at a given T [mgO$_2$·L^{-1}]

DO: Dissolved Oxygen [mgO$_2$·L^{-1}]

DOC: Dissolved Organic Carbon [mgC·L^{-1}]

DO$_{sat}^{(T)}$: Saturated dissolved oxygen concentration at a given T [mgO$_2$·L^{-1}]

EC: Electrical Conductivity [µS·cm^{-1}]

FA: Free Ammonia [mgN-NH$_3$·L^{-1}]

FB: Fed-Batch

FISH: Fluorescent *in situ* Hybridisation

FNA: Free Nitrous Acid [mgN-HNO$_2$·L^{-1}]

H$_2$CO$_3$: Carbonic acid [mgC-H$_2$CO$_3$·L^{-1}]

HCO$_3^-$: Bicarbonate [mgC-HCO$_3^-$·L^{-1}]

HCO$_3^-$$_{inf}$: Bicarbonate concentration at the influent [mol HCO$_3^-$·L^{-1}]

HCO$_3^-$$_{eff}$: Bicarbonate concentration at the effluent [mol HCO$_3^-$·L^{-1}]

HCO$_3^-$$_{AOB}$: Bicarbonate used to balance proton production by AOB [mol HCO$_3^-$·L^{-1}]

HCO$_3^-$$_{stripping}$: Bicarbonate removed from the system and not used to balance proton production by AOB [mol HCO$_3^-$·L^{-1}]

HRT: Hydraulic Retention Time [d]

IC: Inorganic Carbon [mgC·L^{-1}]

i$_{CBM}$: Carbon content of the biomass [gC·gCOD^{-1}]

i$_{CSS}$: Carbon content of Ss [gC·gCOD^{-1}]

i$_{CXI}$: Carbon content of X_I [gC·gCOD^{-1}]

i$_{CXS}$: Carbon content of X_S [gC·gCOD^{-1}]

i$_{NBM}$: Nitrogen content of the biomass [gN·gCOD^{-1}]

i$_{NSS}$: Nitrogen content of Ss [gN·gCOD^{-1}]

i$_{NXI}$: Nitrogen content of X_I [gN·gCOD^{-1}]

i$_{NXS}$: Nitrogen content of X_S [gN·gCOD^{-1}]

i$_{PBM}$: Phosphorus content of the biomass [gP·gCOD^{-1}]

i$_{PSS}$: Phosphorus content of Ss [gP·gCOD^{-1}]

i$_{PXI}$: Phosphorus content of X_I [gP·gCOD^{-1}]

i$_{PXS}$: Phosphorus content of X_S [gP·gCOD^{-1}]

J^2: Janus coefficient

k_{BOD}: First order constant of BOD [d^{-1}]

K$_{e,CO2}$: Chemical equilibrium constant of carbon dioxide [mmol·m^{-3}]

K$_{e,H2PO4}^-$: Chemical equilibrium constant of dihydrogen phosphate [mmol·m^{-3}]

K$_{e,HCO3}^-$: Chemical equilibrium constant of bicarbonate [mmol·m^{-3}]

$K_{e,HNO2}$: Chemical equilibrium constant of nitrous acid [mmol·m⁻³]

$K_{e,NH3}$: Chemical equilibrium constant of ammonia [mmol·m⁻³]

K^H: Maximum specific hydrolysis rate [gCOD·(gCOD·d)⁻¹]

K_{HCO3^-}: Half saturation constant for HCO_3^- [gC·m⁻³]

K_{HNO2}^{NOB}: Nitrous acid substrate saturation constant for NOB [gN·m⁻³]

$K_{I,HNO2}^{AOB}$: Free nitrous acid inhibition constant for AOB [gN·m⁻³]

$K_{I,HNO2}^{NOB}$: Free nitrous acid inhibition constant for NOB [gN·m⁻³]

$K_{I,NH3}^{AOB}$: Free ammonia inhibition constant for AOB [g N·m⁻³]

$K_{I,NH3}^{NOB}$: Free ammonia inhibition constant for NOB [g N·m⁻³]

$K_{i,O2}$: Oxygen inhibition constant for denitrifiers [gO₂·m⁻³]

k_La_i: Volumetric mass transfer coefficient of i [h⁻¹]

K_{NH3}^{AOB}: Ammonia substrate saturation constant for AOB [gN·m⁻³]

K_{NO2}: Saturation constant of S_{NO2} for endogenous respiration [gN·m⁻³]

K_{NO2}^{dNO2}: Nitrite substrate saturation for nitrite denitrifiers [gN·m⁻³]

K_{NO3}: Saturation constant of S_{NO3} for endogenous respiration [gN·m⁻³]

K_{NO3}^{dNO3}: Nitrite substrate saturation for nitrate denitrifiers [gN·m⁻³]

K_{O2}^i: Oxygen substrate saturation constant for i (i as AOB, NOB or H) [gO₂·m⁻³]

K_{pH}: Saturation constant of pH

K_{SS}: Heterotrophic bacteria half-saturation constant for ready biodegradable substrate [gCOD·m⁻³]

K_T: Kinetic parameter at a temperature T

K_{Tref}: Kinetic parameter at a T_{ref}

K_w: Chemical equilibrium constant of water [mmol·m⁻³]

K_x: Saturation constant for slowly biodegradable substrate [gCOD·m⁻³]

MAE: Mean Absolute Error

MAP: Magnesium Ammonium Phosphate

m_i: Henry coefficient for i (i as CO_2, N_2, O_2 and NH_3)

MLSS: Mixed Liquor Suspended Solids [mgSS·L⁻¹]

NAC: Non-ACclimated sludge

NLR: Nitrogen Loading Rate [kgN·m⁻³·d⁻¹]

N-NH₄⁺: Ammonium [mgN-NH₄⁺·L⁻¹]

NH₄⁺$_{AOB}$: Ammonium oxidised by AOB [molN-NH₄⁺·L⁻¹]

N-NO₂⁻: Nitrite [mgN-NO₂⁻·L⁻¹]

N-NO₃⁻: Nitrate [mgN-NO₃⁻·L⁻¹]

NOB: Nitrite Oxidising Bacteria

NOCRI: NOn-Competitive Reversible Inhibition

NPR: Nitrite Production Rate [kgN·m⁻³·d⁻¹]

NPR$_{obs}$: Nitrite Production Rate observed [kgN·m⁻³·d⁻¹]

NPR$_{obs}^{max}$: Maximum Nitrite Production Rate observed [kgN·m⁻³·d⁻¹]

N-TKN: Total Kjeldahl Nitrogen [mgN-TKN·L⁻¹]

OC: Oxygen Consumed [mgO₂·L⁻¹·d⁻¹]

OLAND: Oxygen Limited Autotrophic Nitrification Denitrification

ORP: Oxidation Reduction Potential [mV]

OTU: Organism Taxonomic Units

OUR: Oxygen Uptake Rate [mgO₂·L⁻¹ h⁻¹]

OUR$_{obs}$: Oxygen Uptake Rate observed [mgO₂·L⁻¹ h⁻¹]

OUR$_{obs}^{max}$: Maximum Oxygen Uptake Rate observed [mgO₂·L⁻¹ h⁻¹]

PCR: Polymerase Chain Reaction

PN-SBR: Partial Nitration-Sequencing Batch Reactor

Q_{acid}: Acid flow rate [L·d⁻¹]

Q_{base}: Base flow rate [L·d⁻¹]

$Q_{Csource}$: Carbon source flow rate [L·d⁻¹]

Q_{evap}: Volumetric reactor liquid loss due to evaporation [L·d⁻¹]

$Q_L^{in,}$**net**: Net inflow [L·d⁻¹]

Q_L^{in}: Inflow [L·d⁻¹]

Q_L^{out}: Outflow [L·d⁻¹]

Q_L^{waste}: Waste flow [L·d⁻¹]

r^2: Square of the correlation coefficient

RBC: Rotating Biological Contactor

$r_{i,L}$: Volumetric conversion rate of component i [mg·L⁻¹·d⁻¹]

RMSE: Root Mean Squared Error

SBR: Sequencing Batch Reactor

SF: Step-Feed

SHARON: Single reactor High activity Ammonia Removal Over Nitrite

S_I: Inert soluble organic matter state variable [gCOD·m⁻³]

S_{IC}: Total inorganic carbon state variable [gC·m⁻³]

S$_{IP}$: Total inorganic phosphorus state variable [gP·m^{-3}]

S$_{N2}$: Total nitrogen gas state variable [gN·m^{-3}]

S$_{ND}$: Soluble organic nitrogen state variable [gN·m^{-3}]

S$_{NH}$: Total ammonium and ammonia nitrogen state variable [gN·m^{-3}]

S$_{NO2}$: Total nitrite and nitrous acid nitrogen state variable [gN·m^{-3}]

S$_{NO3}$: Total nitrate nitrogen state variable [gN·m^{-3}]

S$_{O2}$: Dissolved oxygen state variable [gO$_2$·m^{-3}]

SRT: Sludge Retention Time [d]

S$_S$: Ready biodegradable organic matter state variable [gCOD·m^{-3}]

T: Temperature [ºC]

TAN: Total Ammonium as Nitrogen [mgN·L^{-1}]

TNO$_2$: Total Nitrite [mgN·L^{-1}]

TOC: Total Organic Carbon [mgC·L^{-1}]

T$_{ref}$: Reference temperature [ºC]

TSS: Total Suspended Solids [mgTSS·L^{-1}]

VER: Volumetric Exchange Ratio

V$_{max}$: Maximum water volume [L]

V$_{min}$: Minimum water volume [L]

VSS: Volatile Suspended Solids [mgVSS·L^{-1}]

WWTP: WasteWater Treatment Plant

X$_{AOB}$: Ammonium oxidizing bacteria biomass state variable [gCOD·m^{-3}]

X$_H$: Heterotrophic biomass state variable [gCOD·m^{-3}]

X$_{i,exp}$: Experimental value for an output i [mg·L^{-1}]

X$_{i,theo}$: Theoretical value for an output i [mg·L^{-1}]

X$_I$: Inert particulate organic matter state variable [gCOD·m^{-3}]

X$_{ND}$: Particulate organic nitrogen state variable [gN·m^{-3}]

X$_{NOB}$: Nitrite oxidizing bacteria biomass state variable [gCOD·m^{-3}]

X$_S$: Slowly biodegradable substrates state variable [gCOD·m^{-3}]

Y$_{AOB}$: Yield of ammonia oxidation [gCOD·gN^{-1}]

Y$_{H,NO2}$: Yield of denitrification via nitrite [gCOD·gCOD^{-1}]

Y$_{H,NO3}$: Yield of denitrification via nitrate [gCOD·gCOD^{-1}]

Y$_H$: Yield of aerobic organic matter oxidation [gCOD·gCOD^{-1}]

y$_i$: Model output value

Y$_{NOB}$: Yield of nitrite oxidation [gCOD·gN^{-1}]

Z$^+$: Net positive charges [molZ$^+$·m^{-3}]

α$_i$= Fraction of i in the media (i as CO$_3^{2-}$, HCO$_3^-$ or H$_2$CO$_3$)

γ$_K$: Collinearity index

δ$_j^{msqr}$: Sensitive measure

θ: Temperature correction coefficient [ºC^{-1}]

v: Maximum activity

v$_{Gs}$: Superficial gas velocity [m·s^{-1}]

v$_{limited}$: Observed activity

Table of contents

List of Figures

List of Tables

Chapter 1.   INTRODUCTION

1.1 Urban landfill leachate: problem definition

Every year, millions of tones of urban solid wastes potentially harmful for the environment and requiring a proper treatment are produced globally. Landfilling is one of the most widely employed methods for its management (Kurniawan *et al.*, 2006; Renou *et al.*, 2008), and landfill sites have been developed as highly engineered facilities designed to minimise the negative effects of the waste on the surrounding environment (Wiszniowski *et al.*, 2006). These negative effects include possible contamination of the groundwater and surface water regimes, the uncontrolled migration of landfill gas and the generation of odour, noise and visual nuisances (EPA, 2000). One of the main environmental concerns arising from the management of these sites is the production of urban landfill leachate, highly contaminated wastewater generated from the percolation of rain through the landfill, together with the production of liquids during the stabilisation of the solid waste.

Urban landfill leachates are characterised by a wide range of contaminants. According to Kjeldsen *et al.* (2002), the pollutants can be divided into four groups:

1. Organic matter, including dissolved organic matter, volatile fatty acids and more refractory compounds such as fulvic and humic acids.
2. Inorganic macrocomponents: calcium (Ca^{2+}), magnesium (Mg^{2+}), sodium (Na^+), potassium (K^+), ammonium (NH_4^+), iron (Fe^{2+}), manganese (Mn^{2+}), chloride (Cl^-), sulphate (SO_4^{2-}) and hydrogen carbonate (HCO_3^-).
3. Heavy metals: cadmium (Cd^{2+}), chromium (Cr^{3+}), copper (Cu^{2+}), lead (Pb^{2+}), nickel (Ni^{2+}) and zinc (Zn^{2+}).
4. Xenobiotic organic compounds, including a huge variety of aromatic hydrocarbons, phenols, pesticides, among others. These compounds are usually present at very low concentrations.

The composition of landfill leachate changes as the landfill ages. Generally, leachates produced in younger landfills are characterised by the presence of substantial amounts of volatile fatty acids. In mature landfills, the greater portion of organics in leachate are humic and fulvic-like fractions (Kulikowska and Klimiuk, 2008). On the other hand, ammonium is released from the waste by the decomposition of organic matter, therefore reaching significantly high concentrations in the first stages of the waste degradation process. This high ammonium levels may slightly decrease over time due to the landfill maturation.

Figure 1.1 depicts the evolution of different compounds in leachate throughout the degradation process.
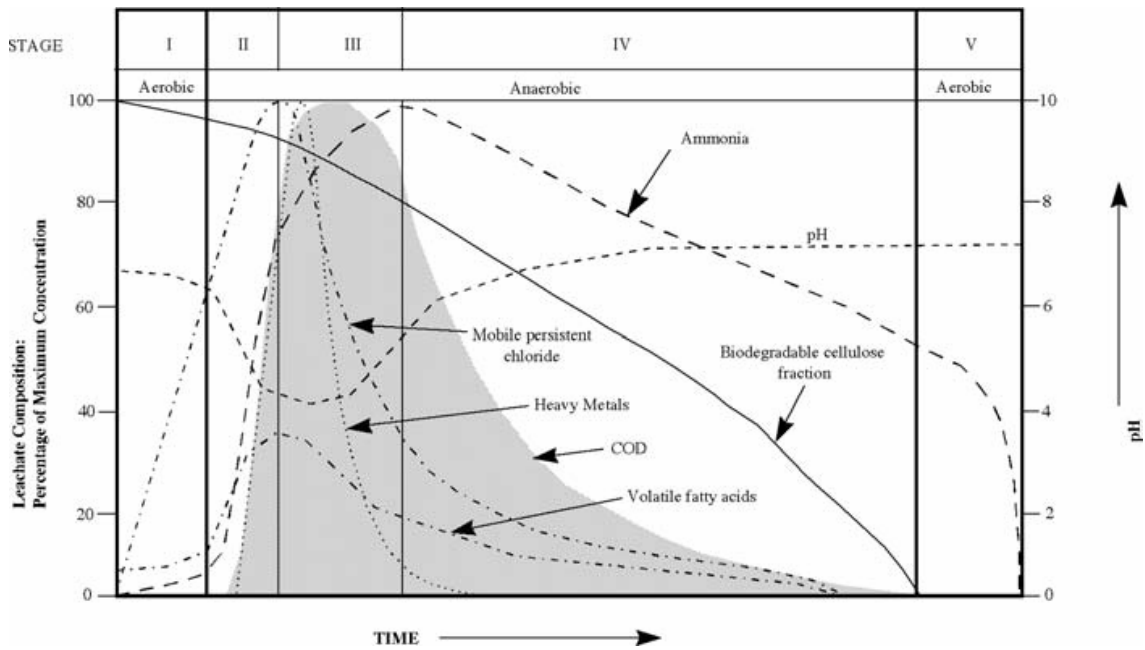
Figure 1.1 Changes in leachate composition (EPA, 2000)

The principal organic content of leachate is formed during the breakdown processes at the beginning of degradation, and the quality of municipal landfill leachate changes with time as the degradation of the waste continues inside the landfill. The process is generally divided into five successive stages, namely (i) aerobic, (ii) hydrolysis and fermentation, (iii) acetogenesis (iv) methanogenic and (v) the aerobic phase. These processes are dynamic, each stage being dependent on the creation of a suitable environment by the preceding one (EPA, 2000). Leachate generated at the early stages, termed young leachate, is characterized by elevated ammonium concentrations and organic matter with a high biodegradable content. As it ages, the ammonium concentrations increase while the biodegradable fraction declines due to the stabilisation process. Leachate with these characteristics is termed mature or old leachate.

Finally, leachate composition among landfills may vary significantly depending on the type of municipal solid wastes dumped, the degree of solid waste stabilisation, site hydrology, moisture content, seasonal weather variations, age of the landfill and the stage of the decomposition in the landfill (Kurniawan et $al.$, 2006). An example of different leachate characteristics can be found in Table 1.1. This table clearly depicts the elevated ammonium concentration of this wastewater (in the majority of the studies between 1,000 and 3,000 $mgN\text{-}NH_4^+\cdot L^{-1}$), reaching values up to 5,500 $mgN\text{-}NH_4^+\cdot L^{-1}$ for mature leachate. This review also shows the significant presence of organic matter in the leachate, with concentrations frequently much higher than 1,000 $mgCOD\cdot L^{-1}$, and its low biodegradable content. Young leachate (such as that treated in the study of Kulikowska et $al.$, 2008) with low nitrogen and organic matter content is also shown in this table. With regards to bicarbonate, concentration in leachate was also high, mainly ranging between 3,000 and 10,000 $mgHCO_3^-\cdot L^{-1}$. Finally, pH was in the majority of the studies slightly basic, with pH values up to 9.

4

Table 1.1 Ammonium and organic matter content of different leachates

Source	NH_4^+ $mgN\text{-}NH_4^+ \cdot L^{-1}$	COD $mgO_2 \cdot L^{-1}$	BOD $mgO_2 \cdot L^{-1}$	HCO_3^- $mgHCO_3^- \cdot L^{-1}$	pH -
Kjeldsen et al. (2002)	50-2,200	140-152,000	20-57,000	-	4.5-9
Kalyuzhnyi and Gladchenko (2004)	780-1,080	9,660-20,560	-	-	5.99-7.52
Liang et al. (2007)	1,600-3,100	1,500-16,000	-	9,200-17,250	8.0-9.0
Vilar et al. (2007)	1,275-5,500	14,600-70,800	-	-	6-8.8
Bohdziewicz et al. (2008)	750-840	2,800-5,000	-	5,612-9,638	8.0-8.9
Kulikowska et al. (2008)	66-364	580-1,821	76-701	-	7.29-8.61
Spagni et al. (2008)	167-1,540	528-3,060	30-1,000	2,135-9,882	7.55-8.9
Spagni et al. (2009)	933-1,406	1,769-2,623	-	5,734-9,882	7.93-8.23
Monclús et al. (2009)	535-1,489	810-2,960	254-368	3,353-8,093	-

When all these factors are taken into account, the treatment of this wastewater turns out to be a highly complex issue. The processes currently used often require combined techniques which are designed as modular or multistage units skilled in the treatment of contaminants which vary in concentration over the years (Wiszniowski *et al.*, 2006).

Because of its elevated concentrations during the degradation process and its high toxicity for aquatic life, ammonia has been identified by many researchers as the contaminant in the leachate with the potentially greatest adverse effect in the long term (Robinson, 1995; Krumpelbeck and Ehrig, 1999; Christensen *et al.*, 1994).

1.2 Nitrogen removal from landfill leachate

The treatment of leachate is complicated due to the wide range of contaminants to be removed (organic matter, salts, nitrogen, metals). This study specifically focuses on the elimination of nitrogen. In the following section, the most commonly-used technologies for ammonium removal of landfill leachate are briefly described. Physical-chemical treatments, as well as biological methods, are included.

1.2.1 Physical-chemical treatments

The treatment of urban landfill leachate by physical-chemical treatments is common due to the constraints imposed by the characteristics of this kind of wastewater: elevated concentrations of ammonium, high concentrations of refractory COD and low biodegradable organic matter content. But these treatments may also allow the elimination of other contaminants, depending

on the technology applied. In terms of nitrogen removal, treatment of landfill leachate can be achieved by adsorption processes in activated carbon (Abdul Aziz *et al.*, 2004), membrane filtration processes (Di Palma *et al.*, 2002; Ozturk *et al.*, 2003), chemical precipitation (Li *et al.*, 1999; Altinbas *et al.*, 2002; Zhang *et al.*, 2009) and ammonia stripping (Cheung *et al.*, 1997; Marttinen *et al.*, 2002; Ozturk *et al.*, 2003; Calli *et al.*, 2005). Of these, the most widely-used technologies for N removal are the chemical precipitation and the ammonia stripping treatments, which are further described below.

1.2.1.1 <u>Chemical precipitation</u>

Due to its effectiveness, the simplicity of the process and the fact that the equipment employed is inexpensive, chemical precipitation has been extensively used for the removal of non-biodegradable organic compounds, $N-NH_3$ and heavy metals from landfill leachate (Li *et al.*, 1999; Altinbas *et al.*, 2002; Zhang *et al.*, 2009). During chemical precipitation, dissolved ions in the solution are converted to the insoluble solid phase via chemical reactions. Typically, the nitrogen precipitate from the solution is in the form of struvite (magnesium ammonium phosphate, MAP). To achieve this goal $MgCl_2 \cdot 6H_2O$ and $Na_2HPO_4 \cdot 12H_2O$ are usually employed as precipitants, as shown in the following reaction (Kurniawan *et al.*, 2005).

$$MgCl_2 \cdot 6H_2O + Na_2HPO_4 + NH_4^+ \leftrightarrow MgNH_4PO_4 \cdot 6H_2O \downarrow +2NaCl + H^+ \qquad \textbf{(Eq. 1.1)}$$

The advantage of struvite precipitation is that the sludge produced after treatment may be utilised as a nitrogen fertiliser if the leachate does not contain any heavy metals. However, there are major drawbacks to chemical precipitation, including the high dose of precipitant required, the sensitivity to pH of the process employed, the generation of sludge and the need for further disposal of this sludge (Kurniawan *et al.*, 2005).

1.2.1.2 <u>Ammonia stripping</u>

Because of its effectiveness, ammonia stripping is the most widely-used method for the removal of NH_3 from landfill leachate (Kurniawan *et al.*, 2005). This treatment is based on a mass transfer process from the liquid to the gas phase. Landfill leachate containing NH_3 and the air phase are allowed to interact in a counter-current flow, resulting in the transfer of ammonia from the waste stream to the air.

However, the ammonia/ammonium equilibrium has to shift to free ammonia prior to the stripping in order to facilitate the stripping of NH_3. This can be achieved by adjusting the pH of the leachate to values over 10. The alkali requirements for achieving such a high pH vary from one leachate to another. For instance, about 0.5 kg lime·m^{-3} may be needed when dealing with

methanogenic leachates, while up to 6 kg·m^{-3} would be necessary for acetogenic leachates (EPA, 2000).

Ammonia stripping is usually carried out in stripping towers, and the ratio between air and leachate critically affects the process performance. Therefore, the greater the ratio, the more efficient the process and the lower the relative cost (EPA, 2000). The concentration of ammonia released in a stripping tower exhaust is typically a couple of hundred milligrams per cubic metre, which is below the level of toxic effect of 1,700 mg·m^{-3}, but above the odour threshold of 35 mg·m^{-3}, meaning there would be detectable odour near the plant. Consequently, a proper treatment of this gas would be required (EPA, 2000). In addition, effluent may be neutralised with acid prior to discharge.

Figure 1.2 shows a scheme of a typical ammonia stripping process.
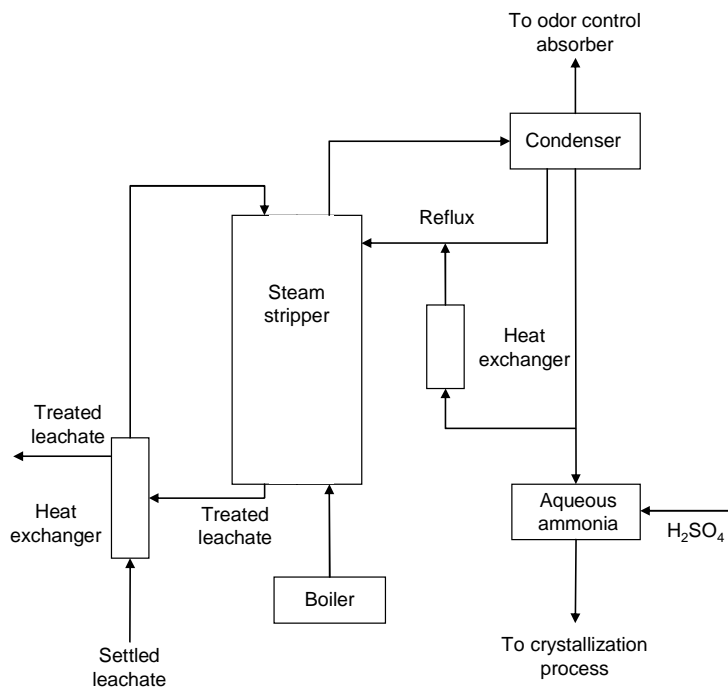
Figure 1.2 Scheme of an ammonia steam stripping process (Tchobanolgous *et al.,* 2003)

It is important to point out that the process is non-selective, so that other contaminants such as volatile organic species may also be released into the atmosphere.

To sum up, ammonia stripping is a good treatment for ammonium removal from urban landfill leachate and allows the ammonium discharge standards to be met. In terms of operational costs, it is more economically appealing than other physical-chemical treatments such as reverse osmosis or nanofiltration. A major drawback of ammonia stripping, however, is the environmental impact of the release of NH$_3$ gas, which makes further treatment of the gas with HCl or with H$_2$SO$_4$ necessary, thus increasing the operational costs of waste treatment due to

chemicals. The other limitations of this technique are the $CaCO_3$ scaling of the stripping tower when lime is employed for pH adjustment, the need for pH adjustment to the treated effluent prior to discharge, and the difficulty in removing ammonia with concentrations of less than 100 $mg \cdot L^{-1}$ (Kurniawan *et al.*, 2005).

1.2.2 Conventional biological treatments

Nitrogen can also be removed from landfill leachate by a conventional biological nitrification/denitrification process. Here, ammonium is biologically oxidised to nitrate under aerobic conditions (Eq. 1.2). This nitrate is reduced to N_2 gas under anoxic conditions by heterotrophic bacteria, which utilise organic matter in wastewater ($C_{10}H_{19}O_3N$) as the electron donor (Eq. 1.3).

$$NH_4^+ + 2HCO_3^- + 2O_2 \rightarrow NO_3^- + 3H_2O + 2CO_2 \tag{Eq. 1.2}$$

$$C_{10}H_{19}O_3N + 10NO_3^- \rightarrow 5N_2 + 10CO_2 + 3H_2O + NH_3 + 10OH^- \tag{Eq. 1.3}$$
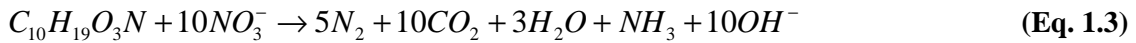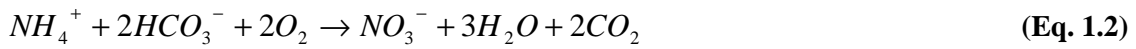
These metabolic pathways can be effected under different technologies. The different configurations that are usually employed for N-biological treatment in urban landfill leachate are presented next.

1.2.2.1 <u>Rotating Biological Contactor (RBC)</u>

The rotating biological contactor (RBC) is an attached growth technology that consists of a series of closely spaced circular disks mounted centrally on a horizontal shaft (Tchobanoglous *et al.*, 2003). These disks are approximately 40% submerged in a tank containing wastewater and are slowly rotated by either a mechanical or a compressed air drive. The rotation of the assemblage ensures that the media are alternately in air and wastewater, resulting in the development of a biofilm (EPA, 2000). Figure 1.3 depicts a rotating biological contactor.

Figure 1.3 View of a rotating biological contactor

This technology has been widely used for the treatment of ammonium from landfill leachate. Examples of it can be found in Henderson *et al.* (1997) and Castillo *et al.* (2007), among others. Finally, it should be noted that the development of anaerobic ammonium oxidation (ANAMMOX) metabolism has been observed on several occasions in RBCs treating landfill leachate (Hippen *et al.*, 1997; Helmer and Kunst, 1998; Siegrist *et al.*, 1998; Helmer *et al.*, 2001).

1.2.2.2 <u>Aerated lagoons/Extended aeration</u>

This is one of the simplest forms of on-site treatment of landfill leachate. It is carried out in ponds operating at long retention times, between 3 and 10 days (Haarstad and Mæhlum, 1999). These systems are provided with artificial aeration (usually by motor driven aerators, but also carried out by diffusers injecting air). Aeration systems play a dual role: on the one hand they supply oxygen to the microorganisms, and on the other they allow biological solids to be kept in suspension (Tchobanoglous *et al.*, 2003). Anoxic conditions have to be provided for the denitrification process, which is usually achieved in specific anoxic ponds. The advantages of this treatment method include its high flexibility, which may allow it to cope with a wide range of flows and strengths of leachate. Nevertheless, it also has drawbacks, including the large area required for the treatment, low energy efficiency, and odour and aerosol formation (EPA, 2000). Some examples of the application of this technology to landfill leachate treatment can be found in Robinson and Grantham (1988), Frascari *et al.* (2004) and Mehmood *et al.* (2009).

1.2.2.3 <u>Activated sludge</u>

The activated sludge process is a suspended growth biological treatment where wastewater is constantly supplied. By definition, activated sludge systems consist of three basic components: i) the activated sludge unit or reactor ii) a liquid-solid separation unit, usually a settler, and iii) a recycle which returns the solids to the reactor (Tchobanoglous *et al.*, 2003). The activated sludge unit can be operated as a continuous stirred tank reactor or a plug flow. In addition, to remove nitrogen, the activated sludge unit has to provide aerobic and anoxic zones. This can be achieved in the same tank or in different tanks, with a subsequent need for internal recirculation. A scheme of this technology is depicted in Figure 1.4.
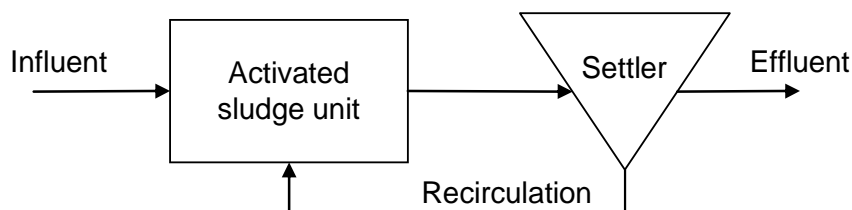
Figure 1.4 Scheme of an activated sludge process

Activated sludge systems for nitrogen removal from landfill leachate are widespread. Examples can be found in Knox (1985), Lin and Sah (2002), Vilar *et al.* (2007), among others.

1.2.2.4 Sequencing Batch Reactors (SBRs)

The SBR is a fill-and-draw activated sludge system for wastewater treatment. While in continuous systems the reaction and settling occur in different tanks, in an SBR all the processes are conducted in a single reactor following a sequence of fill, reaction, settling and draw phases (see Figure 1.5). The cycle configuration depends on the wastewater's characteristics and legal requirements (Puig, 2008).

| FILL | REACTION | SETTLE and wastage | DRAW |
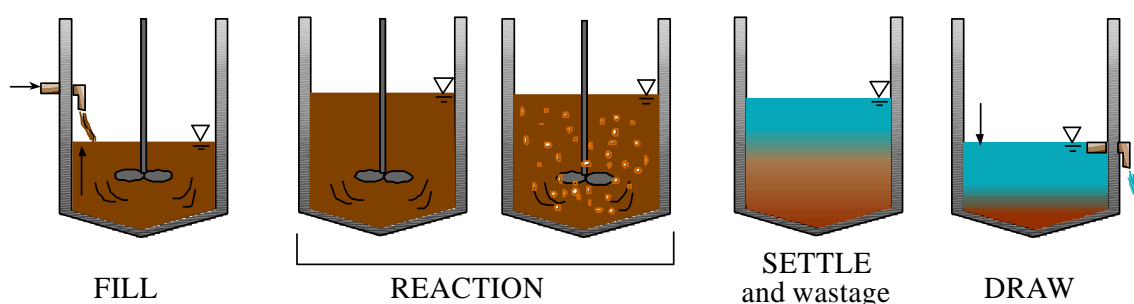
Figure 1.5 Sequence of phases in an SBR operation (Puig, 2008)

This technology has been extensively used for the treatment of landfill leachate (Yilmaz *et al.*, 2001; Uygur and Kargi, 2004; Neczaj *et al.*, 2005; Monclús *et al.*, 2009). Among the main advantages of an SBR are the high flexibility and controllability of the system, which also leads to a reduction in the treatment costs. On the other hand, SBRs require higher levels of control and automation than activated sludge systems when high nitrogen and phosphorus removal is required.

1.3 Autotrophic nitrogen removal

The treatment of high nitrogen loaded wastewaters with low carbon:nitrogen (C:N) ratios by a conventional autotrophic nitrification – heterotrophic denitrification process is expensive due to high aeration requirements and the need for an external carbon supply. In light of this, the development of processes based on anaerobic ammonium oxidation metabolism (anammox) has resulted in a revolution in the field of nutrient removal, since it has paved the way to fully autotrophic nitrogen elimination.

In the late seventies, Broda (1977) demonstrated the feasibility of a metabolic pathway based on ammonium oxidation under anoxic/anaerobic conditions by means of thermodynamic calculations. But it was not until 1995 that this metabolism was first reported, in the wastewater treatment plant (WWTP) of Gist-Brocades, in the Netherlands (Mulder *et al.*, 1995). The

10

process, as well as the organism responsible for it, was named ANAMMOX. Three years later, Strous and co-workers (1998) proposed an experimentally obtained stoichiometry for this process (Eq. 1.4). In their studies they observed that ammonium was converted to nitrogen gas, using nitrite as an electron acceptor, and also that small amounts of nitrate were produced in the reaction.

$$NH_4^+ + 1.32NO_2^- + 0.066HCO_3^- + 0.13H^+ \rightarrow 1.02N_2 + 0.26NO_3^- + 2.03H_2O$$
$$+ 0.066CH_2O_{0.5}N_{0.15}$$

(Eq. 1.4)
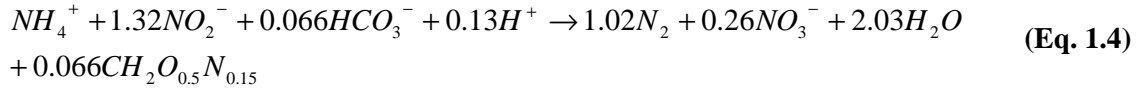
However, this process has also drawbacks. Anammox organisms have a very low growth rate (duplication time around 11 days; Strous *et al.*, 1998), dependent on temperature and pH. In addition their growth is negatively affected by several other factors. Anammox activity is inhibited by oxygen (Strous *et al.*, 1997; Egli *et al.*, 2001) and nitrite (Strous *et al.*, 1999) and the presence of biodegradable organic matter allows the development of heterotrophic bacteria which may compete with anammox for the substrate, NO_2^- (Chamchoi *et al.*, 2008; Ruscalleda *et al.*, 2008).

Finally, the anammox process requires a preliminary stage in which a suitable influent (1.32 moles of nitrite per mole of ammonium; Equation 1.4) must be produced. About half of the ammonium must be partially oxidised to nitrite, with a fraction of ammonium remaining unconverted. This preliminary biological process is named partial nitritation.

1.3.1 Fully autotrophic partial nitritation-anammox systems

At the present, the fully autotrophic partial nitritation-anammox process is still under development. There are very few full-scale facilities around the world, despite the fact that several investigative studies have focused on this issue. In the following sections, different experiences involving the application of a partial nitritation-anammox process in one- or two-reactor systems are presented.

1.3.1.1 Two-reactor systems

There are several studies reporting successful experiences featuring a combined partial nitritation-anammox process in two separate reactors. The majority concern lab-scale applications dealing with sludge digester supernatant, such as van Dongen *et al.* (2001) and Caffaz *et al.* (2006). Hwang *et al.* (2005) and Yamamoto *et al.* (2008) focused their research on the treatment of piggery wastewater, with ammonium concentrations of around 1,000 mgN-$NH_4^+ \cdot L^{-1}$. Also at lab-scale, Liang *et al.* (2008) dealt with landfill leachate containing ammonium concentrations up to 2,800 mgN-$NH_4^+ \cdot L^{-1}$. Several authors have also reported

successful results at the pilot-scale, such as Fux *et al.* (2002), Gut *et al.* (2006) and Qiao *et al.* (2009), with the first two treating sludge digester supernatant (ammonium concentration of around 700 mgN-NH$_4^+$·L^{-1}), and the last livestock manure (with concentrations of about 1,500 mgN-NH$_4^+$·L^{-1}). With regards to full-scale application of this technology, the first facility was in a WWTP in Rotterdam treating sludge digester supernatant with ammonium concentrations of 1,000-1,500 mgN-NH$_4^+$·L^{-1} (van der Star *et al.*, 2007; Abma *et al.*, 2007a). The start-up of this plant took more than three years. However, there are now other full-scale facilities around the world, such as the anammox plant in Lichtenvoorde (the Netherlands) for the treatment of tannery effluents, and the two-step anammox system treating effluents from a semiconductor plant in Japan (Abma *et al.*, 2007b).

1.3.1.2 **One-reactor systems**

Autotrophic nitrogen removal can be also achieved in one-reactor systems where, despite their different metabolic requirements, aerobic and anoxic ammonium oxidising bacteria coexist. To this end, different technologies/configurations have been successfully applied. For instance, Helmer *et al.* (2001), Seyfried *et al.* (2001) and Cema *et al.* (2007) reported good results with the application of a one-step process for the treatment of landfill leachate, dealing with ammonium concentrations lower than 1,500 mgN-NH$_4^+$·L^{-1}. This process included partial nitritation and anammox, and was named as one-stage deammonification. In the late nineties Kuai and Verstraete (1998) developed the oxygen limited autotrophic nitrification denitrification (OLAND) process, which also combines partial nitritation and anammox metabolism in a single reactor. This configuration has been further studied, and successfully applied at lab scale to the treatment of synthetic media (Pynaert *et al.,* 2002; Windey *et al.*, 2005) and digested black waters from vaccum toilets, with concentrations of around 1,000 mgN-NH$_4^+$·L^{-1} (Vlaeminck *et al.*, 2009). The CANON (completely autotrophic nitrogen-removal over nitrite) process (Strous, 2000) was developed along similar lines in Delft (the Netherlands). Experiments relating to this configuration mainly concern lab-scale set-ups, treating synthetic media (Third *et al.*, 2001; Sliekers *et al.*, 2002; Sliekers *et al.*, 2003), although CANON technology has also been successfully applied to full-scale treatment of the effluent of a potato factory (Abma *et al.*, 2007b). Finally, it is also important to mention the DEMON® process, consisting of an SBR for combined nitritation/anammox with continuous feeding, intermittent aeration and pH-control (Wett, 2006). This technology has been successfully applied in at least two full-scale plants: Strass (Austria, since 2004) and Glarnerland (Switzerland, since 2007) (Wett, 2007).

1.4 Partial nitritation

The oxidation of ammonium to nitrite is called nitritation, while the nitrite conversion to nitrate is termed nitratation. The term "partial nitritation" refers to the partial oxidation of ammonium to nitrite, with a fraction of ammonium remaining unconverted. This biological process is the conditioning step in the anammox process and is subject to many factors and parameters.

1.4.1 Fundamentals of nitrification

Nitrification has traditionally been considered as a single process (Eq. 1.2), but from a biological point of view it is composed of two steps. Ammonium is first oxidised to nitrite (Eq. 1.5) by ammonium oxidising bacteria (AOB), while further oxidation of nitrite to nitrate (Eq. 1.6) is carried out by a different bacterial population, called nitrite oxidising bacteria (NOB).

$$NH_4^+ + 2HCO_3^- + 1.5O_2 \rightarrow NO_2^- + 3H_2O + 2CO_2 \qquad \textbf{(Eq. 1.5)}$$

$$NO_2^- + 0.5O_2 \rightarrow NO_3^- \qquad \textbf{(Eq. 1.6)}$$
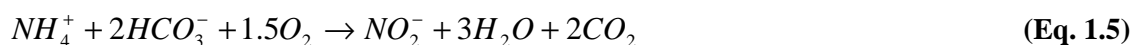
Ammonia and nitrite oxidising bacteria activity is influenced by several parameters and factors. The most important are briefly described in the following sections.

1.4.1.1 Temperature

Temperature (T) is a key factor in biological processes. Biological and chemical reactions take place at higher rates when temperature increases. However, at a certain level, high temperatures result in the denaturalisation of proteins and damage to bacterial membranes, which in turn leads to a sharp reduction in biological activity. We can say, therefore, that microorganisms are conditioned by lower temperatures (below which no growth is detected), an optimal temperature (where the growth rate is at its maximum) and a maximum temperature (over which no growth is possible) (Madigan *et al.*, 1997). Nitrification can take place in the range 4º to 40ºC, with a maximum activity between 30º and 37ºC.

The kinetic parameters are influenced by temperature and their value has to be corrected accordingly. The most widely-used equation to estimate this dependence is the van't Hoff-Arrhenius relationship (Equation 1.7) (Tchobanoglous *et al.*, 2003), but the fact that the estimation may be biased at very high temperatures, or when the temperature is significantly different from the reference, needs to be remembered.

$$K_T = K_{T_{ref}} \cdot e^{\theta(T-T_{ref})}$$ **(Eq. 1.7)**

where K_T is the kinetic parameter at temperature T, K_{Tref} is the value of the kinetic parameter at reference temperature T_{ref} and θ is the temperature coefficient.

Next, Figure 1.6 presents the change in maximum nitrification activity by the increase in temperature. In addition, the estimation of the maximum growth rate (μ_{max}) by the Arrhenius relationship is also depicted in the graph.
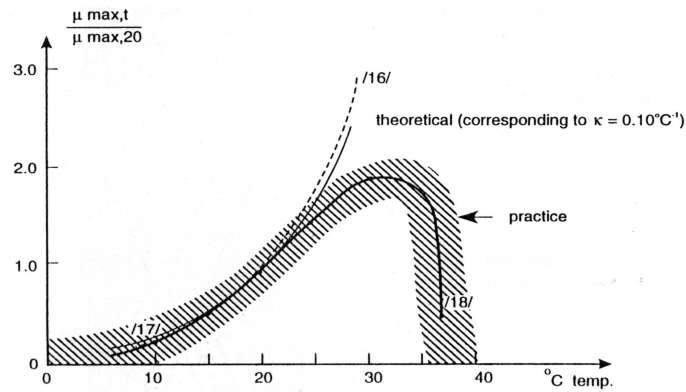
Figure 1.6 Effects of temperature over nitrification (Henze *et al.*, 1995)

Temperature has a differential effect on AOB and NOB activity. Within the temperature range usually found in wastewater treatment plants (10º - 20ºC), nitrite oxidisers grow faster than ammonium oxidisers and under such conditions ammonium is completely oxidised to nitrate. However, at temperatures over 25ºC the situation is the opposite: AOB grow faster than NOB, and nitrite may accumulate (Hellinga *et al.*, 1998). To address this issue, Figure 1.7 shows the minimum sludge retention time needed for the development of both communities, as a function of temperature.
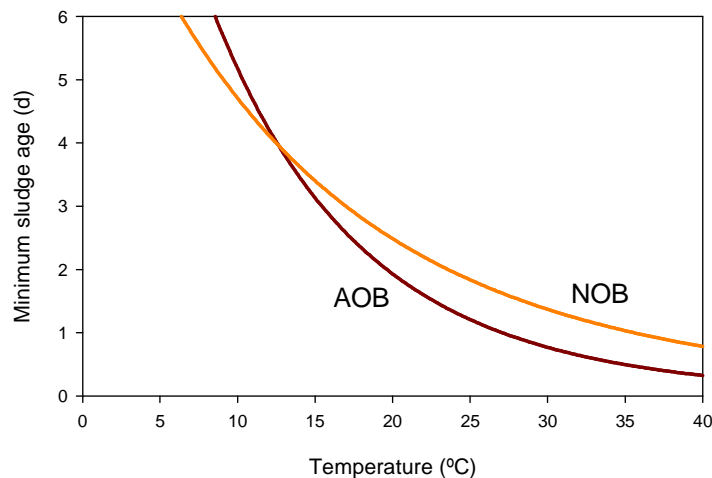
Figure 1.7 Minimum residence time for AOB and NOB as a function of temperature (Hellinga *et al.*, 1998)

14

Temperature also governs the solubility of oxygen in water. A temperature increase leads to a reduction in the solubility of gases, which in turn may increase aeration costs. Finally, temperature also affects the dissociation of chemical equilibriums such as NH_3 - NH_4^+, HNO_2^- - NO_2^- and CO_2 - HCO_3^- - CO_3^{2-}.

1.4.1.2 <u>pH</u>

Nitrification is pH sensitive, and reaction rates decline significantly at pH values below 6.8. At pH values around 5.8 to 6 the rates may be 10 to 20 percent of the rate at pH 7 (Tchobanoglous *et al.*, 2003). On the other hand, pH over 8 may also lead to the inhibition of nitrifying activity. This effect is due to the activation-deactivation of the nitrifying bacteria, linked to the inhibition of active sites of enzymes by the bonding of H^+ and OH^- (García and Fernández-Polanco, 1996).

In addition, pH also governs the chemical equilibrium of substrates (NH_3 - NH_4^+, HNO_2^- - NO_2^- and CO_2 - HCO_3^- - CO_3^{2-}) and inhibitors (NH_3 - NH_4^+, HNO_2 - NO_2^-).

1.4.1.3 <u>Dissolved oxygen</u>

Nitrification is an aerobic process, so the availability of dissolved oxygen (DO) in the media is essential for the development of AOB and NOB activity. However, these two bacterial groups have different affinities to this substrate. In general, NOB organisms have less affinity for DO (K_{O2}^{NOB}=1.1 $mgO_2 \cdot L^{-1}$, Wiesmann, 1994; K_{O2}^{NOB}=1.75 $mgO_2 \cdot L^{-1}$, Guisasola *et al.*, 2005) in comparison with AOB (K_{O2}^{AOB}=0.3 $mgO_2 \cdot L^{-1}$, Wiesmann, 1994; K_{O2}^{AOB}=0.74 $mgO_2 \cdot L^{-1}$, Guisasola *et al.*, 2005).

1.4.1.4 <u>Free ammonia and free nitrous acid: substrates and inhibitors</u>

Free ammonia, rather than ammonium is the substrate for AOB organisms (Suzuki *et al.*, 1974; Wiesmann, 1994), while NOB use the unionised form of nitrite, HNO_2, as their electron donor (Wiesmann, 1994). But, free ammonia (FA) and free nitrous acid (FNA) are also inhibitors of AOB and NOB activity (widely described by Anthonisen *et al.*, 1976; Vadivelu *et al.*, 2007; Van Hulle *et al.*, 2007, among others). Nitrite oxidising organisms are more sensitive to the inhibitions of both compounds than AOB (Vadivelu *et al.*, 2007), although there is a huge disparity in the inhibitory values found in the literature. Therefore, Anthonisen and co-workers (1976) found the FA inhibition range for AOB and NOB to be 10-150 $mgNH_3 \cdot L^{-1}$ and 0.1-1 $mgNH_3 \cdot L^{-1}$, respectively, and also stated that FNA had an impact on NOB (inhibition range of 0.2-2.8 $mgHNO_2 \cdot L^{-1}$), but not over AOB. These results are quite different from those found by Vadivelu *et al.* (2007) who did not detect any inhibition in AOB activity at FA concentrations up to 16 $mgN-NH_3 \cdot L^{-1}$, but observed a total inhibition of such activity at an FNA concentration of 0.4 $mgHNO_2 \cdot L^{-1}$. With regards to NOB, they observed total inhibition at concentrations

higher than 6 mgN-NH$_3$·L^{-1} and 0.02 mgHNO$_2$·L^{-1}. These differences may have been due to different bacterial communities and acclimation to stringent conditions.

1.4.1.5 Salinity

The presence of salts in the media may negatively affect bacteria and inhibit their activity. Campos *et al.* (2002) observed complete inhibition of nitrification activity at high concentrations of different salts (250-300 mM). Similarly, Moussa *et al.* (2006) obtained a 95% reduction in activity in NaCl concentrations of 40gCl$^-$·L^{-1}. In addition, some studies, such as that of Dahl *et al.* (1997), observed nitrite as the end product when treating saline wastewaters. This is in accordance with the findings of Vredenbergt *et al.* (1997) and Dincer *et al.* (1999), who pointed out that salinity favoured AOB rather than NOB. Conversely, Moussa *et al.* (2006) found AOB organisms to be more sensitive to salinity than NOB. This disparity in results may have been due to the sludge used in the experiments, the experimental conditions (pH, temperature, dissolved oxygen, among others), or the specific salts used.

1.4.1.6 Toxics

Nitrification can also be influenced by inorganic toxics such as heavy metals (Dahl *et al.,* 1997). For instance, Skinner and Walker (1961) reported complete inhibition of ammonia oxidation at 0.25 mg·L^{-1} of nickel, 0.25 mg·L^{-1} of chromium and 0.1 mg·L^{-1} of copper. In addition, organic compounds (solvent organic chemicals, amines, proteins, tannins, phenolic compounds, among others) may also inhibit nitrifying activity (Blum and Speece, 1991).

1.4.2 Nitritation

Nitrite concentrations are seldom detected in conventional WWTPs because NOB usually have higher reaction rates than AOB. In fact, ammonium oxidation is the rate-limiting step while nitrite is consumed at the same time it is produced. This means that the accumulation of nitrite in a system is achieved by promoting AOB rather than NOB activity. The previous section has depicted some factors that negatively affect nitrite oxidisers in contrast to ammonia oxidisers. Based on these, several methodologies have been developed to favour AOB activity and avoid nitrate production. In the following section the techniques for nitritation most commonly applied are briefly presented.

1.4.2.1 Operation at high temperatures and short sludge retention times

At room temperature, NOB reaction rates are higher than for AOB organisms, but this changes at temperatures higher than 25ºC (Hellinga *et al.*, 1998). This situation is accentuated at a temperature of 35ºC, where the AOB reaction rate is almost double that of NOB. Thus, when applying a sludge retention time (SRT) lower than the minimum SRT needed for NOB

development, but still high enough for AOB, it is possible to achieve a complete washout of NOB. Such an SRT has been determined to be about 1-1.5 days (Hellinga *et al.*, 1998). This is the theoretical basis of SHARON (Single reactor High activity Ammonia Removal Over Nitrite) technology (Hellinga *et al.*, 1998; van Dongen *et al.*, 2001), which has been mainly applied to the treatment of sludge digester supernatant (Hellinga *et al.*, 1998; Fux *et al.*, 2002; Gut *et al.*, 2006, among others). However, there have been experiences with this configuration for the treatment of other N-strong wastewater, such as piggery waste (Hwang *et al.*, 2005) and effluents from a fish cannery (Mosquera-Corral *et al.*, 2005; Dapena-Mora *et al.*, 2006).

1.4.2.2   Inhibition of NOB activity by free ammonia and/or free nitrous acid

Several studies have reported that non-ionised forms of ammonium and nitrite, free ammonia (FA) and free nitrous acid (FNA), can inhibit AOB and NOB activity (Anthonisen *et al.,* 1976; Villaverde *et al.*, 2000; Vadivelu *et al.*, 2007; Van Hulle *et al.,* 2007, among others). However, NOB organisms are more sensitive than AOB to elevated concentrations of these compounds and reactors operating at high ammonium concentrations may lead to an inhibition of NOB activity. Such inhibition may subsequently end up in nitrite accumulation, which at the same time may reinforce the inhibitory pressure on NOB organisms. This strategy was successfully applied by Lai *et al.* (2004) in a batch reactor. Yamamoto *et al.* (2008) also relied on FA and FNA inhibition to out-compete NOB from an attached biomass reactor treating swine wastewater digested liquor.

1.4.2.3   Low dissolved oxygen concentrations

AOB and NOB organisms require oxygen for performing their metabolisms. In recent years, several studies have pointed out that NOB have a lower affinity with this substrate than AOB organisms (Wiesmann, 1994; Picioreanu *et al.*, 1997; Guisasola *et al.*, 2005). Under oxygen limited conditions (0.1-1 $mgO_2 \cdot L^{-1}$), NOB activity is severely reduced, leading to a negative selection of this phylogenetical group. Thus, the enrichment of AOB ends-up in nitrite accumulation in the system. Examples of the application of this mechanism for NOB outcompetition can be found in Garrido *et al.* (1997), Joo *et al.* (2000), Bernet *et al.* (2001), Wyffels *et al.* (2003), Chuang *et al.* (2007), Blackburne *et al.* (2008a) and Aslan *et al.* (2009).

1.4.2.4   Aeration duration control

A typical nitrification reaction can be divided into two steps. The first is oxidation of ammonia to nitrite and the second is the conversion of nitrite to nitrate. Terminating the aerobic reaction phase prior to or at the completion of ammonium oxidation process may lead to a nitrite accumulation (Blackburne *et al.*, 2008b), a situation which can be identified by the so-called "ammonia valley" in the pH profile and the DO-break endpoints (Yang *et al.*, 2007). Examples

of the application of successful aeration duration control can be found in Fux *et al.* (2006), Yang *et al.* (2007), Peng *et al.* (2008) and Guo *et al*. (2009).

1.4.3 Modelling nitrite build-up

Nitrification and denitrification have been traditionally modelled as one-stage processes (Henze *et al.*, 2000). This assumption was valid since the accumulation of nitrite rarely takes place in wastewater treatment systems. However, the recent development of new processes and technologies reliant on nitrite has made the inclusion of complete metabolic pathways in the biological models of these systems necessary.

Nowadays there are various different biological models describing nitrite build-up, as reviewed by Sin *et al.* (2008). Some of these models focus on side-stream processes for the treatment of highly nitrogen loaded wastewater (Hellinga *et al.*, 1999; Volcke *et al.*, 2002; Wett and Rauch, 2003; among others), while others are more suited to conventional wastewater systems (e.g. Sin and Vanrolleghem, 2006; Kaelin *et al.*, 2009). With regards to organic matter, the majority of the side-stream models have been developed for applications without significant amounts of biodegradable organic matter in the system, and with an occasional external carbon source dosage. As a result, side-stream models seldom feature on a detailed modelling of heterotrophic conversions or organic matter availability and transformations. Finally, models also differ in terms of pH inclusion. pH plays an important role in highly N-loaded streams and, therefore, some models take it up. The main biokinetic models for nitrite build-up, together with their principal features are summarised in Table 1.2 below.

Table 1.2 Summary of biological models taking up nitrite

Model reference	High nitrogen strength streams	2-step nitrification	2-step denitrification	Complex organic matter	pH
Hellinga *et al.* (1999)	✓	✓	✓		✓
Volcke *et al.* (2002)	✓	✓	✓		✓
Hao *et al.* (2002)	✓	✓			
Wett and Rauch (2003)	✓	✓	✓	✓	✓
Moussa *et al.* (2005)	✓	✓			
Van Hulle *et al.* (2005)	✓	✓	✓	✓	✓
Pambrun *et al.* (2006)	✓	✓			
Sin and Vanrolleghem (2006)		✓	✓	✓	
Jones *et al.* (2007)	✓	✓	✓	✓	✓
Magrí *et al.* (2007)	✓	✓		✓	✓
Kampschreur *et al.* (2007)		✓	✓		
Kaelin *et al.* (2009)		✓	✓	✓	

With regards to denitrification, it should be noted that most models assume a sequential denitrification mechanism, i.e. $NO_3^- \rightarrow NO_2^- \rightarrow 1/2N_2$, while Hellinga *et al.* (1999) and Volcke (2006) considered parallel denitrification, i.e. $NO_3^- \rightarrow 1/2N_2$ and $NO_2^- \rightarrow 1/2N_2$ for the sake of simplicity (Sin *et al.*, 2008).

Finally, it is important to highlight that, independent of its characteristics and features, any model may have to be adapted, calibrated and validated for a specific application.

Chapter 2. OBJECTIVES

2.1 Problem definition

The treatment of urban landfill leachate (with high nitrogen concentrations and low biodegradable organic matter content) by classical biological nitrification/denitrification methods is expensive due to high aeration requirements, the need for an external organic matter supply and elevated sludge production. The treatment of such leachate by a combined partial nitritation-anammox system is a more economical alternative to conventional processes. As a preparative step for an anammox reactor, the leachate must be pre-treated in a partial nitritation step.

2.2 Objectives

The main objective of this PhD thesis is study the feasibility of the partial ammonium oxidation to nitrite of landfill leachate, as a prior step for a subsequent anammox process. The working objectives started at a lab-scale level and focused on the acquisition of basic knowledge relating to the partial nitritation of highly ammonium-loaded leachate. The following step was a scale-up to an industrial pilot-plant, aiming at long-term stability of the partial nitritation process. Final efforts focused on process modelling, for the development of a mathematical tool for the study of the system, the simulation of different operational strategies and future process control.

In order to achieve the main goal, the following secondary objectives were established:

> Lab-scale work was directed at the identification of suitable nitrite build-up operational conditions and strategies, focusing on:
>   - SBR cycle definition: Feeding strategies
>   - Study of the inhibitory effects of FA, FNA and HCO_3^- limitation over AOB.
>   - Process assessment by:
>   - Knowledge acquired from in-cycle dynamic profiles of on-line and off-line parameters.
>   - Key parameters for process control relating to influent composition, effluent quality assessment and biological status of the process.

> Once the lab-scale goals had been achieved, the process was scaled up to an industrial pilot-plant with the following aims:
>   - Obtaining a stable effluent of the desired effluent composition, with a view to subsequent anammox reactor.
>   - Reduction of oxygen consumption and total nitrogen in the effluent by taking advantage of the biodegradable organic matter content of landfill leachate.

- Validation of the assessment tools proposed in the lab-scale experiences.
- Microbiological and kinetic characterisation of the bacterial community of the reactor.

➢ Finally, the mathematical model for a partial nitritation process was developed, with the focus on:
- Adaptation of a previously developed model for partial nitritation of highly nitrogen-loaded landfill leachate, looking at:
  - Processes involving heterotrophic and autotrophic bacterial communities
  - Physical and chemical processes
- Refinement of an existing modelling guideline
- Calibration and validation of the partial nitritation model using historical data
- Utilisation of the model for a simulation case study: Impact of different factors on the long-term effluent speciation of a reactor.

Chapter 3.   MATERIALS AND METHODS

This chapter gathers general materials and methods used among the different chapters. Additional *Materials and methods* sections have been also included in Chapters 4 and 5 to briefly describe specific materials and methodologies of these chapters.

3.1 Chemical analyses

Different analytical methods have been used in this study. Among these, the majority are in accordance with Standard Methods (APHA, 2005), except for the biochemical oxygen demand analysis, which was based on a Euro Norm. Next, Table 3.1 summarises the different analytical methods and their references.

Table 3.1 Analytical methods

Analysis	Compound	Reference
$N-NH_4^+$	Ammonium	APHA-4500-NH$_3$.B-C5220B
$N-NO_2^-$	Nitrite	APHA-4110B
$N-NO_3^-$	Nitrate	APHA-4110B
N-TKN	Total Kjeldahl Nitrogen	APHA-4500-Norg.B
COD	Chemical Oxygen Demand	APHA-5220B
BOD	Biochemical Oxygen Demand	Euro Norm EN 1899-1/1998
TOC	Total Organic Carbon	APHA-S310
IC	Inorganic Carbon	APHA- S310
TSS	Total Suspended Solids	APHA- 2540D
VSS	Volatile Suspended Solids	APHA- 2540E

3.2 Free ammonia and free nitrous acid

Concentrations of free ammonia (FA) and free nitrous acid (FNA) were calculated as a function of pH, temperature and total ammonium as nitrogen (TAN), for FA, or total nitrite (TNO$_2$), for FNA (Eqs 3.1 to 3.4; Anthonisen *et al.*, 1976):

$$K_{e,NH_3} = e^{\frac{-6344}{273+T}}$$

(Eq. 3.1)

$$K_{e,HNO_2} = e^{\frac{-2300}{273+T}}$$

(Eq. 3.2)

$$FA \ (mgN \cdot L^{-1}) = \frac{TAN}{1 + \left(\dfrac{10^{-pH}}{K_{e,NH_3}} \right)}$$ **(Eq. 3.3)**

$$FNA \ (mgN \cdot L^{-1}) = \frac{TNO_2}{1 + \left(\dfrac{K_{e,HNO_2}}{10^{-pH}} \right)}$$ **(Eq. 3.4)**

3.3 Carbonate equilibrium

Concentrations of H_2CO_3, HCO_3^- and CO_3^{2-} were calculated as a function of the total inorganic carbon (IC).

$$[CO_3^{2-}] = \alpha_{CO_3^{2-}} \cdot [IC]$$ **(Eq. 3.5)**

$$[HCO_3^-] = \alpha_{HCO_3^-} \cdot [IC]$$ **(Eq. 3.6)**

$$[H_2CO_3] = \alpha_{H_2CO_3} \cdot [IC]$$ **(Eq. 3.7)**

where α_{CO32}^- accounts for the fraction of CO_3^{2-} in the media, α_{HCO3}^- for the fraction of HCO_3^- in the media and α_{H2CO3}^- for the fraction of H_2CO_3

These α values can be obtained from Equations 3.8, 3.9 and 3.10.

$$\alpha_{CO_3^{2-}} = \frac{K_{e,CO_2} \cdot K_{e,HCO_3^-}}{[H^+]^2 + [H^+] \cdot K_{e,CO_2} + K_{e,CO_2} \cdot K_{e,HCO_3^-}}$$ **(Eq. 3.8)**

$$\alpha_{HCO_3^-} = \frac{[H^+] \cdot K_{e,CO_2} \cdot}{[H^+]^2 + [H^+] \cdot K_{e,CO_2} + K_{e,CO_2} \cdot K_{e,HCO_3^-}}$$ **(Eq. 3.9)**

$$\alpha_{H_2CO_3} = \frac{[H^+]^2}{[H^+]^2 + [H^+] \cdot K_{e,CO_2} + K_{e,CO_2} \cdot K_{e,HCO_3^-}}$$ **(Eq. 3.10)**

where $[H^+]$ accounts for the proton concentration (mole·L^{-1}), $K_{e,CO2}$ is the first acid dissociation constant (mole·m^{-3}) and $K_{e,HCO3-}$ is the second acid dissociation constant (mole·m^{-3}).

These dissociation constants can be calculated from the following equilibrium relationships, according to Tchobanoglous *et al.* (2003).

$$K_{e,CO_2} = \frac{[H^+] \cdot [HCO_3^-]}{[H_2CO_3]}$$

(Eq. 3.11)

$$K_{e,HCO_3^-} = \frac{[H^+] \cdot [CO_3^{2-}]}{[HCO_3^-]}$$

(Eq. 3.12)

Finally, equilibrium constants $K_{e,CO2}$ and $K_{e,HCO3-}$ are affected by temperature, and can be calculated from the following temperature-dependent equations, obtained from Stumm and Morgan (1996).

$$K_{e,CO_2} = 10^{\left(-356.3094 - 0.06091964 \cdot T + \frac{21834.37}{T} + 126.8339 \cdot \log_{10} T - \frac{1684915}{T^2}\right)}$$

(Eq. 3.13)

$$K_{e,HCO_3^-} = 10^{\left(-107.8871 - 0.03252849 \cdot T + \frac{5151.79}{T} + 38.92561 \cdot \log_{10} T - \frac{563713.9}{T^2}\right)}$$

(Eq. 3.14)

3.4 Off-line Oxygen Uptake Rate calculation

During aerobic phases of the cycle, and assuming no outflow is taking place and only a negligible oxygen supply from the inflow, the DO mass balance in the mixed liquor can be represented by Equation 3.15.

$$OUR(t) = K_L a^{(T)} \left(DO_{sat}^{(T)} - DO^{(T)}(t)\right) - \frac{dDO}{dt}$$

(Eq. 3.15)

where OUR is the calculated oxygen uptake rate ($mgO_2 \cdot L^{-1} \cdot h^{-1}$), $K_L a^{(T)}$ is the mass transfer coefficient (h^{-1}), DO is the dissolved oxygen in the SBR ($mgO_2 \cdot L^{-1}$), and DO_{sat} is the saturation dissolved oxygen as a function of temperature (T) ($mgO_2 \cdot L^{-1}$)

Oxygen uptake rates (OUR, $mgO_2 \cdot L^{-1} \cdot h^{-1}$) were calculated off-line and based on the general oxygen mass balance in the reactor. Therefore, during air-off periods, due to the on/off control strategy, oxygen uptake rates were calculated from the slope of the oxygen decrease over time (Equation 3.14), in accordance with Puig *et al.* (2005).

$$OUR = -\frac{dDO}{dt}$$

(Eq. 3.16)

OUR values were corrected by the volume or the total amount of VSS in the reactor, to take into account SBR volume variations in feeding during the cycle.

3.5 Oxygen Consumed calculation

The total amount of Oxygen Consumed (OC) during a cycle can be calculated from an OUR profile of a cycle. The area below an OUR curve is assumed to be the oxygen consumed during the cycle. In this sense, OC can be calculated by integrating the OUR profile.

$$OC = \int_t OUR \cdot dt$$

(Eq. 3.17)

Chapter 4. LAB-SCALE EXPERIENCES ON PARTIAL NITRITATION

This chapter formed the basis of the following publications:

Ganigué, R., López, H., Balaguer, M.D. and Colprim, J. 2007. Partial ammonium oxidation to nitrite of high ammonium content urban landfill leachates. *Water Res*. **41**(15), 3317-3326.

Ganigué, R., López, H., Ruscalleda, M., Balaguer, M.D. and Colprim, J. 2008. Operational strategy for a Partial Nitritation-SBR (PN-SBR) treating urban landfill leachate to achieve a stable influent for an anammox reactor. *J. Chem. Technol. Biot.* **83** (3), 365-371.

4.1 Motivation

In recent years, the feasibility of treating highly-loaded nitrogen streams with a low C:N ratio by means of a combined partial nitritation-anammox process has been demonstrated, and been proved to be a promising alternative to conventional nitrification/denitrification systems. The majority of the reported experiences have focused on the treatment of sludge digester supernatant (van Dongen *et al.*, 2001; Fux *et al.*, 2002; Wett, 2007, among others), with only a few studies dealing with other N-loaded wastewater, such as piggery wastes (Ahn *et al.*, 2004; Hwang *et al.*, 2005; Waki *et al.*, 2007; Molinuevo *et al.*, 2009) or canning effluents (Mosquera-Corral *et al.*, 2005; Dapena-Mora *et al.*, 2006). Experiences with fully autotrophic partial nitritation-anammox for the treatment of urban landfill leachate are very few, and only Liang and Liu (2008) have reported the successful application of this technology to leachate.

The partial nitritation step has usually been achieved using SHARON technology (Hellinga *et al.*, 1998; Mulder *et al.*, 2001). However, there are other suitable configurations which could be used, such as sequencing batch reactor (SBR) technology (Lai *et al.*., 2004; Galí *et al.*, 2007) or biofilm airlift reactors (Garrido *et al.*, 1997; Kim *et al.*, 2006). There is just one reported experience with partial nitritation of landfill leachate prior to an anammox reactor. Liang and Liu (2007) achieved a suitable partial nitritation of the ammonium present in leachate with an up-flow fixed bed bio-film reactor, operating at a temperature of 30ºC.

As far as SBR technology is concerned, different strategies can be used to operate these reactors. A batch strategy based on a short feeding event at the beginning of a cycle is one of the simplest cycle designs, and is especially suitable for the treatment of low and medium nitrogen loads. Using this strategy, Galí *et al.* (2007) achieved partial nitritation of a synthetic feed using a 4 h cycle, with a short feeding phase followed by a long aerobic reaction phase. A similar cycle was used by Pambrun *et al.* (2006) to achieve complete nitritation of a synthetic influent which emulated the characteristics of a sludge digester supernatant. Another option is the step-feed strategy (SF), based on multiple feeding events. This can be used in systems which alternate different reaction phases, such as nitrification/denitrification systems (Puig *et al.*, 2004), or when dealing with nitrogen concentrations higher than in the batch strategy (one feeding event). Fux *et al.* (2003) successfully applied a step-feed strategy (composed of three short feeding events, followed by aerobic phases and anoxic periods with external carbon source addition) for the nitritation and denitritation of the nitrogen content of a sludge digester effluent. On the other hand, full-scale SBR plants or SBR plants treating high loads (Haro *et al.*, 2007; Damasceno *et al.*, 2007) usually operate using a fed-batch strategy (FB), where the influent is progressively supplied throughout the entire cycle. Fux *et al.* (2006) used this strategy alternating aerobic and anoxic conditions, to achieve a nitritation/denitritation of the ammonium present in sludge dewatering liquor. To sum up, then, we can say that a suitable cycle definition

depends on the characteristics of the wastewater, the goal of the process and the technical requirements and/or limitations.

4.2 Objectives

This chapter aims principally to evaluate the feasibility of achieving a successful partial nitritation of the ammonium present in leachate from urban landfill sites, using SBR technology, as a preparative step for an anammox reactor. Specifically, the study focuses on the identification of a suitable feeding strategy for the operation of a partial nitritation-sequencing batch reactor (PN-SBR), and its proper operational conditions. In addition, the chapter seeks to gain insight into the inhibitory effect of free ammonia (FA) and free nitrous acid (FNA) over ammonium oxidising bacteria (AOB). Finally, another important aim is the process performance assessment with a view to scale-up.

4.3 Materials and methods

4.3.1 Experimental set-up

The experiments were carried out with a lab-scale SBR, located in the Faculty of Sciences of the University of Girona. The set-up was composed principally of a storage tank, a 20-L reactor and a control system. A scheme of the set-up and views of the lab-scale plant are depicted in Figure 4.1 and Figure 4.2 respectively.

① STORAGE TANK	⑤ pH CONTROL	⑧ DISCHARGE VALVE
② INFLUENT PUMP	⑥ PROBES (ORP, DO, T, pH)	⑨ DO VALVE
③ JACKETED SBR	⑦ STIRRER	⑩ CONTROL PANEL
④ THERMOSTATIC BATH		
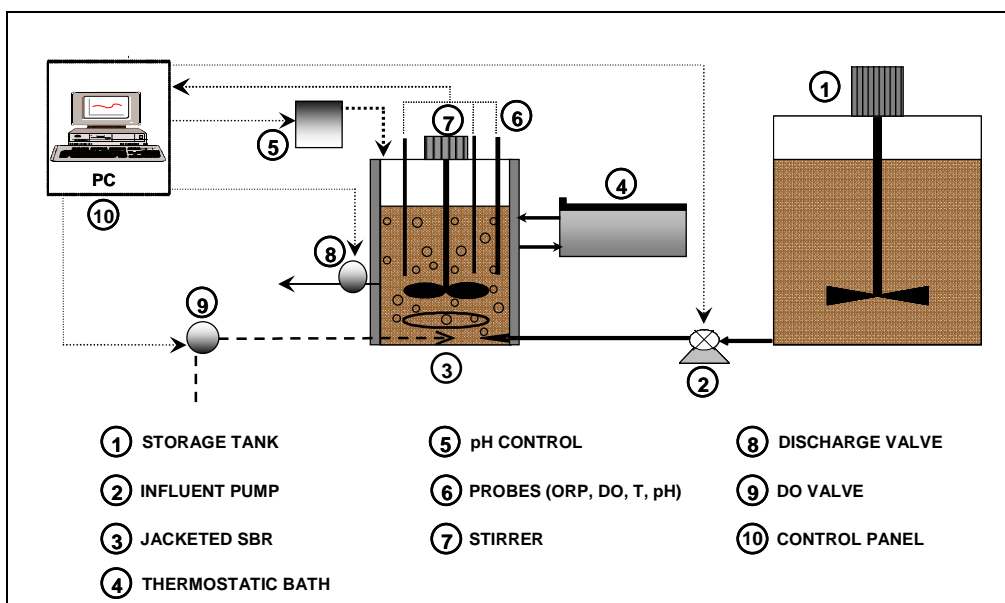
Figure 4.1. Scheme of the lab-scale set-up

The reactor (Figure 4.2b), constructed in A-316 stainless steel, was of cylindrical shape, with a height of 0.55m and an internal diameter of 0.2m. It was water jacketed, thus allowing temperature to be controlled by means of a thermostated water bath. Complete mixture was achieved during the filling and reaction phases with a mechanical stirrer (Stuart Scientifics SS10). The SBR was operated with a minimum water volume (V_{min}) of 9.7 L and a volume exchange ratio (VER, ratio of the volume fed per cycle to the maximum reactor volume) of about 0.225. Aeration was carried out with air diffusers, located at the bottom of the reactor, and the air flow was switched on and off by an electro-valve to maintain the desired DO concentration. The influent, stored at 4 ℃ in a 150-L stirred tank, was pumped with a peristaltic pump (Watson Marlow 505S) to the bottom of the reactor. The SBR was drawn by gravity discharge using an electro-valve, until the V_{min} was reached. The pilot plant was also equipped with a monitoring and control system (Figure 4.2c). On-line data provided by pH, oxidation reduction potential (ORP), DO and temperature probes (CPF 81, CPF 82 and OXYMAX-W COS-41, from Endress-Hauser) were acquired by means of an interface card (PCL-812 PG from National Instruments) and our own software developed using LabWindows® (Puig *et al.*, 2005). Program commands were transmitted to the pilot plant through the same interface card and a relays output board, which controlled the on/off switch of all electrical devices, thereby allowing a previously defined operational cycle to be repeated over time.
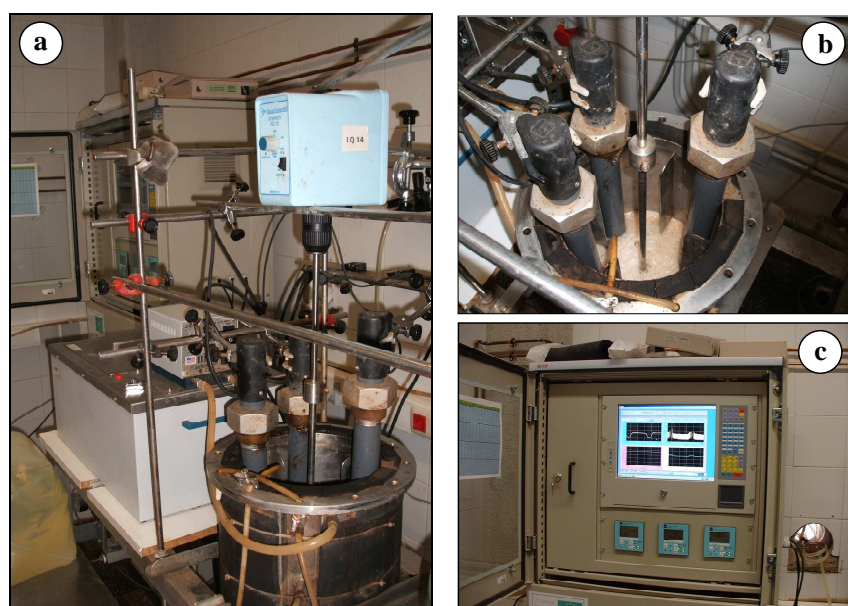
Figure 4.2. Lab-scale pilot plant. a) General view; b) Reactor; c) Control panel

4.3.2 Synthetic feed

The synthetic feed used in this study (Table 4.1) was mainly composed of a mixture of NH_4Cl, $NaHCO_3$, phosphate buffer solution (Puig *et al.*, 2007) and a micronutrient solution (adapted from Dangcong *et al.*, 2000).

Table 4.1 Synthetic wastewater composition

Compound	Formula	Concentration	Solution
Ammonium chloride	NH_4Cl	Variable[*]	Ammonium source
Sodium bicarbonate	$NaHCO_3$	Variable[*]	Alkalinity source
Manganese (II) chloride tetrahydrate	$MnCl_2 \cdot 4H_2O$	$0.19 \text{ mg} \cdot L^{-1}$	
Zinc chloride dehydrate	$ZnCl_2 \cdot 2H_2O$	$0.0018 \text{ mg} \cdot L^{-1}$	Microelement solution
Copper (II) chloride dehydrate	$CuCl_2 \cdot 2H_2O$	$0.022 \text{ mg} \cdot L^{-1}$	
Magnesium sulphate heptahydrate	$MgSO_4 \cdot 7H_2O$	$5.6 \text{ mg} \cdot L^{-1}$	
Iron (III) chloride hexahydrate	$FeCl_3 \cdot 6H_2O$	$0.88 \text{ mg} \cdot L^{-1}$	
Calcium chloride dehydrate	$CaCl_2 \cdot 2H_2O$	$1.3 \text{ mg} \cdot L^{-1}$	
Potassium dihydrogen phosphate	KH_2PO_4	$7.0 \text{ mg} \cdot L^{-1}$	Phosphorus source
Dipotassium hydrogen phosphate	K_2HPO_4	$18 \text{ mg} \cdot L^{-1}$	
Disodium hydrogen phosphate heptahydrate	$Na_2HPO_4 \cdot 7H_2O$	$14 \text{ mg} \cdot L^{-1}$	

[*] concentration dependent on the leachate composition and the percentage of leachate in the feed

Raw leachate was diluted with synthetic feed to progressively acclimate the biomass to the wastewater, as further described in Section 4.3.5. In light of this, ammonium concentration in the synthetic media was calculated based on the dilution of the raw leachate and the desired ammonium concentration in the influent. On the other hand, bicarbonate concentration was defined to keep the same bicarbonate to ammonium molar ratio in the feed than the raw landfill leachate.

4.3.3 Urban landfill leachate

The raw leachate used in this study came from the Corsa urban landfill site (41° 6' 28" N, 1° 7' 4" E; Reus, Catalonia, Spain), and presented a high variability on its composition. The concentration range and mean values of the principal chemical compounds are summarised in Table 4.2.

Table 4.2 Urban landfill leachate characterisation

Compound	Units	Range	Mean ± σ
Ammonium, NH_4^+	$\text{mg N-}NH_4^+ \cdot L^{-1}$	1,346 – 3,149	2,520 ± 523
Nitrite, NO_2^-	$\text{mg N-}NO_2^- \cdot L^{-1}$	0.0 – 17.8	4.9 ± 5.8
Nitrate, NO_3^-	$\text{mg N-}NO_3^- \cdot L^{-1}$	0.0 – 4.8	1.1 ± 1.6
Alkalinity	$\text{mg } HCO_3^- \cdot L^{-1}$	8,156 – 17,894	12,894 ± 2,645
Chemical Oxygen Demand, COD	$\text{mg } O_2 \cdot L^{-1}$	2,880 – 4,860	4,048 ± 376
Biochemical Oxygen Demand, BOD_5	$\text{mg } O_2 \cdot L^{-1}$	114 – 492	338 ± 134
Total Organic Carbon, TOC	$\text{mg C} \cdot L^{-1}$	1,079 – 2,246	1,686 ± 276
Inorganic Carbon, IC	$\text{mg C} \cdot L^{-1}$	688 – 2,399	1,445 ± 329
HCO_3^-:NH_4^+ molar ratio	-	0.56 – 1.95	1.16 ± 0.19
pH	-	8.13 – 9.27	8.68 ± 0.24

4.3.4 Inoculum

The reactor was inoculated using biomass from the Sils-Vidreres wastewater treatment plant (41° 47' 58" N, 2° 45' 7" E; Catalonia, Spain). Sludge was taken from the aerobic tank and washed three times with tap water prior to the inoculation.

4.3.5 Experimental procedure

The experiments focused on assessing the feasibility of achieving partial nitrification in an SBR, and evaluating different strategies and operational conditions. Once these aims had been achieved, an analysis of FA and FNA inhibition and HCO_3^- limitation over AOB was carried out. Finally, efforts were directed at an assessment of process performance with a view to a scaling-up to pilot plant.

4.3.5.1 Operational strategy: fed-batch vs. step-feed

Two separate experiments were carried out, using two different feeding strategies: fed-batch (Run A) and step-feed (Run B). In each run, the reactor was inoculated with nitrifying sludge from the Sils-Vidreres WWTP (10L with a TSS and VSS concentration of 3,400 and 2,200 mgSS·L^{-1} respectively). During the start-up and acclimatising period of each run, the reactor was initially fed with a mixture of synthetic feed and raw urban landfill leachate. The percentage of leachate in the feed was progressively increased to the point where solely urban landfill leachate was being treated. During Run A the reactor was operated using a fed-batch strategy, based on a long feeding phase where influent was supplied continuously (Figure 4.3). The 8 h cycle consisted of an aerobic feeding phase of 360 min, followed by an aerobic reaction phase of 80 min. The aim of this phase was to serve as a safety period. The cycle ended with a settling phase of 15 min and a draw phase of 25 min. During Run B, the PN-SBR was operated using a step-feed strategy (Figure 4.3), also with a cycle length of 8 h. The SBR cycle was composed of 11 aerobic feeding phases of 30 min each (except for the last one of 25 min), followed by aerobic reaction phases of 10 min, then a settling phase of 20 min and a draw phase of 25 min.
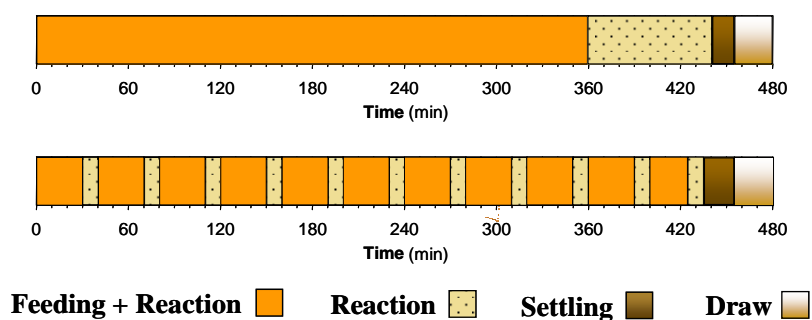
Figure 4.3 Scheme of the cycle design of each strategy

During both runs dissolved oxygen (DO) was controlled at a set-point value of 2 $mgO_2 \cdot L^{-1}$ and the temperature was kept at 36±1 ℃. The reactor was operated with 1–2 days of hydraulic retention time (HRT), maintaining a minimum volume of 9.7 L. Sludge retention time (SRT) ranged from 3 to 7 days (with an average value of around 5 days). The SRT was calculated as depicted in Equation 4.1, taking into account the effluent total suspended solids (TSS) concentration and the mixed liquor suspended solids (MLSS), maintained throughout the entire study at 500–1,000 $mgSS~L^{-1}$ with a volatile fraction of between 66% and 75%.

$$SRT = \frac{V_{max} \cdot MLSS}{Q_{eff} \cdot TSS_{eff}}$$
(Eq. 4.1)

where V_{max} (L) is the maximum volume of the reactor in a certain cycle, and Q_{eff} is the outflow ($L \cdot d^{-1}$).

To avoid FA inhibitory effects, the maximum pH inside the reactor was controlled by means of HCl (1 M) dosage. Based on Equations 3.3 and 3.4 (Anthonisen *et al.*, 1976), a maximum pH set-point was defined as a function of reactor temperature and the total ammonium as nitrogen (TAN), taking the worst scenario (i.e. the TAN concentration inside the reactor being the same as that of influent TAN), and permitting a maximum FA of 8.23 $mgN–NH_3~L^{-1}$ (the lowest value in the AOB activity inhibitory range due to FA, according to Anthonisen *et al.*, 1976). Therefore, the pH set-point was variable during the whole study, and mainly dependent on influent ammonium concentration.

Table 4.3 summarises the main operational parameters of both runs.

Table 4.3 Summary of the main PN-SBR operational conditions during the experimental period

Parameter	Units	Fed-batch	Step-feed
Length of the period	d	250	160
Volumetric exchange ratio (VER)	-	0.16-0.33	0.16-0.33
Hydraulic retention time (HRT)	d	1-2	1-2
Sludge retention time (SRT)	d	3-7	3-7
Total suspended solids (TSS)	$mgTSS \cdot L^{-1}$	500-1,000	500-1,000
Volatile suspended solids (VSS)	$mgVSS \cdot L^{-1}$	300-750	300-750
Nitrogen loading rate (NLR)	$kgN \cdot m^{-3} \cdot d^{-1}$	0.5-1.5	0.5-2

Once a proper and stable operation of the reactor had been achieved, each run was characterised by fixed cycle concentration profiles, where the main physical-chemical parameters along a cycle were monitored.

Finally, the two strategies were compared and evaluated in terms of general performance and from the information obtained in the cycle analyses.

4.3.5.2 Inhibitory effect of FA, FNA, and HCO_3^- limitation on AOB

In order to assess the inhibitory effect of FA and FNA on AOB activity, as well as possible HCO_3^- limitation, experiments based on a stepwise increase in pH (from 6.2 to 8.3, with a step size of 0.1 pH units) were conducted. These experiments, carried out subsequent to the fed-batch run, were performed during the reaction phase with feeding of four different SBR cycles (i.e. from minute 0 to minute 360 of the 8 h cycle). During the experiment, the pH value was automatically controlled with NaOH (1 M) or HCl (1 M) by using an Endress Hausser LIQUISYS M CPM 223/253 controller. At each pH step, after the pH value had been stabilised and the performance of the system was steady, a sample from the SBR was obtained and prepared for analysis of ammonium, nitrite, nitrate and inorganic carbon. Afterwards, the pH set-point was again increased by 0.1 units, repeating the same procedure. Figure 4.4 depicts the pH profile during the feeding phase (360 minutes) of one of the four cycles in which the experiment for the assessment of the inhibitions was carried out.
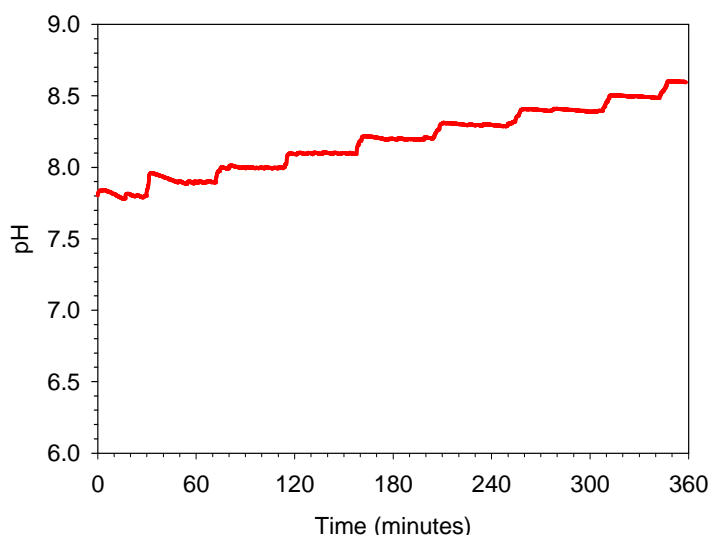
Figure 4.4 pH profile during the feeding phase of a cycle in which the experiment took place

4.3.5.3 Assessment of the process in view of the scale-up

Once the feasibility of achieving partial nitrification in a lab-scale SBR had been evaluated, and the most suitable operational conditions and cycle design identified, efforts were focused on increasing process knowledge with a view to scaling it up. To this end, the reactor was restarted using 10L of sludge from the Sils-Vidreres wastewater treatment plant (SST = 4,360 mgSS·L^{-1}, VSS = 2,770 mgSS·L^{-1}), and operated under the feeding strategy which had yielded the best results (see Section 4.3.5.1).

Table 4.4 summarises the main operational conditions of the PN-SBR in this experiment.

Table 4.4 Main PN-SBR conditions during the process assessment period

Parameter	Units	Value
Length of the period	d	190
Volumetric exchange ratio (VER)	-	0.06-0.10
Hydraulic retention time (HRT)	d	3-6
Sludge retention time (SRT)	d	3-16
Total suspended solids (TSS)	$mgTSS \cdot L^{-1}$	250-400
Volatile suspended solids (VSS)	$mgVSS \cdot L^{-1}$	100-250
Nitrogen loading rate (NLR)	$kgN \cdot m^{-3} \cdot d^{-1}$	0.5-1

During this stage, the assessment of the process was complemented by monitoring of organic matter. In addition, new parameters for the assessment of the reactor's performance were proposed, based on dissolved oxygen: the oxygen uptake rate (OUR, calculated as explained in Section 3.4) and the oxygen consumed (OC, calculated as explained in Section 3.5).

4.4 Results and discussion

This section deals with the feasibility of achieving partial nitritation of the ammonium present in urban landfill leachate, using SBR technology. It also seeks to find a suitable feeding strategy, identify the most important operational parameters and investigate the inhibition of AOB by free ammonia and free nitrous acid. Finally the results of the process performance assessment are presented.

4.4.1 Operational strategy: fed-batch vs. step-feed

The purpose of this section is demonstrate the feasibility of achieving partial nitritation of the ammonium present in urban landfill leachate, using SBR technology, and evaluate two different feeding strategies, fed-batch and step-feed, for the operation of the reactor.

4.4.1.1 Fed-batch strategy

The PN-SBR reactor was started up on a fed-batch strategy (Figure 4.3), being fed with synthetic media for a week (data not shown). After this short start-up period, the reactor was fed with a mixture of synthetic feed and landfill leachate. The percentage of leachate in the feed was progressively increased in order to acclimatise the bacteria to the raw leachate.

Figure 4.5 shows the evolution of influent ammonium and the nitrogen loading rate (NLR; $kgN \cdot m^{-3} \cdot d^{-1}$) (Figure 4.5a), and effluent ammonium, nitrite and nitrate concentrations (Figure 4.5b).

The influent ammonium concentration was progressively increased, until it reached 1,474 mg $N-NH_4^+ \cdot L^{-1}$ on day 167. Concentrations of nitrite and nitrate in the influent were negligible, as shown in Table 4.2. The NLR initially applied to the system was 0.35 $kgN \cdot m^{-3} \cdot d^{-1}$, rising to 1.1 $kgN \cdot m^{-3} \cdot d^{-1}$. In terms of the concentration of nitrogen compounds in the effluent, Figure 4.5b shows that during this period ammonium was partly converted to nitrite, without any significant further oxidation to nitrate. Ammonium and nitrite concentration started to increase from day 0, until it reached concentrations of 729 and 610 $mgN \cdot L^{-1}$ respectively on day 167. Effluent nitrate concentration that day was 5.2 $mgN-NO_3^- \cdot L^{-1}$.
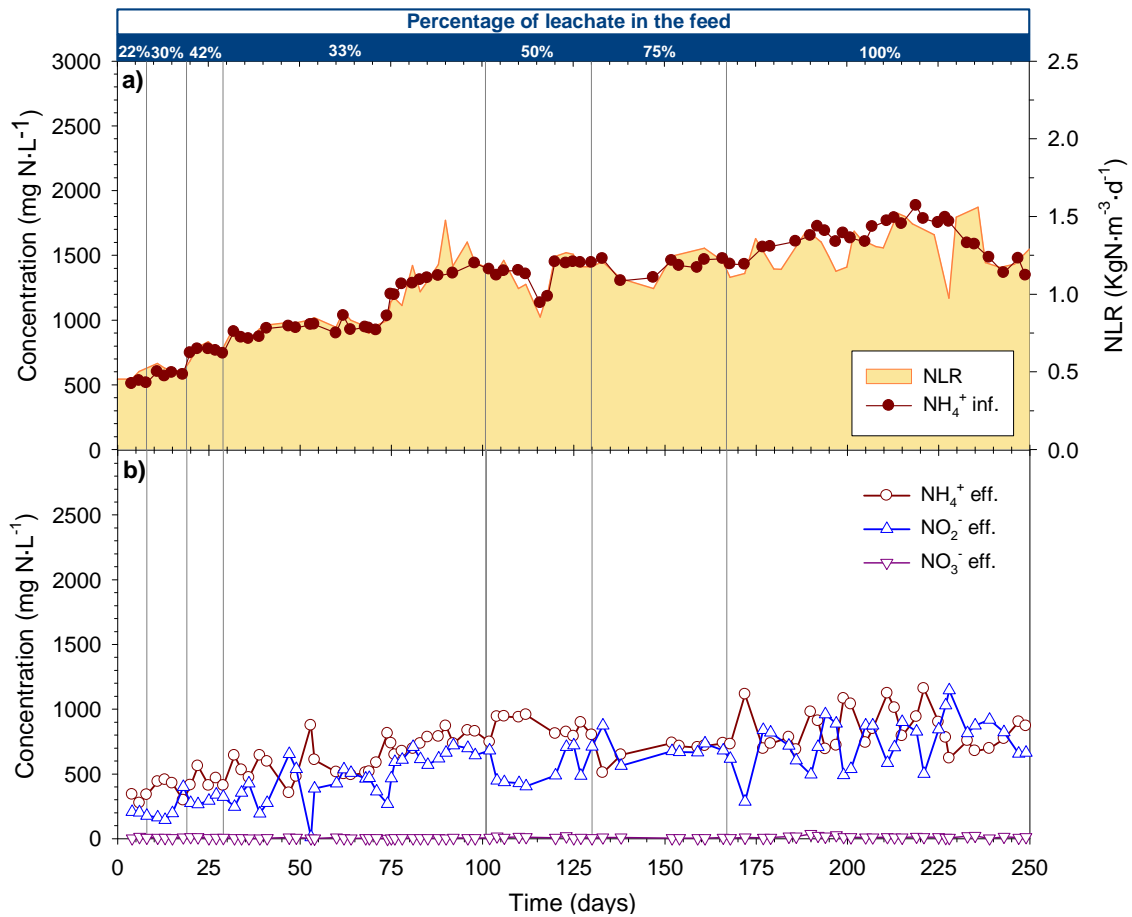
Figure 4.5 Evolution of the PN-SBR using a fed-batch strategy a) Influent ammonium concentration and NLR; b) Effluent nitrogen compounds

For the next 83 days, during which raw urban landfill leachate only was supplied to the system, the NLR was kept at around 1.25, ranging from 0.97 to 1.56 $kgN \cdot m^{-3} \cdot d^{-1}$. The influent ammonium concentration was kept about 1,500 $mgN-NH_4^+ \cdot L^{-1}$. On the other hand, the effluent concentration of ammonium and nitrite during this period fluctuated between 750-1,000 $mgN-NH_4^+ \cdot L^{-1}$ and 500-750 $mgN-NO_2^- \cdot L^{-1}$ respectively, indicating that the desired partial nitritation had been achieved. Furthermore, the nitrate concentration remained close to zero.

The bicarbonate concentration in the influent and effluent was also assessed throughout the entire period, and is shown in Figure 4.6. As can be seen from the graph, influent bicarbonate concentration rose continuously during the first 167 days, starting from 2,500 $mgHCO_3^-\cdot L^{-1}$ and rising to about 10,000 $mgHCO_3^-\cdot L^{-1}$. This augmentation was due to the progressive increase of leachate in the feed. From day 167, bicarbonate concentration remained at this level. In contrast, bicarbonate in the effluent was almost negligible throughout the study. This showed that the majority of the bicarbonate supplied was always removed from the system.
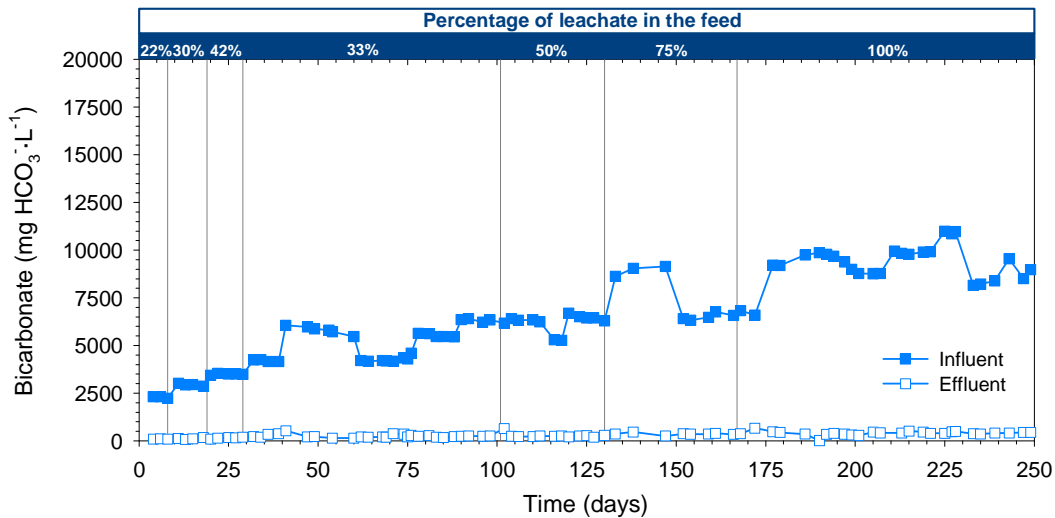
Figure 4.6 Evolution of bicarbonate concentration in the influent and effluent of a PN-SBR using a fed-batch strategy

In terms of process performance, Figure 4.7 shows the nitrogen compound effluent speciation. The orange and green dashed-dotted lines have been included in the graph to serve as a reference for the ideal nitrite and ammonium speciation for an anammox reactor (57% of NO_2^- and 43% of NH_4^+ respectively).
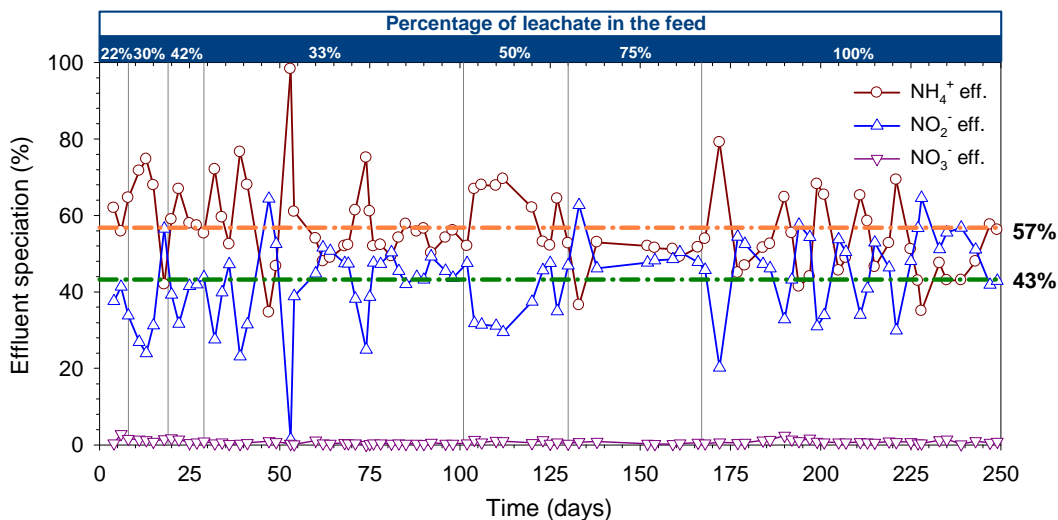
Figure 4.7 Evolution of the nitrogen compound effluent speciation on a fed-batch strategy

42

As depicted in Figure 4.7, nitritation efficiency between 30% and 55% was reached during the majority of the fed-batch operation, with a very low percentage of nitrate production (i.e. less than 2%). These results clearly point to significant fluctuations in the process performance, mainly due to changes in raw leachate and NLR. However, stable performance was recovered after a period of stable influent composition, and the percentage of nitritation evolved to 40–55%. This effect was possibly related to the AOB's slow response to an increasing loading rate. Finally, it is important to note that the fluctuations in the process performance during the period in which only leachate was being fed led to an average nitrite to ammonium molar ratio of 0.94, slightly lower than the stoichiometry of the anammox process.

With regards to on-line parameter behaviour, Figure 4.8 depicts the evolution of pH, DO, ORP and T along three typical 8-hour cycles corresponding to day 198. It must be emphasised that the initial conditions of each cycle are dependent on the end conditions of the previous one.
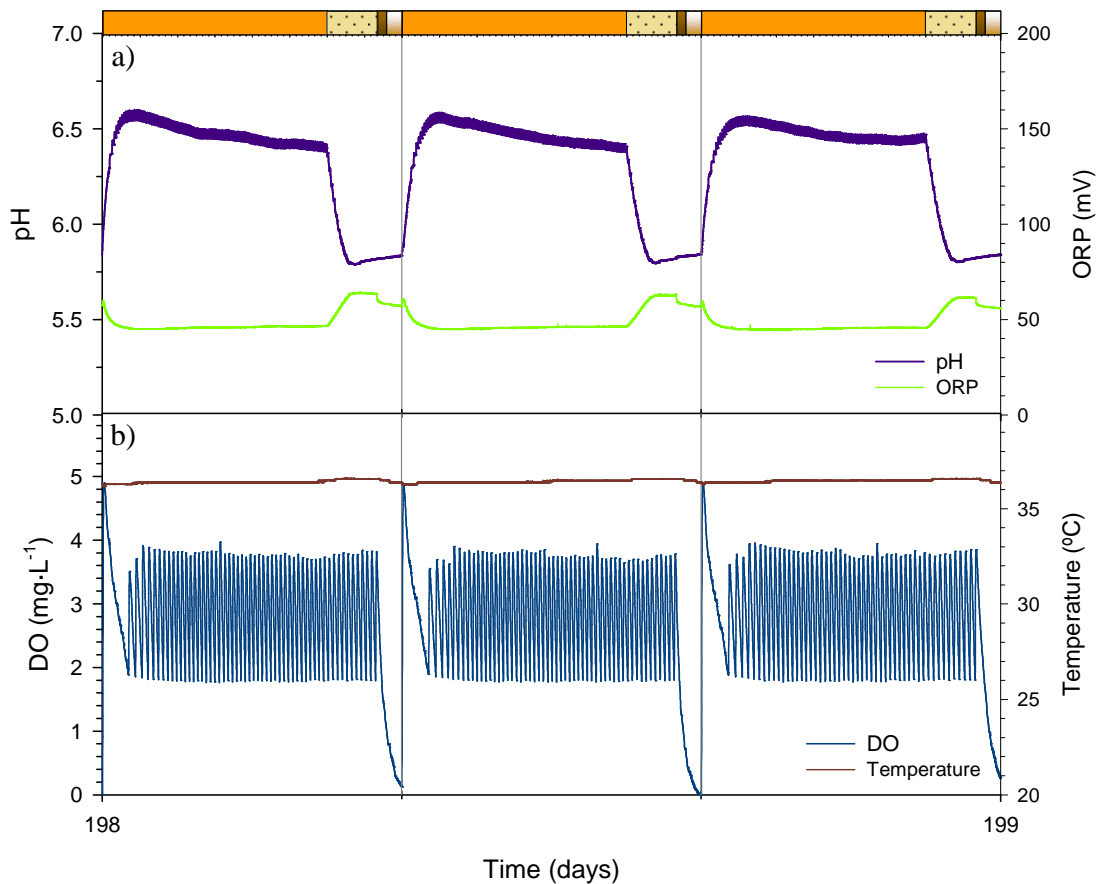
Figure 4.8 Evolution of the main on-line parameters along a day on the fed-batch strategy a) pH and ORP; b) DO and T

Figure 4.8a shows that pH at the beginning of the cycle was very low, around 5.8. However, when the feeding event started, pH quickly increased until it reached a value of 6.6. After that, it stabilised at around 6.5 for the entire feeding phase, since H^+ production by nitritation was

balanced by the alkalinity supplied by the leachate. However, during the aerobic reaction phase, pH plummeted to values lower than 6 because of nitrifying activity and the low buffer capacity of the system. The ORP profile was always higher than 50 mV, with slightly higher values during the reaction phases. Dissolved oxygen values ranged from 2 to 4 $mgO_2 \cdot L^{-1}$ due to the rough on/off control, except in the settling and draw phases when the DO plummeted to 0. The temperature during these cycles was around 36.5°C, and slightly higher during the reaction phases. Finally it is important to notice that on-line parameter values may vary depending on the influent composition, NLR and process conversions, among other factors. Nevertheless, they can be a good indicator of reactor performance.

In order to study the process in more detail, the dynamics of the main physical-chemical parameters were monitored over an 8-hour cycle. Table 4.5 summarises the main characteristics of the influent in this specific cycle.

Table 4.5 Main influent characteristics in the fed-batch cycle profile analysis

Parameter	Units	Value
Ammonium, NH_4^+	$mgN\text{-}NH_4^+ \cdot L^{-1}$	1,761
Nitrite, NO_2^-	$mgN\text{-}NO_2^- \cdot L^{-1}$	5.8
Nitrate, NO_3^-	$mgN\text{-}NO_3^- \cdot L^{-1}$	0.0
Alkalinity	$mgHCO_3^- \cdot L^{-1}$	11,512
Chemical Oxygen Demand, COD	$mgO_2 \cdot L^{-1}$	4,007
Biochemical Oxygen Demand, BOD_5	$mgO_2 \cdot L^{-1}$	492
Total Organic Carbon, TOC	$mgC \cdot L^{-1}$	1,892
Inorganic Carbon, IC	$mgC \cdot L^{-1}$	1,768
pH	-	8.67

The cycle profile for the fed-batch operational strategy is presented in Figure 4.9. In spite of continuous influent feeding, the ammonium and nitrite concentrations inside the PN-SBR remained almost constant (650 $mgN\text{-}NH_4^+ \cdot L^{-1}$ and 1,120 $mgN\text{-}NO_2^- \cdot L^{-1}$) throughout the whole cycle (Fig. 4.9a), indicating that the ammonium was oxidised at the same time it was supplied by the influent flow. It was expected that, during the aerobic reaction phase without filling (i.e. minutes 360–440), ammonium concentration would decrease and nitrite would increase due to the nitritation process. However, analytical data showed slight changes in nitrogen species concentrations. The inorganic carbon (IC, $mgC \cdot L^{-1}$) profile during the cycle was quite different from the nitrogen species profile. Initially, the IC increased slightly until minute 60. It remained stable at around 30 $mgC \cdot L^{-1}$, until the reaction phase without filling, when the concentration quickly diminished to values near zero due to alkalinity consumption by the high ammonium oxidation. The reduction in IC during this final reaction phase without filling was 24 $mgC \cdot L^{-1}$, corresponding to a production of 14 $mgN\text{–}NO_2^- \ L^{-1}$, which cannot be identified because of the graph's scale. In addition, the possibility of IC loss due to CO_2 stripping cannot be discounted.

44
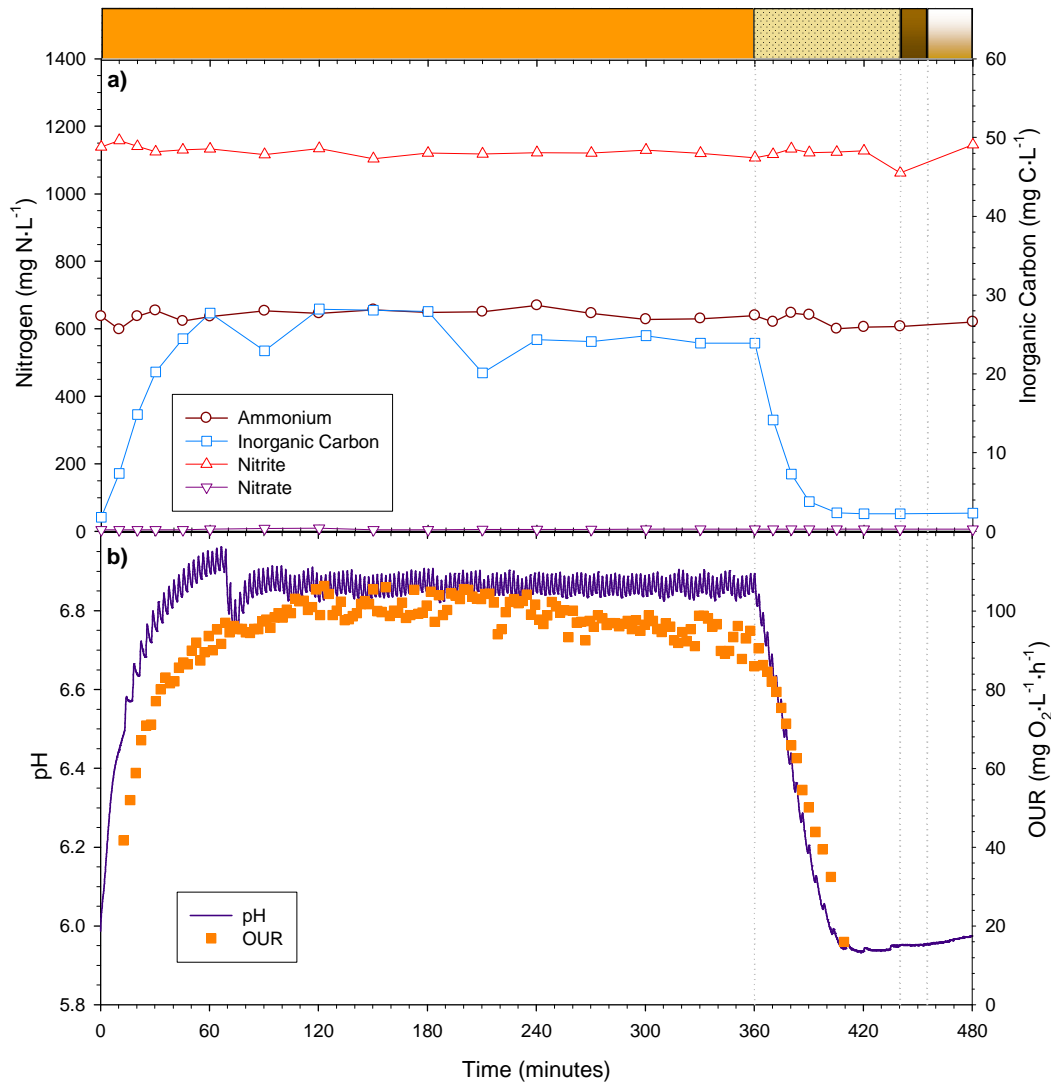
Figure 4.9 Cycle profile evolution of the main physical-chemical parameters over an 8h SBR fed-batch cycle. a) Ammonium, nitrite, nitrate and inorganic carbon concentrations; b) pH and oxygen uptake rate (OUR)

From the pH profile (which has a shape similar to that of the IC profile), it can be seen that during the first 60 min the pH increased to 6.9, which was when the maximum pH set-point was reached and controlled. From about minute 75, the increase on pH due to the OH⁻ supply from the feed was balanced by the proton production, and the pH value stabilised. Later, during the reaction phase, the pH plummeted to values lower than 6 because of nitrifying activity, and the consumption of IC.

The OUR indicated the biological activity in the reactor, which increased sharply during the first 60 min, at which point it stabilised. It then remained at its maximum values (100–110 mgO$_2$·L^{-1}·h^{-1}), until minute 360. In terms of the reaction phase without filling, the OUR decreased, following a similar trend to those of the pH and IC concentrations. From these

observations it can be concluded that biological activity reduction may be related to inhibition factors regulated by pH and/or IC limitation.

4.4.1.2   Step-feed strategy

Once the fed-batch run had finished, the PN-SBR reactor was started up again using seed sludge from the Sils-Vidreres WWTP. The same procedure was followed, but a step-feed strategy was applied. After a short start-up period, the reactor was fed with a mixture of synthetic and real wastewater. Then, after the acclimation period, raw urban landfill leachate was supplied. Next is presented the performance of the reactor for the 160 days during which this second run lasted. Figure 4.10 depicts the evolution of influent and effluent nitrogen compounds, and the NLR, during this second run.
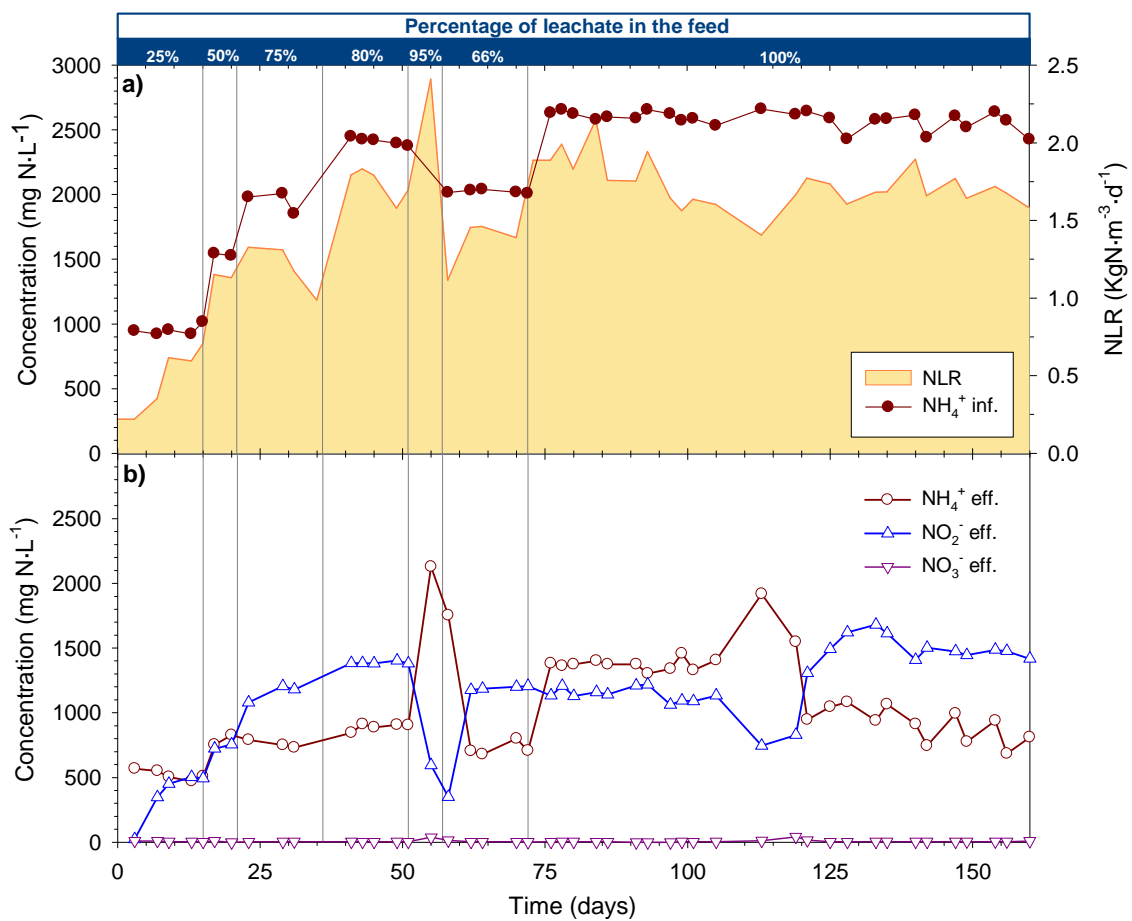
Figure 4.10 Evolution of the PN-SBR on a step-feed strategy a) Influent ammonium concentration and NLR; b) Effluent nitrogen compounds

Influent ammonium at the beginning of this experiment was 1,000 mgN-NH$_4^+$·L^{-1} (see Figure 4.10a). It was progressively increased up to 2,600 on day 75 by increasing the proportion of leachate in the feed. At this point the feed was solely composed of leachate, and ammonium remained at the same level until the end of the run (day 160). The progressive acclimation to the leachate meant an increase in the nitrogen loading rate from 0.25 to 1.8 kgN·m^{-3}·d^{-1} during the

46

first 72 days, with problems only being encountered on day 51 due to an overloading of the system. Once raw leachate feeding had been achieved (days 72-160), the NLR was kept at between 1.5 and 2 $kgN·m^{-3}·d^{-1}$.

During the early days of this run, nitrite started to build up, without any nitrate production (Figure 4.10b). Ammonium and nitrite concentrations increased progressively, reaching concentrations of 800 $mgN-NH_4^+·L^{-1}$ and 1,300 $mgN-NO_2^-·L^{-1}$ by day 72. From that day on, the system performed well, and changes in the effluent ammonium and nitrite concentrations were linked to the raw leachate's characteristics, achieving concentrations on day 160 of 811 $mgN-NH_4^+·L^{-1}$ and 1,417 $mgN-NO_2^-·L^{-1}$ respectively.

With regard to the inorganic carbon, Figure 4.11 shows the evolution of influent and effluent bicarbonate during the 160-day period.
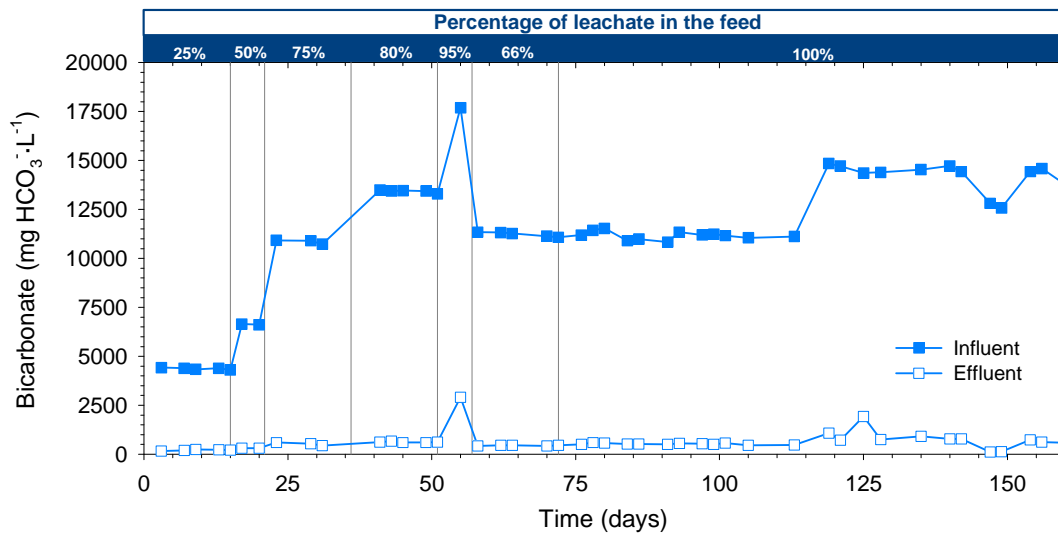
Figure 4.11 Evolution of bicarbonate concentration in the influent and effluent of the PN-SBR on a step-feed strategy

Influent bicarbonate was raised quickly in accordance with influent ammonium concentrations. However, on day 57 the NLR was decreased due to the reactor's poor nitritation performance. This was done by decreasing the percentage of leachate, which resulted in a decrease in the bicarbonate to 11,000 $mgHCO_3^-·L^{-1}$. This concentration was kept fairly constant until day 119 when it was increased to 15,000 $mgHCO_3^-·L^{-1}$. With regards to the effluent, bicarbonate concentrations were very low, although slight accumulations were detected in days 51-56 due to the increase in the influent concentration and the low nitritation performance, and on days 119-130 when it accumulated due to the high bicarbonate concentration in the influent.

Figure 4.12 shows the effluent speciation of the nitrogen compounds. Orange and green dashed-dotted lines have been included in the graph to serve as a reference for the ideal speciation of, respectively, nitrite (57% of NO_2^-) and ammonium (43 of %NH_4^+).
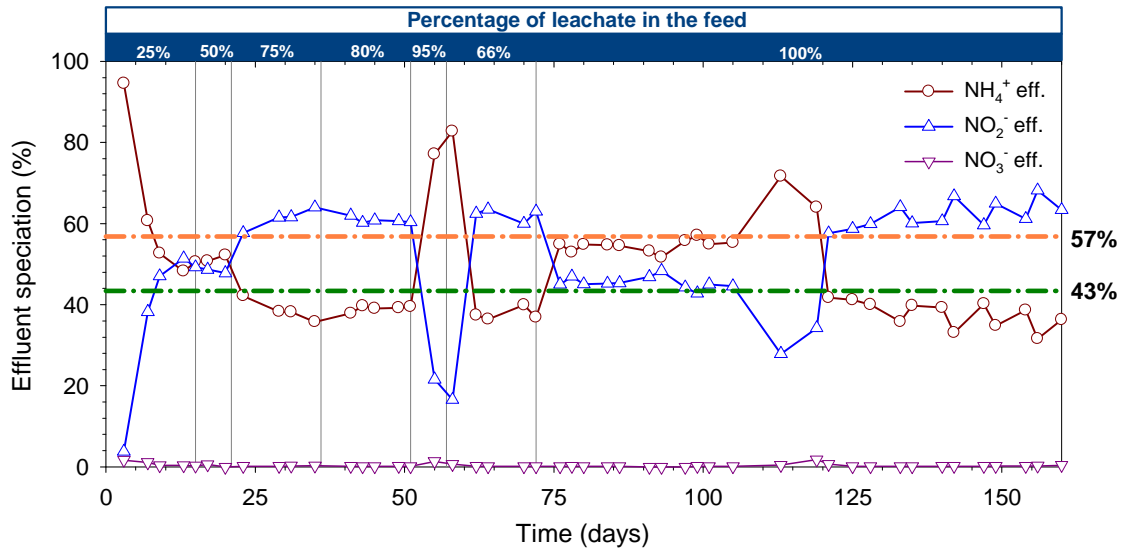
Figure 4.12 Evolution of the nitrogen compounds effluent speciation on a step-feed strategy

As depicted in the graph, the percentage of nitrite in the effluent increased quickly during the first 15 days, until it stabilised at around 45%. Over the next 30 days, nitritation was enhanced, leading to conversions slightly higher than the stoichiometric. With regards to nitrate, there was initially a percentage of 3%, but this rapidly plummeted to values around 0. On day 51 a loading shock ended up on a loss of activity, which led to a sudden decrease in the effluent's nitrite content. Once AOB activity had recovered, nitrite build-up was restored. From day 120 on, the higher bicarbonate concentration in the influent conducted to higher conversions, with an effluent speciation of about 60% of NO_2^- and 40% of NH_4^+. Finally it is important to point out that there were very few fluctuations in effluent speciation, indicating a high level of process stability. This issue is examined further in Section 4.4.1.3.

On-line parameters were also monitored during the step-feed strategy. Figure 4.13 summarises the evolution of pH, ORP, DO and temperature on day 80 of the step-feed operation. The pH followed an increase/decrease pattern, linked to the feeding events: pH increased when leachate was supplied and decreased during reaction phases as a result of proton production. ORP presented values of around 70 mV, with fluctuations caused by the feeding pattern. Figure 4.13b shows that DO was controlled within a suitable range (always above 2mg·L^{-1}), except in the settling and draw phases. To conclude with the analysis of on-line profiles, temperature – also depicted in Figure 4.13.b – presented values around 37ºC, decreasing slightly during the settling and draw events.
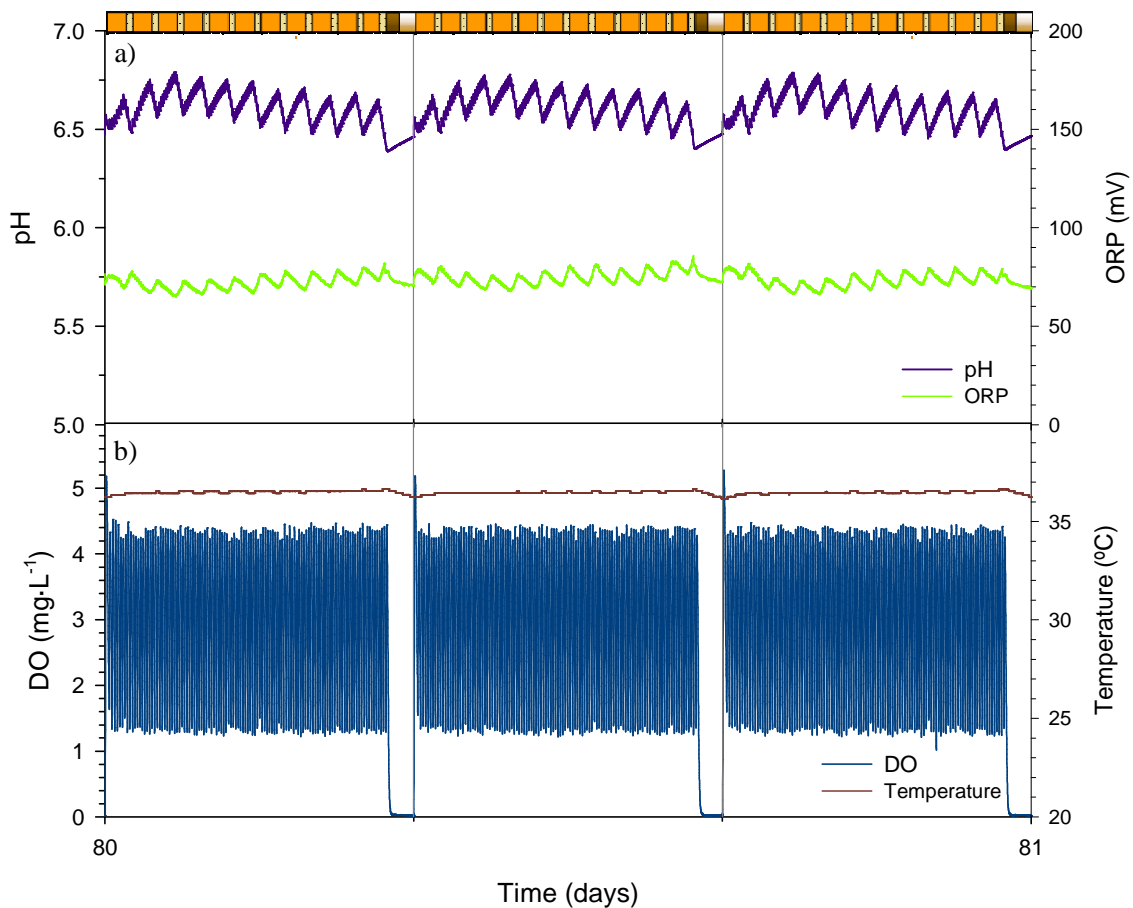
Figure 4.13 Evolution of the main on-line parameters along a day on the step-feed strategy. a) pH and ORP; b) DO and T

A cycle profile analysis for the step-feed strategy was also performed, in order to make it possible to study the process dynamics in more detail. The main characteristics of the influent raw leachate are summarised in Table 4.6, while the profile of the main physical-chemical parameters is shown in Figure 4.14.

Table 4.6 Main influent characteristics in the step-feed cycle profile analysis

Compound	Units	Step-feed
Ammonium, NH_4^+	$mgN\text{-}NH_4^+\cdot L^{-1}$	2,009
Nitrite, NO_2^-	$mgN\text{-}NO_2^-\cdot L^{-1}$	0.3
Nitrate, NO_3^-	$mgN\text{-}NO_3^-\cdot L^{-1}$	3.5
Alkalinity	$mgHCO_3^-\cdot L^{-1}$	11,437
Chemical Oxygen Demand, COD	$mgO_2\cdot L^{-1}$	3,053
Biochemical Oxygen Demand, BOD_5	$mgO_2\cdot L^{-1}$	377
Total Organic Carbon, TOC	$mgC\cdot L^{-1}$	1,085
Inorganic Carbon, IC	$mgC\cdot L^{-1}$	1,863
pH	-	8.84
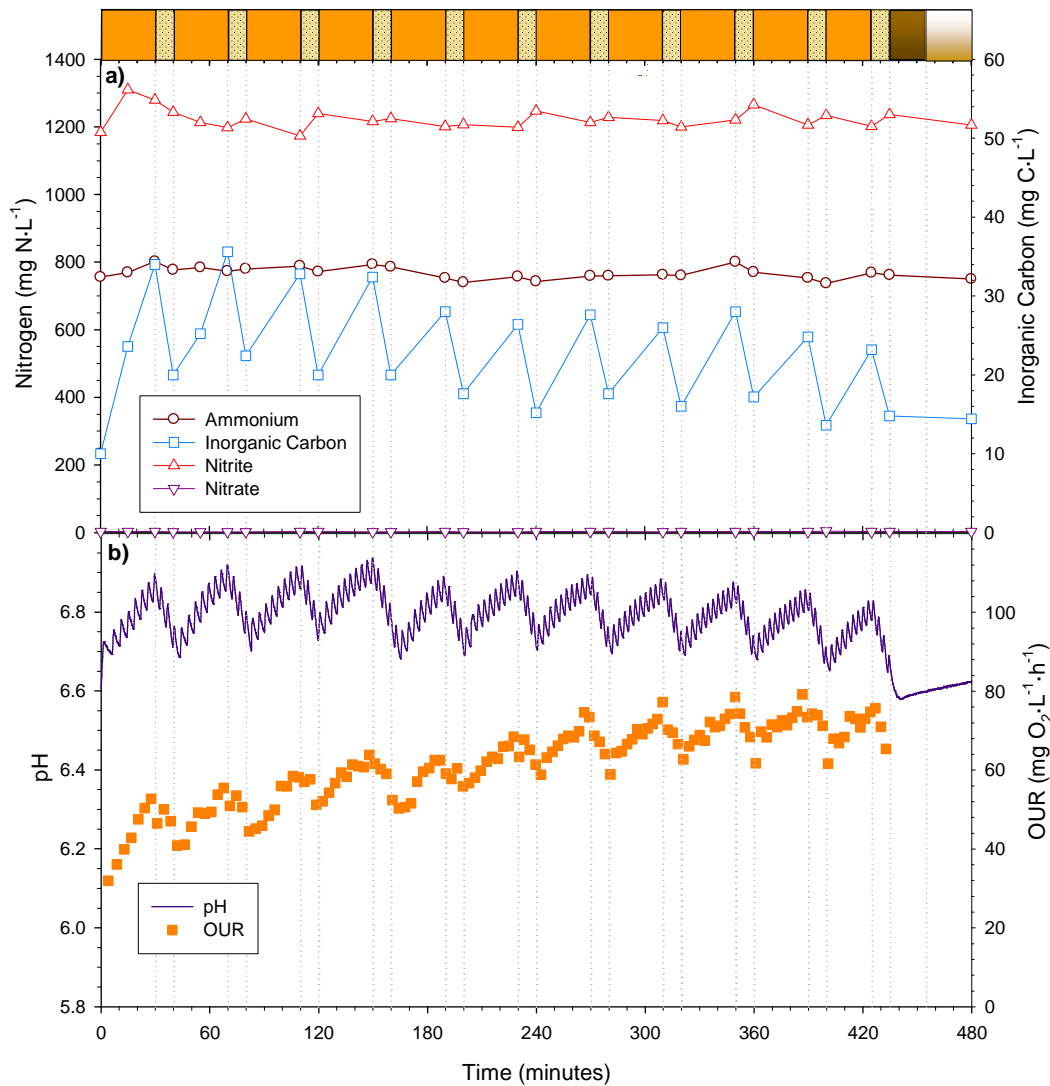
Figure 4.14 Cycle profile evolution of the main physical-chemical parameters over an 8h SBR step-feed cycle. a) Ammonium, nitrite, nitrate and inorganic carbon concentrations; b) pH and oxygen uptake rate (OUR)

Figure 4.14a shows the evolution of nitrogen compounds and inorganic carbon. From the plot it can be seen that NH_4^+ and NO_2^- concentrations remained stable over the cycle at around 750 $mgN-NH_4^+L^{-1}$ and 1,200 $mgN-NO_2^-L^{-1}$, with no nitrate production. However, there were slight variations in the compounds (barely noticeable due to the scale) linked to the feeding strategy. IC concentration at the beginning of the cycle was 11 $mgC \cdot L^{-1}$. During the feeding phases, the concentration inside the reactor increased slightly to values of about 25–30 $mgC \cdot L^{-1}$ due to the high bicarbonate concentration in the influent. Nevertheless, the IC levels decreased during the aerobic reaction phases without filling, as a result of high ammonium oxidation activity. pH (Figure 4.14b) followed the same trend as IC, remaining between 6.7 and 6.9 over the entire cycle, but increasing during the feeding phases (because of the higher pH of the influent), and decreasing during the reaction phases (due to nitritation activity). In the same figure it can also be seen that there was an increase/decrease pattern linked to pH and IC levels in the OUR plot.

However, the overall trend of the OUR profile was one of a progressive increase throughout the cycle until stabilisation, at minutes 250–300, at about 80 $mgO_2 \cdot L^{-1} \cdot h^{-1}$.

4.4.1.3 Comparison of the feeding strategies

Two different feeding strategies (fed-batch and step-feed) were applied to the PN-SBR process. The general performance results show that both strategies allowed the partial nitritation SBR to perform properly: stable partial nitrite build-up was reached in both operating periods. Nevertheless, the experimental results also indicate that the two feeding strategies yielded different reactor performances and process dynamics. In order to visually evaluate the efficacy of each strategy, the theoretical NO_2^-:NH_4^+ effluent molar ratio (calculated from ammonium and bicarbonate at the influent, in accordance with the AOB stoichiometry) was plotted, together with the experimental ratio. In addition, the loss of bicarbonate by stripping was quantified on the basis of mass balances, neglecting inorganic carbon assimilated for cell growth.

$$HCO_{3\ inf}^- = HCO_{3\ AOB}^- + HCO_{3\ eff}^- + HCO_{3\ stripping}^- \qquad \textbf{(Eq. 4.2)}$$

where $HCO_{3\ inf}^-$ is the concentration of bicarbonate at the influent ($mole \cdot L^{-1}$), $HCO_{3\ AOB}^-$ is the amount of bicarbonate used to balance the proton produced by ammonium oxidation ($mole \cdot L^{-1}$), $HCO_{3\ eff}^-$ is the effluent bicarbonate concentration ($mole \cdot L^{-1}$) and $HCO_{3\ stripping}^-$ is the amount of bicarbonate lost from the system and non-used for ammonium oxidation buffering ($mole \cdot L^{-1}$).

Assuming that two moles of bicarbonate are needed to balance the protons produced from the oxidation of one mole of ammonium (Equation 1.5), the amount of bicarbonate lost from the system can be quantified as:

$$HCO_{3\ stripping}^- = HCO_{3\ inf}^- - 2 \cdot NH_{4\ AOB}^+ - HCO_{3\ eff}^- \qquad \textbf{(Eq. 4.3)}$$

where $NH_{4\ AOB}^+$ accounts for the ammonium oxidised ($mole \cdot L^{-1}$).

These findings are presented in Figures 4.15 and 4.16 for the fed-batch and the step-feed strategies respectively.

From a visual comparison of the general performance of the PN-SBR under the two feeding strategies (Figure 4.15a and Figure 4.16a) it can be concluded that, in general terms, the step-feed strategy performed better, since the effluent molar ratio was closer to the theoretical than that of the fed-batch. In addition, the step-feed strategy resulted in a more stable performance, because fewer fluctuations in the effluent composition were detected (Figure 4.10b compared to Figure 4.5b).
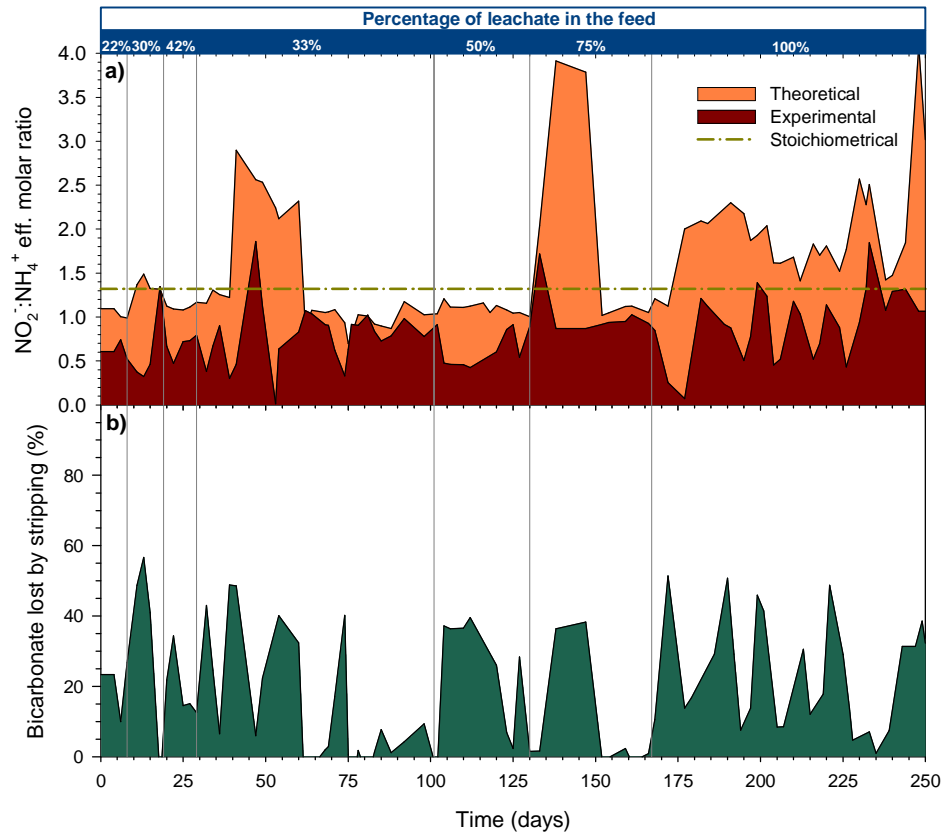
Figure 4.15 Fed-batch operation. a) Theoretical and experimental NO_2^-:NH_4^+ effluent molar ratio; b) Bicarbonate lost by stripping
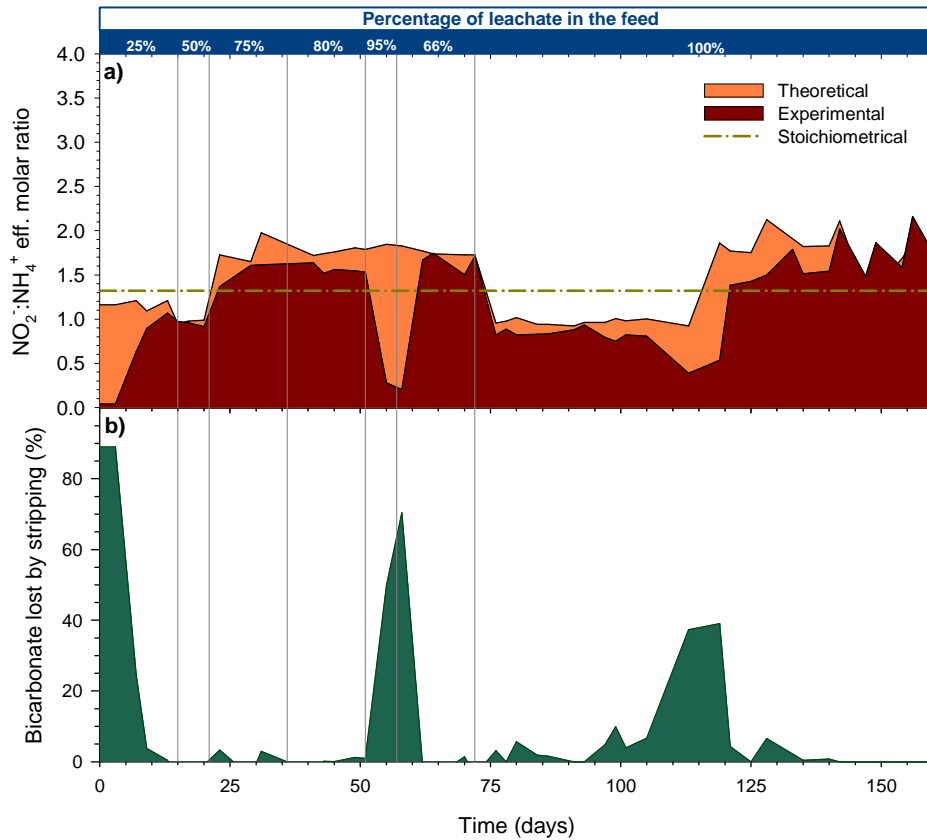
Figure 4.16 Step-feed operation. a) Theoretical and experimental NO_2^-:NH_4^+ effluent molar ratio; b) Bicarbonate lost by stripping

Since the majority of the bicarbonate was always removed from the system independently of process effectiveness, it was expected that a significant amount of bicarbonate would be lost by stripping when the PN-SBR underperformed. Figures 4.15b and 4.16b provide a rough estimation of this bicarbonate loss for the fed-batch and step-feed strategies respectively. As can be seen, there was significant HCO_3^- elimination linked to the stripping process in the fed-batch operation, which at certain moments was about 45-50% of the total HCO_3^- in the influent. In contrast, Figure 4.16b shows that the loss of HCO_3^- was much lower in the step-feed strategy, and was mainly evident during periods of process underperformance.

In order to quantify this observation, the average relative deviation (ARD; Equation 4.4) between the theoretical and observed process performance was calculated for both runs. For this calculation only the period treating raw urban landfill leachate was taken into account.

$$ARD = \frac{1}{n}\sum_{i=1}^{n}\left(\frac{\left|X_{i,theo} - X_{i,\exp}\right|}{X_{i,teo}}\right)$$

(Eq. 4.4)

where $X_{i,theo}$ is the theoretical value of the stoichiometry, and $X_{i,exp}$ is the experimental value.

The results revealed that when operating the reactor under a fed-batch strategy (SF), the PN-SBR presented an important underperformance, with an average relative deviation of 40.9%. On the contrary, the step-feed operation (SF) yielded a lower ARD of 14.1%, which meant that the performance was very close to the theoretical.

The reason for the better performance of the step-feed strategy may be found through cycle profile analysis. When the fed-batch strategy was used, there were significant pH variations in the reactor at the beginning and end of the cycle. From the cycle representation depicted in Figure 4.9, it can be seen that the average pH was 6.65 ± 0.35 and the lowest pH value reached was 5.95. This low pH led to FNA inhibition and a significant loss of IC by stripping. The fed-batch strategy could be improved in this respect by reducing the length of the aerobic reaction phase. In contrast, when the step-feed strategy was used, pH values remained more stable throughout the cycles. Despite the increase/decrease pattern, the average pH was 6.77 ± 0.07, with minimum values of 6.7. The loss of bicarbonate by CO_2 stripping was minor and inhibition of AOB by FNA was much lower.

4.4.2 Inhibitory effect of FA, FNA, and HCO_3^- limitation over AOB

During the feeding phase of four different SBR cycles, an experiment was carried out to assess the effect of free ammonia (FA), free nitrous acid (FNA) and HCO_3^- limitation on AOB activity, by staggerly increasing the pH. OUR values, NH_4^+, NO_2^- and IC concentrations were monitored

throughout the experiment. Non-ionic species concentration, FA and FNA, was calculated based on Anthonisen *et al.* (1976) (see Section 3.2 for further details), while HCO_3^- concentration was calculated from the carbonate-bicarbonate equilibrium, taking into account temperature and pH (see Section 3.3). The results of this experiment are presented in Figure 4.17.
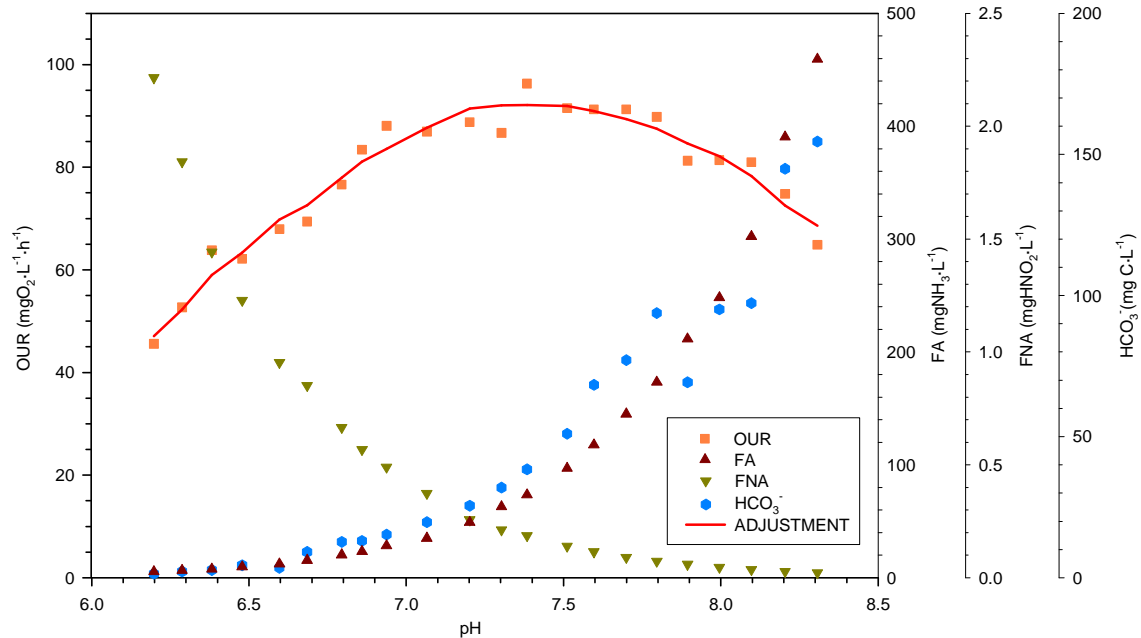
Figure 4.17 Evolution of oxygen uptake rate (OUR), free ammonia (FA), free nitrous acid (FNA) and bicarbonate (HCO_3^-) at different reactor pH, and the adjustment curve

Analyzing the results, AOB activity seemed to be reduced by FA inhibition at high pH, and by FNA inhibition and bicarbonate limitation at low pH. Nevertheless, AOB activity reduction due to the direct effect of pH may also took place at very high/low pH values (above 8 or below 6.5). From Figure 4.17 it can also be seen that OUR were at its maximum in the pH range 7 - 7.7.

In order to study the results in more depth and quantify the inhibitory effects and bicarbonate limitation, the experimental data was fitted to a kinetic model. In the literature, several authors (Carrera, 2001; Magrí *et al.*, 2007; Pambrun *et al.*, 2006) have assumed a Haldane kinetic to be the most suitable model to describe FA inhibition of AOB, since it takes into account the double effect of FA as a substrate and an inhibitor. However, a non-competitive reversible inhibition (NOCRI) term can also be used (Wett and Rauch, 2003; van Hulle *et al.,* 2007). Also a NOCRI term has usually been considered suitable to model FNA inhibition over AOB (Hellinga *et al.*, 1998; Wett and Rauch, 2003; van Hulle *et al.,* 2007; Pambrun *et al.*, 2006). Wett and Rauch (2003) proposed a Sigmoidal function to model the effect of growth reduction due to HCO_3^- limitation. Guisasola *et al.* (2007) also studied this issue and considered other possible kinetic expressions apart from the Sigmoidal term, such as a Monod growth term.

54

Table 4.7 summarises a wide variety of kinetic expressions which could be used for the modelling of free ammonia and free nitrous acid inhibition, together with bicarbonate substrate limitation.

Table 4.7 Summary of kinetic expressions

Compound	Kinetic	Kinetic expressions	References
FA	NOCRI	$v_{limited} = v \cdot \dfrac{k_{I,FA}}{k_{I,FA} + FA}$	Wett and Rauch (2003) van Hulle *et al.* (2007)
	Haldane	$v_{limited} = v \cdot \dfrac{FA}{k_{FA} + FA + \dfrac{FA^2}{k_{I,FA}}}$	Carrera (2001) Magrí *et al.* (2007) Pambrun *et al.* (2006)
FNA	NOCRI	$v_{limited} = v \dfrac{k_{I,FNA}}{k_{I,FNA} + FNA}$	Hellinga *et al.* (1998) Wett and Rauch (2003) van Hulle *et al.* (2007) Pambrun *et al.* (2006)
HCO_3^-	Monod	$v_{limited} = v \dfrac{HCO_3^-}{k_{HCO_3^-} + HCO_3^-}$	Guisasola *et al.* (2007)
	Sigmoidal	$v_{limited} = v \cdot \dfrac{e^{((HCO_3^- - k_{HCO_3^-})/a)}}{e^{((HCO_3^- - k_{HCO_3^-})/a)} + 1}$	Wett and Rauch (2003) Guisasola *et al.* (2007)

where $v_{limited}$ is the observed activity, v is the maximum activity, $k_{I,FA}$ the inhibition constant for NH_3 ($mgNH_3 \cdot L^{-1}$), FA the calculated NH_3 concentration ($mgNH_3 \cdot L^{-1}$), k_{FA} the substrate half saturation constant for NH_3 ($mgNH_3 \cdot L^{-1}$), $k_{I,FNA}$ the inhibition constant for HNO_2 ($mgHNO_2 \cdot L^{-1}$), and FNA the calculated HNO_2 concentrations ($mgHNO_2 \cdot L^{-1}$). HCO_3^- is the bicarbonate concentration ($mgC \cdot L^{-1}$), $k_{HCO_3^-}$ the half-saturation constant for the HCO_3^- ($mgC \cdot L^{-1}$), and a a kinetic constant.

Among the expressions for modelling FA inhibition, a non-competitive reversible inhibition term was chosen in this experiment because when the substrate is not limiting, the Haldane model becomes mathematically equal to the NOCRI. However, it was decided to consider both possible kinetics for the bicarbonate substrate limitation.

OUR can be understood as a measure of AOB activity, but this is only true if the contribution of heterotrophic metabolism to the oxygen consumption is negligible. This is a plausible assumption if the low biodegradable organic matter content of the leachate is taken into account. Therefore, two different kinetic models (Equation 4.5 and 4.6) were fitted to the experimental data:

$$OUR_{obs} = OUR_{obs}^{max} \cdot \frac{k_{I,FA}}{k_{I,FA} + FA} \cdot \frac{k_{I,FNA}}{k_{I,FNA} + FNA} \cdot \frac{e^{((HCO_3^- - k_{HCO_3^-})/a)}}{e^{((HCO_3^- - k_{HCO_3^-})/a)} + 1} \qquad \textbf{(Eq. 4.5)}$$

$$OUR_{obs} = OUR_{obs}^{max} \cdot \frac{k_{I,FA}}{k_{I,FA} + FA} \cdot \frac{k_{I,FNA}}{k_{I,FNA} + FNA} \cdot \frac{HCO_3^-}{k_{HCO_3^-} + HCO_3^-} \qquad \textbf{(Eq. 4.6)}$$

where OUR_{obs} is the observed OUR ($mgO_2 \cdot L^{-1} \cdot h^{-1}$) and OUR_{obs}^{max} the theoretical maximum OUR value ($mgO_2 \cdot L^{-1} \cdot h^{-1}$),

The results of both adjustments are summarised in Table 4.8.

Table 4.8 Results of the adjustment for the two kinetics

Kinetic model	r^2	$k_{I,FA}$ mgN·L^{-1}	$k_{I,FNA}$ mgN·L^{-1}	k_{HCO3-} mgC·L^{-1}
$OUR_{obs} = OUR_{obs}^{max} \cdot \dfrac{k_{I,FA}}{k_{I,FA}+FA} \cdot \dfrac{k_{I,FNA}}{k_{I,FNA}+FNA} \cdot \dfrac{e^{((HCO_3^- - k_{HCO_3^-})/a)}}{e^{((HCO_3^- - k_{HCO_3^-})/a)}+1}$	0.912	751.30±177.21	9.29±33.99	$1.04 \cdot 10^{-7}$±3.54
$OUR_{obs} = OUR_{obs}^{max} \cdot \dfrac{k_{I,FA}}{k_{I,FA}+FA} \cdot \dfrac{k_{I,FNA}}{k_{I,FNA}+FNA} \cdot \dfrac{HCO_3^-}{k_{HCO_3^-}+HCO_3^-}$	0.957	605.48±87.18	0.49±0.09	0.01±0.16

Equation 4.6 yielded a better adjustment than Equation 4.5 (r^2 = 0.957 vs. r^2 = 0.912). The best fitting is shown in Figure 4.17 in a red continuous line. As can be observed, both adjustments yielded similar results for the $k_{I,FA}$, while there was a huge disparity in $k_{I,FNA}$ values. The results for Equation 4.6 were adopted because of higher correlation of the adjustment and fewer standard errors.

In order to validate these constants, they were compared with the literature. Table 4.9 summarises the results of this study, as well as those reported by other authors.

Table 4.9 Comparison of different reported inhibition and half-saturation coefficients for FA, FNA and IC, according to reactor operational conditions

	Reactor conditions			Constant values		
Reference	NH_4^+ (NH_3) mgN·L^{-1}	NO_2^- (HNO_2) mgN·L^{-1}	Temp ºC	$k_{I,FA}$ mgN·L^{-1}	$k_{I,FNA}$ mgN·L^{-1}	k_{HCO3-} mgC·L^{-1}
This stud	1,812-2,230 (6-516)	641-788 (0.01-2.58)	36	605.48±87.18	0.49±0.09	0.01±0.16
Hellinga *et al.* (1998)	130 (1.77)	300 (0.17)	35	-	0.2	-
Carrera (2001)	1.7-441 (0.13-35.15)	411-2,275 (0.11-0.61)	20	95.72	0.18	-
Wett and Rauch (2003)	100 (1-3)	100 (0.03)	30-35	3,000	2.8	50
Pambrun *et al.* (2006)	0-2,000 (0-325)	200-500 (0.04-0.1)	30	241	0.05	-
Van Hulle *et al.* (2007)	0-2,000 (0-1,000)	0-2,000 (0-1.5)	35	-	2.04	-
Magrí *et al.* (2007)	417.8-675 (0-45.8)	246.2-685.1 (0-0.43)	35	45.8	0.24	-
Guisasola *et al.* (2007)	-	-	25	-	-	13.32

An analysis of the results collected in this table reveals significant variation among the constant values detected. Specifically, the $k_{I,FA}$ value obtained in this study is not as high as that obtained by Wett and Rauch (2003), or as low as that obtained by the other authors. The $k_{I,FNA}$ value is also quite different from the literature, although the constant values range is not as big as for the $k_{I,FA}$. It has an intermediate value, located between the high values found by Wett and Rauch (2003) and van Hulle *et al.* (2007), and the low ones found by Carrera (2001), Pambrun *et al.* (2006) and Magrí *et al.* (2007). In terms of bicarbonate, the half saturation coefficient (k_{HCO3-}) obtained for this study is much lower than that obtained by Wett and Rauch (2003) or Guisasola *et al.* (2007). However, since the results were obtained using two different kinetic expressions, they may not be comparable.

Several factors may explain this deviation. Among others, these are a possible acclimation of the biomass to the inhibitory effects of FA and FNA due to a long term exposure to high concentrations, differences in the microbial community, and a different kinetic model choice. It must also be taken into account that a possible correlation between the parameters may bias the results when determining different parameters using the same data set. In particular, inhibition by FNA and growth limitation due to low concentrations of HCO_3^- occurred simultaneously when pH decreased. Thus, for this experiment it is difficult to clearly distinguish the reduction linked to each phenomenon. Both effects need to be investigated in depth in further studies in order to identify the contribution of each to global activity reduction.

4.4.3 Assessment of the process with a view to scale-up

Previous experiments have demonstrated the feasibility of using SBR technology for achieving a partial nitritation of the ammonium present in urban landfill leachate and allowed the correct operating conditions and a suitable feeding strategy to be identified. However, there are still some issues remaining which need to be clarified prior to scaling-up the process to pilot scale.

Urban landfill leachate contains low biodegradable organic matter content, but the degradation of this fraction may influence the partial nitritation process, so it was decided that partial nitritation would be studied together with organic matter removal.

The main aim of a partial nitritation process is to obtain a suitable stream for feeding an anammox reactor. Therefore, it was also decided efforts would be focused on the assessment of process performance to identify the keys for proper operation of the PN-SBR.

To this end, experiments were carried out with the lab-scale PN-SBR. The reactor was started up with sludge from the Sils-Vidreres WWTP using a step-feed strategy. The system was directly fed with urban landfill leachate, in contrast to previous experiments in which bacteria were progressively acclimated to the leachate. Figure 4.18a depicts the evolution of influent ammonium concentration and NLR, as well as the effluent nitrogen compound concentration (Figure 4.18b) and organic matter (Figure 4.18c).

The NLR was progressively increased from 0 to 0.95 $kgN \cdot m^{-3} \cdot d^{-1}$ during the first 25 days. The N-load was then kept at this level until day 110. During this period, the process performed properly, and effluent concentrations of ammonium and nitrite remained at 1,000 - 1,600 $mgN\text{-}NH_4^+ \cdot L^{-1}$ and 1,700 - 2,100 $mgN\text{-}NO_2^- \cdot L^{-1}$, respectively. With regard to organic matter, influent TOC concentrations were around 1,600 - 1,800 $mgC \cdot L^{-1}$. On day 25, about 40% of influent organic matter was removed heterotrophically. This fraction diminished progressively to under

10% by day 110 due to a decline in the organic matter biodegradability (BOD_5 from 480 $mgO_2 \cdot L^{-1}$ on day 10 to 114 $mgO_2 \cdot L^{-1}$ on day 110). Such a change on the biodegradability was attributable to the leachate supplied from the landfill site.
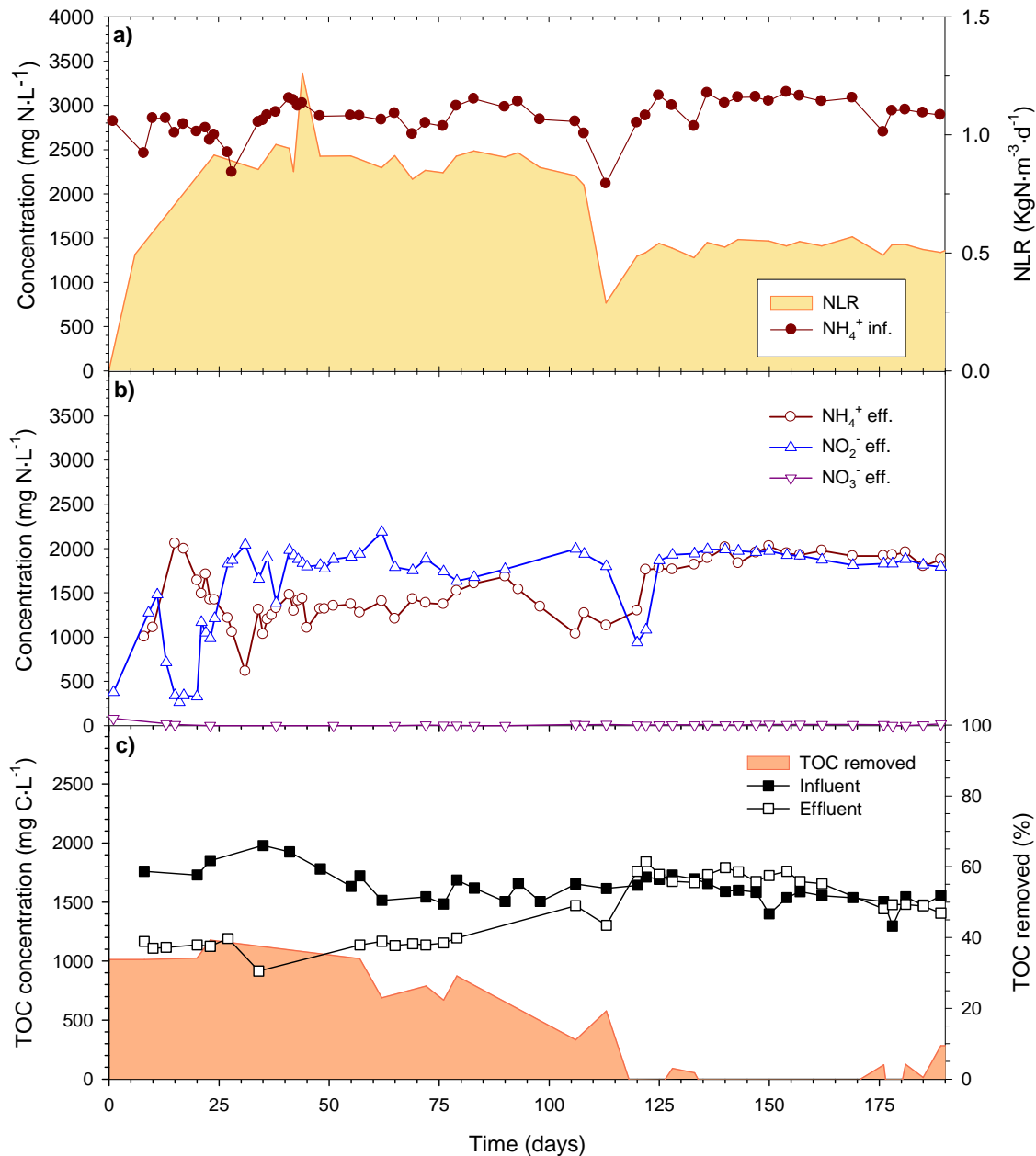
Figure 4.18 Evolution of the PN-SBR a) Influent ammonium concentration and NLR; b) Effluent nitrogen compounds; c) influent and effluent TOC, and percentage of TOC removed from the system

On day 115, the process performance diminished and ammonium started to accumulate. It was therefore decided to decrease the NLR to avoid further process inhibition and restore proper nitritation. To this end, the nitrogen load was set to 0.5 $kgN \cdot m^{-3} \cdot d^{-1}$. The NLR was kept at this level for the rest of the period, with the aim of ensuring a stable reactor performance. In terms of effluent compounds, when stability was recovered the ammonium and nitrite effluent concentrations both remained at about 1,900 $mgN \cdot L^{-1}$ for the rest of the period. With regards to

organic matter, influent TOC remained at around 1,500 - 1,600 mgC·L^{-1} until the end of the experiment. In this final period, effluent TOC concentrations were close to those of the influent, indicating minimal organic matter removal. Specifically, effluent organic matter was sometimes slightly higher than that of the influent, which can be attributed to organic matter released by biomass decay processes. Moreover, TOC measurements only include dissolved organic matter, so the contribution of solids was not considered when measuring the organic matter in the influent.

Stoichiometrically, anammox bacteria need 1.32 moles of nitrite per mole of ammonium (Equation 1.4), and achieving a suitable NO_2^- to NH_4^+ in the effluent of the PN-SBR is crucial for the proper operation of an anammox reactor. From the AOB's stoichiometry (Equation 1.5), 1.14 moles of bicarbonate per mole of ammonium are theoretically needed to reach such a conversion. In this sense, the assessment of influent bicarbonate to ammonium and effluent nitrite to ammonium molar ratios may provide deeper insight into process performance. Figure 4.19 depicts the evolution of experimental influent $HCO_3^-:NH_4^+$ and effluent $NO_2^-:NH_4^+$ molar ratios. In addition, the reference values with which to achieve a suitable feed for an anammox reactor are shown in dashed-dotted lines.
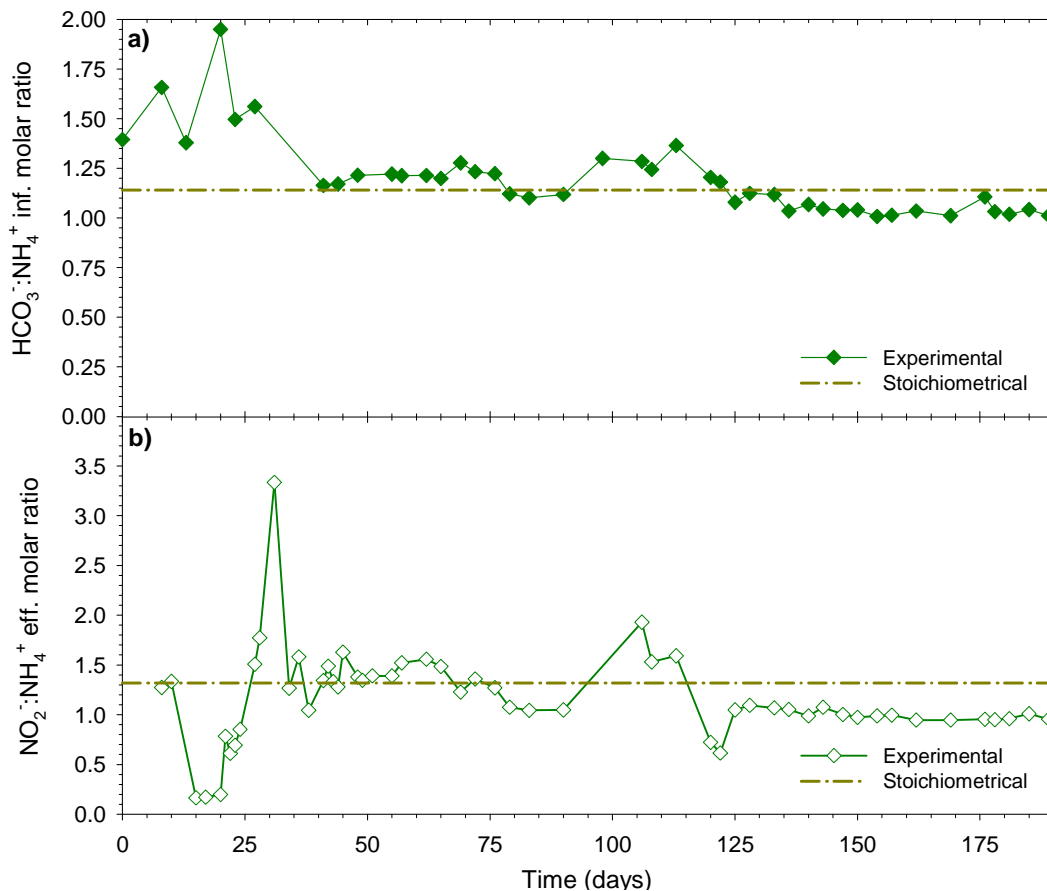
Figure 4.19 a) Evolution of $HCO_3^-:NH_4^+$ influent molar ratio; b) Evolution of $NO_2^-:NH_4^+$ effluent molar ratio

The influent HCO_3^-:NH_4^+ molar ratio was much higher during the first 35 days, than the theoretical stoichiometric value needed to reach the ideal effluent of 1.32 moles of nitrite per mole of ammonium. Then, due to the decrease in influent bicarbonate concentration, this ratio got to between 1.25 and 1, close to the stoichiometry. Regarding the nitrite to ammonium effluent molar ratio (Figure 4.19b), this relationship was initially much lower than expected, due to the underperformance of the reactor. Once a suitable process performance was reached, the NO_2^-:NH_4^+ effluent molar ratio stabilised at around 1.32. On day 105, the influent molar ratio increased due to a decline in the influent ammonium concentration, which also resulted in a higher NO_2^-:NH_4^+ effluent molar ratio (up to 2 moles of nitrite per mole of ammonium). Nevertheless, over the following days, both the influent and effluent molar ratios stabilised at around 1 due to the recovery in influent ammonium concentration and a decline in bicarbonate concentration.

In Figure 4.20, NO_2^-:NH_4^+ effluent molar ratio values have been plotted against the influent HCO_3^-:NH_4^+ molar ratio to establish a relationship between the influent HCO_3^-:NH_4^+ molar ratio and process conversion. In addition the theoretical effluent NO_2^-:NH_4^+ molar ratio (calculated on the basis of the AOB's stoichiometry; Equation 1.5) has been included as a red dashed line. Finally, it should be noted that results from days 0 to 25 have been excluded from the plot to avoid biased results linked to the effects of start up and dilution.
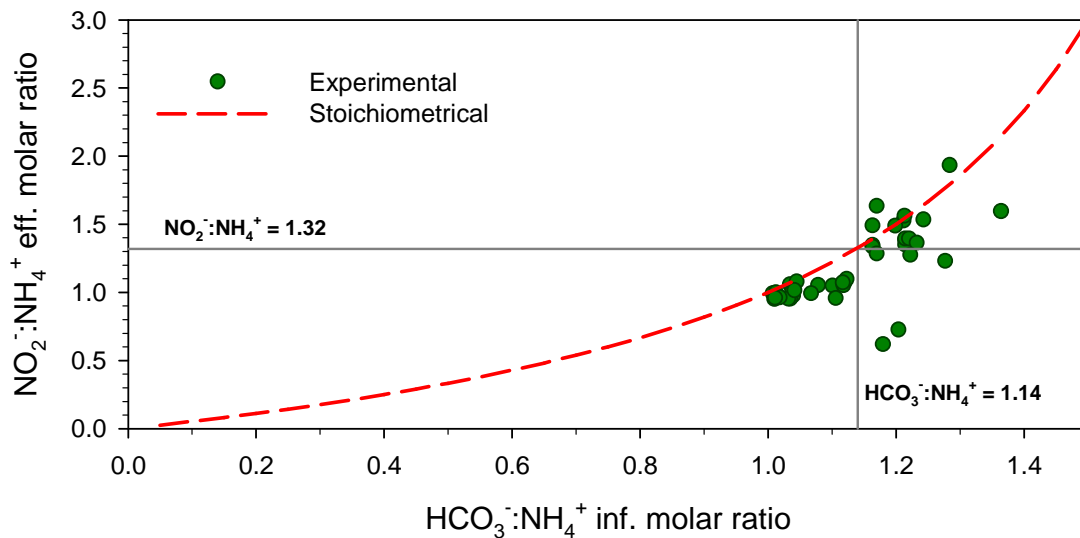
Figure 4.20 Experimental and stoichiometric nitrite to ammonium effluent molar ratio versus bicarbonate to ammonium influent molar ratio

As can be seen, experimental results fit quite well with the stoichiometric curve and confirm bicarbonate as the key to controlling the conversion of ammonium to nitrite. However, there are several experimental features that deviate from theoretical behaviour, and which provide information about process performance and ongoing phenomena. If the effluent molar ratio is lower than the theoretical, this can be attributed to a bias linked to bicarbonate loss due to CO_2

stripping. On the other hand, a higher than theoretical effluent ratio could be related to ammonium removal from the system due to NH_3 stripping, and/or to additional CO_2 coming from organic matter elimination, which may allow a higher conversion if being supplied as bicarbonate. In this period, several experimental points were significantly below the theoretical curve, corresponding to days 111-125. The reactor was partially inhibited and a significant amount of bicarbonate was removed from the system by stripping. Finally, it should be noted that these results need to be validated for a wider $HCO_3^-:NH_4^+$ range.

The assessment of the PN-SBR's performance during the lab-scale experiments was carried out through periodic analytical monitoring. However, the evaluation of process performance by on-line parameters may turn out to be an important milestone in terms of process control. In this way, efforts were also focused on the identification of possible on-line parameters which may help operators to evaluate plant performance.

The OUR, whose measurement can be understood as an indicator of biological activity, has been used for control purposes in several studies (e.g. Johansen *et al.*, 1997; Puig *et al.*, 2005). If the small quantity of biodegradable organic matter removed in the process is taken into account, it can be assumed that the oxygen consumption in the PN-SBR is due solely to AOB activity, and the OUR would then be a good indicator of AOB performance. Figure 4.21 shows the evolution of maximum and minimum OURs, and the nitrite production rate (NPR, kgN-$NO_2^-\cdot m^{-3}\cdot d^{-1}$). The graph covers the period between days 40 and 190, when the process was performing properly.
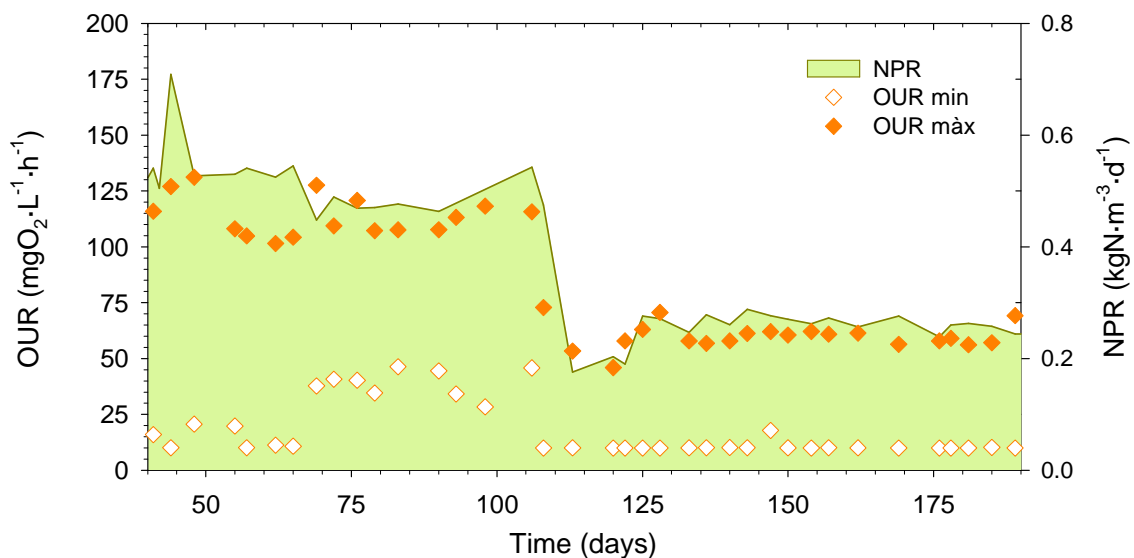
Figure 4.21 Maximum and minimum OUR, together with the nitrite production rate (NPR)

It can be seen from Figure 4.21 that the maximum OUR during the time period from day 40 to day 106 was between 100 and 125 mgO$_2\cdot$L$^{-1}\cdot$h^{-1}, while the minimum OUR fluctuated between 10 and 50 mgO$_2\cdot$L$^{-1}\cdot$h^{-1}. The decrease in the nitrite production rate from 0.5 to 0.25 kgN$\cdot$m$^{-3}\cdot$d^{-1}

led to lower maximum OUR (60 mgO$_2$·L^{-1}·h^{-1}), while the minimum rate stabilised at around 10 mgO$_2$·L^{-1}·h^{-1}. Thus, a significant relationship between the NPR and the maximum OUR can be observed in the graph.

Nevertheless, OURs are dependent on the amount of active biomass in the system, traditionally assimilated to VSS. Therefore, because of the important errors linked to the VSS analysis, it was decided that the total amount of oxygen consumed during a day (OC; mgO$_2$ per litre of reactor per day) would be a better indicator of process performance, calculated according to Section 3.5. The OC and NPR data are presented in Figure 4.22.
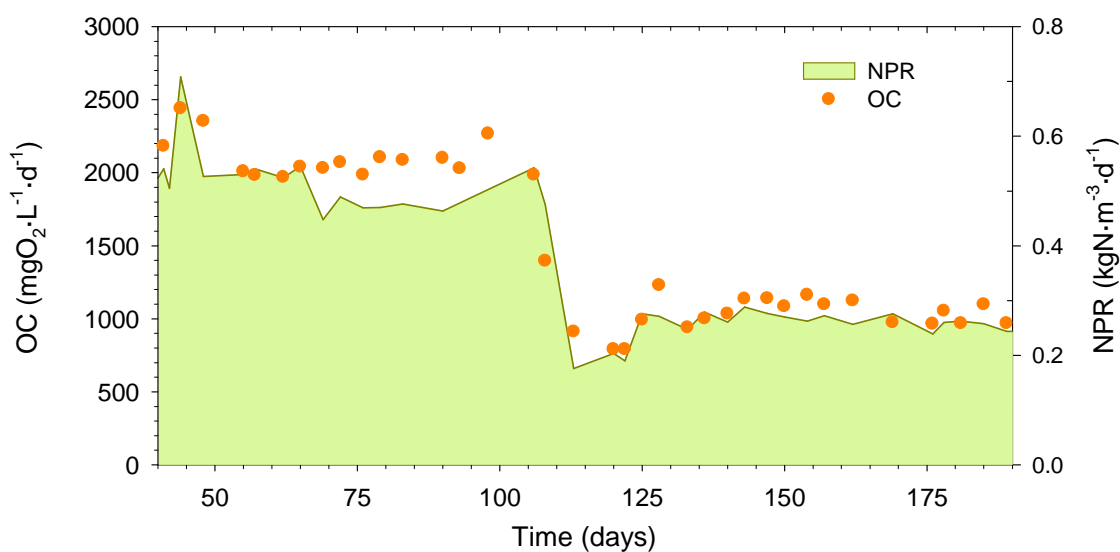
Figure 4.22 Oxygen consumed (OC), together with the nitrite production rate (NPR)

As depicted in the figure, there is a good agreement between the NPR and OC. Values for OC of around 2,100 mg·L^{-1}·d^{-1} were obtained for an NPR of 0.5, and when NPR decreased to 0.25, OC followed suit, presenting values of between 900 and 1,200 mgO$_2$·L^{-1}·d^{-1}.

Given a certain NLR, the NPR of a partial nitritation reactor should be about 50-55% of it, in order to achieve a suitable influent to feed an anammox reactor. Therefore, and because of the strong correlation between the NPR and OC, process performance could be monitored on-line by assessing the oxygen consumed. This could prove interesting in terms of a future on-line control of the process.

4.5 Conclusions

It proved possible to achieve stable partial nitrification of the ammonium present in urban landfill leachate using the SBR technology. On the basis of the conditions of the system, and according to the literature, it may be concluded that this nitrite build-up was achieved by the out-competition of NOB due to inhibition by FA and/or FNA. However, the contribution of

other factors such as IC limitations and temperature, among others, is still not clear. Further experiments must be carried out to confirm this hypothesis.

The PN-SBR was operated under two different feeding strategies: fed-batch and step-feed. Although both allowed partial nitrification to be successfully achieved, the step-feed strategy yielded a more suitable performance. Its overall performance was better, and was linked to a more efficient use of the available bicarbonate (its ARD value was of 14.1%, while the ARD for the fed-batch strategy was 40.9%) and a higher stability. The cycle profiles obtained show that when a fed-batch strategy was applied, the inorganic carbon and pH profile values were low at the end of the cycle (2 mgC·L^{-1} and pH = 5.8 respectively), which concluded with a significant reduction in AOB activity and a loss of HCO$_3^-$ by stripping. In contrast, during the step-feed operation, the pH and inorganic carbon profiles presented a more stable behaviour, in spite of an increase/decrease pattern, which in turn resulted in a NO$_2^-$:NH$_4^+$ effluent molar ratio with fewer fluctuations.

From the batch studies of OUR to PN-SBR pH value, high pH values indicated an OUR reduction caused by FA inhibition, while on the other hand there was an activity reduction at low pH related to an inhibitory effect by FNA and a lack of bicarbonate. The inhibition constants for FA and FNA and the semi-saturation constant for HCO$_3^-$ were calculated from the experimental data, with values of $k_{I,FA}$ (mg N–NH$_3$·L^{-1}) = 605.48±87.18, $k_{I,FNA}$ (mg N–HNO$_2$·L^{-1}) = 0.49±0.09 and k_{HCO3^-} (mg·CL^{-1}) = 0.01±0.16. However, further in-depth studies are necessary to validate this set of parameters, and to establish a possible correlation between $k_{I,FNA}$ and k_{HCO3^-}

A successfully start-up of a PN-SBR treating only leachate was achieved under a step-feed strategy, with a NLR of 1 kgN·m^{-3}·d^{-1} being reached in 25 days.

Biodegradable organic matter was completely removed in the PN-SBR, without any harmful effect on process performance. However, the low biodegradable organic matter fraction of the leachate should be noted.

This study allowed identifying bicarbonate as the key to controlling the process conversion. In addition, the assessment of the influent HCO$_3^-$:NH$_4^+$ molar ratio vs. NO$_2^-$:NH$_4^+$ effluent molar ratio provides an insight into process performance.

OC may serve as a good parameter for a PN-SBR's evaluation because of the correlation between this parameter and the nitrite production rate (NPR). This could be used as a tool for the on-line assessment of process performance.

Chapter 5.   PILOT-SCALE EXPERIENCES ON PARTIAL NITRITATION

This chapter formed the basis of the following publication:

Ganigué, R., Gabarró, J., Sànchez-Melsió, A., Ruscalleda, M., López, H., Vila, X., Colprim, J. and Balaguer, M.D. 2009. Long-term operation of a partial nitritation pilot plant treating leachate with extremely high ammonium concentration prior to an anammox process. *Bioresource Technol.* **100** (23), 5624-5632.

5.1 Motivation

In Chapter 4 the feasibility of achieving a mid-term partial nitrification of the ammonium contained in urban landfill leachate was demonstrated at lab scale using the SBR technology. In such a system, NOB out-competition is accomplished by free ammonia (FA) and/or free nitrous acid (FNA) inhibition (Lai *et al.*, 2004). However, some authors (Turk and Mavinic, 1989; Villaverde *et al.*, 2000; Fux *et al.*, 2004) have reported problems in maintaining nitrite build-up over the long term in such systems when the NOB becomes acclimatised to high concentrations of these inhibitory compounds.

The aim of a partial nitritation system is to oxidise about half of the influent ammonium to nitrite. In the particular case of highly ammonium-loaded wastewater like landfill leachate, the ammonium and nitrite concentrations inside a partial nitritation reactor can be very high. This turns to be an operational problem, since AOB can be also inhibited by the unionised forms of their substrate and product, NH_3 and HNO_2 (as detailed in the previous chapter and widely described by other authors such as Anthonisen *et al.*, 1976; Wiesmann, 1994; Vadivelu *et al.*, 2007; Van Hulle *et al.*, 2007). Partial nitritation systems have been extensively used to treat sludge digester supernatants (Hellinga *et al.*, 1998; Fux *et al.*, 2002; among others) with ammonium concentrations between 500 and 1,500 $mgN-NH_4^+ \cdot L^{-1}$. Nevertheless, inhibition can be a critical issue when dealing with landfill leachate, which can present concentrations up to 6,000 mg $N-NH_4^+ \cdot L^{-1}$ (Kurniawan *et al.*, 2006). In light of this, any reduction in total nitrogen concentration inside the partial nitritation reactor must be seen as an opportunity to reduce inhibition factors. Despite the low levels of biodegradable organic matter available in the leachate, the inclusion of anoxic phases during the feeding events may help to reduce the nitrogen content by heterotrophic denitrification via nitrite, and diminishing inhibition over AOB.

Finally, several studies (Wett and Rauch, 2003; Guisasola *et al.,* 2007) have suggested that bicarbonate substrate limitation can reduce AOB activity at quite high concentrations. This is in contradiction to the results obtained in the previous chapter. However, these results are subject to uncertainty due to the determination of two different parameters using the same data set.

5.2 Objectives

The primary aim of this section is to demonstrate the feasibility of treating urban landfill leachate with extremely high ammonium concentrations (up to 5,000 mg $N-NH_4^+ \cdot L^{-1}$) by means of a 250L pilot-scale partial nitritation-sequencing batch reactor (PN-SBR), as a step prior to an anammox reactor. Specifically, the study seeks to achieve the stable production of a suitable

mixture of ammonium and nitrite, and to demonstrate the viability of long-term nitrite build-up in a biomass retention system. This study also focuses on harnessing the low levels of available biodegradable organic matter for denitrification purposes. The assessment of the process performance has been also defined as one of the goals of this chapter. Finally, the characterisation of the microbial populations involved in the aerobic processes of N-compound oxidation (AOB and NOB) by DNA-based molecular techniques and kinetic batch studies has been performed to attain a better understanding of the partial nitritation process.

5.3 Materials and methods

5.3.1 Experimental set-up

5.3.1.1 <u>250L PN-SBR pilot plant</u>

This study was conducted in a PN-SBR pilot plant, located inside a container to allow transportation. The set-up was placed outside the Faculty of Sciences of the University of Girona so that analytical monitoring could be carried out in the Laboratory of Chemical and Environmental Engineering (LEQUIA) facilities. Urban landfill leachate was provided from the Corsa uban landfill site by 1,000L cubicontainers, located outside the facility. Effluent from the treatment was also stored using empty cubicontainers. An outside view of the experimental set-up is depicted in Figure 5.1.

Figure 5.1 Exterior view of the pilot plant

The pilot plant was composed of a reactor, a storage tank and a control panel. A scheme of the pilot-plant is presented in Figure 5.2, while Figure 5.3 provides a detailed view of the main parts of the plant.
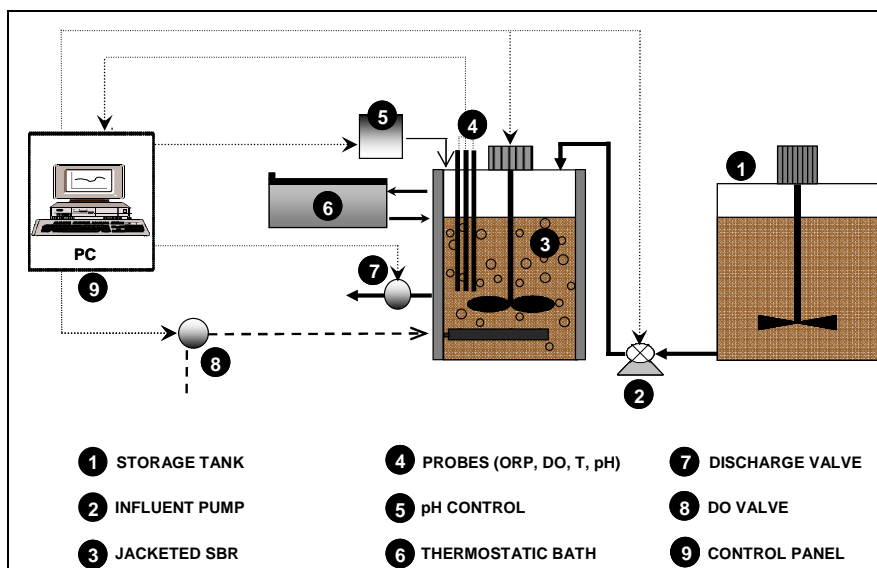
Figure 5.2. Scheme of the pilot-scale set-up

1	STORAGE TANK	**4**	PROBES (ORP, DO, T, pH)	**7**	DISCHARGE VALVE
2	INFLUENT PUMP	**5**	pH CONTROL	**8**	DO VALVE
3	JACKETED SBR	**6**	THERMOSTATIC BATH	**9**	CONTROL PANEL
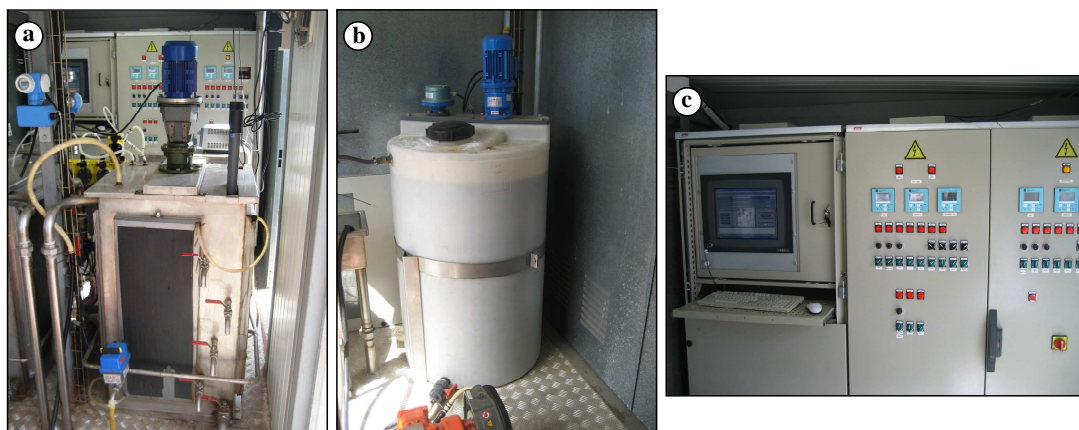
Figure 5.3. Pilot-scale set-up. a) Reactor; b) Storage tank; c) Control panel

The reactor, constructed of stainless steel, had a square-base shape, with a side-length of 0.6m and a height of 1.1m (an effective volume of 250L). It was operated between a minimum and maximum volume of 111 and 165 litres respectively. The reactor was water jacketed, allowing temperature control by means of a thermostated water bath. A complete mixture was achieved by means of a mechanical stirrer, and aeration was carried out using air diffusers (Magnum, from OTT System GmbH & Co.) located at the bottom of the reactor. Raw leachate was stored in a 300 litre storage tank prior to treatment, and supplied to the reactor from the top. The pilot plant was also equipped with a monitoring and control system. On-line data provided by pH, ORP, DO, and temperature probes (CPF 81, CPF 82 and OXYMAX-W COS-41 from Endress-Hauser) were acquired by means of interface cards (PCI-1711 and PCLD-8710 from Advantech) and by our own software, which was developed using Lab-View®. Program commands were transmitted to the pilot plant through another interface card (PCI-885 from Advantech) and a relays output board, which controlled the on/off switch of all electrical devices and thus allowed the repetition of a previously defined operational cycle.

5.3.1.2 Batch reactors

The batch reactors (BIOSTAT B PLUS-SARTORIUS AG) (Figure 5.4) were two cylindrical glass vessels of 5L and 10L of maximum capacity. They were jacketed to allow temperature control, and were equipped with a mechanical stirrer to achieve ideal mixing. The vessels were provided with pH, DO, ORP and T probes. The set-ups were monitored by control units which allowed the stirring velocity, maximum and minimum pH, DO level, and temperature of the mixed liquor to be controlled. The system was supervised by software which enabled acquiring on-line data.
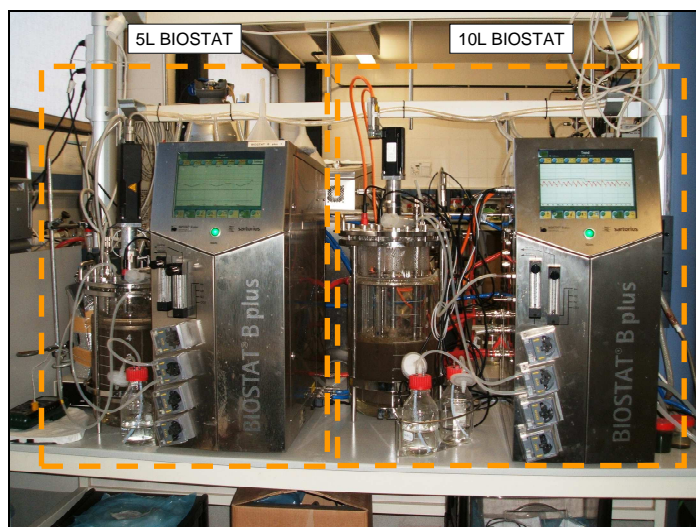
Figure 5.4 Batch reactors

5.3.2 Operational conditions

Temperature in the reactor was maintained at $36\pm1°C$ and dissolved oxygen (DO) was controlled at a set-point concentration of 2 mg·L^{-1} during the aerobic reaction phases. The pH was kept below a maximum set-point value of 8 through the addition of hydrochloric acid (1 M).

The reactor was operated according to an anoxic-aerobic step-feed strategy (DN/PN; Figure 5.5). In contrast to the lab-scale experiments, a 24h cycle was used because of the elevated ammonium concentration, the high pH and the technical limitations. The cycle consisted of 14 feeding events under anoxic conditions (the volume added per feeding ranged between 0.21 and 3.86L), homogeneously distributed over a total reaction phase of 1,400 minutes. The cycle could therefore be divided into 14 identical sub-cycles of 100 minutes, each consisting of 15 minutes of anoxic phase (feeding between minutes 4 to 14) followed by 85 minutes of aerobic reaction. The cycle ended with a 20-minute settling phase followed by 20 minutes of draw.
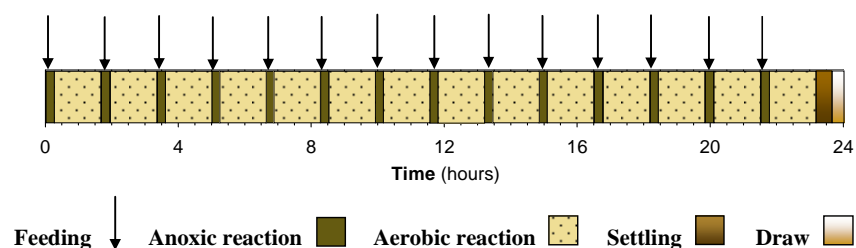
Figure 5.5 Scheme of the anoxic-aerobic step-feed strategy cycle design

5.3.3 Urban landfill leachate

The raw leachate used in this study came from the Corsa urban landfill site (41° 6' 28" N, 1° 7' 4" E; Reus, Catalonia, Spain), supplied in 1,000L cubicontainers. This wastewater varied greatly in its composition during the study. The concentration range and mean values of the principal chemical compounds are summarised in Table 5.1.

Table 5.1 Urban landfill leachate characterisation

Compound	Units	Range	Mean ± σ
Ammonium, NH_4^+	mg N-NH_4^+·L^{-1}	2,237 – 4,938	3,772 ± 956
Nitrite, NO_2^-	mg N-NO_2^-·L^{-1}	0.0 – 1.2	0.2 ± 0.5
Nitrate, NO_3^-	mg N-NO_3^-·L^{-1}	0.0 – 8.0	1.4 ± 3.2
Alkalinity	mg HCO_3^-·L^{-1}	2,059 – 11,223	8,638 ± 3314
Total Kjeldahl Nitrogen, TKN	mg N·L^{-1}	2,494 – 5,540	4,058 ± 987
Chemical Oxygen Demand, COD	mg O_2·L^{-1}	2,480 – 7,040	4,357 ± 692
Biological Oxygen Demand, BOD_5	mg O_2·L^{-1}	230 – 1,025	810 ± 278
Total Organic Carbon, TOC	mg C·L^{-1}	1,509 – 2,420	1,946 ± 457
Inorganic Carbon, IC	mg C·L^{-1}	1,336 – 1,904	1,571 ± 296
Conductivity, EC	µS·cm^{-1}	60,600 – 70,500	68,065 ± 1,863
pH	-	7.48 – 8.56	8.11 ± 0.20

5.3.4 Pilot-plant operation methodology

The SBR was inoculated with a mixture of nitrifying sludge from the Sils-Vidreres municipal WWTP (41° 47' 58" N, 2° 45' 7" E; Catalonia, Spain) and the Orís urban landfill leachate treatment plant (42° 03' 28" N, 2° 14' 15" E; Catalonia, Spain). After a brief start-up, the PN-SBR was operated under a DN/PN strategy (Figure 5.5).

Influent and effluent periodic samples (2-3 per week) were taken for NH_4^+, NO_x^-, TKN, alkalinity, COD, TOC, IC and EC determination. With regards to suspended solids, influent, effluent and reactor TSS and VSS were also analysed 2-3 times per week. BOD analyses were usually performed twice a month.

OUR and OC were calculated from on-line data, according to the methodology described in 3.4 and 3.5.

5.3.5 Molecular analyses

Different molecular techniques to characterise the microbial community were used in this study. All these techniques, except for the FISH analyses, were carried out with the help of the Laboratory of Molecular Microbial Ecology of the University of Girona.

5.3.5.1 <u>FISH analyses</u>

Periodically, sludge samples were taken from the reactor for further fluorescent *in situ* hibridization (FISH) analysis. This technique was performed following the procedure described in Amann (1995). Samples were fixed and stored prior to the analysis. A *Cy5* labelled EUBMIX probe was used to target the entire bacterial community, while specific probes labelled with *Fluos* and *Cy3* were used to target ammonium and nitrite oxidising bacteria (AOB and NOB) respectively. The probed sludge was self-examined using a Leica confocal laser scanning microscope from the Autonomous University of Barcelona. The area containing specific labelled probe cells (*Cy3* and *Fluos*) was quantified as a percentage of the total bacteria, corresponding to the area labelled with EUBMIX (*Cy5*). The probes used in this study are summarised in Table 5.2.

Table 5.2 Oligonucleotide probes used in this thesis

	Probe name	Sequence (5'-3')	Specificity	% Formamide	Reference
EUBMIX	EUB338	GCTGCCTCCCGTAGGAGT	Eubacteria	0-80	Amann *et al.* (1990)
	EUB338II	GCAGCCACCCGTAGGTGT	*Planctomyces* branch	0-80	Daims *et al.* (1999)
	EUB338III	GCTGCCACCCGTAGGTGT	*Verrucomicrobia*	0-80	Daims *et al.* (1999)
AOB	NSO190	TCCCCGCCTAAAGGGCTT	Ammonia oxidising β-*proteobacteria*	40	Mobarry *et al.* (1996)
	NSO1225	CGCCATTGTATTACGTGTGA	Ammonia oxidising β-*proteobacteria*	35	Mobarry *et al.* (1996)
NOB	NIT3	CCTGTGCTCCATGCTCCG	*Nitrobacter*	40	Wagner *et al.* (1996)
	Ntspa662	GGAATTCCGCGCTCCTCT	*Nitrospira*-like organisms	35	Daims *et al.* (2001)
	compNIT3	CCTGTGCTCCAGGCTCCG	To be used with NIT3	-	Wagner *et al.* (1996)
	compNtspa663	GGAATTCCGCTCTCCTCT	To be used with Ntspa662	-	Daims *et al.* (2001)

5.3.5.2 <u>Community assessment by molecular techniques</u>

Sludge samples from the reactor were screened to assess the composition and evolution of AOB and NOB populations. Different molecular techniques were needed to reach this goal, and the complete procedure is briefly described next.

DNA isolation

DNA was isolated from the samples using a DNeasy Blood & Tissue commercial kit (Qiagen, Venlo, The Netherlands) in accordance with the manufacturer's instructions for gram-negative microorganisms. The DNA isolation efficiency was verified in a 0.8% (w/v) electrophoresis gel.

Polymerase Chain Reaction (PCR)

Different combinations of primer sets were used to obtain DNA amplification from all the organisms tagged in the aims of the study. AOB and NOB populations were searched through the amplification of the 16S rDNA operon with specific primer sets, gathered in Table 5.3.

Table 5.3 Forward and reverse primers used to amplify the main bacterial groups in the PN-SBR.

Primer	Specificity	Sequence (5'-3')	Reference
CTO 189F A/B[1]	AOB	GGAGRAAAGCAGGGGATCG	
CTO 189F C[1]	AOB	GGAGGAAAGTAGGGGATCG	Kowalchuk *et al.* (1997)
CTO 654R	AOB	CTAGCYTTGTAGTTTCAAACGC	
FGPS 872F	*Nitrobacter*	CTAAAACTCAAAGGAATTGA	Degrange and Bardin (1995)
FGPS 1269R	*Nitrobacter*	TTTTTTGAGATTTGCTAG	
NSR 1113F	*Nitrospira*	CCTGCTTTCAGTTGCTACCG	Dionisi *et al.* (2002)
NSR 1264R	*Nitrospira*	GTTTGCAGCGCTTTGTACCG	

[1] CTO189F is a 2:1 mixture of CTO189F A/B and CTO189F C

All the PCR analyses were carried out with the PCR programs described in their respective references. 16S rDNA sequences were amplified in a GeneAmp PCR system 2700 thermocycler (Applied Biosystems, Perkin-Emer, CA, USA). The reaction volumes were 50 µL, and each reaction contained 0.8 mM premixed dNTPs (GeneAmp, Applied Biosystems, Warrington, UK), 1.5 mM $MgCl_2$, 1 U Taq polymerase (Applied Biosystems, Warrington, UK) and 5X buffer, plus the respective primers at 0.5 µM.

Cloning, sequencing and identification

The cloning procedure was performed when different DNA sequences were amplified in the same PCR product, making necessary to separate them for successful sequencing and identification. To this end, the different PCR products were ligated to pGEM Teasy vectors (Promega) and transformed into Top10 *Escherichia coli* cells following the manufacturer's instructions. The vectors were then isolated from *E. coli* colonies growing in LB + Ampicillin medium using the Ultraclean 6 minute Mini Plasmid Prep Kit (MoBio). This procedure was only necessary for DNA amplifications performed with CTO primers. PCR products obtained with *Nitrobacter* and *Nitrospira* primer sets were sequenced directly, since only a single phylotype was detected from their respective PCRs. 16S rDNA fragments were sequenced by Macrogen (Seoul Korea), and the partial sequences were compared with the National Center for

Biotechnology Information (NCBI) database using the BLASTn algorithm tool (Altschul *et al.*, 1990) to identify their closest relatives. The presence of chimeras was checked using the Bellerophon tool from the Greengenes website (www.greengenes.lbl.gov).

5.3.6 Batch experiments

Batch experiments were performed to complement the microbial characterisation of the bacterial populations and acquire more in-depth knowledge of the impact of different factors on them. Prior to each experiment, a mixed liquor aliquot from the sludge was taken and pre-conditioned by washing it three times with tap water, thereby acclimating it to the temperature and oxygen conditions of the experiment.

5.3.6.1 <u>Bicarbonate substrate limitation</u>

The aim of these experiments was to determine the role of bicarbonate in process performance, specially focusing on possible substrate limitation. The studies were conducted with a 5L batch reactor at 35ºC, using sludge from the PN-SBR pilot-plant. Dissolved oxygen was kept above 3 mg·L^{-1} by a PID controller to avoid oxygen limitation, and pH was controlled at a set-point of 7.2 by the addition of NaOH or HCl (1M).

Once the sludge had been acclimated to the batch conditions, a pulse of ammonium and bicarbonate was dosed to achieve initial concentrations of 200 mgN-NH$_4^+$·L^{-1} and 120 mgC·L^{-1} respectively. A micronutrient solution and phosphate buffer were also provided to avoid any growth limitation. The evolution of the main chemical compounds was assessed by intensive sampling and monitoring of the concentrations of NH$_4^+$, NO$_2^-$, NO$_3^-$ and IC. The concentration of bicarbonate was calculated based on the carbonate chemical equilibrium, according to Section 3.3. The speciation curves at 35ºC are depicted in Figure 5.6.
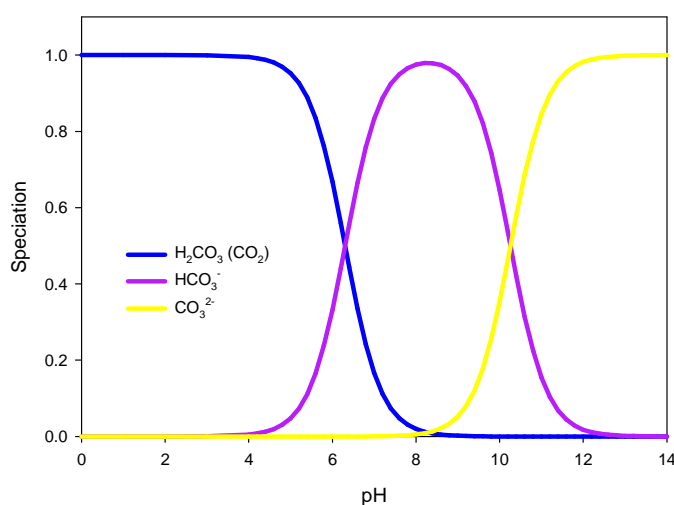
Figure 5.6 Carbonate chemical equilibrium speciation

5.3.6.2 Temperature and free ammonia

These experiments focused on assessing the impact of free ammonia, and temperature on the AOB population of PN-SBR sludge. The studies were conducted on a 5L batch reactor using sludge from the industrial PN-SBR, at different temperatures and initial ammonium concentrations. In addition, experiments were also performed for sludge from a conventional WWTP (non-acclimated sludge) in order to compare the results. In all the experiments, dissolved oxygen was kept above 3 mg·L^{-1} to avoid oxygen limitation, and pH was controlled at 7.2 by means of NaHCO$_3$ or HCl (1M). The complete set of experiments is summarised in Table 5.4.

Table 5.4 Summary of batch experiments

Sludge	Temperature (ºC)	Initial NH$_4^+$ concentration (mg N·L^{-1})	Initial FA concentration (mg N·L^{-1})
Acclimated	35	200	3.53
	35	2,000	35.31
	25	200	1.78
	25	2,000	17.85
	15	200	0.86
	15	2,000	8.56
Non-acclimated	35	200	3.53
	35	2,000	35.31
	25	200	1.78
	25	2,000	17.85
	15	200	0.86
	15	2,000	8.56

The amount of ammonium needed to achieve the desired initial concentration was spiked at the beginning of each experiment, together with bicarbonate (an initial concentration equal to 100 mgC·L^{-1}), a micronutrient solution and phosphate buffer. Bicarbonate substrate limitation was avoided by the NaHCO$_3$ dosage by pH control. The evolution of the main chemical compounds was assessed by a sampling campaign, monitoring the concentration of NH$_4^+$, NO$_2^-$, NO$_3^-$ and IC.

5.4 Results and discussion

A suitable nitrite-to-ammonium ratio in the influent of around 1.32 is crucial for the proper operation of an anammox reactor. Experiments were conducted in an industrial-scale PN-SBR to achieve the desired conversion, and to highlight the keys to this proper operation. In the previous chapter, the step-feed strategy was proven to be a good cycle design for achieving stable partial nitrition, as well as for allowing successful organic matter removal under aerobic conditions. Nevertheless, because of the high nitrogen concentrations and the biodegradable organic matter present in the influent, anoxic phases were included during feeding events to promote heterotrophic denitrification. The diminished total nitrogen inside the reactor could

then reduce the nitrogen load applied to the anammox reactor and inhibition over AOB, thus improving process performance and stability. It should be noted, moreover, that organic matter removal under anoxic conditions may lead to a reduction in energy consumption by aeration.

5.4.1 PN-SBR operation

The pilot-scale PN-SBR reactor was inoculated with sludge from the Sils-Vidreres WWTP and the Orís urban landfill leachate treatment plant. It was directly fed with landfill leachate and was successfully operated for 450 days, according to an anoxic-aerobic step-feed strategy (Figure 5.5), treating this wastewater. Figure 5.7 shows the influent ammonium concentration and nitrogen loading rate (NLR; Figure 5.7a), the evolution of effluent nitrogen compounds (Figure 5.7b) and the bicarbonate supplied in the influent and effluent of the reactor (Figure 5.7c). Furthermore, the theoretical stoichiometric bicarbonate requirements to produce 1.32 moles of nitrite per mole of ammonium, calculated based on the nitritation stoichiometry (Eq. 1.5) and the influent ammonium concentration, are also depicted in Figure 5.7c. It should be noted that the graph has been divided into three sections, corresponding to the different operational stages, based on the bicarbonate dosage.

As depicted in Figure 5.7a, for the first 23 days the reactor was initially fed with a leachate containing about 5,000 mgN-NH$_4^+$·L^{-1}, and was operated at a NLR of between 0.6 and 0.8 kgN·m^{-3}·d^{-1}. Nitrite build-up started to take place in the system, and reached concentrations around 1,200 mgN-NO$_2^-$·L^{-1} in the effluent. Significant ammonium accumulation occurred during these first few days, with ammonium concentrations of up to 3,800 mgN-NH$_4^+$. The low nitrite conversion was a consequence of a shortage of alkalinity in the influent. From Figure 5.7c it can be seen that the bicarbonate supplied to the system by the influent (about 11,000 mgHCO$_3^-$·L^{-1}) was much lower than the theoretical stoichiometric requirements.

On day 24 the influent ammonium concentration diminished to 4,000 mgN-NH$_4^+$·L^{-1} due to a change in the leachate supplied. However, process performance was not significantly enhanced. The elevated ammonium levels coupled with the high pH (around 8) led to process inhibition caused by free ammonia (concentrations up to 350 mgN-NH$_3$·L^{-1}), and feeding had to be stopped on day 34. Because of these severe conditions, it was decided to dilute the reactor content with tap water in order to facilitate process performance recovery. Ammonium and nitrite concentrations were decreased to 850 and 200 mgN·L^{-1}, respectively. Feeding was re-started on day 48 with a NLR of 0.3 kgN·m^{-3}·d^{-1}, but the NH$_4^+$ concentration started to rise sharply again.

To reduce ammonium accumulation and bring the experimental nitrite-to-ammonium effluent molar ratio to the desired 1.32, it was decided on day 59 to enhance the conversion by the addition of external alkalinity (Period II). To this end, a bicarbonate dosage (NaHCO$_3$ 0.5M)

was implemented, based on a pH control. This addition was made when the pH decreased below a set-point value of 7.2.
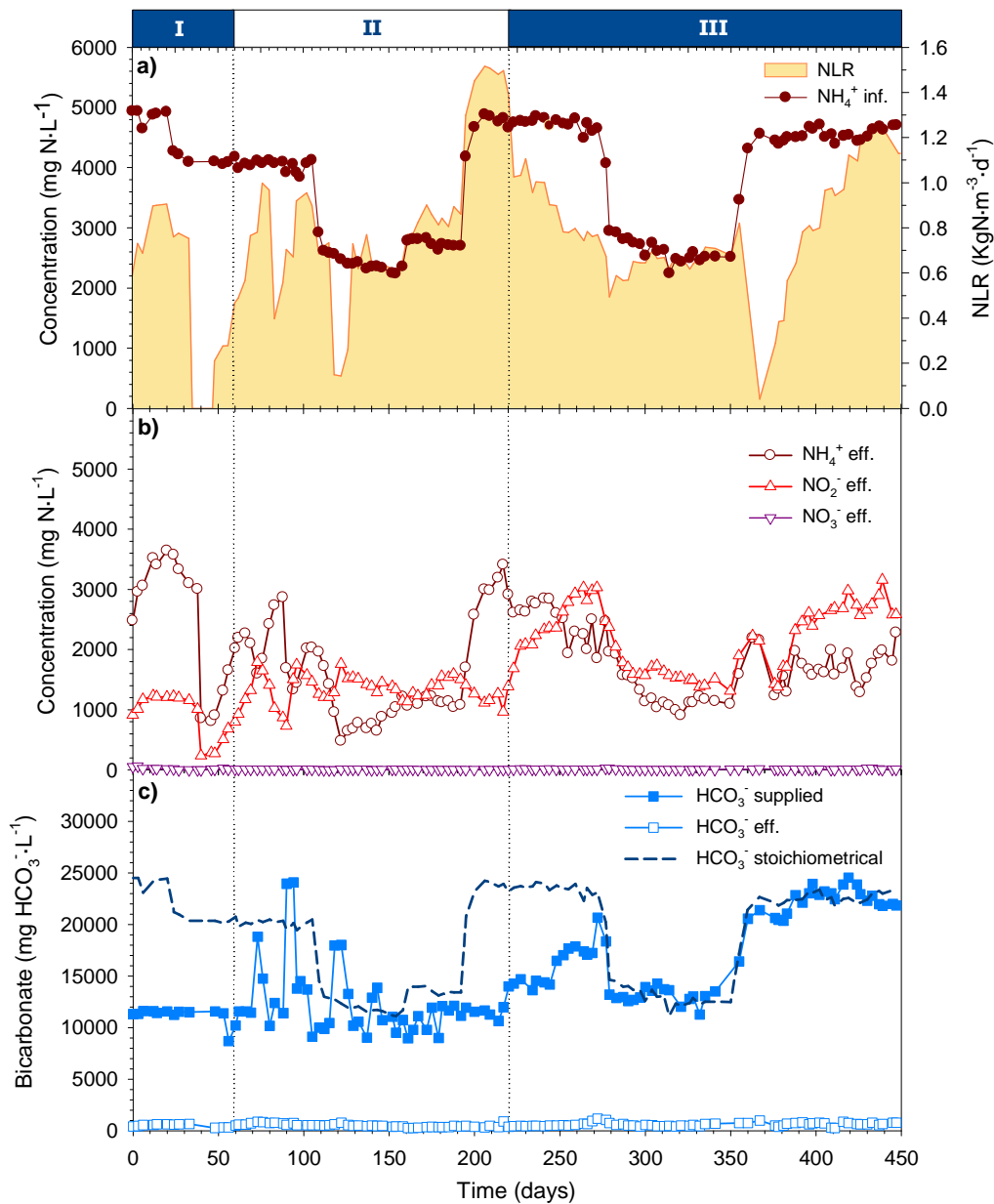
Figure 5.7 Evolution of the PN-SBR. a) Influent ammonium concentration and NLR; b) Effluent nitrogen compounds

This control led to an increase in the HCO_3^- supplied, but with a fluctuating behaviour pattern (Figure 5.7c). As a consequence, nitrite build-up increased substantially, resulting in an effluent with 1,789 $mgN\text{-}NO_2^-\cdot L^{-1}$ and 1,599 $mg\ N\text{-}NH_4^+\cdot L^{-1}$ on day 73. Under these conditions, the system's performance was still fairly unstable. On day 110 the influent ammonium concentration fell to 2,500 $mgN\text{-}NH_4^+\cdot L^{-1}$ due to a change in the leachate supplied. On subsequent days, the nitrite concentration remained at between 1,200 and 1,600 $mgN\text{-}NO_2^-\cdot L^{-1}$, while ammonium concentration was from 1,000 to 1,200 $mgN\text{-}NH_4^+\cdot L^{-1}$. Nevertheless, on day 195, ammonium concentration in the influent increased again to 5,000 $mgN\text{-}NH_4^+\cdot L^{-1}$ (NLR of

1.5 kgN·m^{-3}·d^{-1}), and ammonium started to accumulate because the control system was unable to supply enough bicarbonate (Figure 4.7c), finally reaching ammonium concentrations of over 3,000 mgN-NH$_4^+$·L^{-1}.

To overcome this situation, solid bicarbonate started to be added to the pre-treatment tank (Period III). The amount of bicarbonate added was calculated on the basis of the stoichiometric requirements for achieving a suitable effluent to feed an anammox reactor. During Period III, the minimum pH was also controlled by the bicarbonate solution dosage, and as a result, the bicarbonate supplied to the system got very close to the stoichiometric. Thus, during the last 200 days of the period, the production of an influent suitable to feed an anammox reactor was reached, despite the variations on the influent. Ammonium and nitrite concentrations in the effluent were about 1,800 mgN-NH$_4^+$·L^{-1} and 2,600 mgN-NO$_2^-$·L^{-1} respectively, and with the NO$_2^-$ to NH$_4^+$ ratio approaching the desired value of 1.32. During this period, the system was operated at NLR higher than 0.75 kgN·m^{-3}·d^{-1}, reaching a maximum of 1.25 kgN·m^{-3}·d^{-1}.

Finally, it is important to note that no significant nitrate production was detected during the whole 450-day period, except for at the beginning of the start-up. NO$_3^-$ concentration throughout the study was always below 25 mgN-NO$_3^-$·L^{-1}. It should also be pointed out that all the bicarbonate supplied was eliminated from the system in the three periods, since the very low effluent concentrations.

All biodegradable organic matter needs to be removed in the partial nitritation step to avoid operational problems in an anammox reactor. Figure 5.8 shows the organic matter evolution of both influent and effluent in terms of TOC values and removal percentage.
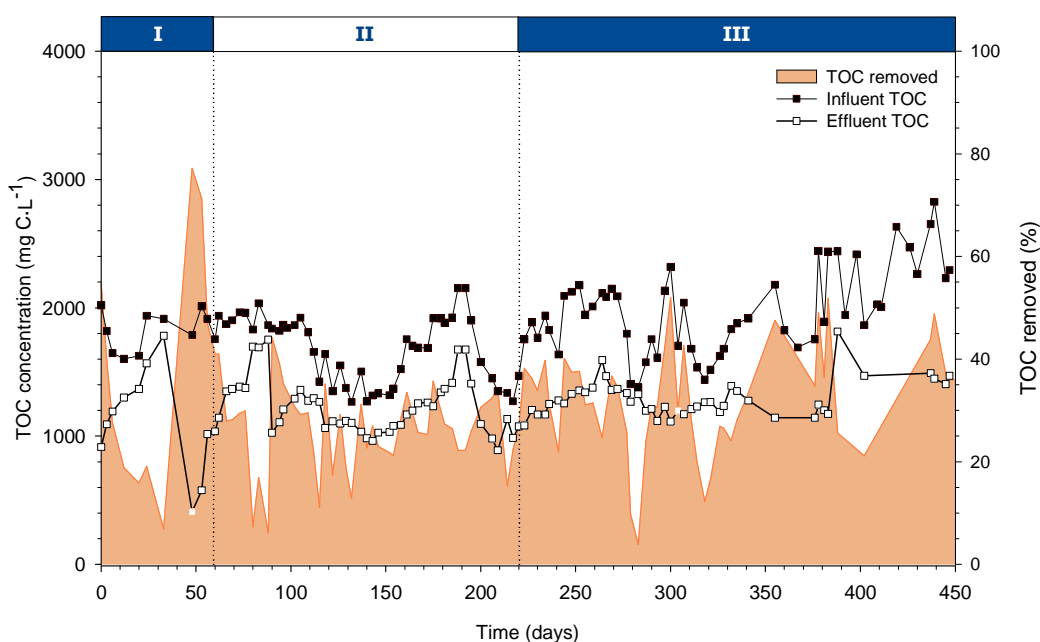
Figure 5.8 Evolution of influent and effluent TOC, and the percentage of TOC removed

78

The raw leachate had influent TOC concentrations of around 1,500-3,000 mgC·L^{-1}. The biodegradable fraction of this organic matter was removed in the PN-SBR process (either aerobically or anoxically). Except for the periods with operational problems, TOC concentrations in the effluent were higher than 1000 mgC·L^{-1} throughout the study. This means that less than 50% of the TOC was removed in the system, which shows the high inert organic matter fraction of the raw leachate. This was confirmed by a mean BOD$_u$ to COD ratio of 0.32 in the raw leachate and a soluble BOD$_u$ of zero in the effluent.

Next, Figure 5.9 shows the evolution of TSS and VSS concentrations in the reactor and in the effluent of the PN-SBR.
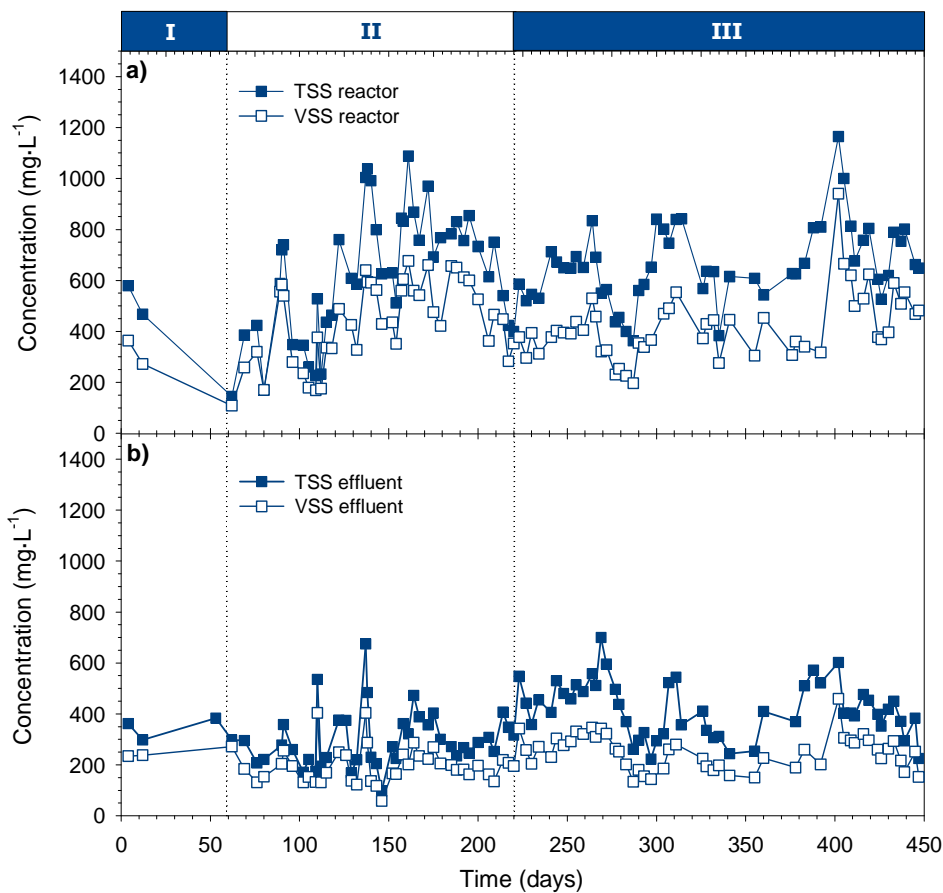
Figure 5.9 Evolution of TSS and VSS concentrations. a) Reactor; b) Effluent

During Period I, the amount of TSS and VSS in the mixed liquor decreased sharply due to low process conversion and the dilution to avoid inhibition problems. In contrast, effluent SS (Figure 5.9b) remained quite stable and at very high values (around 375 mgTSS·L^{-1} and 250 mgVSS·L^{-1} respectively). However, the addition of bicarbonate to the system, which enhanced process performance, supposed a stabilisation of the amount of TSS in the reactor at around 800 mgTSS·L^{-1}, with peaks up to 1,100 mgTSS·L^{-1}. The ratio between VSS and TSS in the reactor was around 75% and the effluent remained at its elevated values, reaching peaks of 700 mgTSS·L^{-1} (450 mgVSS·L^{-1}).

From these results it can be clearly concluded that the amount of biomass retained in the reactor was enough to achieve the desired conversion, despite the elevated concentrations of suspended solids drawn by the outflow. This loss of solids may be linked to deficient settling, probably associated with the high conductivity of leachate (always higher than 60,000 μS·cm^{-1}) as pointed out by Wu *et al.* (2008). An increase in settling characteristics may suppose an increase in the MLSS, which could allow the treatment of higher NLR and/or a reduction in the cycle duration.

Due to significant variations in the raw leachate ammonium concentration, the inflow of the PN-SBR had to be adjusted to keep the nitrogen loading rate (NLR) close to -but below- the maximum nitrifying capacity of the system to avoid loading shocks. This caused significant hydraulic retention time (HRT) fluctuations, ranging from 3 to 6 days. Under these conditions the sludge retention time (SRT) was not a controlled system parameter, but could be calculated based on reactor MLSS and effluent suspended solids concentrations, according to Equation 4.1. The evolution of reactor SRT is depicted in Figure 5.10.
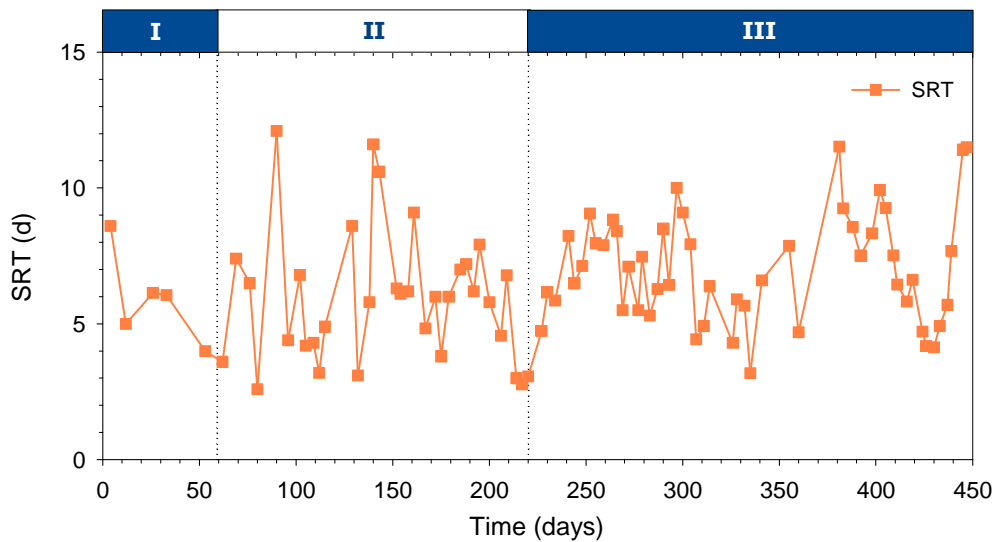
Figure 5.10 Sludge age evolution during the experiment

As can be seen from the plot, the SRT of the reactor fluctuated throughout the study, in the range 3.1 to 12 days. The average SRT value was 6.44 ± 2.34 days. Finally, it is important to note that only 82.6% of this SRT was under aerobic reaction conditions.

5.4.2 Assessment of the process performance

Various tools for the assessment of process performance were proposed in the previous chapter. In this section their utility is verified by their application at pilot scale and, due to changes on the operational mode (alternation of aerobic and anoxic phases), new aspects have been evaluated.

5.4.2.1 Influent bicarbonate to ammonium molar ratio

As previously observed, process performance is closely related to the alkalinity/bicarbonate availability. Accordingly, the monitoring of the HCO_3^-:NH_4^+ influent molar ratio may allow the process conversion to be predicted, and the outcome of the system could be controlled by adjusting this ratio.

Figure 5.11 shows the evolution of the HCO_3^-:NH_4^+ influent molar ratio (Figure 5.11a) and the NO_2^-:NH_4^+ effluent molar ratio (Figure 5.11b). It should be noted that the bicarbonate supplied by the pH control has also been taken up in the calculation. The required HCO_3^-:NH_4^+ influent and desired NO_2^-:NH_4^+ effluent molar ratios have been depicted in dotted horizontal lines.
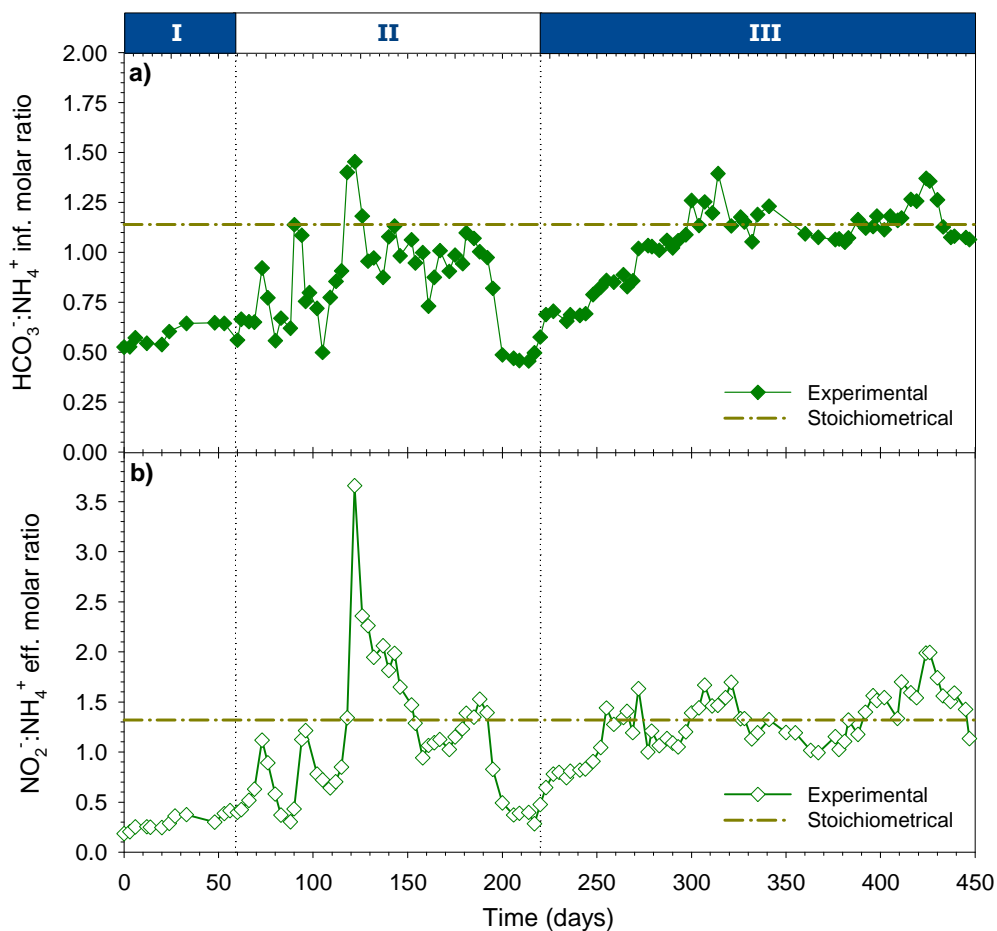
Figure 5.11 a) Evolution of the HCO_3^-:NH_4^+ influent molar ratio; b) Evolution of the NO_2^-:NH_4^+ effluent molar ratio

During Period I, the influent had HCO_3^-:NH_4^+ molar ratios around 0.6, which led to effluent molar ratios between 0.18 and 0.41, a long way from the stoichiometric requirements of the further anammox process (a NO_2^-:NH_4^+ molar ratio of 1.32). The external $NaHCO_3$ dosage during Period II resulted in an increase in the HCO_3^-:NH_4^+ influent molar ratio, which manifested in an increased nitrite to ammonium effluent molar ratio. However, the dosage strategy also induced significant fluctuations, with values ranging from 0.3 to 3.7.

Preconditioning the influent with solid $NaHCO_3$ addition (Period III) provided a more stable $HCO_3^-:NH_4^+$ influent molar ratio; this kept the effluent molar ratio within a suitable range over the 200 days, at between 1 and 1.5 moles of NO_2^- per mole of NH_4^+, with peaks of up to 2. It should be mentioned that the denitrification process might have slightly affected the NO_2^- to NH_4^+ effluent molar ratio.

With the aim of further evaluating reactor performance, a data subset was selected whereby the reactor operated under stable conditions. Figure 5.12 shows the experimental nitrite to ammonium effluent molar ratio versus the influent bicarbonate to ammonium molar ratio. The theoretical effluent $NO_2^-:NH_4^+$ molar ratio was calculated based on the AOB stoichiometry (Equation 1.5), and is shown in a dashed red line. The ideal effluent molar ratio (1.32), together with the stoichiometric bicarbonate to ammonium influent molar ratio (1.14) are also depicted, in grey lines.
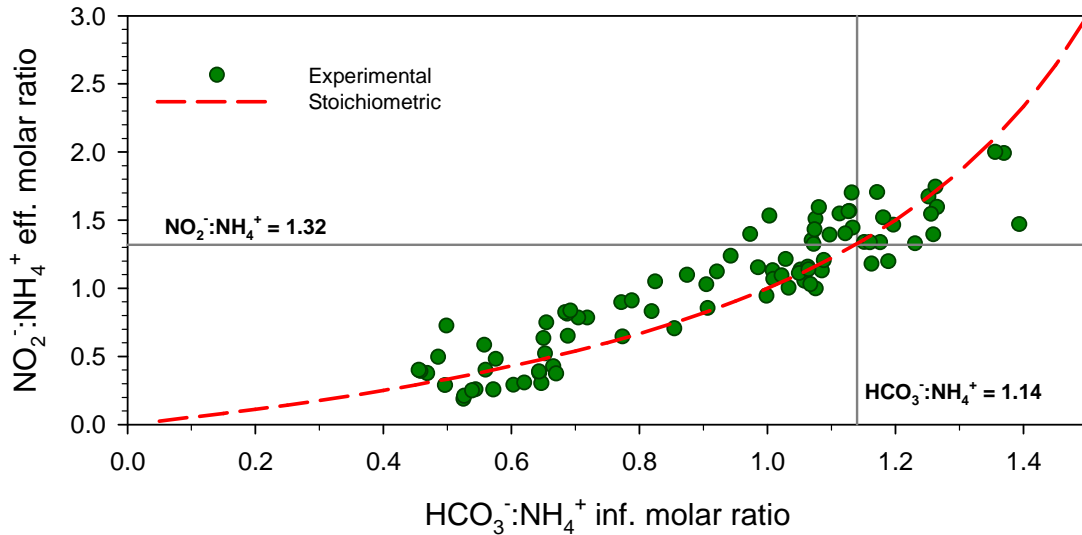
Figure 5.12 Experimental and stoichiometric nitrite to ammonium effluent molar ratio versus bicarbonate to ammonium influent molar ratio

As can be seen in the figure, the experimental results fit quite well with the stoichiometric curve, which validates bicarbonate as the key to controlling the conversion of ammonium to nitrite. Deviations from theoretical behaviour in the experiment provided information about the process performance and the ongoing phenomena. When the effluent molar ratio was lower than the theoretical, this can be attributed to a bias linked to the heterotrophic denitrification process and/or bicarbonate loss by CO_2 stripping. On the other hand, a higher than theoretical effluent molar ratio could be related to ammonium removal from the system due to NH_3 stripping. Additional inorganic carbon coming from the elimination of organic matter may also allow a higher conversion. Nevertheless, this depends on whether IC is produced as CO_2 or HCO_3^-.

5.4.2.2 **Heterotrophic denitritation**

The nitrogen balance and organic matter removal over a period of stable operation were assessed to estimate the amount of nitrogen removal by denitritation (Figure 5.13). Based on this stability requirement, the assessment was done between days 145 and 335 (Periods II and III), ignoring all data biased due to influent composition changes. The theoretical amount of COD necessary for denitrification was calculated and plotted, based on Tchobanoglous *et al.* (2003), obtaining a theoretical ratio of 1.97 gCOD per gN-NO$_2^-$. Results are depicted in Figure 5.13b.

The average amount of nitrogen eliminated in the system was about 200-250 mg N·L^{-1}. As can be observed in Figure 5.13a, 15 to 20% of the influent nitrogen was removed by heterotrophic denitritation between days 145 and 225 (Period II), declining to 5% over the next 110 days (Period III).
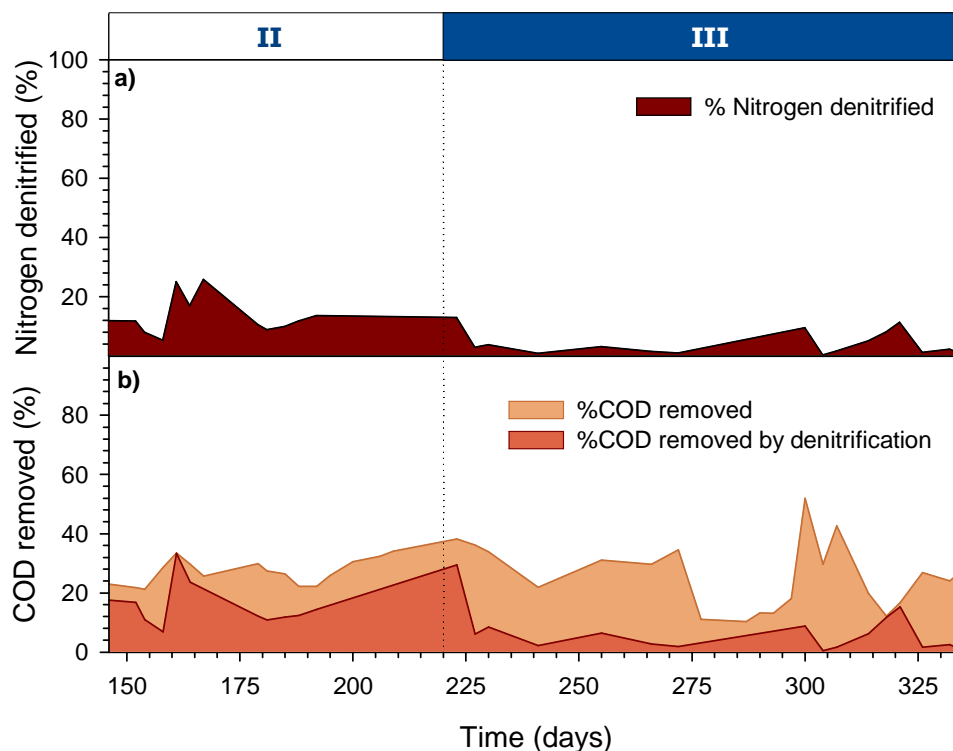
Figure 5.13 Denitrification assessment. a) Evolution of the percentage of nitrogen denitrified; b) Evolution of the percentage of COD removed from the reactor, along with the theoretical amount of COD necessary to achieve the denitritation

Figure 5.13b presents the amount of COD eliminated in respect to the total organic matter in the influent. The COD removed from the system over this 190-day period was about 25 to 30%. During Period II, more than half of the biodegradable organic matter was used for denitrification purposes; this value fell sharply to less than 10% in Period III. It is important to point out that denitrification performance declined when solid bicarbonate began to be dosed in the influent (day 220). This external bicarbonate dosage conducted to a higher conversion,

which meant that nitrite concentration in the system became more elevated. Inhibition of heterotrophic bacteria by FNA has been reported by some authors (Abeling and Seyfried, 1992; Glass *et al.*, 1997). Accordingly, the denitrification efficiency has been plotted together with the evolution of the maximum FNA in the cycle, and the results are shown in Figure 5.14.
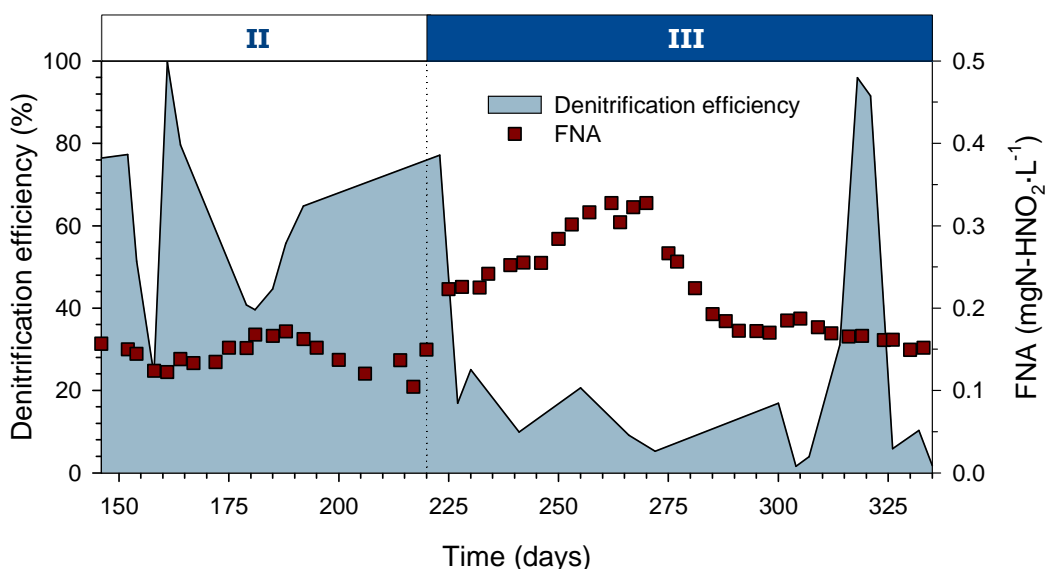
Figure 5.14 Assessment of denitrification efficiency, together with the evolution of FNA levels

As can be observed, there is a high correlation between efficiency and the FNA levels. The increase in the FNA may have led to a higher inhibition of the heterotrophic bacteria, resulting in a decrease in organic matter removal. Nevertheless, further targeted experiments would be needed to validate this hypothesis and quantify the inhibitory effects.

5.4.2.3 Cycle analysis: on-line parameters

In order to clearly understand the behaviour of the system, it is necessary to monitor on-line parameters over the course of a cycle. To illustrate this, Figure 5.15 shows the pH and DO profiles over the anoxic-aerobic step-feed cycle of day 392 (DN/PN; Figure 5.5) in Period III, as well as the specific OUR.

The pH fluctuated from 7.2 to 7.9, increasing during anoxic phases due to the high pH of the influent leachate (around 8.2), coupled with OH$^-$ production linked to a possible heterotrophic denitritation process. The pH decrease was caused by the proton production of ammonium oxidation during the aerobic phases. Figure 5.15a shows the DO profile. Oxygen levels were always over 2 mg·L^{-1} except during anoxic phases, when they plummeted to values close to zero due to the cessation of aeration. Oxygen consumption was mainly due to the nitritation process, as part of the organic matter was removed under anoxic conditions. The specific OUR plot

(Figure 5.15b) also shows an increase/decrease pattern similar to the pH, with specific OUR values ranging between 60 and 310 $mgO_2 \cdot gVSS^{-1} \cdot h^{-1}$.
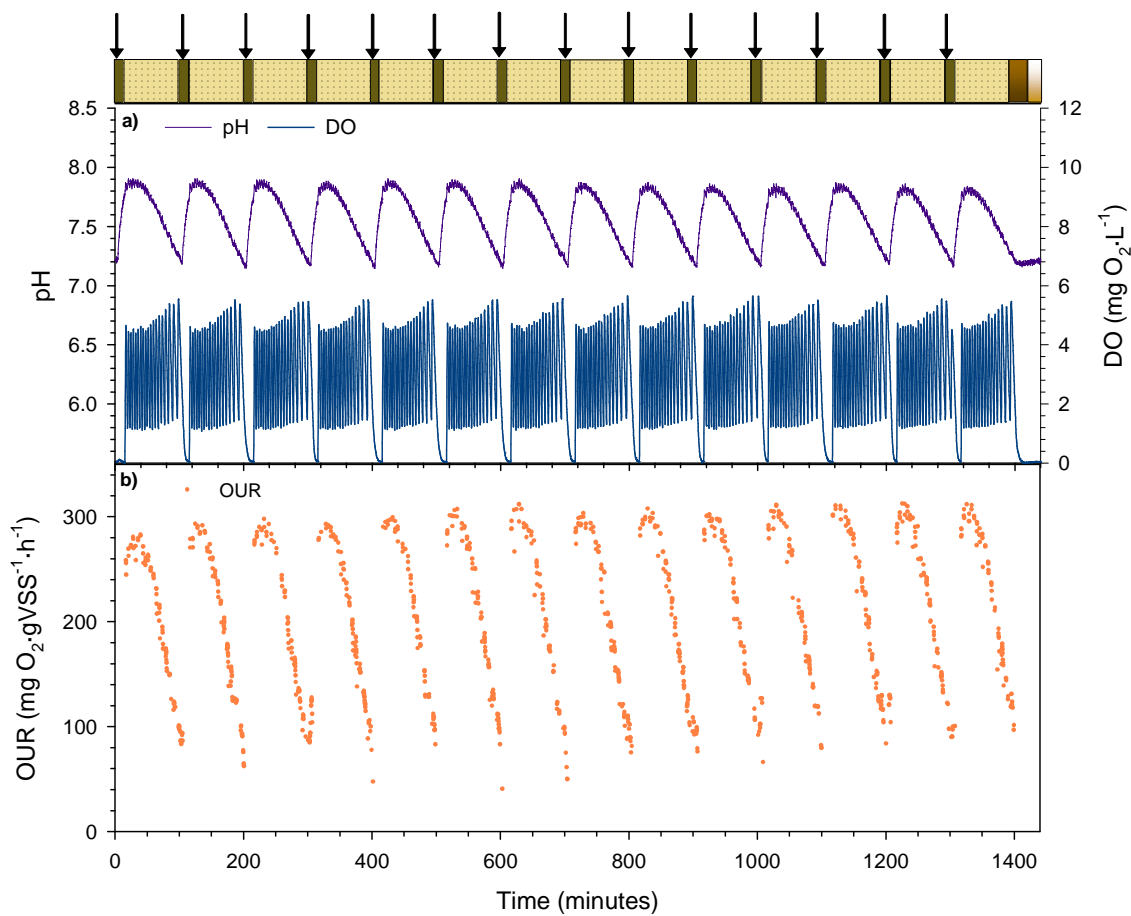
Figure 5.15 a) Evolution of pH and DO throughout the cycle; b) Calculated specific OURs

To further study the dynamics of these three parameters, a specific aerobic-anoxic sub-cycle (100 minutes out of the whole 1440 minute cycle) is shown in Figure 5.16. The graph is divided into three sections: aerobic reaction (beige-dotted area of the bar), anoxic reaction (green area of the bar) and feeding in anoxic conditions (white-striped area of the bar).

At the beginning of the reaction phase, pH values were around 7.7-7.8. During the aerobic reaction phase they declined to 7.2 due to proton production linked to AOB activity. At minute 305, pH increased sharply during the feeding event partly because of the high pH of the influent (about 8.2), but also due to the OH^- contribution of the denitritation process. Concerning the specific OUR, this was initially about 260 $mgO_2 \cdot gVSS^{-1} \cdot h^{-1}$, increasing to 300 $mgO_2 \cdot gVSS^{-1} \cdot h^{-1}$ after only 20 minutes of aeration. From this point on, it decreased slightly up to the end of the aerobic phase. At the beginning of the anoxic phase (minute 300), the DO concentration was still around 5 $mgO_2 \cdot L^{-1}$, which meant that aerobic reactions could continue. At minute 304 the feeding event started, with raw leachate being supplied to the PN-SBR. This contribution induced an initial increase in specific OUR values until the DO declined to values near zero. By

minute 312 the oxygen had been completely depleted, and the strict anoxic conditions necessary for denitrification process had been reached. Nevertheless, the presence of available oxygen during part of the anoxic feeding period enabled aerobic consumption of the biodegradable organic matter supplied in the influent, which may explain the poor denitrification performance. Denitritation could be then enhanced by extending the anoxic periods before and after the feeding events. The optimisation of the DO control may also help to improve the denitrification process. Nevertheless, the inhibition of denitrifying bacteria by FNA cannot be discarded as a possible cause for such an underperformance, and remains as an open issue for further investigations.
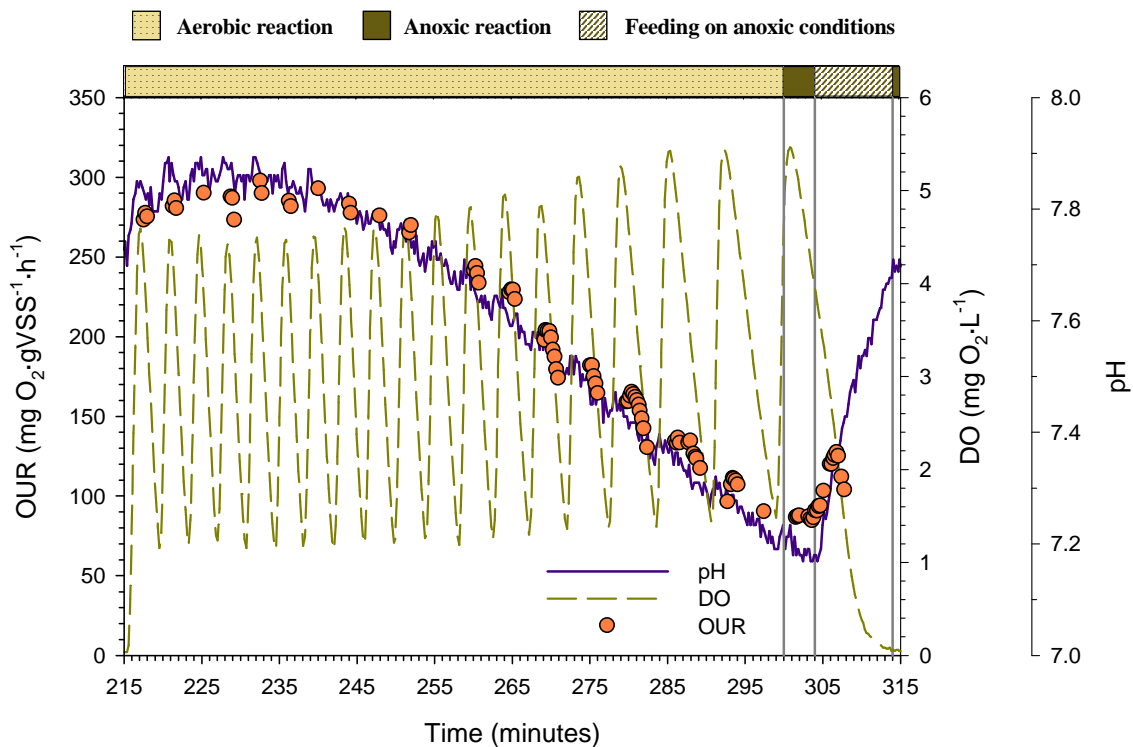
Figure 5.16 Specific oxygen uptake rates (OURs), dissolved oxygen (DO) and pH, from minutes 215 to 315 of a 1440 minute cycle

Finally, it is important to point out the close relationship between pH and specific OURs, since both parameters declined following exactly the same trend. It could be thought that pH directly governs AOB activity. The relationship between the two parameters could be also explained by the progressive inhibition of AOB by FNA (Vadivelu *et al.*, 2007; Van Hulle *et al.*, 2007), because of the increase in its concentration due to the pH decline. The low bicarbonate concentrations in the mixed liquor may also contributed to this reduction in activity. On the one hand, such low concentrations might allow a faster decrease in pH. On the other, they could also have caused a reduction in growth due to a substrate limitation (as reported in Guisasola *et al.,* 2007 or Wett and Rauch, 2003). Further studies are needed to clarify this issue.

5.4.2.4 Oxygen consumption

In the previous chapter the close relationship between the nitrite production rate (NPR) and the oxygen consumed (OC) was experimentally demonstrated. This relationship was validated by the pilot-scale PN-SBR, and was used for the assessment of process performance. Figure 5.17 depicts the evolution of OC and NPR during the study. Note that data from day 415 to 450 is missing due to a problem with the data acquisition.
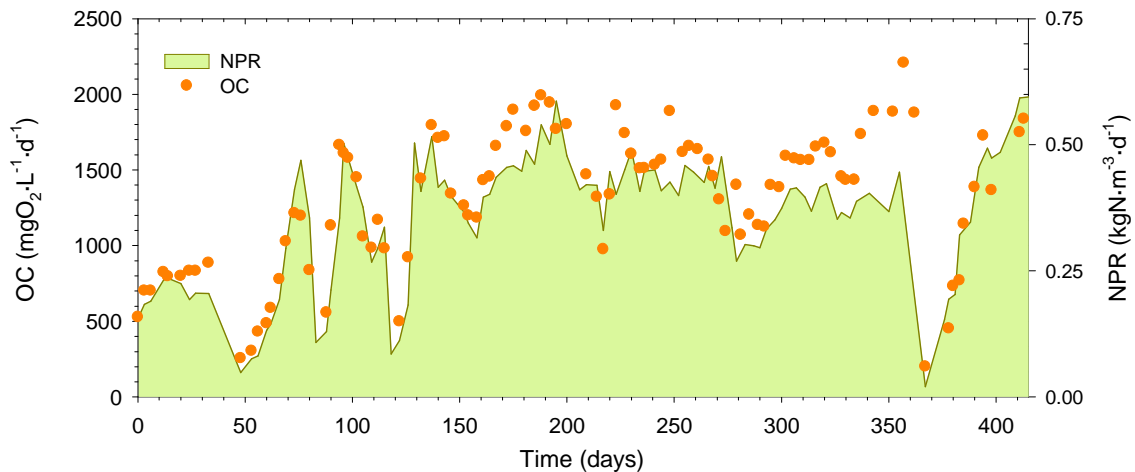
Figure 5.17 Oxygen consumption (OC) and nitrite production rate (NPR)

As shown in Figure 5.17, a very good fitting was reached for the majority of the data set, although OC values from days 300 to 360 are slightly higher than should theoretically be the case. Taking into account the poor denitrification performance during this period (see Figure 5.13b), such deviation could be attributed to aerobic organic matter degradation.

On a theoretical basis, about 3.43 mg of oxygen are consumed per mg of ammonium oxidised to nitrite. Higher ratios may be linked to other oxygen consumption processes (i.e. heterotrophic organic matter oxidation, aerobic endogenous respiration processes etc). Accordingly, OC was plotted against the NPR in order to assess this stoichiometric relationship (see Figure 5.18).

As can be seen from the graph, there is good agreement between the experimental data and the stoichiometry. In general, oxygen consumptions are slightly higher than the stoichiometry, reassuring the aerobic heterotrophic organic matter removal. There exist also a few experimental points which are under the stoichiometric consumption. Such behaviour may be attributed to biases on the NPR and OC calculations.
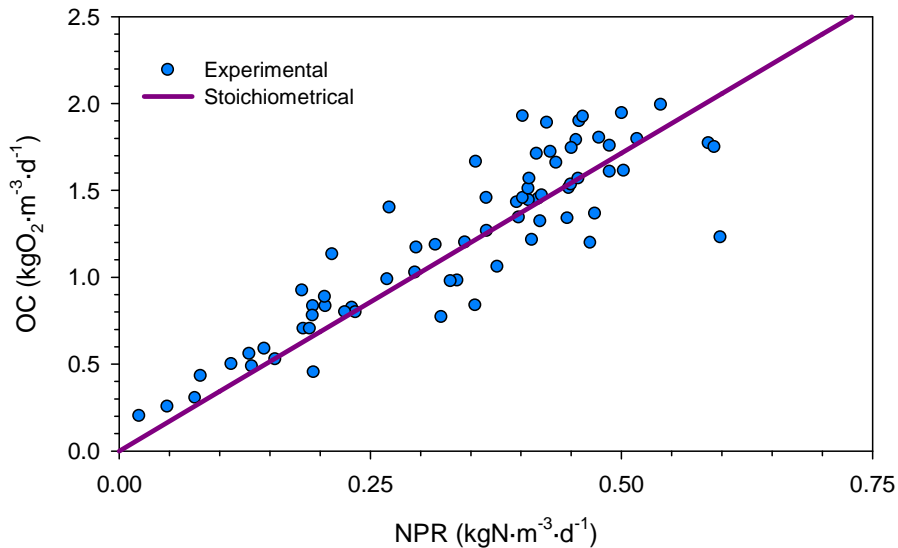
Figure 5.18 Oxygen consumption (OC) versus nitrite production rate (NPR)

These results validate OC as a tool for on-line process performance assessment, being specially suited for systems treating wastewater with low biodegradable organic matter content.

5.4.3 Characterisation of AOB and NOB populations

Another important issue in view of further application of this technology is the acquisition of a better understanding of the bacterial community responsible for the biochemical transformations. To this end, efforts were made to identify and evaluate the bacterial community, as well as their kinetic characterisation.

5.4.3.1 Bacterial community characterisation by molecular techniques

One of the aims of this study was to identify the initial AOB and NOB populations and analyse their evolution over the course of a long-term operation. Given the high ammonium and nitrite concentrations in the bulk media (both higher than 1,000 $mgN \cdot L^{-1}$), the elevated salinity (always above 60,000 $\mu S \cdot cm^{-1}$) and high temperature (36ºC), identifying the AOB capable of resisting such extreme conditions would represent an important microbiological feature with potential environmental implications. Given the low level of nitrate production during the study, the microbial community analysis was also intended to determine whether or not NOB organisms were present in the community after long-term operation. With these purposes, five samples were collected and their genomic DNA was isolated and processed. R0 was an aliquot from the initial sample from the mixture of nitrifying sludges used to inoculate the reactor, while R192, R288, R415 and R450 were obtained from the PN-SBR after 192, 288, 415 and 450 days respectively.

All DNA isolations were screened by PCR using different combinations of primers, each of them specific to a bacterial group. Positive PCR amplifications with the CTO primer sets confirmed the presence of AOB throughout the entire working period. Based on these results, only R0 and R450 were cloned since no changes were detected between days 192 and 450 (data not shown). 16S rDNA sequences obtained from the cloning procedure showed a high homology with known uncultured bacteria phylotypes, all of them related to *Nitrosomonas*-like species. Phylotypes detected in R0 were grouped into five organism taxonomic units (OTUs), while all R450 sequences clustered together in one OTU (OTU 5), which arose as dominant in the reactor (Table 5.5). This OTU showed a high similarity (98-99%) with *Nitrosomonas* sp. IWT514, which was therefore positively selected by the severe operational conditions in the reactor.

Table 5.5 Summary of NCBI closest relatives of the OTUs detected from CTO primer set amplification

	OTU	Closest BLASTn phylotype	NCBI accession number	% phylotypes
	OTU 1	Uncultured bacterium clone IIIEA1-rp-O2 nit	gi|161367780|gb|EU267435.1|	27
	OTU 2	Nitrosomonas sp. Is32	gi|40994846|emb|AJ621027.1|	27
R0	OTU 3	Uncultured bacterium clone S_1	gi|121592404|gb|EF175894.1|	20
	OTU 4	Uncultured bacterium clone 58	gi|89348071|gb|DQ413117.1|	10
	OTU 5	*Nitrosomonas* sp. IWT514	gi|13958147|gb|AF363293.1|AF363293	10
R450	OTU 5	*Nitrosomonas* sp. IWT514	gi|13958147|gb|AF363293.1|AF363293	100

Despite the stable nitrite build-up over the long term, positive PCR amplifications were also obtained for NOB in all the DNA isolations using FGPS (*Nitrobacter*) and NSR (*Nitrospira*) primer sets, which were chosen to search for the main NOB groups in wastewater treatment plants. Sequences for *Nitrobacter* showed high homology with *Nitrobacter winogradskyi* (99%), while *Nitrospira* sequences matched perfectly (100% homology) with *Candidatus* Nitrospira defluvii. All the sequences from each amplification belonged to the same phylotype, and no changes were detected between the inoculum and the reactor samples. It was initially expected that such extreme conditions would completely remove NOB from the reactor. However, results proved that both *Nitrobacter* and *Nitrospira* were still present in the system and coexisted after 450 days of operation, which explains the very low nitrate production level (below 20 mgN-NO$_3^-$·L^{-1}) throughout the study (Figure 5.7). Finally it is important to note that despite being strongly inhibited, changes in environmental conditions may lead to the development of NOB populations and the expression of nitrite oxidation activity.

Once the different species involved in the process had been identified, efforts were focused on assessing their abundance. For this purpose, the FISH technique was used. A sample from day 450 was hybridised using different probes and analysed with a confocal laser scanning microscope. Figure 5.19 shows two FISH images, corresponding to a sample from day 450.

Figure 5.19a depicts an image hybridised with a general eubacteria probe (EUBMIX), a probe labelling all AOB (NSO190) and a specific probe for *Nitrobacter* (NIT3), while Figure 5.19b shows the results of hybridisation with a general eubacteria probe (EUBMIX), a probe labelling all AOB (NSO1225) and a specific probe for *Nitrospira* (Ntspa662).
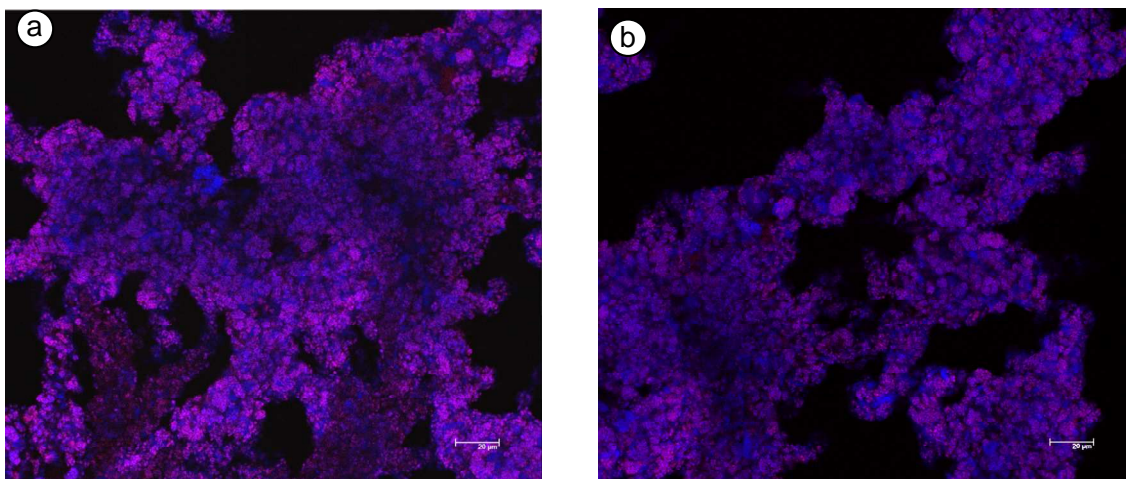
Figure 5.19 In situ hybridisation of PN-SBR sludge samples from day 450. a) probes EUBMIX (Cy5; in blue), NSO190 (FLUOS; in red) and NIT3 (Cy3; in green). b) probes EUBMIX (Cy5; in blue), NSO1225 (FLUOS; in red) and Ntspa662 (Cy3; in green)

As can be seen in the pictures, the two AOB family probes (NSO190 and NSO1225) yielded similar results, pointing to an elevated enrichment of AOB in the PN-SBR sludge. On the other hand, any presence of *Nitrobacter* or *Nitrospira* was visually undetectable.

In order to obtain an estimated quantification of AOB enrichment, FISH images quantification was performed from four different photos. The results, expressed as a percentage of the total bacteria (EUBMIX), are summarised in Table 5.6. NOB were considered as the sum of *Nitrobacter* and *Nitrospira*.

Table 5.6 Summary of FISH quantification on day 450

	Range	**Average**	**Units**
AOB	55.48-74.50	65.4±7.8	%
NOB	0.07-0.11	0.09±0.02	%

The results shown in the table corroborate the initial visual judgement. Thus, almost two out of three bacteria present in the reactor corresponded to AOB, whereas NOB were present in very low numbers (below 0.5%). The remaining bacteria fraction, about 33%, was assumed to consist of heterotrophic organisms growing on organic matter from the leachate and death products from the decay processes.

5.4.3.2 **Kinetic characterisation of the bacterial community**

Molecular techniques revealed the enrichment of the bacterial community with one AOB phylotype, although NOB organisms were still present in the system, despite the severe inhibitory conditions. Accordingly, batch experiments were carried out to gain insight, mainly, on the AOB kinetics. Studies were first focused on the assessment of possible AOB bicarbonate limitation. Then, the short-term impact of temperature and free ammonia concentration on the kinetics of not only AOB, but also NOB, were studied.

Bicarbonate substrate limitation

Batch experiments were performed to assess bicarbonate substrate limitation on AOB, according to the methodology previously described (Section 5.3.6.1). Two replicas of the experiment were carried out on different days. Figure 5.20 depicts the evolution of nitrogen compounds, as well as bicarbonate concentration during the batch experiments.
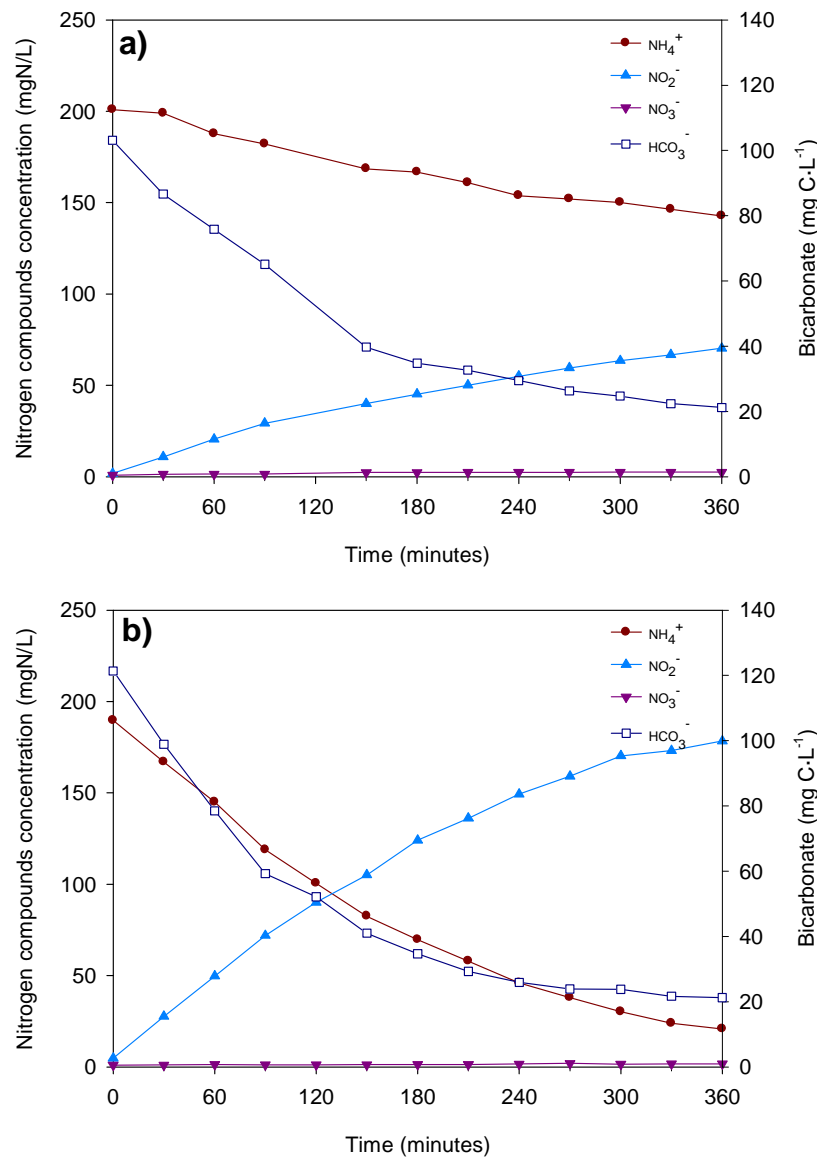
Figure 5.20 Bicarbonate limitation batch profiles at 35°C. a) Replica 1; b) Replica 2

As can be observed, in both batch experiments ammonium was progressively converted to nitrite, while no nitrate production was detected. Both graphs in Figure 5.20 depict a progressive decline in nitrite production, together with bicarbonate depletion. Finally, the difference between the reaction rates of the two replicas should be noted; this may be attributed to the much higher biomass concentration in Replica 2 than in the first batch. In addition, the AOB enrichment of the sludge may also have led to variations in the results.

Under batch conditions, AOB activity may only be limited by bicarbonate substrate limitation. Therefore, the NPR observed (linked to bicarbonate concentrations) may be related to the maximum NPR by substrate limiting kinetic expression. In the previous chapter, a Monod-type equation yielded a better fit with the experimental data than a Sigmoidal kinetic (proposed by Wett and Rauch, 2003, and Guisasola *et al.*, 2007). However, it is also important to keep in mind the important uncertainty associated to that fitting since FNA inhibition also contributed to the reduction in activity.

In order to study bicarbonate substrate limitation more deeply, the experimental data was fitted to two kinetic expressions (Equations 5.1 and 5.2).

$$NPR_{obs} = NPR_{obs}^{max} \cdot \frac{HCO_3^-}{k_{HCO_3^-} + HCO_3^-} \qquad \textbf{(Eq. 5.1)}$$

$$NPR_{obs} = NPR_{obs}^{max} \cdot \frac{e^{((HCO_3^- - k_{HCO_3^-})/a)}}{e^{((HCO_3^- - k_{HCO_3^-})/a)} + 1} \qquad \textbf{(Eq. 5.2)}$$

The experimental data, as well as the adjustment of the two kinetic expressions to these data, are depicted in Figure 5.21. The results of the adjustment are gathered in Table 5.7.
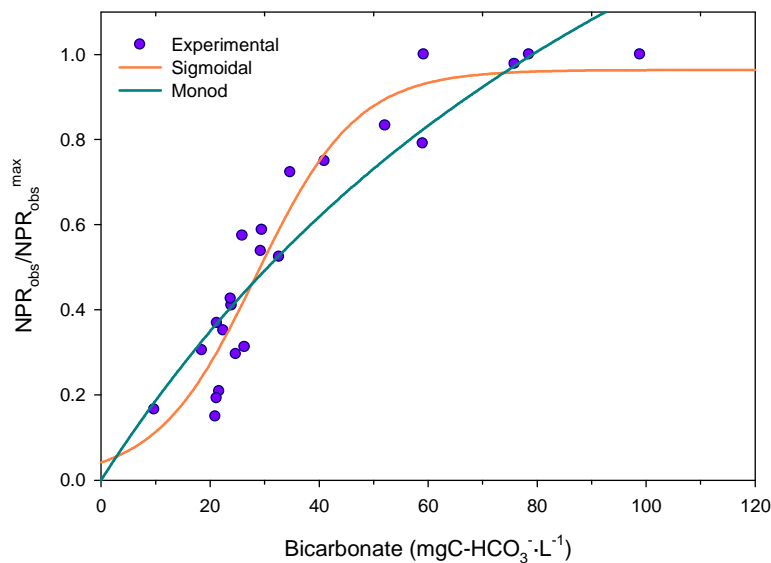
Figure 5.21 Experimental data and kinetic fitting

Table 5.7 Results of the adjustment of the two kinetic expressions

Kinetic expression	r^2	$k_{HCO_3^-}$ [mgC-HCO$_3^-$·L^{-1}]
Sigmoidal	0.9138	28.49±1.49
Monod	0.8517	134.28±53.21

From a visual point of view, as well as from the adjustment results, the Sigmoidal kinetic yielded a much better fitting than the Monod expression. In this experiment, a bicarbonate half-saturation constant of 28.5 mgC-HCO$_3^-$·L^{-1} for AOB organisms was found, which is a long way from the value determined in the previous chapter, but is more trustworthy, since it was obtained from specifically targeted experiments. In order to widen the perspective of the analysis, this result is compared with that obtained by other authors (see Table 5.8).

Table 5.8 Comparison of different half-saturation constants for bicarbonate

Source	Constant value	Units
This study	28.5	mgC-HCO$_3^-$·L^{-1}
Wett and Rauch (2003)	50	mgC-HCO$_3^-$·L^{-1}
Guisasola *et al.* (2007)	13.32	mgC-HCO$_3^-$·L^{-1}

As can be seen from the table, the bicarbonate half-saturation constant obtained in this study is lower than the one found by Wett and Rauch (2003) and slightly higher than the one determined by Guisasola *et al.* (2007). Nevertheless, all three constants are at a similar order of magnitude and point to a significant growth-reduction effect linked to bicarbonate substrate limitation. It must be emphasised that different AOB phylotypes may present different kinetic characteristics, which could explain the differences between the constants determined in each study.

Determination of the bicarbonate substrate limitation constant may allow the results obtained in the analysis of the inhibitory effect of FA, FNA, and HCO$_3^-$ limitation on AOB (Section 4.4.2) to be reassessed. Once IC substrate limitation is quantified, inhibition of FA and FNA may be evaluated more properly. Nevertheless, it is also important to take into account that this exercise might be biased since the two experiments were performed for two different bacterial communities, which could be composed by different phylotypes, and present different degrees of AOB enrichment.

Therefore, results were recalculated to take into account the findings of the specifically targeted experiment for the assessment of bicarbonate substrate limitation. The kinetic fitting was redone, using the Sigmoidal kinetic and the half-saturation constant value, and the results for both adjustments are shown in Table 5.9.

Table 5.9 Results of the kinetic fitting obtained in Section 4.4.2 and the new proposal

Kinetic model	r^2	OUR max $mgO_2 \cdot L^{-1}$	$k_{I,FA}$ $mgN \cdot L^{-1}$	$k_{I,FNA}$ $mgN \cdot L^{-1}$	k_{HCO3-} $mgC \cdot L^{-1}$
$OUR_{obs} = OUR_{obs}^{max} \frac{k_{I,FA}}{k_{I,FA} + FA} \frac{k_{I,FNA}}{k_{I,FNA} + FNA} \frac{HCO_3^-}{k_{HCO_3^-} + HCO_3^-}$	0.9571	112.97±4.14	605.48±87.18	0.49±0.09	0.01±0.16
$OUR_{obs} = OUR_{obs}^{max} \frac{k_{I,FA}}{k_{I,FA} + FA} \frac{k_{I,FNA}}{k_{I,FNA} + FNA} \frac{e^{((HCO_3^- - k_{HCO_3^-})/a)}}{e^{((HCO_3^- - k_{HCO_3^-})/a)} + 1}$	0.9593	230.83±8.27	435.00±135.20	0.49±0.05	28.49±1.49

As can be observed, results obtained using the Sigmoidal kinetic to model bicarbonate limitation (setting the bicarbonate half-saturation constant at 28.5 mgC-HCO$_3^-$·L^{-1}) are slightly different; the maximum activity predicted is twice as high as that previously obtained (113 mgO$_2$·L^{-1} vs. 231 mgO$_2$·L^{-1}). A lower value for the FA inhibition constant was obtained, while the FNA inhibition constant presented the same value. It must be mentioned that the *a* value obtained for this fitting was much higher (475.26) than that obtained in the specifically targeted experiment (9.1849). Finally it is important to emphasise that results are not comparable, since were obtained for different kinetic expressions.

Temperature and free ammonia

Batch experiments were performed in the fermenters at three temperatures - 15, 25 and 35ºC - with the aim of evaluating the short-term impact of temperature on the AOB and NOB populations of the reactor, However, these studies had a double aim since also pretended to assess the effects of free ammonia on the two bacterial populations, and its role as a substrate and inhibitor. The experiments were carried out at initial concentration of 200 and 2,000 mgN-NH$_4^+$·L^{-1}. The batch studies mainly focused on sludge acclimated to high ammonium concentrations and temperature (acclimated sludge; AC), but non-acclimated sludge (NAC) from a conventional WWTP was also used in the assays. The experiments with non-acclimated sludge were used to assess the behaviour of a NAC to different characteristics, and examine its differential response in comparison with PN-SBR sludge (acclimated sludge).

The experiments were conducted in accordance with the methodology described in Section 5.3.6.2. Each batch was performed twice to get two data set replicas. As an example of the batch results, the evolutions of ammonium, nitrite and nitrate for the first replica are shown in Figure 5.22 as percentages. Figure 5.22a and Figure 5.22b correspond to acclimated sludge at the two influent ammonium concentrations (200 mgN-NH$_4^+$·L^{-1} and 2,000 mgN-NH$_4^+$·L^{-1}), while Figure 5.22c and Figure 5.22d relate to non-acclimated sludge. Finally, the graphs distinguish between temperatures (15, 25 and 35ºC).
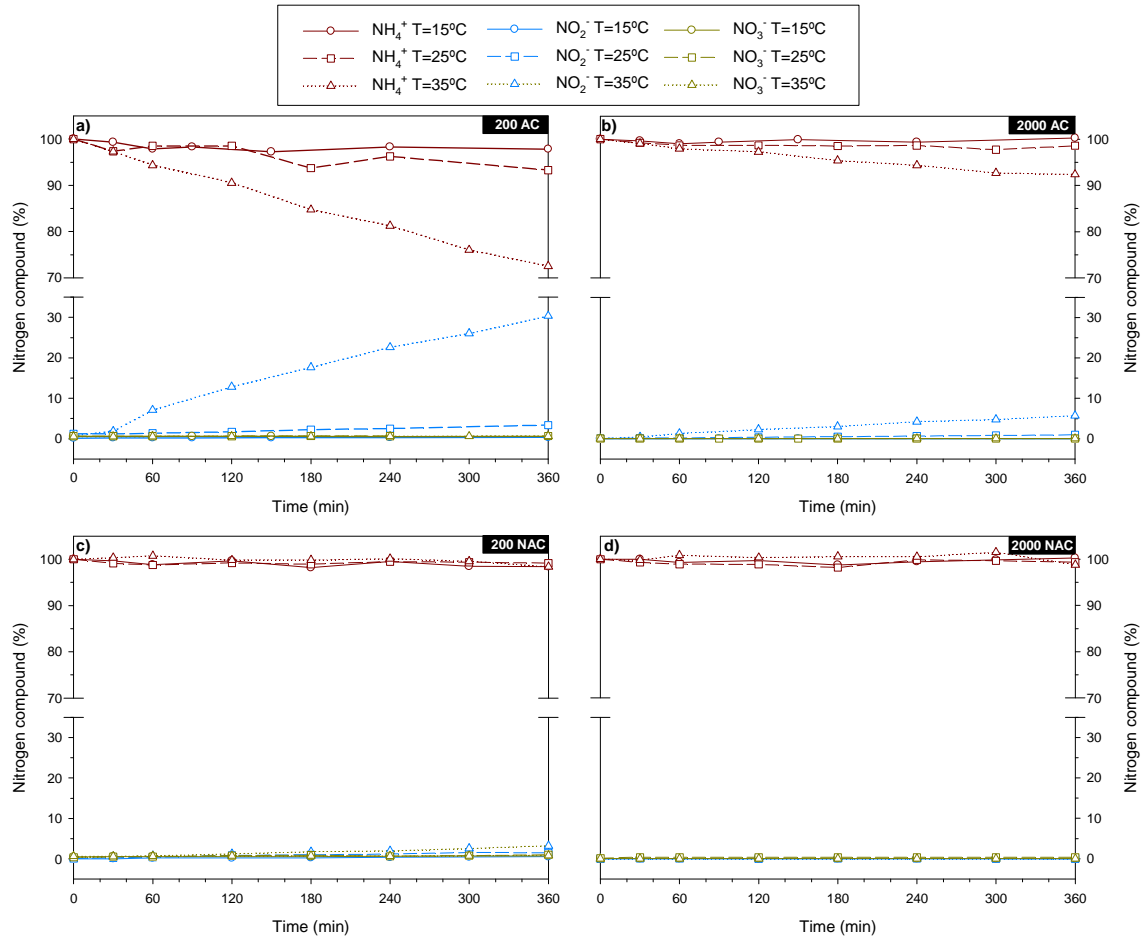
Figure 5.22 First batch replica. Evolution of the nitrogen compounds as percentages for temperatures of 15ºC, 25ºC and 35ºC. a) 200mgN-$NH_4^+\cdot L^{-1}$ and AC sludge; b) 2,000mgN-$NH_4^+\cdot L^{-1}$ and AC sludge; c) 200mgN-$NH_4^+\cdot L^{-1}$ and NAC sludge; d) 2,000mgN-$NH_4^+\cdot L^{-1}$ and NAC sludge

From Figure 5.22 it can be clearly observed that nitrogen conversions were apparently higher in the acclimated sludge experiments, and that reaction rates were higher for higher temperatures. In addition, it can be also seen that no nitrate production was detected at any concentration or temperature for the acclimated sludge. Regarding NAC sludge, very few changes in the nitrogen compounds were detected. In this way, almost no activity was observed at 15ºC and 200 mgN-$NH_4^+\cdot L^{-1}$ (Figure 5.22c). However, at this concentration slight amounts of nitrite were produced at 25ºC, which increased at 35ºC. In contrast to the situation with acclimated sludge, significant nitrate production was observed for non-acclimated sludge at different temperatures. Regarding the behaviour of NAC sludge at 2,000 mgN-$NH_4^+\cdot L^{-1}$ (Figure 5.22d), insignificant nitrite and nitrate production was detected at all temperatures, indication that AOB and NOB activity were severely inhibited.

The changes in the nitrogen profiles depicted in Figure 5.22 are barely noticeable due to the scale of the graphs, but in any case the interpretation of these profiles it is not straightforward, because biological conversion rates are subject to the amount of biomass in each batch. Accordingly, in order to summarise all this information in a clear and understandable way, the

ammonium and nitrite oxidation rates (AOR and NOR) have been calculated for each batch, and averaged for the two replicas. Results for acclimated (AC) sludge are represented as a function of temperature, distinguishing between 200 and 2,000mgN·L^{-1} as the initial ammonium concentration (Figure 5.23a). Figure 5.23b also depicts the initial free ammonia levels as a function of temperature and initial ammonium concentration.
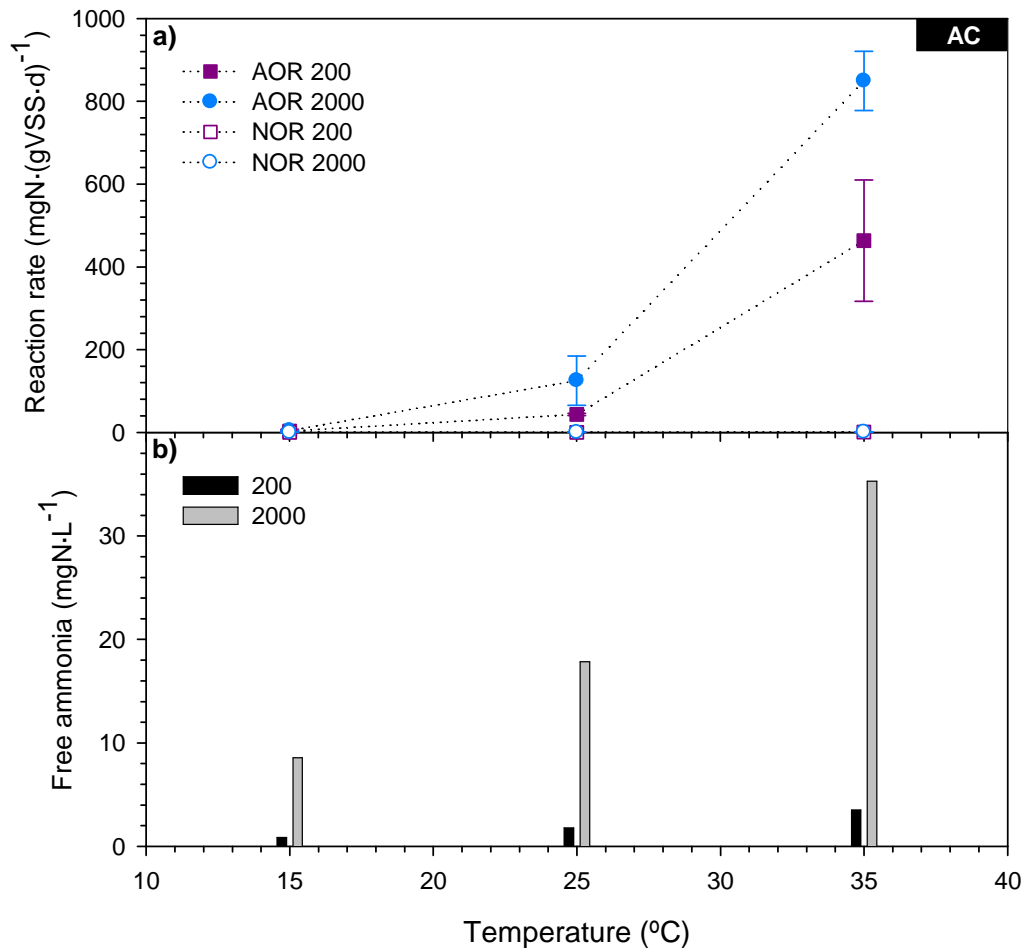
Figure 5.23 Acclimated sludge. a) AOR and NOR as a function of temperature and initial ammonium concentration; b) Initial free ammonia as a function of temperature and initial ammonium concentration

Figure 5.23a shows that the AOR and NOR were very low at a temperature of 15ºC for both initial ammonium concentrations. With an increase in temperature it can be seen how the AOR increased slightly, while the NOR evolved to values close to zero. However, the figure also shows differential behaviour between the batches at initial ammonium concentrations of 200 and 2,000 mgN·L^{-1}. Thus, experiments at 2,000 mgN·L^{-1} yielded a higher AOR (between 100 and 150 mgN·gVSS^{-1}·d^{-1}) than that obtained at 200 mgN·L^{-1} (around 50 mgN·gVSS^{-1}·d^{-1}). The same behaviour can be observed at 35ºC if AORs at 200 and 2,000 mgN·L^{-1} are compared. In this case, the disparity is visually clearer. One hypothesis for this differential behaviour is AOB activity reduction due to free ammonia substrate limitation. Lochtman (1995) reported a K$_{NH3}$ of 0.468 mgN-NH$_3$·L^{-1}, and Wiesmann (1994) and Van Hulle *et al.* (2007) found higher constant

values of 0.71 mgN-NH$_3$·L^{-1} and 0.75 mgN-NH$_3$·L^{-1} respectively. When these constant values and the FA measurements are taken into account, noticeable activity reduction may take place under batch conditions. The magnitude of the activity loss is dependent on the constant, but could reach 20% and 30% of activity reduction at 35ºC and 25ºC respectively.

These findings are in agreement with the bacterial community characterisation. Molecular techniques identified *Nitrosomonas* as the dominant AOB species in the acclimated sludge. This AOB group is known to be an r-strategist, with low affinity for the substrate, but high reaction rates (Sundberg *et al.*, 2007; Yuan *et al.*, 2008).

Results of the experiments with the non-acclimated (NAC) sludge are summarised in Figure 5.24.
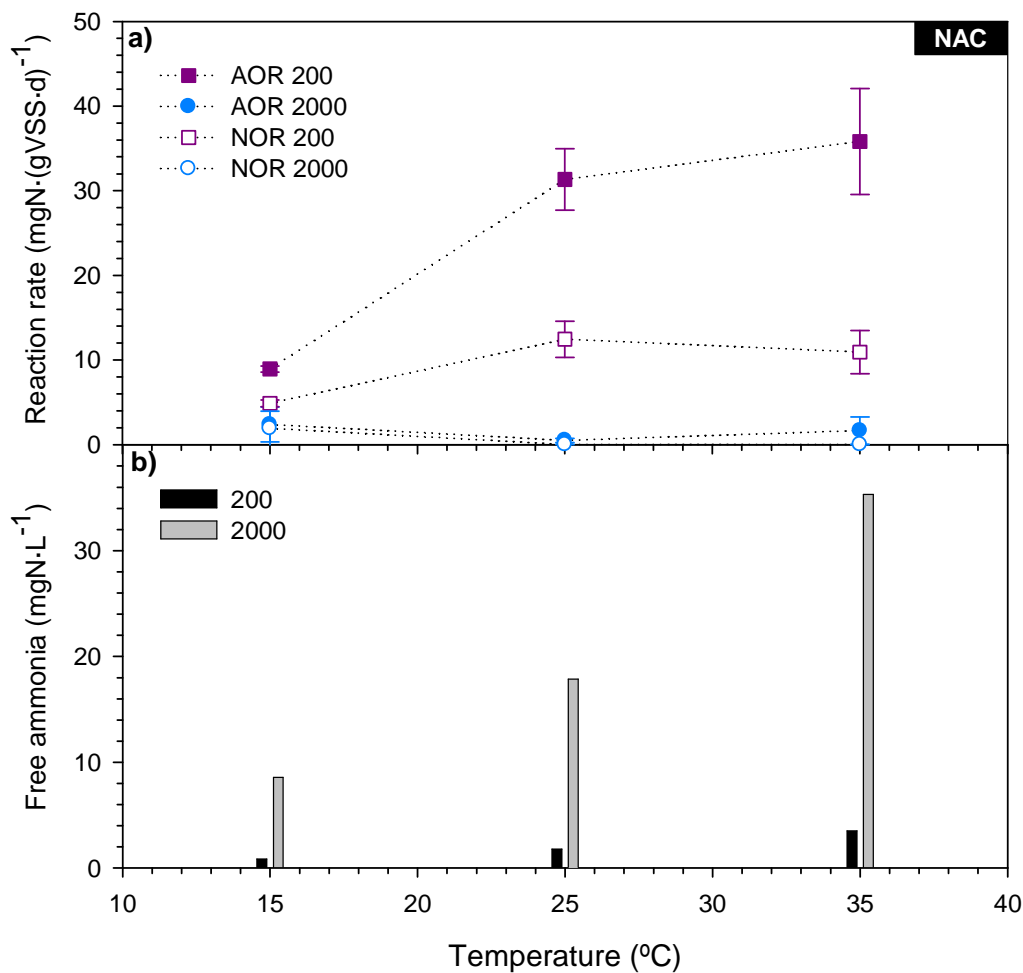
Figure 5.24 Non-acclimated sludge. a) AOR and NOR as a function of temperature and initial ammonium concentration; b) Initial free ammonia as a function of temperature and initial ammonium concentration

As depicted in Figure 5.24a, the AOR and NOR for the batch at 200 mgN·L^{-1} were quite low, about 10 mgN·(gVSS·d)$^{-1}$, although unlike acclimated sludge, the NOR were not 0. The batch

experiments yielded significantly higher rates for both AOR and NOR at a temperature of 25ºC. Regarding the results with an initial concentration of 200 mgN·L^{-1} at 35ºC, the AOR measured in the batch were slightly higher (about 40 mgN·gVSS·d^{-1}) than those measured at 25ºC. Nevertheless, the rise in the ammonium oxidation rates was less significant than the obtained when the temperature was increased from 15º to 25ºC. On the other hand, the NOR at 35ºC were slightly lower than those measured at 25ºC lower. With regards to the batch at an initial ammonium concentration of 2,000 mgN·L^{-1}, both AOR and NOR measured at 15ºC were lower than for the low concentration batch, yielding values around 2 mgN·gVSS·d^{-1}. These low AOR and NOR rates declined with an increase in temperature.

From these results, one can conclude a different behaviour of the non-acclimated sludge, in contrast to the sludge from the PN-SBR. Reaction rates were more elevated at lower FA concentration, indicating that FA substrate limitation must be less important than the inhibitory effects of free ammonia. Non-acclimated sludge usually presents a higher affinity for the substrate, but is more sensitive to the low concentrations of this compound and may be inhibited at very low FA levels. This is consistent with the findings of these experiments. Furthermore, NOB are more susceptible to inhibitions than AOB (Anthonisen *et al.*, 1976; Vadivelu *et al.*, 2007), explaining why AOR are always higher than NOR. These results confirm the importance of free ammonia as a mechanism for out-competing NOB organisms, but also as a threat to AOB development, due to the potential it has to inhibition to their activity.

As a final remark, it should be noted that the experiments with acclimated and non-acclimated sludge were performed very close to each other in time, so that no significant changes in the bacterial community could take place. Therefore, the correction to the reaction rates by the amount of active biomass is enough to make the results comparable, since one can assume the same proportion of AOB in the sludge. However, attention should be paid when comparing AC and NAC results, since the reactor rate correction by VSS does not take into account the enrichment of sludge in AOB and NOB. Acclimated sludge may present higher amounts of AOB organisms per gram of VSS (and probably lower quantities of NOB) than non-acclimated sludge coming from the Sils-Vidreres WWTP, and therefore non-acclimated sludge could not yield similar specific rates than acclimated sludge, even under optimal operational conditions. This may explain the wide differences between the AOR of acclimated and non-acclimated sludge.

5.5 Conclusions

This chapter has proven the feasibility of long-term stable nitrite build-up in a PN-SBR treating raw urban landfill leachate with extremely high ammonium concentrations (up to 5,000 mgN–

$NH_4^+ \cdot L^{-1}$). During the period under study a suitable influent to feed an anammox reactor (about 1.32 moles of nitrite per mole of ammonium) was produced.

The operational strategy, based on an anoxic–aerobic step-feed cycle, helped to reduce the amount of total nitrogen in the reactor and diminish the inhibition of FA and FNA over AOB. However, the denitritation process still required upgrading, since an optimal cycle design may lead to a higher organic matter removal under anoxic conditions.

The control of the $HCO_3^-:NH_4^+$ molar ratio in the influent was confirmed as the key for achieving a suitable nitrite to ammonium effluent molar ratio. On-line parameter analyses enabled the different phenomena taking place in the reactor to be identified. Finally, oxygen consumption was verified as a useful tool for the process assessment, and could be used in view of an on-line control of the system.

Molecular techniques enabled the identification of *Nitrosomonas sp.* IWT514 as the only AOB phylotype present in the reactor at the end of the study. *Nitrobacter winogradskyi* and *Candidatus* Nitrospira defluvii were also detected, revealing that NOB were not completely removed from the system. In addition, FISH analyses allowed a relative quantification of AOB enrichment in the sludge, with percentages of 66% of AOB, in respect to the total *Eubacteria*. In contrast, the percentages for NOB were below 1%.

Kinetic characterisation allowed the boundaries of bicarbonate substrate limitation in this AOB population to be identified. Batch experiments also highlighted the important temperature dependency of AOB activity. Finally these experiments allowed characterising the AOB population in the acclimated sludge, presenting high tolerance to FA inhibitory effects and low substrate affinity.

Chapter 6. MODELLING PARTIAL NITRITATION

6.1 Motivation

The previous chapters demonstrated the feasibility of achieving successful partial nitritation using sequencing batch reactor (SBR) technology for the treatment of highly-loaded nitrogen streams. However, despite the experience acquired, the reactor's response to changes in the operational conditions and influent characteristics was not always easy to understand or predict, given the complexity of the system in terms of interactions between oxygen supply, CO_2 stripping, alkalinity, pH, inhibition effects and nitrification kinetics, among others factors.

Mathematical models can be useful tools for increasing the process knowledge and helping to acquire a better understanding of the biological processes and physical phenomena taking place in a partial nitritation-sequencing batch reactor (PN-SBR). Traditional modelling has assumed nitrification and denitrification as single-step processes (Henze *et al.*, 2000), but when modelling a partial nitritation system it is necessary to consider nitrite as an intermediary step in nitrification and denitrification. There are, nowadays, several biological models describing nitrite build-up, as reviewed by Sin *et al.* (2008). Some of these models focus on the treatment of highly-loaded streams (Hellinga *et al.*, 1999; Volcke *et al.*, 2002; Wett and Rauch, 2003; among others) and can be used as a basis when modelling specific processes. Nevertheless, it is clear that existing models may need to be modified or extended to include all physical-chemical processes and biochemical transformations relevant to a given application. Besides, the model needs to be calibrated for specific influent and process parameters. This is illustrated in this study for partial nitrification of landfill leachate in an SBR, aimed at increasing process knowledge (e.g. quantifying interactions between aeration, CO_2 stripping, alkalinity, pH, nitrification kinetics) and focusing on the short-term dynamics (based on the cycle). The work also deals with the usefulness of a systematic calibration guideline and its refinement.

6.2 Objectives

The main aim of this chapter is develop, calibrate and validate a mathematical model of a partial nitritation-sequencing batch reactor (PN-SBR) for the treatment of urban landfill leachate. The model will focus on increasing process understanding. During the calibration procedure, the calibration guideline will be refined by adding an identifiability analysis step and statistics for the quality check at the evaluation stage. Finally, once the tool has been developed, it will be applied to a specific problem, the assessment of nitrite build-up under different influent and operational conditions.

6.3 Model development

The partial nitritation SBR model was based on the SHARON model developed by Volcke *et al.* (2002). The model mainly consists of a liquid phase in which the biological reactions and the physical-chemical phenomena take place. This liquid phase is in equilibrium with a gas phase, both assumed to be perfectly mixed. Transport phenomena between these phases are taken up, and the model also considers pH calculation.

6.3.1   Liquid phase mass balance

The liquid phase volume and the concentration of individual compounds were calculated from mass balances. The mathematical development of these balances is briefly described next. A deeper insight can be found in Volcke (2006a).

6.3.1.1   General liquid phase mass balance

In general terms, the liquid volume in an SBR reactor is determined by the influent and effluent mass flow rates, the waste flow, and the volume added from external sources (pH control, and carbon source addition among others). Evaporation phenomena can sometimes significantly affect the liquid balances when dealing with small reactors. However, this balance only holds true if a constant density for all the streams is assumed. Equation 6.1 shows the general mass balance.

$$\frac{d(V_L)}{dt} = Q_L^{in} + Q_{acid} + Q_{base} + Q_{C\,source} - Q_L^{out} - Q_L^{waste} - Q_{evap.} \qquad \textbf{(Eq. 6.1)}$$

where V_L is the reactor volume (L), Q_L^{in} is the inflow (L·d^{-1}), Q_{acid} is the amount of acid dosed (L·d^{-1}), Q_{base} is the amount of base dosed (L·d^{-1}), $Q_{Csource}$ is the amount of carbon source added to the system (L·d^{-1}), Q_L^{out} is the outflow (L·d^{-1}), Q_L^{waste} is the waste flow (L·d^{-1}) and $Q_{evap.}$ is the volumetric reactor liquid loss due to evaporation (L·d^{-1}).

Depending on the phases, some of these terms would be equal to zero (i.e. during the filling events, leachate is supplied from the inflow, but the reactor is not drawn). In addition, the volumetric overall mass balance for the PN-SBR could be simplified, since no base and carbon source were added, and no purge was carried out. From experimental data the contribution of evaporation effects was determined as negligible. The simplified overall liquid phase balance could be expressed as:

$$\frac{d(V_L)}{dt} = Q_L^{in} + Q_{acid} - Q_L^{out} = Q_L^{in,net} - Q_L^{out} \qquad \textbf{(Eq. 6.2)}$$

where $Q_L^{in,net}$ is the net inflow (L·d^{-1})

Finally, it is important to mention the fact that the reactor draw was performed by gravity discharge, meaning that reactor volume could never become lower than the minimum water volume (V_{min}).

6.3.1.2 **Individual mass balances**

The model aims to predict the biochemical transformations of nitrogen and organic matter by different bacterial groups. The growth of these organisms is also dependent on other substrates, such as oxygen, inorganic carbon, phosphorus etc., which must also be taken up. Accordingly, a total of 21 components were considered in the liquid phase: NH_4^+, NH_3, NO_2^-, HNO_2^-, NO_3^-, N_2, CO_3^{2-}, HCO_3^-, CO_2, $H_2PO_4^-$, HPO_4^{2-}, X_{AOB}, X_{NOB}, X_H, S_S, S_I, X_S, X_I, O_2, H^+ (pH) and Z^+ (which is an artificial variable accounting for the amount of net positive charges of ionised species originating from acids or bases). Note that the first dissociation for the phosphate equilibrium has not been taken up since occurs at a pH of around 2, where biological reactions may not take place.

The concentration of some of these compounds is governed by chemical equilibriums subject to pH and temperature variations. These equilibriums are shown in Equations 6.3 to 6.7, while the equilibrium constants as a function of temperature are listed in Table 6.1.

$$NH_4^+ \Leftrightarrow NH_3 + H^+ \qquad \text{(Eq. 6.3)}$$

$$HNO_2 \Leftrightarrow NO_2^- + H^+ \qquad \text{(Eq. 6.4)}$$

$$CO_2 + H_2O \Leftrightarrow HCO_3^- + H^+ \Leftrightarrow CO_3^{2-} + 2H^+ \qquad \text{(Eq. 6.5)}$$

$$H_2PO_4^- \Leftrightarrow HPO_4^{2-} + H^+ \qquad \text{(Eq. 6.6)}$$

$$H_2O \Leftrightarrow OH^- + H^+ \qquad \text{(Eq. 6.7)}$$
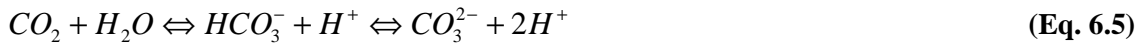
Table 6.1 Chemical equilibrium constants as a function of temperature

Constant	Expression	Units	Source
K_{e,NH_3}	$\exp\left(-\dfrac{6344}{T}\right)$	mmole·m^{-3}	Anthonisen *et al.* (1976)
K_{e,HNO_2}	$\exp\left(-\dfrac{2300}{T}\right)$	mmole·m^{-3}	Anthonisen *et al.* (1976)
K_{e,CO_2}	$10^{\left(-356.3094-0.06091964\cdot T+\frac{21834.37}{T}+126.8339\cdot\log_{10}T-\frac{1684915}{T^2}\right)}$	mmole·m^{-3}	Stumm and Morgan (1996)
K_{e,HCO_3^-}	$10^{\left(-107.8871-0.03252849\cdot T+\frac{5151.79}{T}+38.92561\cdot\log_{10}T-\frac{563713.9}{T^2}\right)}$	mmole·m^{-3}	Stumm and Morgan (1996)
$K_{e,H_2PO_4^-}$	$-\dfrac{1979.5}{T}+5.3541-0.01984\cdot T$	mmole·m^{-3}	Helgeson (1967)
K_w	$10^{\left(-283.971+\frac{13323}{T}-0.05069842\cdot T+102.24447\cdot\log_{10}T-\frac{1119669}{T^2}\right)}$	mmole^2·m^{-6}	Stumm and Morgan (1996)

Changes in equilibrium compounds affect the concentration of each individual chemical component involved in the equilibrium. To solve this, Volcke (2006a) suggested grouping the equilibrium compounds in lumped components accounting for the sum of the total concentration of each active component. In the model, therefore, lumped components were taken up in the individual mass balances, instead of equilibrium components. Equations 6.8 - 6.11 summarise these lumped compounds, and their composition.

$$NH = NH_4^+ + NH_3 \qquad \text{(Eq. 6.8)}$$

$$NO2 = NO_2^- + HNO_2 \qquad \text{(Eq. 6.9)}$$

$$IC = CO_3^{2-} + HCO_3^- + CO_2 \qquad \text{(Eq. 6.10)}$$

$$IP = HPO_4^{2-} + H_2PO_4^- \qquad \text{(Eq. 6.11)}$$

Next step was the definition of the different state variables considered in the model. These variables were defined in the classical activated sludge models (ASM) nomenclature (Henze *et al.*, 2000) and expressed in the same units, in contrast to the model developed by Volcke (2006a), which included state variables on a molar basis.

Table 6.2 gathers together the state variables taken up in the liquid phase.

Table 6.2 State variables in the liquid phase

Variable	Description	Units
S_{NH}	Total ammonium and ammonia nitrogen	$gN \cdot m^{-3}$
S_{NO2}	Total nitrite and nitrous acid nitrogen	$gN \cdot m^{-3}$
S_{NO3}	Total nitrate nitrogen	$gN \cdot m^{-3}$
S_{N2}	Total nitrogen gas	$gN \cdot m^{-3}$
S_{IC}	Total inorganic carbon	$gC \cdot m^{-3}$
S_{O2}	Dissolved oxygen	$gO_2 \cdot m^{-3}$
S_{IP}	Total inorganic Phosphorus	$gP \cdot m^{-3}$
X_{AOB}	Ammonium oxidising bacteria biomass	$gCOD \cdot m^{-3}$
X_{NOB}	Nitrite oxidising bacteria biomass	$gCOD \cdot m^{-3}$
X_H	Heterotrophic biomass	$gCOD \cdot m^{-3}$
S_S	Readily biodegradable organic matter	$gCOD \cdot m^{-3}$
S_I	Inert soluble organic matter	$gCOD \cdot m^{-3}$
X_S	Slowly biodegradable substrates	$gCOD \cdot m^{-3}$
X_I	Inert particulate organic matter	$gCOD \cdot m^{-3}$
Z^+	Net positive charges	$moleZ^+ \cdot m^{-3}$

It is important to note that H^+ concentration was not included as a state variable, since it was calculated from a charge balance. The pH calculation procedure is further discussed in *pH calculation* (Section 6.3.3.1).

106

Once the different state variables in the liquid phase had been identified, the next step was to define the individual mass balance. Equation 6.12 depicts the general mass balance for a certain compound, i, with a concentration of C_i. It is important to highlight that this mass balance is only valid for SBR operational phases with a complete mixture (feeding, aerobic reaction, anoxic reaction etc.).

$$\frac{d(V_L \cdot C_{L,i})}{dt} = Q_L^{in} \cdot C_{L,i}^{in} - Q_L^{out} \cdot C_{L,i} + k_L a_i \cdot (C_{L,i}^* - C_{L,i}) \cdot V_L + r_{i,L} \cdot V_L \qquad \textbf{(Eq. 6.12)}$$

where $C_{L,i}$ is the concentration of the component i in the liquid phase (mg·L^{-1}), $C_{L,i}^{in}$ is the concentration of the component i in the influent (mg·L^{-1}), $k_L a_i$ is the volumetric mass transfer coefficient (d^{-1}), $C_{L,i}^*$ is the saturation concentration of the component i (mg·L^{-1}), and $r_{i,L}$ is the volumetric conversion rate of the component i (mg·L^{-1}·d^{-1}).

This general expression quantifies the accumulation of a certain component in the liquid phase, and takes into account the influent ($Q_L^{in} \cdot C_{L,i}^{in}$) and effluent ($Q_L^{out} \cdot C_{L,i}$) fluxes, the transference between the liquid and the gas phase ($k_L a_i \cdot (C_{L,i}^* - C_{L,i})$), and the biological transformations ($r_{i,L} \cdot V_L$).

Assuming that:

$$\frac{d(V_L \cdot C_{L,i})}{dt} = V_L \cdot \frac{d(C_{L,i})}{dt} + C_{L,i} \cdot \frac{d(V_L)}{dt} \qquad \textbf{(Eq. 6.13)}$$

Then the general equation can be expressed as Equation 6.14.

$$V_L \frac{d(C_{L,i})}{dt} + C_{L,i} \cdot \frac{d(V_L)}{dt} = \left[Q_L^{in} \cdot C_{L,i}^{in} - Q_L^{out} \cdot C_{L,i} \right] + k_L a_i \cdot (C_{L,i}^* - C_{L,i}) \cdot V_L + r_{i,L} \cdot V_L \quad \textbf{(Eq. 6.14)}$$

Nevertheless, given the overall liquid mass balance (Eq. 6.2), the previous expression can be converted to Equation 6.15.

$$V_L \frac{d(C_{L,i})}{dt} = \left[Q_L^{in} \cdot C_{L,i}^{in} - Q_L^{out} \cdot C_{L,i} \right] + k_L a_i \cdot (C_{L,i}^* - C_{L,i}) \cdot V_L + r_{i,L} \cdot V_L - C_{L,i} \cdot (Q_L^{in,net} - Q_L^{out}) \quad \textbf{(Eq. 6.15)}$$

Finally, the individual mass balance of a component can be written as follows:

$$\frac{d(C_{L,i})}{dt} = \frac{\left[Q_L^{in} \cdot C_{L,i}^{in} - Q_L^{in,net} \cdot C_{L,i} \right]}{V_L} + k_L a_i \cdot (C_{L,i}^* - C_{L,i}) + r_{i,L} \qquad \textbf{(Eq. 6.16)}$$

This general expression is valid for state variables affected by biological conversion, and involved in transport phenomena between the liquid and the gas phase, such as S_{NH}, S_{N2}, S_{IC} and S_{O2}. However, it must be adapted for each specific compound. For variables with no liquid-air transference (S_{NO2}, S_{NO3}, S_{IP}, S_S, X_{AOB}, X_{NOB}, X_H, X_S and X_I), it could be simplified to Equation 6.17:

$$\frac{d(C_{L,i})}{dt} = \frac{\left[Q_L^{in} \cdot C_{L,i}^{in} - Q_L^{in,net} \cdot C_{L,i}\right]}{V_L} + r_{i,L}$$

(Eq. 6.17)

The differential equation for S_I and Z^+ can be simplified in the same way, since these variables are not involved in any biological conversion and/or transferences to the gas phase. Thus, the specific expression for them is:

$$\frac{d(C_{L,i})}{dt} = \frac{\left[Q_L^{in} \cdot C_{L,i}^{in} - Q_L^{in,net} \cdot C_{L,i}\right]}{V_L}$$

(Eq. 6.18)

Finally, SHARON reactors are operated on a continuous fashion. Therefore, no separation between solid and liquid was considered in the model developed by Volcke (2006a). Nevertheless, SBR are operated discontinuously with solid-liquid separation, and settling and draw phases were modelled considering the PN-SBR as a point settler without reaction, with a fraction of suspended solids being removed by the outflow (which is further described in the definition of the settler model). The reactor volume decreased until it reached the minimum volume, while the concentration of soluble compounds remained unaltered during these phases. Conversely, the concentration of particulate state variables (X_{AOB}, X_{NOB}, X_H, X_S and X_I) diminished due to the loss of suspended solids by the draw. This is represented by f_{ns}, the fraction of non-settable suspended solids. The concentration of particulate state variables on the reactor and outflow was calculated at the end of the draw phase by algebraic equations. The concentration of effluent particulate compounds can be expressed as:

$$C_{L,i}^{out} = \frac{C_{L,i} \cdot V_L \cdot f_{ns}}{V_{max} - V_{min}}$$

(Eq. 6.19)

where f_{ns} is the non-settable fraction of the particulate compounds, and V_{max} is the reactor volume at the end of the cycle (L), which should be equal to V_L

Based on this balance, the concentration of the particulate state variables (X_{AOB}, X_{NOB}, X_H, X_S and X_I) in the reactor at the end of the draw phase can be calculated as:

$$C_{L,i}^{reactor} = \frac{C_{L,i} \cdot (1 - fns) \cdot V_L}{V_{min}}$$

(Eq. 6.20)

108

6.3.2 Biological conversion reactions

The biological model was adapted from the SHARON model defined by Volcke (2006a) -on its turn based on the one from Hellinga (1999)- and extended on the basis of the specificities of the process under study. Thus, ammonium and nitrite oxidation kinetics were modified by including growth limitation terms, and organic matter processes were also adapted. The system modelled by Volcke presented low concentrations of organic matter, and heterotrophic bacteria activity was only considered to take place under methanol dosing. In contrast, the leachate treated in the PN-SBR presented high amounts of organic matter, with variable biodegradable fractions. Accordingly, the biological model included aerobic and anoxic organic matter consumption, as well as the hydrolysis of the slowly biodegradable fraction. These processes were adopted from different sources (basically from ASM models). In addition, the endogenous respiration of each biomass under aerobic and anoxic conditions was also included.

Next, the 15 processes considered in the biological model, as well as their kinetics are described in detail. With regards to the model stoichiometry, is presented afterwards in Table 6.6.

1. <u>Aerobic ammonium oxidation:</u> This process describes the oxidation of NH_4^+ to NO_2^-, carried out by ammonium oxidising bacteria (AOB) under aerobic conditions. The kinetic equation, adapted from Hellinga *et al.* (1999), has been modified to take into account possible AOB inhibition due to NH_3 (in accordance with the results obtained in Chapter 4). An inorganic carbon growth limitation term has also been included to take into account possible growth reduction due to a lack of carbon source. In addition, a pH dependency term has been considered using the relationship from Henze *et al.* (1995). The same term is applied for all the microbial growth rates (μ_{max}^{AOB}; μ_{max}^{NOB}, μ_{max}^{H}) assuming they all have the same pH dependency (Volcke, 2006). It is important to keep in mind that this assumption is not strictly correct from a biological point of view, since each bacterial group (X_{AOB}, X_{NOB}, X_H) has a different optimal pH and suitable pH operating range. Nevertheless, such a simplification may not lead to significantly different results, and is a good first approach to modelling the pH effect on biological activity.

$$\rho_1 = \mu_{max}^{AOB} \cdot \frac{S_{NH_3}}{K_{NH_3}^{AOB} + S_{NH_3}} \cdot \frac{S_{O_2}}{K_{O_2}^{AOB} + S_{O_2}} \cdot \frac{K_{I,NH_3}^{AOB}}{K_{I,NH_3}^{AOB} + S_{NH_3}} \cdot \frac{K_{I,HNO_2}^{AOB}}{K_{I,HNO_2}^{AOB} + S_{HNO_2}} \cdot \frac{S_{HCO_3^-}}{K_{HCO_3^-} + S_{HCO_3^-}} \cdot \frac{K_{pH}}{K_{pH} - 1 + 10^{|pH_{opt} - pH|}} \cdot X_{AOB} \qquad \textbf{(Eq. 6.21)}$$

2. <u>Aerobic nitrite oxidation:</u> This process describes the oxidation of NO_2^- to NO_3^-, carried out by nitrite oxidising bacteria (NOB) under aerobic conditions. The equation, adapted from Hao *et al.* (2002), has been modified to take into account possible NOB inhibition

due to NH_3 and HNO_2. An inorganic carbon growth limitation term has also been included to take into account possible growth reduction due to a lack of carbon source, and a pH dependency term has also been considered.

$$\rho_2 = \mu_{max}^{NOB} \cdot \frac{S_{HNO_2}}{K_{HNO_2}^{NOB} + S_{HNO_2}} \cdot \frac{S_{O_2}}{K_{O_2}^{NOB} + S_{O_2}} \cdot \frac{K_{I,HNO_2}^{NOB}}{K_{I,HNO_2}^{NOB} + S_{HNO_2}} \cdot \frac{K_{I,NH_3}^{NOB}}{K_{I,NH_3}^{NOB} + S_{NH_3}} \cdot \frac{S_{HCO_3^-}}{K_{HCO_3^-} + S_{HCO_3^-}} \cdot \frac{K_{pH}}{K_{pH} - 1 + 10^{|pH_{opt} - pH|}} \cdot X_{NOB} \qquad \textbf{(Eq. 6.22)}$$

3. <u>Aerobic organic matter oxidation</u>: Heterotrophic biomass oxidises readily biodegradable organic matter substrates (S_S) under aerobic conditions. Accordingly, the equation has been adapted from ASM1 (Henze *et al.*, 2000), but including a pH dependency term.

$$\rho_3 = \mu_{max}^{H} \cdot \frac{S_{O_2}}{K_{O_2}^{H} + S_{O_2}} \cdot \frac{S_S}{K_{S_S}^{H} + S_S} \cdot \frac{K_{pH}}{K_{pH} - 1 + 10^{|pH_{opt} - pH|}} \cdot X_H \qquad \textbf{(Eq. 6.23)}$$

4. <u>Denitrification via nitrite</u>: Heterotrophic biomass oxidises readily biodegradable organic matter (S_S) under anoxic conditions, using nitrite as an electron acceptor. The equation, adapted from van Hulle *et al.* (2005), includes a pH dependency growth term to take into account the effect of pH on biomass growth.

$$\rho_4 = \mu_{max}^{H} \cdot \eta \cdot \frac{S_{NO_2}}{K_{NO_2}^{dNO_2} + S_{NO_2}} \cdot \frac{S_S}{K_{S_S}^{H} + S_S} \cdot \frac{S_{NO_2}}{S_{NO3} + S_{NO_2}} \cdot \frac{K_{I,O_2}}{K_{I,O_2} + S_{O_2}} \cdot \frac{K_{pH}}{K_{pH} - 1 + 10^{|pH_{opt} - pH|}} \cdot X_H \qquad \textbf{(Eq. 6.24)}$$

5. <u>Denitrification via nitrate</u>: Heterotrophic biomass oxidises readily biodegradable organic matter (S_S) under anoxic conditions using nitrate as an electron acceptor. The equation, adapted from van Hulle *et al.* (2005), also includes a pH dependency growth term to take into account the effect of pH on biomass growth.

$$\rho_5 = \mu_{max}^{H} \cdot \eta \cdot \frac{S_{NO_3}}{K_{NO_3}^{dNO_3} + S_{NO_3}} \cdot \frac{S_S}{K_{S_S}^{H} + S_S} \cdot \frac{S_{NO_3}}{S_{NO_3} + S_{NO_2}} \cdot \frac{K_{I,O_2}}{K_{I,O_2} + S_{O_2}} \cdot \frac{K_{pH}}{K_{pH} - 1 + 10^{|pH_{opt} - pH|}} \cdot X_H \qquad \textbf{(Eq. 6.25)}$$

6. <u>Aerobic hydrolysis of X_S</u>: This process makes slowly biodegradable substrates (X_S) contained in the influent available to an activated sludge system (Henze *et al.*, 2000). To model this process the approach proposed in ASM3 has been used.

$$\rho_6 = K_H \cdot \frac{X_S / X_H}{K_X + X_S / X_H} \cdot X_H \qquad \textbf{(Eq. 6.26)}$$

7, 10, 13. <u>Aerobic endogenous respiration of X_{AOB}, X_{NOB} and X_H:</u> This process describes all the forms of biomass loss and energy requirements not associated with growth by considering related respiration under aerobic conditions: decay (maintenance),

endogenous respiration, lysis, predation, motility, death etc. (Henze *et al.,* 2000). To model this process the ASM3 approach has been used.

$$\rho_7 = b_{AOB} \cdot \frac{S_{O_2}}{K_{O_2}^{AOB} + S_{O_2}} \cdot X_{AOB} \tag{Eq. 6.27}$$

$$\rho_{10} = b_{NOB} \cdot \frac{S_{O_2}}{K_{O_2}^{NOB} + S_{O_2}} \cdot X_{NOB} \tag{Eq. 6.28}$$

$$\rho_{13} = b_H \cdot \frac{S_{O_2}}{K_{O_2}^{H} + S_{O_2}} \cdot X_H \tag{Eq. 6.29}$$

8, 11, 14. Anoxic endogenous respiration of X_{AOB}, X_{NOB} and X_H on nitrate: This process is similar to the aerobic endogenous respiration of each biomass, but occurs under anoxic conditions. The equation has been adapted from Hao *et al.* (2002), but considering only NO_3^-. In addition, an extra term has been added to the equation to avoid the possibility of the denitrification rate in the presence of both NO_3^- and NO_2^- being greater than if only one of the two were present.

$$\rho_8 = b_{AOB} \cdot \eta \cdot \frac{K_{I,O_2}}{K_{I,O_2} + S_{O_2}} \cdot \frac{S_{NO_3}}{K_{NO_3} + S_{NO_3}} \cdot \frac{S_{NO_3}}{S_{NO3} + S_{NO_2}} \cdot X_{AOB} \tag{Eq. 6.30}$$

$$\rho_{11} = b_{NOB} \cdot \eta \cdot \frac{K_{I,O_2}}{K_{I,O_2} + S_{O_2}} \cdot \frac{S_{NO_3}}{K_{NO_3} + S_{NO_3}} \cdot \frac{S_{NO_3}}{S_{NO3} + S_{NO_2}} \cdot X_{NOB} \tag{Eq. 6.31}$$

$$\rho_{14} = b_H \cdot \eta \cdot \frac{K_{I,O_2}}{K_{I,O_2} + S_{O_2}} \cdot \frac{S_{NO_3}}{K_{NO_3} + S_{NO_3}} \cdot \frac{S_{NO_3}}{S_{NO3} + S_{NO_2}} \cdot X_H \tag{Eq. 6.32}$$

9, 12, 15. Anoxic endogenous respiration of X_{AOB}, X_{NOB} and X_H on nitrite: This process is similar to the aerobic endogenous respiration of each biomass, but occurs under anoxic conditions. The equation has been adapted from Hao *et al.* (2002), but considering only NO_2^-. In addition, an extra term has been added to the equation to avoid the possibility of the denitrification rate of both NO_3^- and NO_2^- being greater than if only one of the two were present.

$$\rho_9 = b_{AOB} \cdot \eta \cdot \frac{K_{I,O_2}}{K_{I,O_2} + S_{O_2}} \cdot \frac{S_{NO_2}}{K_{NO_2} + S_{NO_2}} \cdot \frac{S_{NO_2}}{S_{NO3} + S_{NO_2}} \cdot X_{AOB} \tag{Eq. 6.33}$$

$$\rho_{12} = b_{NOB} \cdot \eta \cdot \frac{K_{I,O_2}}{K_{I,O_2} + S_{O_2}} \cdot \frac{S_{NO_2}}{K_{NO_2} + S_{NO_2}} \cdot \frac{S_{NO_2}}{S_{NO3} + S_{NO_2}} \cdot X_{NOB} \tag{Eq. 6.34}$$

$$\rho_{15} = b_H \cdot \eta \cdot \frac{K_{I,O_2}}{K_{I,O_2} + S_{O_2}} \cdot \frac{S_{NO_2}}{K_{NO_2} + S_{NO_2}} \cdot \frac{S_{NO_2}}{S_{NO3} + S_{NO_2}} \cdot X_H \tag{Eq. 6.35}$$

Tables 6.3 and 6.4 show the default stoichiometric and kinetic parameters used in the model. Table 6.5 gathers together the θ factors used for the temperature correction. Finally, Table 6.6 summarises the stoichiometric matrix of the model.

Table 6.3 Stoichiometric parameters

Symbol	Definition	Value	Units	Reference
Y_{AOB}	Yield of ammonia oxidation	0.15	$gCOD\cdot(gN)^{-1}$	Wiesmann (1994)
Y_{NOB}	Yield of nitrite oxidation	0.041	$gCOD\cdot(gN)^{-1}$	Wiesmann (1994)
Y_H	Yield of aerobic organic matter oxidation	0.67	$gCOD\cdot(gCOD)^{-1}$	Henze *et al.* (2000); ASM1
$Y_{H,NO2}$	Yield of denitrification via nitrite	0.53	$gCOD\cdot(gCOD)^{-1}$	adapted from Muller *et al.* (2003)
$Y_{H,NO3}$	Yield of denitrification via nitrate	0.53	$gCOD\cdot(gCOD)^{-1}$	Muller *et al.* (2003)
i_{NBM}	Nitrogen content of the biomass	0.070	$gN\cdot(gCOD)^{-1}$	Henze *et al.* (2000); ASM3
i_{PBM}	Phosphorus content of the biomass	0.021	$gP\cdot(gCOD)^{-1}$	Volcke (2006b)
i_{CBM}	Carbon content of the biomass	0.36	$gC\cdot(gCOD)^{-1}$	Volcke (2006b)
i_{NXS}	Nitrogen content of X_S	0.04	$gN\cdot(gCOD)^{-1}$	Henze *et al.* (2000); ASM3
i_{PXS}	Phosphorus content of X_S	0.0089	$gP\cdot(gCOD)^{-1}$	Volcke (2006b)
i_{CXS}	Carbon content of X_S	0.3	$gC\cdot(gCOD)^{-1}$	Volcke (2006b)
i_{NSS}	Nitrogen content of S_S	0.03	$gN\cdot(gCOD)^{-1}$	Henze *et al.* (2000); ASM3
i_{PSS}	Phosphorus content of S_S	0.0089	$gC\cdot(gCOD)^{-1}$	Volcke (2006b)
i_{CSS}	Carbon content of S_S	0.3	$gC\cdot(gCOD)^{-1}$	Volcke (2006b)
fx_I	Production of X_I in endogenous respiration	0.08	$gCOD\cdot(gCOD)^{-1}$	Henze *et al.* (2000); ASM1
i_{NXI}	Nitrogen fraction in X_I	0.02	$gN\cdot(gCOD)^{-1}$	Henze *et al.* (2000); ASM3
i_{PXI}	Phosphorus fraction in X_I	0.00064	$gP\cdot(gCOD)^{-1}$	Volcke (2006b)
i_{CXI}	Carbon fraction in X_I	0.36	$gC\cdot(gCOD)^{-1}$	Volcke (2006b)

Table 6.4 Kinetic parameters

Symbol	Characterisation	Value (T=35ºC)	Units	Reference
μ_{max}^{AOB}	Maximum growth rate AOB	2.1	d^{-1}	Lochtman (1995)
b^{AOB}	Aerobic endogenous respiration rate for AOB	0.1944	d^{-1}	Wiesmann (1994)
K_{NH3}^{AOB}	Ammonia substrate saturation for AOB	0.75	$gN\cdot m^{-3}$	Van Hulle *et al.* (2007)
K_{O2}^{AOB}	Oxygen substrate saturation for AOB	0.3	$gO_2\cdot m^{-3}$	Wiesmann (1994)
$K_{I,NH3}^{AOB}$	Free ammonia inhibition constant for AOB	605.48	$gN\cdot m^{-3}$	This study (Chapter 4)
$K_{I,HNO2}^{AOB}$	Nitrous acid inhibition constant for AOB	0.49	$gN\cdot m^{-3}$	This study (Chapter 4)
K_{HCO3^-}	Inorganic carbon substrate saturation	0.01	$gC\cdot m^{-3}$	This study (Chapter 4)
K_{pH}	Saturation constant for pH	8.21	-	Van Hulle *et al.* (2007)
pH_{opt}	Optimum pH	7.23	-	Van Hulle *et al.* (2007)
μ_{max}^{NOB}	Maximum growth rate NOB	1.05	d^{-1}	Lochtman (1995)
b^{NOB}	Aerobic endogenous respiration rate for NOB	0.0795	d^{-1}	Wiesmann (1994)
K_{HNO2}^{NOB}	Nitrite substrate saturation for NOB	$3.2\cdot10^{-5}$	$gN\cdot m^{-3}$	Wiesmann (1994)
K_{O2}^{NOB}	Oxygen substrate saturation for NOB	1.1	$gO_2\cdot m^{-3}$	Wiesmann (1994)
$K_{I,HNO2}^{NOB}$	Nitrous acid inhibition constant for NOB	0.26	$gN\cdot m^{-3}$	Wiesmann (1994)
$K_{I,NH3}^{NOB}$	Free ammonia inhibition constant for NOB	14.8	$gN\cdot m^{-3}$	Magrí *et al.* (2007)
μ_{max}^{H}	Maximum growth rate for heterotrophic biomass	16.97	d^{-1}	Henze *et al.* (2000); ASM1
b^{H}	Aerobic endogenous respiration rate for heterotrophic biomass	3.18	d^{-1}	Henze *et al.* (2000); ASM1
K_{O2}^{H}	Oxygen saturation for heterotrophic biomass	0.2	$gO_2\cdot m^{-3}$	Henze *et al.* (2000); ASM1
K_{SS}	Substrate saturation for heterotrophic biomass	20	$gCOD\cdot m^{-3}$	Henze *et al.* (2000); ASM1
K_{NO2}^{dNO2}	Nitrite substrate saturation for nitrite denitrifiers	0.119	$gN\cdot m^{-3}$	Wiesmann (1994)
K_{NO3}^{dNO3}	Nitrate substrate saturation for nitrate denitrifiers	0.14	$gN\cdot m^{-3}$	Wiesmann (1994)
K_{NO2}	Saturation constant of SNO2 for endogenous respiration	0.5	$gN\cdot m^{-3}$	Henze *et al.* (2000); ASM1
K_{NO3}	Saturation constant of SNO3 for endogenous respiration	0.5	$gN\cdot m^{-3}$	Henze *et al.* (2000); ASM1
$K_{I,O2}$	Oxygen inhibition constant for denitrifiers	0.20	$gO_2\cdot m^{-3}$	Henze *et al.* (2000); ASM1
η	Anoxic reduction factor	0.6	-	Henze *et al.* (2000); ASM3
K_H	Maximum specific hydrolysis rate	15.59	$gCOD\cdot(gCOD\cdot d)^{-1}$	Henze *et al.* (2000); ASM1
K_X	Saturation constant for slowly biodegradable substrate	0.1559	$gCOD\cdot gCOD^{-1}$	Henze *et al.* (2000); ASM1

Table 6.5 Temperature correction factors

Symbol	Characterisation	Value (ºC^{-1})
θ^{AOB}	Theta value for AOB	0.086
θ^{NOB}	Theta value for NOB	0.056
θ^{H}	Theta value for heterotrophic organisms	0.104

Table 6.6 Stoichiometric matrix

Process	S_{NH} g N·m⁻³	S_{NO2} g N·m⁻³	S_{NO3} g N·m⁻³	S_{N2} g N·m⁻³	S_{IC} g C·m⁻³	S_{O2} g O₂·m⁻³	S_{IP} g P·m⁻³	X_{AOB} g COD·m⁻³	X_{NOB} g COD·m⁻³	X_{H} g COD·m⁻³	S_{S} g COD·m⁻³	X_{S} g COD·m⁻³	X_{I} g COD·m⁻³
Aerobic ammonium oxidation	$-\dfrac{1}{Y_{AOB}}-i_{NBM}$	$\dfrac{1}{Y_{AOB}}$	-	-	$-i_{CBM}$	$-\dfrac{3.43-Y_{AOB}}{Y_{AOB}}$	$-i_{PBM}$	1	-	-	-	-	-
Aerobic nitrite oxidation	$-i_{NBM}$	$-\dfrac{1}{Y_{NOB}}$	$\dfrac{1}{Y_{NOB}}$	-	$-i_{CBM}$	$-\dfrac{1.14-Y_{NOB}}{Y_{NOB}}$	$-i_{PBM}$	-	1	-	-	-	-
Aerobic organic matter oxidation	$\dfrac{1}{Y_H}\cdot i_{NSS}-i_{NBM}$	-	-	-	$\dfrac{1}{Y_H}\cdot i_{CSS}-i_{CBM}$	$-\dfrac{1-Y_H}{Y_H}$	$\dfrac{1}{Y_H}\cdot i_{PSS}-i_{PBM}$	-	-	1	$-\dfrac{1}{Y_H}$	-	-
Denitrification of nitrite	$\dfrac{1}{Y_{H,NO_2}}\cdot i_{NSS}-i_{NBM}$	$-\dfrac{1-Y_{H,NO_2}}{1.71\cdot Y_{H,NO_2}}$	-	$\dfrac{1-Y_{H,NO_2}}{1.71\cdot Y_{H,NO_2}}$	$\dfrac{1}{Y_{H,NO_2}}\cdot i_{CSS}-i_{CBM}$	-	$\dfrac{1}{Y_{H,NO_2}}\cdot i_{PSS}-i_{PBM}$	-	-	1	$-\dfrac{1}{Y_{H,NO_2}}$	-	-
Denitrification of nitrate	$\dfrac{1}{Y_{H,NO_3}}\cdot i_{NSS}-i_{NBM}$	$\dfrac{1-Y_{H,NO_3}}{1.14\cdot Y_{H,NO_3}}$	$-\dfrac{1-Y_{H,NO_3}}{1.14\cdot Y_{H,NO_3}}$	-	$\dfrac{1}{Y_{H,NO_3}}\cdot i_{CSS}-i_{CBM}$	-	$\dfrac{1}{Y_{H,NO_3}}\cdot i_{PSS}-i_{PBM}$	-	-	1	$-\dfrac{1}{Y_{H,NO_3}}$	-	-
Hydrolysis of X_S	$i_{NXS}-i_{NSS}$	-	-	-	$i_{CXS}-i_{CSS}$	-	$i_{PXS}-i_{PSS}$	-	-	-	1	-1	-
Aerobic endogenous respiration of X_{AOB}	$i_{NBM}-fx_I\cdot i_{NXI}$	-	-	-	$i_{CBM}-fx_I\cdot i_{CXI}$	$-(1-fx_I)$	$i_{PBM}-fx_I\cdot i_{PXI}$	-1	-	-	-	-	fx_I
Anoxic endogenous respiration of X_{AOB} on NO₃⁻	$i_{NBM}-fx_I\cdot i_{NXI}$	$\dfrac{1-fx_I}{1.14}$	$-\dfrac{1-fx_I}{1.14}$	-	$i_{CBM}-fx_I\cdot i_{CXI}$	-	$i_{PBM}-fx_I\cdot i_{PXI}$	-1	-	-	-	-	fx_I
Anoxic endogenous respiration of X_{AOB} on NO₂⁻	$i_{NBM}-fx_I\cdot i_{NXI}$	$-\dfrac{1-fx_I}{1.71}$	-	$\dfrac{1-fx_I}{1.71}$	$i_{CBM}-fx_I\cdot i_{CXI}$	-	$i_{PBM}-fx_I\cdot i_{PXI}$	-1	-	-	-	-	fx_I
Aerobic endogenous respiration of X_{NOB}	$i_{NBM}-fx_I\cdot i_{NXI}$	-	-	-	$i_{CBM}-fx_I\cdot i_{CXI}$	$-(1-fx_I)$	$i_{PBM}-fx_I\cdot i_{PXI}$	-	-1	-	-	-	fx_I
Anoxic endogenous respiration of X_{NOB} on NO₃⁻	$i_{NBM}-fx_I\cdot i_{NXI}$	$\dfrac{1-fx_I}{1.14}$	$-\dfrac{1-fx_I}{1.14}$	-	$i_{CBM}-fx_I\cdot i_{CXI}$	-	$i_{PBM}-fx_I\cdot i_{PXI}$	-	-1	-	-	-	fx_I
Anoxic endogenous respiration of X_{NOB} on NO₂⁻	$i_{NBM}-fx_I\cdot i_{NXI}$	$-\dfrac{1-fx_I}{1.71}$	-	$\dfrac{1-fx_I}{1.71}$	$i_{CBM}-fx_I\cdot i_{CXI}$	-	$i_{PBM}-fx_I\cdot i_{PXI}$	-	-1	-	-	-	fx_I
Aerobic endogenous respiration of X_{H}	$i_{NBM}-fx_I\cdot i_{NXI}$	-	-	-	$i_{CBM}-fx_I\cdot i_{CXI}$	$-(1-fx_I)$	$i_{PBM}-fx_I\cdot i_{PXI}$	-	-	-1	-	-	fx_I
Anoxic endogenous respiration of X_{H} on NO₃⁻	$i_{NBM}-fx_I\cdot i_{NXI}$	$\dfrac{1-fx_I}{1.14}$	$-\dfrac{1-fx_I}{1.14}$	-	$i_{CBM}-fx_I\cdot i_{CXI}$	-	$i_{PBM}-fx_I\cdot i_{PXI}$	-	-	-1	-	-	fx_I
Anoxic endogenous respiration of X_{H} on NO₂⁻	$i_{NBM}-fx_I\cdot i_{NXI}$	$-\dfrac{1-fx_I}{1.71}$	-	$\dfrac{1-fx_I}{1.71}$	$i_{CBM}-fx_I\cdot i_{CXI}$	-	$i_{PBM}-fx_I\cdot i_{PXI}$	-	-	-1	-	-	fx_I

6.3.3 Physical-chemical phenomena

6.3.3.1 pH calculation

Nitrification of wastewater streams with high ammonium concentrations combined with CO_2 stripping causes high pH variations. In turn, pH affects the chemical equilibrium of substrates and inhibitory compounds. It is therefore essential to take up pH as a model variable.

In the PN-SBR model, pH calculation was carried out according to Volcke (2006a), based on a charge balance. In this approach, pH and concentrations of equilibrium components are calculated by means of a charge balance (an electro-neutrality equation) in the reactor. This balance takes into account the equilibrium species previously defined (see Section 6.3.1.2), the nitrate concentration, and the concentration of the artificial variable, Z^+, representing the amount of net positive charges coming from strong acid and bases. The balance is defined by an algebraic equation, computed at each time step. Thus, pH is not a state variable, since its concentration is not calculated from a mass balance (which would result in a differential equation). Equation 6.36 presents the charge balance over the reactor, expressing the fact that the sum of all charges must be zero.

$$\Delta_{ch} = [H^+] - [OH^-] + [NH_4^+] - [NO_2^-] - [NO_3^-] - [HCO_3^-] - 2 \cdot [CO_3^{2-}] - [H_2PO_4^-] - 2 \cdot [HPO_4^{2-}] + [Z^+] \qquad \textbf{(Eq. 6.36)}$$

A detailed description and development of the pH calculation is given in Volcke (2006a).

6.3.3.2 Transport between gas and liquid phase

The model assumes a perfect mixture between liquid and gas phases. Under these conditions, the liquid-gas transfer phenomena may take place between the two phases. The transport of oxygen, carbon dioxide and nitrogen were taken up in the model by exchange terms (Equation 6.37). In addition, liquid-gas transport of ammonia was included to the model. As previously shown, the transport of these compounds may influence the individual mass balances of some components.

$$TR = k_L a_i \cdot (C_{L,i}^* - C_{L,i}) \qquad \textbf{(Eq. 6.37)}$$

These transfer terms are dependent on the concentration of each component in the liquid phase and the saturation concentration in the gas phase, which is governed by the Henry's law. The temperature dependent expressions of the Henry constants are listed in Table 6.7. The transport rate is reliant on the volumetric mass transfer coefficient, $k_L a_i$.

Table 6.7 Temperature dependent Henry coefficients

Constant	Expression	Source
m_{O_2}	$-403 + 2.52 \cdot T - 3.56 \cdot 10^{-3} \cdot T^2 -$	Lochtman, (1995)
m_{CO_2}	$2.8 - 3.87 \cdot 10^{-2} \cdot T + 1.12 \cdot 10^{-4} \cdot T^2$	Lochtman, (1995)
m_{N_2}	$-7.47 + 4.74 \cdot T - 6.77 \cdot 10^{-3} \cdot T^2$	Lochtman (1995)
m_{NH_3}	$\dfrac{1}{1499.18 \cdot 10^{\left(4100 \cdot \left(\frac{1}{T} - \frac{1}{310}\right)\right)}}$	Sander, R. (1999)

6.3.4   Model implementation

The development of the model was carried out using MATLAB/Simulink software (MathWorks, Natick, Massachusetts, USA). This general purpose simulation environment provided enormous flexibility in terms of model construction. In addition, it allowed advanced mathematical calculation, easy matrix manipulation, plotting of functions and data, and implementation of algorithms, among other features.

The model structure was built in Simulink, and the different parts of the model (liquid phase, gas phase, pH calculation algorithm etc.) were implemented by blocks. In addition, DO and pH on-off controls were included in the model. A general scheme of the implementation is depicted in Figure 6.1.
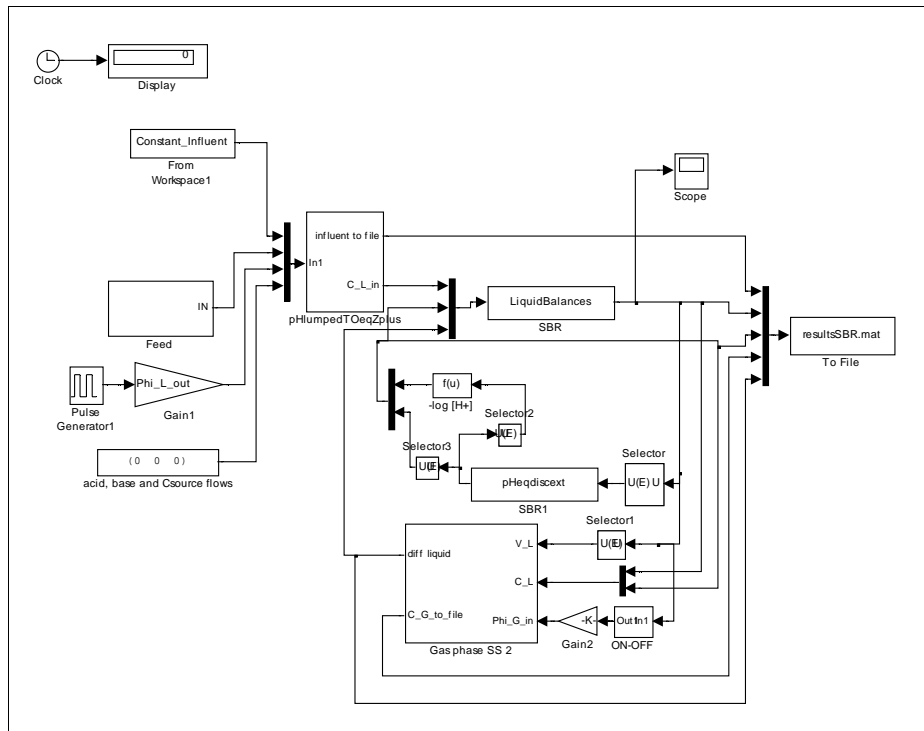
Figure 6.1 Simulink implementation of the PN-SBR model

Finally, it should be mentioned that the ode23t solver was selected to compute differential equations. This method, based on an implementation of the trapezoidal rule using "free" interpolation, is specially suited for stiff models.

6.4 Calibration of the PN-SBR model

Prior to their utilisation, mathematical models should be calibrated to ensure a proper representation of the system under study. In order to perform the calibration procedure in a systematic and organised way, the guideline presented in Corominas (2006) for SBR systems, based on the BIOMATH protocol (Vanrolleghem *et al.*, 2003), was followed. Nevertheless, due to the specific features of the PN-SBR system, minor modifications had to be introduced to this guideline. These changes included: (i) the adaptation of the influent wastewater characterisation to the available historical data, (ii) the inclusion of an identifiability analysis to find an identifiable parameter subset for model fine-tuning (Ruano *et al.*, 2007) and (iii) the use of additional statistical tests for the evaluation of the model fits to data.

The calibration procedure was divided into five stages and nine steps. The structure of the procedure is summarised in Figure 6.2.
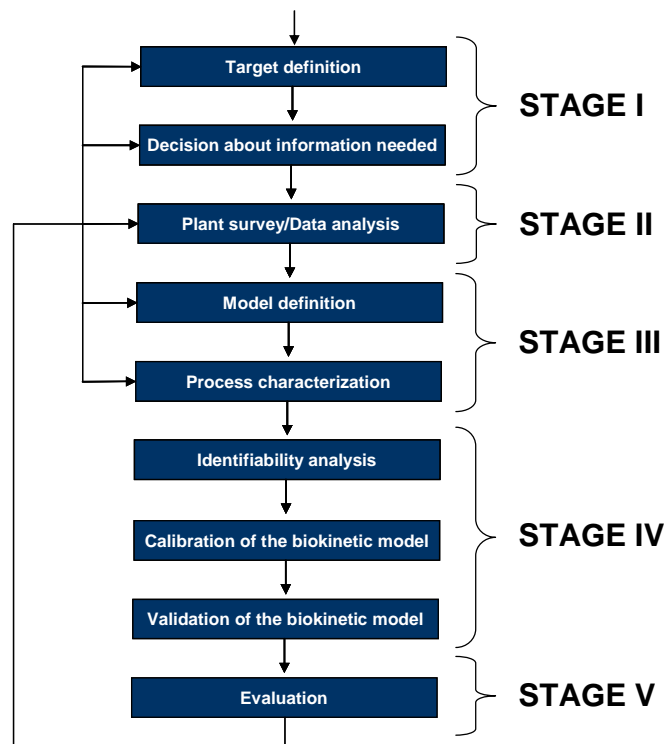
Figure 6.2 Scheme of the calibration procedure

6.4.1   STAGE 1: Defining the target

6.4.1.1   Step 1: Target definition

The main aim of this work was to develop a mathematical model of a partial nitritation-SBR for the treatment of raw urban landfill leachate, as a tool to increase the knowledge of the process. To this end, the model had to be able to accurately describe the main process involving nitrogen and organic conversion under aerobic and anoxic conditions, as well as the behaviour of the pH. The calibration of the model focused on short-term rather than long-term evolutions, taking into account the important dynamics of this system.

6.4.1.2   Step 2: Decision about the information needed

This step looks at everything related to planning the calibration procedure. On the one hand, the logistic aspects such as the equipment and material used, the timing and software are considered, while there is the planning on the information needed about the plant, and especially the decision about monitoring intensity (Corominas, 2006).

Since the model was calibrated and validated using historical data, no measurement campaign was needed. Concerning the simulation environment, the MATLAB/Simulink software was chosen due to its high flexibility.

6.4.2   STAGE 2: Plant survey

6.4.2.1   Step 3: Plant survey/Data analysis

This step comprises a complete process description, the collection of the data needed (design, operational, measurements) …

The calibration and validation of the model was performed using historical data. Two data sets were available, with one being used for calibration and the other for validation. In each period the PN-SBR was operated under a different strategy: The data set used for calibration was obtained when the reactor was operated in a fed-batch strategy (one long feeding phase), while in the set of data used for the validation, the reactor was operated on a step-feed strategy (multiple feeding phases). A scheme of the SBR cycle definition in each period is presented in Figure 6.3.
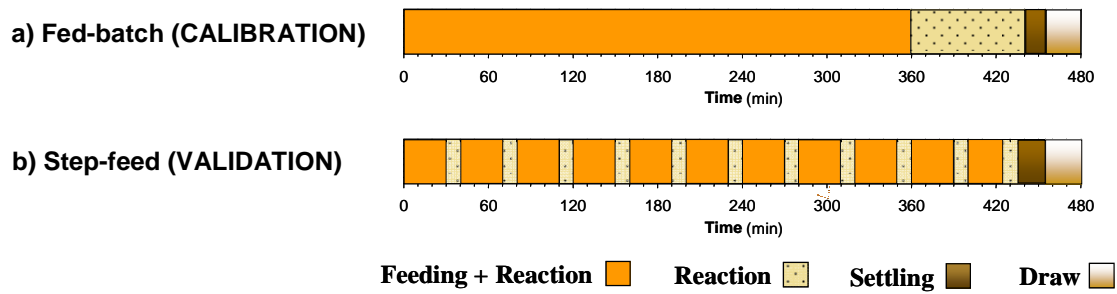
Figure 6.3 SBR cycle definition in both periods. a) Fed-batch and b) Step-feed

The main operational features of the reactor during the calibration and validation periods are presented in Table 6.8.

Table 6.8 Main operational characteristics of the set-up

Description	Units	Calibration	Validation
Influent flow (Q_I)	L·d^{-1}	10.5	8.3
Total cycle length	h	8	8
Volume exchange ratio (V_{EX})	-	0.26	0.22
Minimum volume (V_{MIN})	L	9.8	9.8
Hydraulic Retention Time (HRT)	d	1.27	1.5
Sludge Retention Time (SRT)	d	3-5	3-5
Temperature (T)	ºC	36	36

Focusing on the data available, the calibration and validation data sets were composed of single cycle profiles, including physical-chemical analysis and on-line measurements. The information available for each set is given in Table 6.9.

Table 6.9 Available data for the Calibration and Validation steps

Measurements	Cycle profile	
	Calibration	Validation
TKN*	Total	Total
NH_4^+	Total	Total
NO_2^-	Soluble	Soluble
NO_3^-	Soluble	Soluble
COD*	Filtrated (1.2µm)	Filtrated (1.2µm)
BOD_x	-	-
TOC	Soluble	Soluble
TC	Soluble	Soluble
IC	Soluble	Soluble
TSS	Yes	Yes
Alkalinity*	Total	Total
VSS	Yes	Yes
On-line measurements	pH, DO, ORP, T	pH, DO, ORP, T

* Due to the high volume needed for this analysis, data is only available at the influent and effluent.

Additional data concerning the evolution of the PN-SBR prior to the cycle analysis were also available, and used for organic matter fractionation.

Before starting the calibration procedure, the data quality has to be checked. The nitrogen balance was verified over the calibration and validation cycles. Assuming that no denitrification processes had taken place, total nitrogen at the influent should have been equal to the total nitrogen at the effluent, plus the nitrogen assimilated through bacterial growth. Accordingly, the nitrogen mass balance was defined as:

$$TKN_{inf} + NO_2^-{}_{inf} + NO_3^-{}_{inf} = TKN_{eff} + NO_2^-{}_{eff} + NO_3^-{}_{eff} + (\Delta MLSS \cdot i_{NBM})$$ **(Eq. 6.38)**

where $\Delta MLSS$ represents the increase in the concentration of mixed liquor suspended solids due to growth processes, and i_{NBM} accounts for the nitrogen content of the biomass..

From this balance, a difference between the influent and effluent total nitrogen lower than 10% was observed, which could be attributed to analytical error if the high nitrogen concentrations in the wastewater (higher than 1,000 mgN-NH$_4^+$·L^{-1}) are taken into account. Hence, the nitrogen mass balance was considered as closed.

6.4.3   STAGE 3: Model structure and process characterisation

6.4.3.1   Step 4: Model definition
4a. Mass transfer

In terms of mass transfer, two main aspects have to be taken into account: hydraulic characterisation and volumetric mass transfer efficiency (k_La). Since ideal mixing can be assumed when dealing with a lab-scale SBR, this step only focused on the determination of the volumetric mass transfer coefficients for the different components.

The calculation of this term is critical, since it governs the liquid-gas transport phenomenon. As in Volcke (2006a), the calculation of k_La_{O2} was performed on the basis of the superficial gas velocity, v_{Gs}, which can be calculated by dividing the air flow and the reactor cross section. This relationship (Eq. 6.39) was obtained from van der Lans (2000) and is only valid for low flow rates ($v_{Gs}<0.1$m·s^{-1}) and coarse bubbles (about 6 mm in diameter).

$$k_L a_{O_2} = 0.6 \cdot v_{Gs}$$ **(Eq. 6.39)**

Once the k_La_{O2} value is obtained, the volumetric mass transfer coefficient for CO_2, N_2 and NH_3 can be calculated by the following expression, only valid for low water soluble components in turbulent motion (De Heyder et $al.,$ 1997)

$$k_L a_i = k_L a_{O_2} \cdot \sqrt{\frac{D_i}{D_{O_2}}}$$ (Eq. 6.40)

where D_i is the diffusivity of a compound i (m·s^{-2}), and D_{O2} is the diffusivity of O_2.

Finally, Table 6.10 lists the diffusivity values considered in this study.

Table 6.10 Diffusivity constants

Constant	Expression	Units	Source
D_{O_2}	$2.16 \cdot 10^{-4}$	m^2·d^{-1}	Perry (1994)
D_{CO_2}	$1.69 \cdot 10^{-4}$	m^2·d^{-1}	Perry (1994)
D_{N_2}	$1.64 \cdot 10^{-4}$	m^2·d^{-1}	Perry (1994)
D_{NH_3}	$1.73 \cdot 10^{-4}$	m^2·d^{-1}	Perry (1994)

4.b Settler

The settling model was selected according to a decision tree presented in Vanrolleghem et $al.$ (2003) (Figure 6.4).
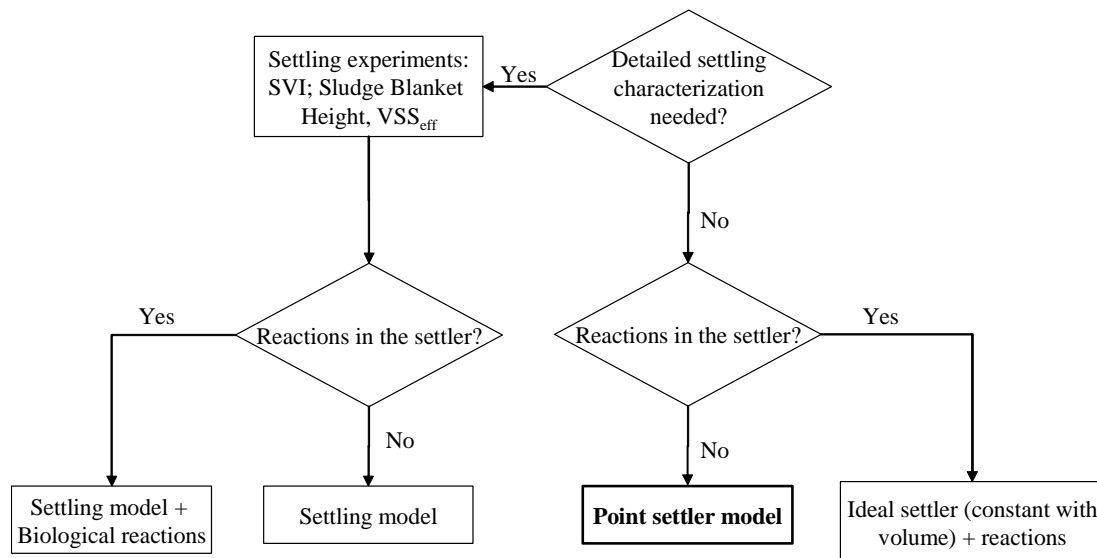
Figure 6.4 Decision tree for selecting the settling model (Vanrolleghem et $al.$, 2003)

There was no available data concerning settling properties, except for the concentration of TSS and VSS in the reactor and effluent. Therefore the simplest option, namely the point settler, was adopted, in which no reactions take place during the settling and draw phases. As an important amount of suspended solids were removed from the system due to inefficient settling, it was

considered that a fraction of the solids in the reactor (f_{ns}) was removed from the system during the draw phases.

4.c Biological model

The guideline proposed the choice of the biological model by using a decision tree defined by Vanrolleghem *et al.* (2003). However, this decision tree only considers the activated sludge models (ASMs) proposed by the IWA task group on mathematical modelling for the design and operation of biological wastewater treatments (Henze *et al.*, 2000). Due to the special features of the system to be modelled, a different approach was considered and a tailor-made biokinetic model was used (previously described in Section 6.2.2).

6.4.3.2   <u>Step 5: Process characterisation</u>

5.a Estimation of ASM parameters

The calibration procedure was carried out using historical data, so it was not possible to estimate any ASM parameter in this study. However, three model parameters ($k_{I,FA}$, $k_{I,FNA}$ and k_{HCO3^-}) had been estimated in previous experiments (see Section 4.4.2), and were taken up in the model. The rest of parameters were taken from the literature (see Tables 6.3 to 6.5).

5.b Influent characterisation

The next step was to achieve a proper characterisation of the influent wastewater. Corominas (2006) performed the influent fractionation following a procedure similar to the STOWA protocol (Roeleveld and Van Loosdrecht, 2002), based on physical-chemical and BOD measurements. Nevertheless, there was some information missing from the data sets under study, and so the characterisation had to be adapted to the data that was available.

Four state variables involving nitrogen fractionation were considered in Corominas (2006): S_{NH} (linked to ammonium), S_{NO} (equivalent to the sum of nitrites and nitrates), and S_{ND} and X_{ND} (which account for the soluble and particulate nitrogen fractions of soluble and particulate organic matter respectively). In contrast, in the partial nitrification model, nitrite and nitrate were considered separately, and S_{ND} and X_{ND} were not taken up, since organic nitrogen was considered as a fraction of the organic matter (S_S, S_I, X_S and X_I).

With regards to the organic matter, Figure 6.5 presents a scheme of the fractionation proposed by Corominas (2006).

The available historical data sets did not contain soluble chemical oxygen demand (COD_S) measurements, essential for organic matter fractionation. Nevertheless, dissolved organic carbon (DOC) measurements were available at the influent and effluent, so COD_S were calculated from

the DOC values, applying empirical ratios. These ratios were experimentally found to be 1.86 mg COD_S per mg DOC at the influent, and 2.3 mg COD_S per mg DOC at the effluent.
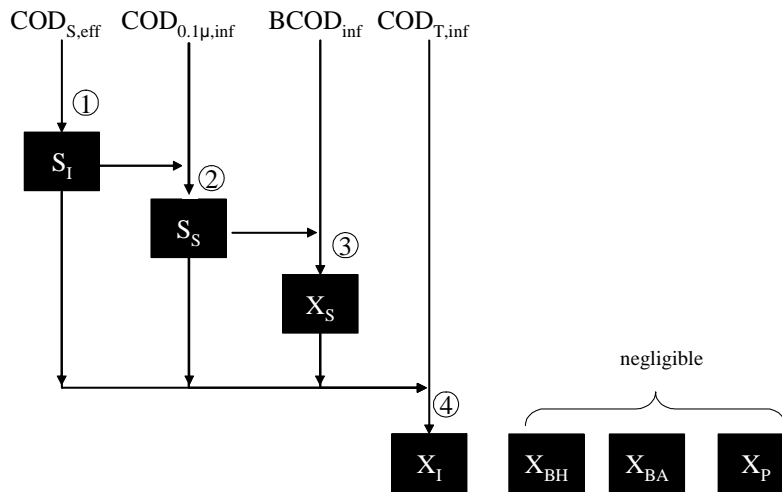
Figure 6.5 Organic matter fractionation (Corominas, 2006).

Biodegradable COD (BCOD) at the influent was also needed for this procedure, but only BOD_5 measurements were available. However, the BCOD can be estimated from these according to Roeleveld and Van Loosdrecht (2002) (Equations 6.41 and 6.42).

$$BOD_{total} = \frac{1}{1 - k^{-k_{BOD} \cdot t}} BOD_t \qquad \textbf{(Eq. 6.41)}$$

$$BCOD = \frac{1}{1 - f_{BOD}} BOD_{total} \qquad \textbf{(Eq. 6.42)}$$

in which k_{BOD} (d^{-1}) is a first order constant of BOD versus time, BOD_t is a biochemical oxygen demand measurement at time t, and f_{BOD} is a correction factor. In this specific case the k_{BOD} of this organic matter was experimentally determined to be 0.13 (from historical data, not shown) and the f_{BOD} was assumed to be 0.15.

From this procedure, influent organic matter was fractionated. The concentration for each state variable and the percentage of each fraction with respect to the total influent COD are given in Table 6.11.

Table 6.11 Organic matter fractionation for both data sets

State variables	CALIBRATION		VALIDATION	
	Concentration (mgCOD·L^{-1})	(%)*	Concentration (mgCOD·L^{-1})	(%)*
S_S	1052.63	25.01	649.94	20.19
S_I	3066.57	72.88	2078.28	64.55
X_S	59.07	1.40	247.42	7.68
X_I	29.51	0.70	244.03	7.58

* This percentage is calculated with respect to the total influent COD.

As can be observed, in both cases the majority of the COD was due to the soluble fractions, with the inert (S_I) being the most important and representing 60-70% of the total influent COD. The readily biodegradable fraction (S_S) only constituted about 20-25% of the total COD. The particulate fractions (X_S and X_I) were negligible in the calibration, while their importance in the validation data set was more significant. Since there is no physical-chemical explanation for such different behaviour, this variation might be attributed to biases linked to the fractionation.

The above organic matter fractionation was believed to be sufficiently accurate for this study. It should be noted that most assumptions relate to the COD fractions, which were expected to have little impact in comparison with the high nitrogen concentrations.

The main influent characteristics for the calibration and validation cycles are summarized in Table 6.12.

Table 6.12 Input state variables

Influent State variables	Units	CALIBRATION	VALIDATION
S_{NH}	mgN·L^{-1}	1761.0	2009.3
S_{NO2}	mgN·L^{-1}	5.7	0.26
S_{NO3}	mgN·L^{-1}	4.0	3.47
S_{IC}	mgC·L^{-1}	1768.0	1863.2
X_{AOB}	mgCOD·L^{-1}	0.01	0.01
X_{NOB}	mgCOD·L^{-1}	0.01	0.01
X_H	mgCOD·L^{-1}	0.01	0.01
S_S	mgCOD·L^{-1}	1052.63	649.94
S_I	mgCOD·L^{-1}	3066.57	2078.28
X_S	mgCOD·L^{-1}	59.07	247.42
X_I	mgCOD·L^{-1}	29.51	244.03
pH	-	8.67	8.84

6.4.4   STAGE 4: Calibration and validation

Model calibration is understood as the estimation of the model parameters to fit a certain set of data obtained from the WWTP under study (Gernaey *et al.*, 2004). To carry out the calibration, modellers usually follow a calibration protocol. However, independently of the protocol, the calibration step is usually achieved through a trial and error approach, in which a number of parameters are changed one at a time to fit the model. The selection of the parameter subset to be tuned is a key point, since an unsuitable subset may lead to poor fitting. Identifiability analysis is a good tool for finding an adequate parameter subset to fine-tune with.

6.4.4.1   Step 6: Identifiability analysis

Prior to the calibration step, an identifiability analysis of the model was performed, using the methodology defined in Brun *et al.* (2002) and based on a local sensitivity analysis. The aim of this analysis was to find an identifiable subset of parameters to calibrate the PN-SBR model. To

be identifiable, a parameter subset K has to fulfil two conditions. First, a model output $y(\theta)$ has to be sufficiently sensitive to individual changes to each parameter in K. This is addressed by the sensitivity measure δ_j^{msqr}. Secondly, variations in the model output due to changes in single parameters may not be approximately cancelled by appropriate changes in other parameters. This analysis of parameter interdependences is addressed by the collinearity index, γ_K. The determinant value, ρ_K, takes into account both identifiability conditions simultaneously and is, therefore, particularly suited for the assessment of the identifiability of parameter subsets.

The first step of the identifiability analysis was the identification of the model parameters to be calibrated. For this purpose, 30 parameters (all kinetic parameters plus the temperature correction coefficients; listed in Tables 6.4 and 6.5) were selected. The identifiability analysis considered five different outputs: NH_4^+, NO_2^-, NO_3^-, IC and pH.

As a starting point, the relative sensitivity of each parameter j (30 in total) to each of the available measurements (henceforth called model outputs) y (five in total) and at each time instant i (S_{ij}), was calculated as:

$$S_{ij} = \frac{\partial y_i}{\partial \theta_j} \cdot \frac{\theta_j}{y_i} \qquad \textbf{(Eq. 6.43)}$$

where $\partial y_i / \partial \theta_j$ is defined as the absolute sensitivity of the model output y_i to the parameter θ_j at each time instant i.

The absolute sensitivity function was approximated using a finite difference method, which is only valid for a small change in the parameters considered, i.e. a small perturbation factor ($\Delta\theta$). Finding proper perturbation factors is a challenging task (De Pauw and Vanrolleghem, 2003). After several trials with a wide range of perturbation factors, ranging from 0.0001% to 50%, a perturbation factor of 10% was found suitable for all the model parameters.

After performing this step it was observed that the resulting plots presented scattering. This noise is probably attributable to a problem of numerical accuracy of the integrator (ode23t) versus the complexity of the model. To solve it, a more accurate integrator (ode45) was tried. Nevertheless, the stiffness of the model led to very slow simulations which made the use of this new integrator unviable. Pre-treatment of the data for the removal of this noise was therefore preferred, and was reached by the use of a one dimensional median filter.

From these sensitivities (S_{ij}) the sensitivity measure (δ_{yj}^{msqr}) was calculated for each parameter and output:

$$\delta_{yj}^{msqr} = \sqrt{\frac{1}{n}\sum_{i=1}^{n}s_{ij}^{2}}$$ **(Eq. 6.44)**

where n is defined as the number of measurements (at different time instants)

This equation measures the mean sensitivity of a model output (y) to a change in the parameter θ_j (in the mean square sense). A high δ_{yj}^{msqr} means that the value of the parameter θ_j has great influence on the simulation result; a value of zero means that the simulation results do not depend on the parameter θ_j (Brun *et al.*, 2002).

The total sensitivity of a parameter (δ_j^{msqr}) was calculated as the sum of the parameter's δ_{yj}^{msqr} over each output (y), according to Equation 6.45.

$$\delta_j^{msqr} = \sqrt{\frac{1}{n}\sum_{i=1}^{n}(\delta_{yj}^{msqr})^2}$$ **(Eq. 6.45)**

The total sensitivities of each parameter are listed in Table 6.13, and the ranking distribution is given in Figure 6.6

Table 6.13 Parameter significance ranking

Ranking	Parameter	δ_j^{msqr}	Ranking	Parameter	δ_j^{msqr}
1	pH_{opt}	1.304	16	$K_{I,NH3}^{NOB}$	0.024
2	μ_{max}^{NOB}	0.179	17	K_{pH}	0.023
3	μ_{max}^{AOB}	0.177	18	K_{O2}^{AOB}	0.022
4	K_{IC}	0.143	19	K_H	0.019
5	$K_{I,HNO2}^{NOB}$	0.102	20	K_{O2}^{H}	0.010
6	b_{AOB}	0.089	21	$K_{I,NH3}^{AOB}$	0.003
7	$K_{I,HNO2}^{AOB}$	0.085	22	K_x	0.003
8	μ_{max}^{H}	0.075	23	θ^{AOB}	0.001
9	K_{SS}	0.073	24	K_{NO2}^{dNO2}	0.001
10	b^{H}	0.068	25	K_{HNO2}^{NOB}	0.001
11	η	0.059	26	K_{NO3}	0.001
12	$K_{I,O2}$	0.057	27	θ^{H}	0.000
13	K_{O2}^{NOB}	0.042	28	θ^{NOB}	0.000
14	b^{NOB}	0.038	29	K_{NO3}^{dNO3}	0.000
15	K_{NH3}^{AOB}	0.035	30	K_{NO2}	0.000

As can be observed, pH_{opt} was by far the most sensitive parameter. Among the others, values were lower and more uniform.

On the basis of this ranking, only the more sensitive parameters could be considered identifiable. There is not a clear cut-off value for the δ_j^{msqr} (Ruano *et al.*, 2007). However, based on experience, a threshold value of 0.05 was chosen as a cut-off value to select the most significant parameters, and reduce the computational time for further collinearity index and

determinant measure calculations. As a result, a subset containing the 12 parameters presenting the higher δ_j^{msqr} was selected.
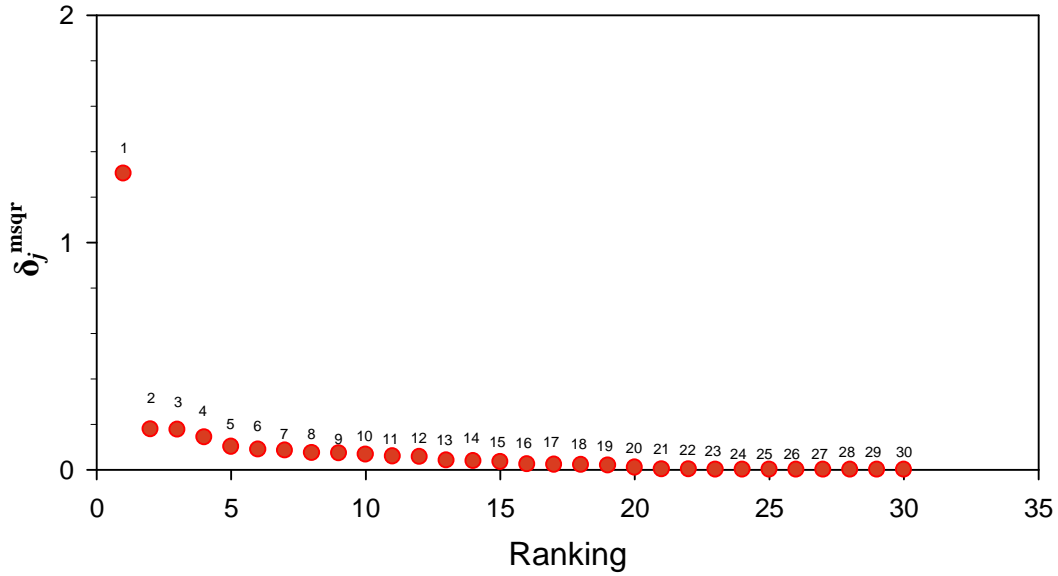
Figure 6.6 Parameter ranking according to the $\boldsymbol{\delta}_j^{msqr}{}_{total}$

The collinearity index (γ_K), associated with a parameter subset K of size k, is defined as:

$$\gamma_K = \frac{1}{\sqrt{\min \tilde{\lambda}_k}} \qquad \textbf{(Eq. 6.46)}$$

where $\min \tilde{\lambda}_k$ is the smallest eigenvalue of the normalised subset matrix $\tilde{S}_K^T \tilde{S}_K$

γ_K measures the degree of near-linear dependence between the sensitivity functions. It equals unity if the columns are orthogonal and it reaches infinity if the columns are linearly dependent. If the columns are nearly linearly dependent, changes in the model output, y, due to small changes in a parameter θ_j can be compensated to a large extent by appropriate changes in other parameters in K. This is indicated by a high collinearity index γ_K. Based on experience, a collinearity value of 5 was chosen as the cut-off value in this study.

The determinant measure (ρ_K) is defined as:

$$\rho_K = \det(S_K^T S_K)^{1/2k} = \left(\prod_{j=1}^{k} \lambda_j \right)^{1/2k} \qquad \textbf{(Eq. 6.47)}$$

where $\det(S_K^T S_K)^{1/2k}$ is the determinant function of the $n \times K$ subset matrix of S.

The determinant measure combines the information provided by δ_j^{msqr} and γ_K in a useful way. ρ_K becomes large if the parameter sensitivities (δ_j^{msqr}) are high and their collinearity (γ_K) is low. A high value of ρ_K; therefore, indicates a good ''conditional identifiability'' of parameter subset K.

126

Since ρ_K is substantially dependent on the choice of the $\Delta\theta_j$, it is generally not possible to define an absolute threshold value. ρ_K is rather a relative measure suited for the comparison of parameter identifiability of different parameter subsets.

Subsequently, the collinearity index (γ) and the determinant measures (ρ) for each output variable were calculated for all possible subsets containing 2 to 12 of the 12 most significant parameters. The results are given in Table 6.14.

Table 6.14 Identifiability results (δ_j^{msqr})

Size	Combinations	γ range	$\gamma < 5$ (%)	γ_{min}	$\rho(\gamma_{min})$	Parameter subset for γ_{min}
2	66	2.90-95.93	19.69	2.90	44.33	b^H, $K_{I,HNO2}^{NOB}$
3	220	4.91-178.26	0.45	4.91	11.20	μ_{max}^{NOB}, b^H, $K_{I,HNO2}^{NOB}$
4	495	6.19-363.62	0	6.19	7.93	No identifiable subset found
5	792	10.14-390.06	0	10.14	22.13	No identifiable subset found
6	924	10.53-397.39	0	10.53	16.88	No identifiable subset found
7	792	12.12-403.13	0	12.12	10.52	No identifiable subset found
8	495	13.58-416.30	0	13.58	11.91	No identifiable subset found

As can be observed in the table, there were many potentially identifiable parameter subsets ($\gamma < 5$), the majority of which were composed of two parameters. In order not to lose valuable information it is important to choose the largest possible parameter subset. In this particular case, the maximum subset size accomplishing the collinearity threshold was three. The largest subset with the lowest collinearity value and the highest determinant (ρ_K) was compound by μ_{max}^{NOB}, b^H and $K_{I,HNO2}^{NOB}$.

Since the calibration method is usually performed output by output following step-wise procedures and experience based protocols (i.e. Insel *et al.*, 2007 and Corominas *et al.*, 2008), the identifiability of the parameters subset for each output was also studied. The identifiability measurements for each output were calculated independently, and the results are summarised in Tables 6.15 to 6.19:

Table 6.15 Identifiability results ($\delta_j^{msqr}{}_{NH4+}$)

Size	Combinations	γ range	$\gamma < 5$ (%)	γ_{min}	$\rho(\gamma_{min})$	Parameter subset for γ_{min}
2	66	1.48-141.51	66.66	1.48	0.84	μ_{max}^{NOB}, K_{SS}^{H}
3	220	1.91-176.68	28.18	1.91	8.14	μ_{max}^{AOB}, μ_{max}^{NOB}, $K_{I,HNO2}^{NOB}$
4	495	2.34-298.96	6.46	2.34	6.00	μ_{max}^{NOB}, η, K_{SS}^{H}, $K_{I,HNO2}^{NOB}$
5	792	4.77-355.27	0.5	4.77	3.50	μ_{max}^{AOB}, μ_{max}^{NOB}, μ_{max}^{H}, b^H, $K_{I,HNO2}^{NOB}$
6	924	14.27-365.45	0	14.27	2.82	No identifiable subset found
7	792	15.83-371.03	0	15.83	3.15	No identifiable subset found
8	495	50.62-375.17	0	50.62	5.47	No identifiable subset found

Table 6.16 Identifiability results (δ_j^{msqr} $_{NO2\text{-}}$)

Size	Combinations	γ range	γ < 5 (%)	γ_{min}	$\rho(\gamma_{min})$	Parameter subset for γ_{min}
2	66	1.59-161.99	45.45	1.59	20.52	μ_{max}^{HET}, b^{AOB}
3	220	4.24-249.86	8.63	4.24	8.57	b^{AOB}, b^{H}, K_{SS}^{H}
4	495	5.98-370.22	0	5.98	2.82	No identifiable subset found
5	792	7.76-457.32	0	7.76	6.89	No identifiable subset found
6	924	45.62-472.40	0	45.62	7.44	No identifiable subset found
7	792	66.78-480.17	0	66.78	3.54	No identifiable subset found
8	495	90.63-496.51	0	90.63	3.09	No identifiable subset found

Table 6.17 Identifiability results (δ_j^{msqr} $_{NO3\text{-}}$)

Size	Combinations	γ range	γ < 5 (%)	γ_{min}	$\rho(\gamma_{min})$	Parameter subset for γ_{min}
2	66	63.84-3307.62	0	63.84	0.03	No identifiable subset found
3	220	133.80-9230.17	0	133.80	0.04	No identifiable subset found
4	495	242.92-17297.22	0	242.92	0.02	No identifiable subset found
5	792	543.02-20163.22	0	543.02	0.08	No identifiable subset found
6	924	973.06-21399.88	0	973.06	0.02	No identifiable subset found
7	792	1936.55-22607.05	0	1936.55	0.02	No identifiable subset found
8	495	2609.83-27031.78	0	2609.83	0.03	No identifiable subset found

Table 6.18 Identifiability results (δ_j^{msqr} $_{IC}$)

Size	Combinations	γ range	γ < 5 (%)	γ_{min}	$\rho(\gamma_{min})$	Parameter subset for γ_{min}
2	66	1.00-83.36	84.85	1.00	1875.88	b^{AOB}, $K_{I,O2}$
3	220	1.01-94.97	63.64	1.01	133.20	b^{AOB}, b^{H}, $K_{I,HNO2}^{NOB}$
4	495	1.72-104.51	41.41	1.72	209.18	b^{AOB}, b^{HET}, $K_{I,O2}$, $K_{I,HNO2}^{NOB}$
5	792	2.45-128.05	19.94	2.45	172.65	μ_{max}^{AOB}, μ_{max}^{HET}, b^{AOB}, b^{H}, $K_{I,O2}$
6	924	3.19-136.12	5.3	3.19	156.73	μ_{max}^{HET}, η, b^{AOB}, $K_{I,O2}$, $K_{I,HNO2}^{NOB}$, pH_{opt}
7	792	4.06-140.94	0.8	4.06	72.48	μ_{max}^{NOB}, μ_{max}^{HET}, η, b^{AOB}, b^{H}, $K_{I,O2}$, $K_{I,HNO2}^{NOB}$
8	495	7.06-145.55	0	7.06	77.79	No identifiable subset found

Table 6.19 Identifiability results (δ_j^{msqr} $_{pH}$)

Size	Combinations	γ range	γ < 5 (%)	γ_{min}	$\rho(\gamma_{min})$	Parameter subset for γ_{min}
2	66	1.00-38.14	90.90	1.00	1.39	μ_{max}^{AOB}, μ_{max}^{H}
3	220	1.18-78.26	75.91	1.18	1.24	η, K_{SS}^{H}, $K_{I,HNO2}^{NOB}$
4	495	1.79-81.00	56.36	1.79	1.57	b^{H}, K_{SS}^{H}, $K_{I,O2}$, $K_{I,HNO2}^{NOB}$
5	792	2.06-85.76	33.33	2.06	6.18	b^{AOB}, b^{H}, $K_{I,O2}$, $K_{I,HNO2}^{NOB}$, pH_{opt}
6	924	2.62-86.06	14.39	2.62	3.02	μ_{max}^{AOB}, μ_{max}^{H}, b^{AOB}, b^{H}, $K_{I,O2}$, $K_{I,HNO2}^{NOB}$
7	792	3.76-86.71	4.17	3.76	2.10	μ_{max}^{H}, η, b^{AOB}, b^{H}, K_{IC}, $K_{I,O2}$, $K_{I,HNO2}^{NOB}$
8	495	4.70-87.67	0.61	4.70	1.29	μ_{max}^{NOB}, μ_{max}^{H}, η, b^{AOB}, b^{HET}, K_{IC}, K_{SS}^{H}, $K_{I,O2}$

As can be observed, maximum subset sizes of 5, 2, 7 and 8 were obtained for ammonium, nitrite, IC and pH, respectively. With regards to nitrate, it should be noted that any combination of the most sensitive parameters accomplished the cut-off value for NO_3^- output.

Once these results were obtained, the next action was to define the parameter subset in order to proceed with Step 7 of the calibration guideline. Accordingly, the parameter subset accomplishing the collinearity threshold and with the highest determinant value was chosen for the NH_4^+, NO_2^-, IC and pH. The selected parameter subsets are summarised in Table 6.20.

Table 6.20 Selected parameters

Output	Parameter subset	γ	ρ
NH_4^+	μ_{max}^{AOB}, μ_{max}^{NOB}, μ_{max}^{H}, b^H, $K_{I,HNO2}^{NOB}$	4.77	3.5
NO_2^-	b^{AOB}, b^H, K_{SS}^{H}	4.23	8.57
IC	μ_{max}^{H}, η, b^{AOB}, b^H, $K_{I,O2}$, $K_{I,HNO2}^{NOB}$, pH_{opt}	4.28	120.50
pH	μ_{max}^{NOB}, μ_{max}^{H}, η, b^{AOB}, b^H, K_{IC}, K_{SS}^{H}, $K_{I,O2}$	4.7	1.29

6.4.4.2   Step 7: Calibration of the biokinetic model

The calibration step was conducted in two stages, as proposed in Corominas (2006), following a step-wise procedure (see Figure 6.7). First, the model was simulated with a constant influent, and the volatile suspended solids (VSS) concentration inside the reactor was adjusted by tuning the f_{ns}. Once proper conditions had been achieved, cycle evolution calibration was performed for each of the selected outputs (NH_4^+, NO_2^-, NO_3^-, IC and pH).
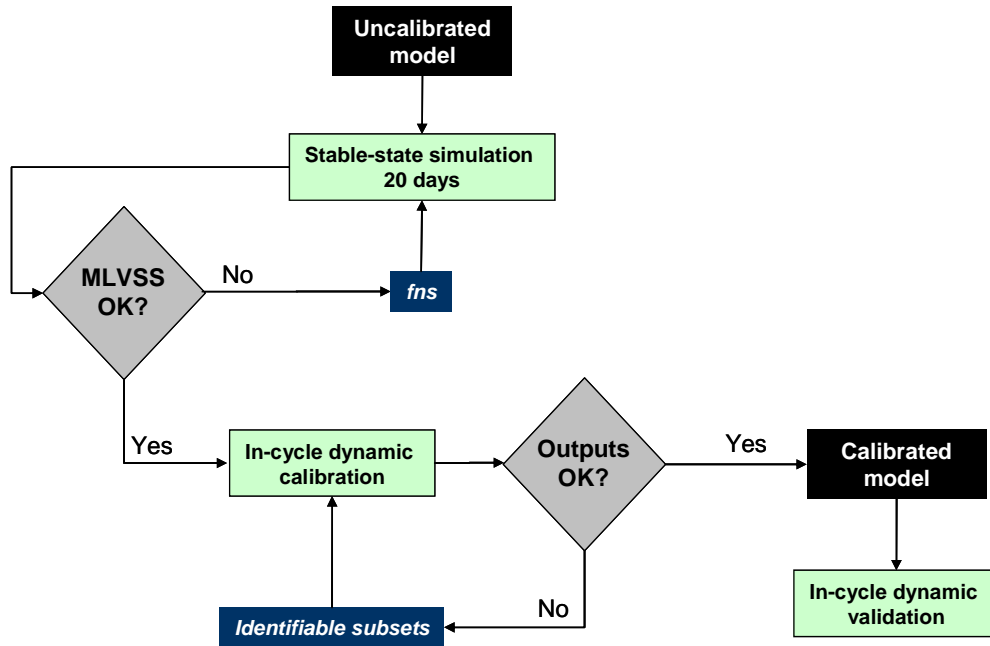
Figure 6.7 Step-wise procedure for calibration and validation

The process dynamics were fitted by manually fine tuning the identifiable parameter subsets previously found in the identifiability analysis (see Table 6.20). A maximum variation of 10% with respect to its default value, was considered acceptable in a parameter, and the model's fitting to the respective output was visually assessed. However, the model turned to be insensitive to the majority of the parameters, and only μ_{max}^{AOB}, μ_{max}^{NOB} and pH_{opt} (accounting for the highest δ_j^{msqr} values) gave a significant response. The initial and final values of the tuned parameters are given in Table 6.21.

Table 6.21 Initial and calibrated values

Parameter	Initial	Calibrated
μ_{max}^{AOB}	2.1	2.31
μ_{max}^{NOB}	1.05	0.945
pH_{opt}	7.23	7.63

Figure 6.8 presents the results of the calibration for the nitrogen compounds (Figure 6.8a), inorganic carbon (Figure 6.8b) and pH (Figure 6.8c).
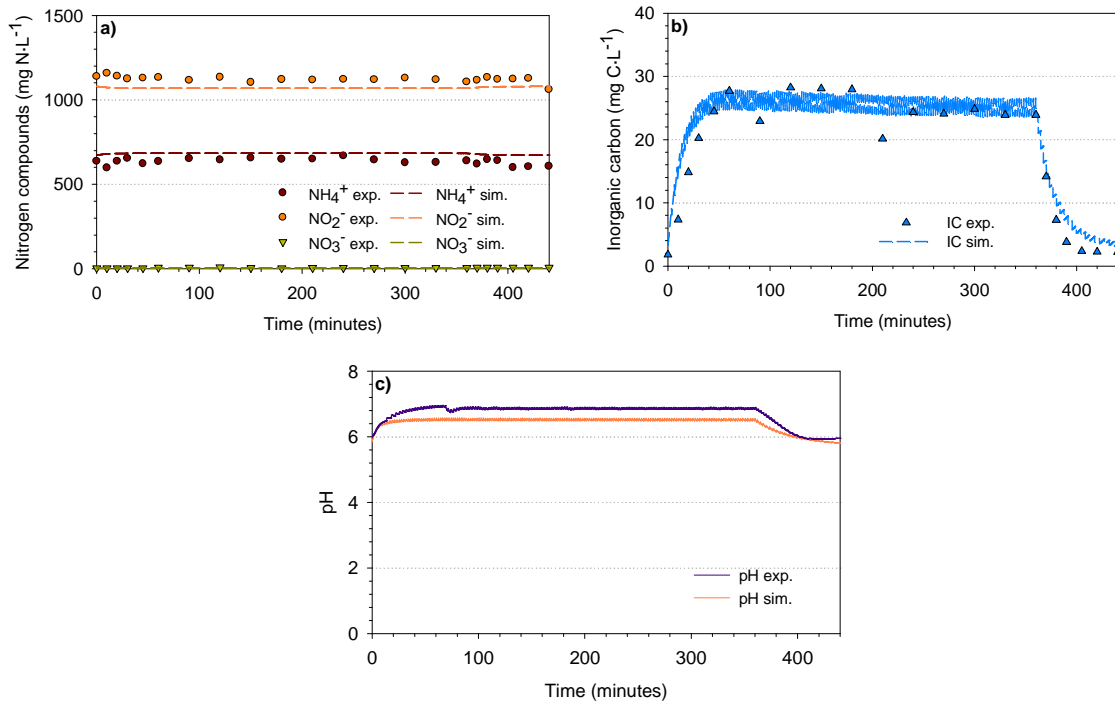
Figure 6.8 Experimental and simulated evolution of the main physical-chemical outputs during the calibration step: a) Nitrogen compounds; b) Inorganic carbon; c) pH

Figure 6.8 shows a good model fit with the data in the calibration step. The model accurately followed the dynamic trends in terms of nitrogen compounds (nitrite build-up, without nitrate production) and inorganic carbon. Figure 6.8c presents the experimental and simulated pH profiles. As can be seen, the model was capable of forecasting the pH dynamics, despite a slight bias (about 0.3-0.4 pH units) between the simulated and the experimental values.

Step 8: Validation of the biokinetic model

After the calibration step was finished, the model was validated using an independent data set from a cycle profile of the reactor operating under a step-feed strategy. Next are presented the experimental and simulated profiles for the nitrogen compounds (Figure 6.9a), inorganic carbon (Figure 6.9b) and pH (Figure 6.9c).

130
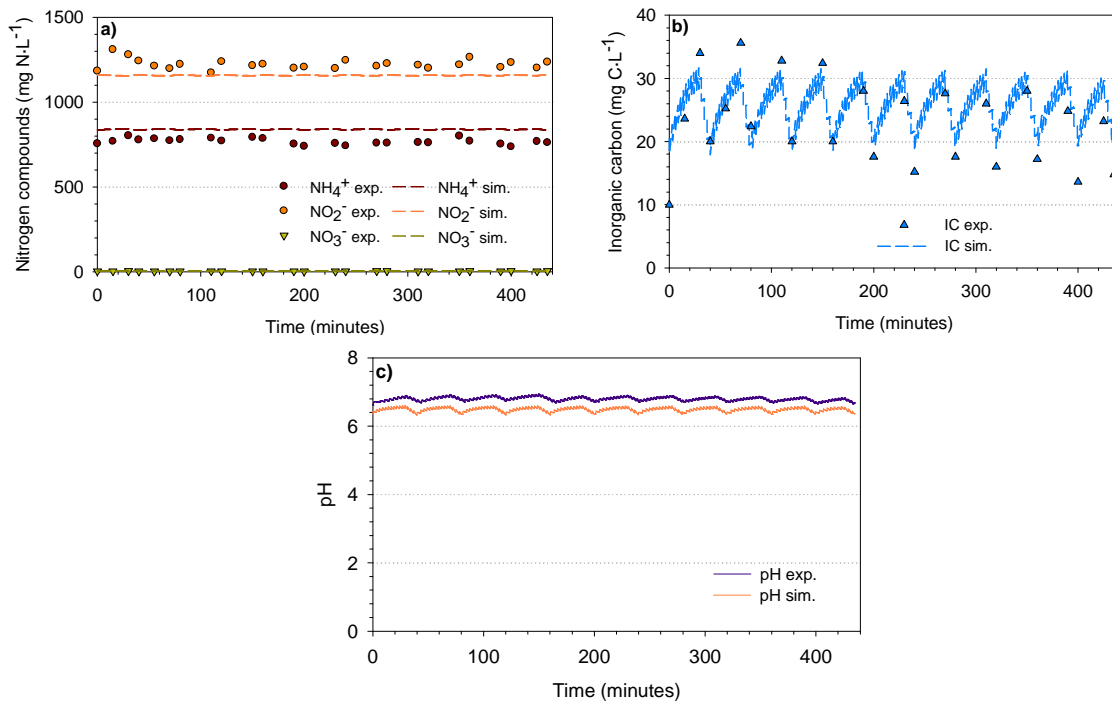
Figure 6.9 Experimental and simulated evolution of the main physical-chemical outputs during the validation step: a) Nitrogen compounds; b) Inorganic carbon; c) pH

As can be seen from Figure 6.9, good results were also obtained for the validation step. The model was able to forecast the evolution of the nitrogen compounds, and a good prediction was reached for the inorganic carbon, despite the increase/decrease pattern. Moreover, the model was also able to forecast pH behaviour, although a similar off-set to that in the calibration step was detected. Taking into account the high sensitivity of pH in non-buffered systems, this deviation is deemed acceptable. One of the most likely hypotheses for the deviation is the effect of salinity. Raw leachate used in this study had a conductivity of above 35,000 $\mu S \cdot cm^{-1}$, and elevated ionic strengths may also affect pH calculation. With such a high value, the use of activities instead of concentrations is recommended (Smith and Chen, 2006).

6.4.5   STAGE 5: Evaluation

6.4.5.1   <u>Step 9: Evaluation of the results</u>

This final step evaluates whether the calibration procedure has accomplished the initial goals. In case of an unsuccessful calibration, the procedure should move back to Step 2.

Corominas (2006) performed the evaluation step by visual judgment and the use of an average relative deviation test (ARD). In the present case, assessment of the calibration of the partial nitrification model was refined by including different statistical tests (Power, 1993) to support the visual evaluation. These tests are summarised in Table 6.22.

Table 6.22 Statistical tests

Mean Absolute Error (MAE)	Root Mean Squared Error (RMSE)	Average Relative Deviation (ARD)	Janus coefficient (J^2)
$MAE = \dfrac{1}{n}\sum_{i=1}^{n}\left\|y_{meas,i} - y(t_i)\right\|$	$RMSE = \sqrt{\dfrac{1}{n}\sum_{i=1}^{n}\left(y_{meas,i} - y(t_i)\right)^2}$	$ARD = \dfrac{1}{n}\sum_{i=1}^{n}\left(\dfrac{\left\|y_{meas,i} - y(t_i)\right\|}{y_{meas,i}}\right)$	$J^2 = \dfrac{\dfrac{1}{n\_val}\sum_{i=1}^{n\_val}\left(y_{meas,i} - y(t_i)\right)^2}{\dfrac{1}{n\_cal}\sum_{i=1}^{n\_cal}\left(y_{meas,i} - y(t_i)\right)^2}$

n is the total number of observations of the variable y; $y_{meas,i}$ is the ith measurement of the variable y, and $y(t_i)$ is the corresponding model output at time i; n_cal and n_val are the total number of measurements in the calibration and validation periods, respectively.

MAE and RMSE are statistical tests directly related to each output, accounting for the same units. On the other hand, ARD is a test that informs about relative deviations. The Janus coefficient measures the predictive accuracy of a model, and its value should be close to 1.

Next, Table 6.23 shows the quantification of the model fit for the calibration and validation data sets on the basis of statistical tests.

Table 6.23 Results of the statistical tests evaluation

Output	MAE		RMSE		ARD		J^2
	Calibration	Validation	Calibration	Validation	Calibration	Validation	
NH_4^+	45.76	70.87	48.71	72.78	0.08	0.10	2.23
NO_2^-	52.83	64.76	54.43	70.96	0.05	0.06	1.70
NO_3^-	1.69	0.7	2.09	0.79	0.29	0.31	0.15
IC	2.80	3.42	3.43	4.15	0.53	0.27	1.47
pH	0.29	0.31	0.31	0.31	0.05	0.05	1.01

As can be seen from the table, ammonium and nitrite had MAE and RMSE values higher than 40. This was due to the elevated concentration of these compounds, and may not imply poor fittings. In such circumstances, ARD can be useful for assessing the adjustment of highly concentrated compounds. Thus, average relative deviations of NH_4^+ and NO_2^- were lower than 10%, pointing to a good adjustment of the model to the experimental data. The higher values of these statistics for the validation could be related to the more elevated nitrogen concentration in the leachate fed in the validation cycle, which was 200 - 300 mgN-$NH_4^+ \cdot L^{-1}$ higher. With regards to nitrate and inorganic carbon, both outputs presented low MAE and RMSE values, which is in accordance with a good model fit. Nevertheless, high values for the ARD statistics were obtained. Such elevated ARDs were due to the very low concentrations of these compounds in the reactor, despite the high nitrogen and IC concentrations in the influent. In this sense, ARD statistic may yield a biased interpretation of the results when dealing with very low concentrations. Finally, the results of the different statistics for pH revealed a similar fitting in the calibration and validation steps, with low MAE, RMSE and ARD values.

In terms of the Janus coefficient, the values obtained for the PN-SBR model were not so far from 1, meaning that the model structure remained unchanged during the calibration and validation periods, thus verifying the predictive accuracy of the model.

6.5 Nitrite build-up in an SBR: A simulation study

The production of an effluent with a proper nitrite to ammonium ratio (1.32) is essential for the anammox process. Bicarbonate is a key parameter for controlling the degree of nitritation (van Hulle *et al.*, 2005). A lack of bicarbonate can be solved by the dosage of external bicarbonate into the influent, as demonstrated in Chapter 5. On the other hand, an excess of bicarbonate can lead to an over-conversion, which may be overcome by by-passing part of the influent. Streams with a bicarbonate excess may also imply other consequences, such as a decrease on the inhibition pressure over NOB, due to the decrease in FA concentration, although this situation may be balanced by increasing the FNA levels.

Leachate composition varies greatly between landfill sites and over time. Excessively low ammonium concentrations may not allow inhibiting NOB organisms, while too high concentrations could imply the loss of the nitrification process due to inhibition by FA. In light of this, partial nitritation in an SBR might not be applicable in all situations. Because of the huge variability that exists among ammonium and bicarbonate concentrations, it is crucial to identify the limits of the system in terms of nitrite build-up. Is it possible to achieve successful nitrite accumulation at any concentration of influent ammonium and bicarbonate to ammonium molar ratio? Does the N load play any role in NO_2^- build-up? A simulation study was designed with the aim of answering these questions and filling these knowledge gaps.

6.5.1   Influent conditions

This study aimed to assess the impact of variations in ammonium and bicarbonate concentrations on nitrite build-up. Accordingly, different concentrations of both chemical species were taken up, being specifically defined for each scenario. On the other hand, only negligible concentrations of nitrite and nitrate were considered, and it was also assumed that AOB, NOB and heterotrophic biomass content in the influent was insignificant. With regards to organic matter, an elevated organic matter concentration in the leachate (4,000 mgCOD·L^{-1}) was considered, similar to the levels reported in this work. Organic matter fractionation was assumed to be similar to that obtained in the calibration step, and a very high soluble inert fraction (S_I) was adopted, being 75% of the total COD. The remaining fraction (25%) was assumed to be biodegradable. A quarter of this fraction was considered as slowly biodegradable (X_S), while the remaining was taken to be readily biodegradable substrate (S_S). The influent characteristics are shown in Table 6.24.

Table 6.24 Influent characteristics

Compound	Units	Influent
NH_4^+	$mgN \cdot L^{-1}$	variable*
NO_2^-	$mgN \cdot L^{-1}$	0.001
NO_3^-	$mgN \cdot L^{-1}$	0.001
HCO_3^-	$mgC \cdot L^{-1}$	variable*
S_S	$mgCOD \cdot L^{-1}$	750
X_S	$mgCOD \cdot L^{-1}$	250
S_I	$mgCOD \cdot L^{-1}$	3,000
X_I	$mgCOD \cdot L^{-1}$	0.001
X_{AOB}	$mgCOD \cdot L^{-1}$	0.001
X_{NOB}	$mgCOD \cdot L^{-1}$	0.001
X_H	$mgCOD \cdot L^{-1}$	0.001

* Concentrations dependent on each scenario

6.5.2 Definition of the scenarios

The goal of the simulation study was to evaluate the impact of leachate composition and operating conditions on nitrite accumulation. Accordingly, scenarios involving different ammonium concentrations and bicarbonate-to-ammonium molar ratios (input variables), were screened for different nitrogen loading rates (the controllable variable of the system). All these conditions are summarised in Table 6.25.

Table 6.25 Scenario conditions

NH_4^+ inf [$mgN\text{-}NH_4^+ \cdot L^{-1}$]	HCO_3^-:NH_4^+ influent molar ratio	NLR [$kgN \cdot m^{-3} \cdot d^{-1}$]
500	0	0.1
1,000	0.5	0.2
2,000	1	0.3
3,000	1.14	0.4
	1.5	0.5
	1.6	1
	1.7	1.5
	1.8	2
	1.9	
	2	

In this way, all possible combinations of these three parameters were analysed, resulting in a total number of 250 scenarios. Unfeasible scenarios, in which the volume fed would be higher than the reaction volume, had been previously discarded.

Simulations were carried out for a period of 200 days, to ensure stable state operation under a step-feed strategy (Figure 6.3b). The temperature of the simulations was set at 35ºC and the DO set-point was chosen as 2 $mgO_2 \cdot L^{-1}$.

6.5.3 Simulation results

Each scenario was simulated for the required influent and operational conditions, and once all the simulations had been performed, the results from each scenario were analysed in terms of nitrite and nitrate production. It was observed that depending on the combination of this 3 conditions (influent ammonium concentration, HCO_3^-:NH_4^+ influent molar ratio and NLR), either nitrite or nitrate was the end-product of the long-term operation of the reactor.

Figure 6.10 shows four graphs depicting the influence of the influent ammonium concentration on the long-term evolution of ammonium, nitrite and nitrate in the reactor. For this case it were chosen scenarios operating the reactor at a NLR of 0.5 kgN·m^{-3}·d^{-1} and a HCO_3^-:NH_4^+ influent molar ratio of 1.6.
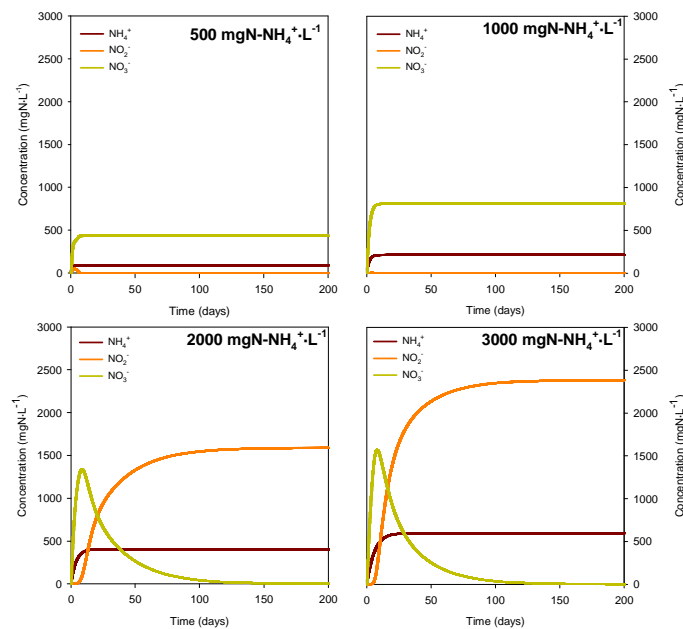
Figure 6.10 Long term evolution of ammonium, nitrite and nitrate in the reactor at a NLR of 0.5 kgN·m^{-3}·d^{-1} and a HCO_3^-:NH_4^+ influent molar ratio of 1.6, when applying different influent ammonium concentrations

According to the stoichiometry, the bicarbonate-to-ammonium molar ratio of the influent allows a conversion of around 80%, and the simulation results depicted in Figure 6.10 are in accordance with this. Nevertheless, differences depending on the influent ammonium concentration can be observed in the final outcome of the system. At the beginning of the scenarios, ammonium is almost completely oxidised to nitrate. But, when high ammonium concentrations are accumulated in the reactor, FA inhibition over NOB leads to a progressive decrease in nitrate concentration and a nitrite build-up. This behaviour, taking place more or less quickly, is clearly observed for influent ammonium concentrations of 2,000 mgN-NH$_4^+$ or higher. In these scenarios, the end-product is NO$_2^-$. Conversely, in the scenarios with a lower

influent ammonium concentration (500 mgN-NH$_4^+$ and 1,000 mgN-NH$_4^+$) nitrate builds up, probably because FA inhibition over NOB is not severe enough to out-compete them.

The HCO$_3^-$:NH$_4^+$ influent molar ratio is the factor that governs the amount of ammonium oxidised. However, it may also affect nitrite production, as depicted in Figure 6.11. These graphs depict the evolution of the different nitrogen compounds in the reactor when applying different influent HCO$_3^-$:NH$_4^+$ molar ratios. For this case, scenarios with 2,000 mgN-NH$_4^+\cdot$L^{-1} and a NLR of 1 kgN$\cdot$m$^{-3}\cdot$d^{-1} were chosen.

Figure 6.11 Long term evolution of ammonium, nitrite and nitrate in the reactor at an influent ammonium concentration of 2,000 mgN-NH$_4^+\cdot$L^{-1} and a NLR of 1 kgN$\cdot$m$^{-3}\cdot$d^{-1}, when applying different bicarbonate to ammonium influent molar ratios

The figure clearly shows the increase in ammonium oxidation alongside the raise in the HCO$_3^-$:NH$_4^+$ influent molar ratio. When no bicarbonate is supplied, insignificant amounts of ammonium are oxidised. From this point, each scenario reflects a decrease in the effluent ammonium concentration that correlates with the AOB stoichiometry (Equation 1.5). In these specific scenarios, the end up product of the process was nitrite in all the scenarios comprised where there were between 0.5 and 1.5 moles of bicarbonate per mole of ammonium in the

136

influent. However, for the last scenario depicted in Figure 6.11, corresponding to a $HCO_3^-:NH_4^+$ influent molar ratio of 2, nitrate is the outcome of the system in the long term. Despite the fact that concentrations of nitrite up to 500 - 600 $mgN-NO_2^-\cdot L^{-1}$ were initially produced, the inhibitory effect of FNA over NOB organisms was insufficient to out-compete them in the long-term. These results indicate that an excessively high bicarbonate concentration in the influent may lead to undesired nitrate build-up in the system.

Finally, the nitrogen load applied to the system may also play an important role in the nitrite build-up process. The NLR is controlled by the volumetric exchange ratio (VER) of the system, which in turns affects the sludge retention time. Figure 6.12 shows the long-term evolution of ammonium, nitrite and nitrate when different nitrogen loading rates are applied. The scenarios depicted concern an ammonium influent concentration of 2,000 $mgN-NH_4^+\cdot L^{-1}$ and a bicarbonate to ammonium molar ratio of 1.14.

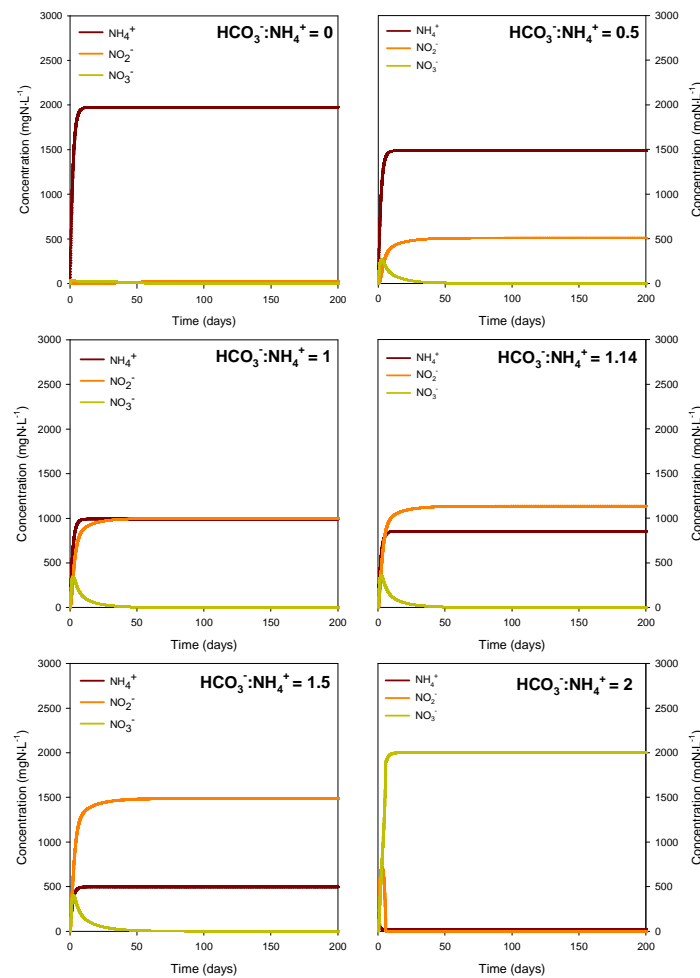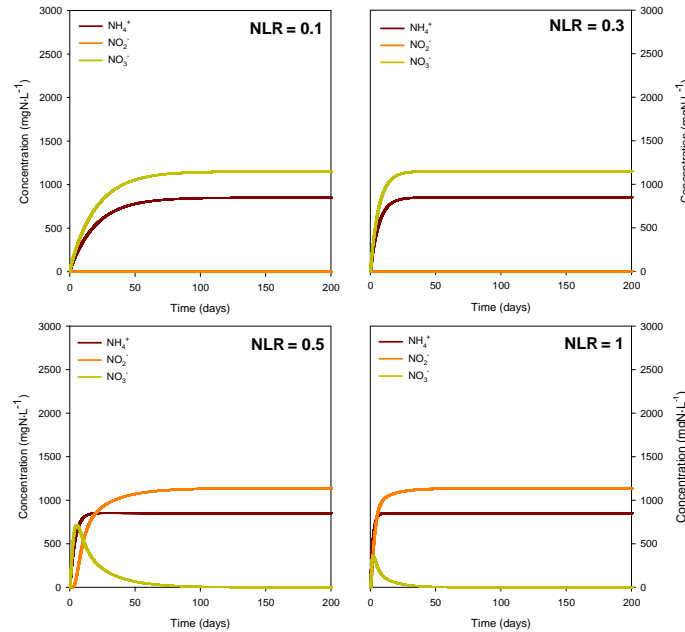**Figure 6.12** Long term evolution of ammonium, nitrite and nitrate in the reactor at an influent ammonium concentration of 2,000 $mgN-NH_4^+\cdot L^{-1}$ and a $HCO_3^-:NH_4^+$ influent molar ratio of 1.14, when applying different nitrogen loading rates (NLRs)

As can be clearly seen from the graphs, about 57% of the influent ammonium was successfully oxidised, but the end-product of the process differed depending on the NLR. Low NLR led to nitrate production, while higher NLR allowed nitrite accumulation in the system. This differential behaviour may be related to a reduction in NOB activity and the VER. If applying low NLR, VER are also low, implying elevated values of SRT. In light of this, the SRT of the system is higher than the minimum sludge age needed for NOB growth and, despite the activity reduction linked to FA inhibition, NOB are spared enough time for development. On the

contrary, higher NLR may lead to an SRT lower than the minimum retention time necessary for NOB development, which in practice means NO_2^- accumulation.

Taking into account that the interaction of these three factors affects the effluent speciation, leading to nitrite or nitrate build-up depending on each case, it can be appreciated that the independent analysis of these 250 scenarios is far from straight forward. In order to clearly summarise the information about all the simulations, the results have been plotted on a contour graph (Figure 6.13), grouped by influent ammonium concentration. White areas in the graphs depict operational conditions not feasible for the reactor under study (i.e. when the volume fed would be higher than the reaction volume).
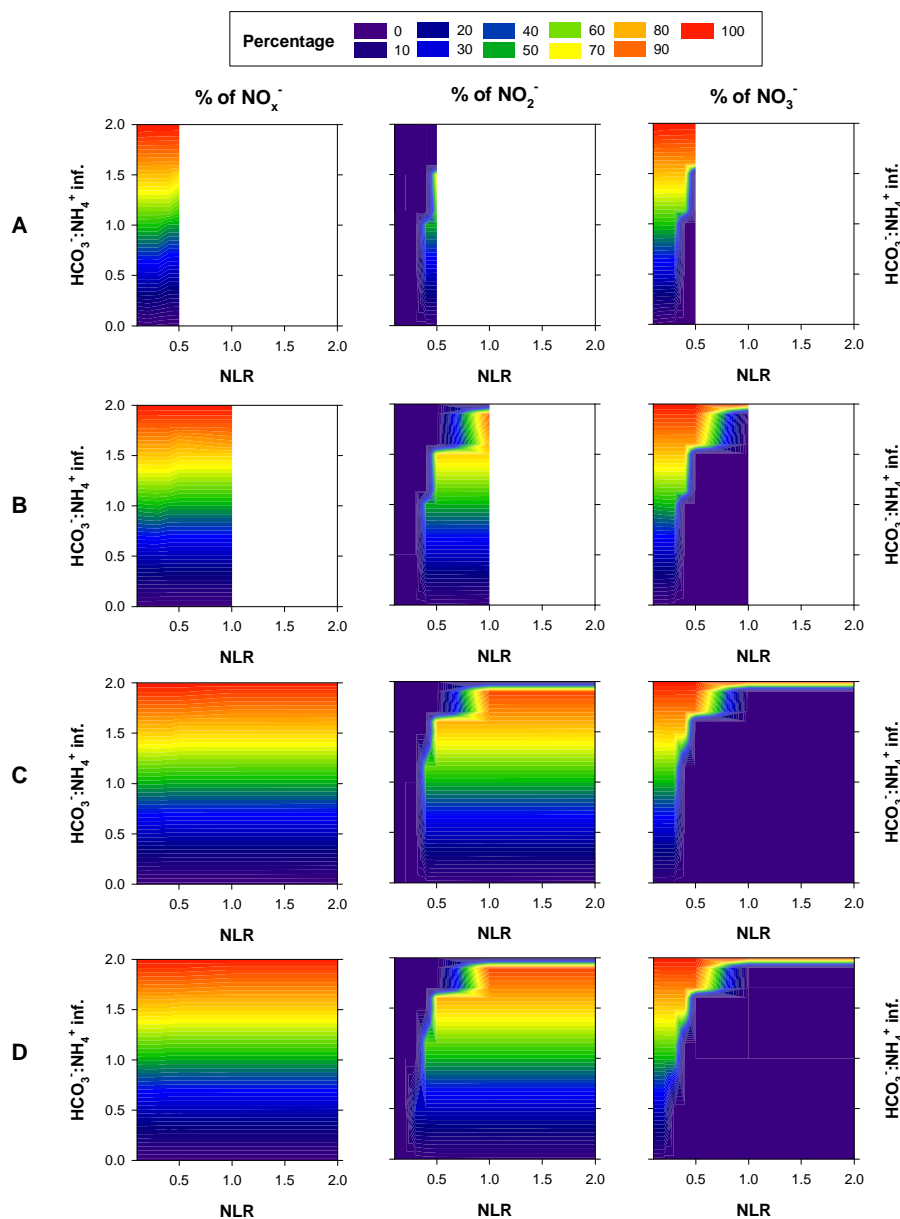
Figure 6.13 Percentage of NO_x^-(NO_2^-+NO_3^-), NO_2^- and NO_3^- at the stable state for different influent ammonium concentrations (A: 500 $mgN-NH_4^+ \cdot L^{-1}$; B: 1,000 $mgN-NH_4^+ \cdot L^{-1}$; C: 2,000 $mgN-NH_4^+ \cdot L^{-1}$; D: 3,000 $mgN-NH_4^+ \cdot L^{-1}$), NLR and HCO_3^-:NH_4^+ influent molar ratios

Figure 6.13 clearly presents the long-term reactor performance. The interaction of the three parameters (influent ammonium concentration, bicarbonate to ammonium influent molar ratio and nitrogen loading rate) govern the final effluent speciation. In general terms, low influent ammonium concentrations, low nitrogen loading rates and/or high $HCO_3^-:NH_4^+$ influent molar ratios lead to nitrate production. This is because reactor conditions (low inhibition and high SRT) are not stringent enough to outcompete NOB from the system. However, when one or more of these parameters becomes too severe for NOB long-term subsistence, nitrite becomes the end-product of the process. Despite the elevated inhibitions also affecting AOB, the system did not suffer a breakdown, although the stringent conditions may have also negatively influenced ammonium oxidation rates. It is important to mention that bicarbonate to ammonium molar ratios of 2 or higher always led to nitrate production at the end of a scenario, because initial inhibitory conditions were not severe enough to wash NOB out of the system. In light of this, the PN-SBR configuration may not be suitable for achieving complete nitritation.

6.6 Conclusions

A mathematical model of a partial nitritation SBR treating raw urban landfill leachate has been successfully constructed, calibrated and validated using historical data. The development of this model was carried out following a systematic guideline, which has been upgraded through the inclusion of an identifiability analysis step and additional statistical tests for the evaluation of the model fitting.

The calibrated PN-SBR model is capable of accurately predicting the behaviour of the main physical-chemical outputs (NH_4^+, NO_2^-, NO_3^- and IC). Good results were also obtained for pH, despite a slight bias in pH forecasting, probably caused by the high salinity of the leachate.

The mathematical model has served as a tool for a simulation study of the impact of influent composition and NLR on nitrite accumulation. In general terms, low ammonium concentration in the influent, too high bicarbonate to ammonium molar ratios and/or too low NLR, result in nitrate production in the system. On the contrary, when one of these parameters becomes too stringent for NOB development, nitrite accumulation takes place. Therefore, this scenario analysis enabled an "applicability map" of the PN-SBR to be obtained which, given the influent ammonium concentration, the bicarbonate to ammonium molar ratio and the NLR, allows the long-term effluent speciation of the system to be predicted.

Future work will be addressed at evaluating the interaction of different factors (aeration, stripping, pH, inhibitions, among others) and their impact on the process.

Chapter 7.   CONCLUSIONS

7.1 General conclusions

This thesis deals with the treatment of landfill leachate by a partial nitritation-SBR, as a preparative step for an anammox reactor. The results of the study have demonstrated the feasibility of this technology for the treatment of landfill leachate. The work evolved from initial lab-scale studies, where the process was first tested, to a successful long-term experiment at pilot-scale. In addition, the thesis also includes the development, calibration and validation of a mathematical model of the process, aiming at increasing process knowledge.

7.2 Lab scale

Experiments at lab scale demonstrated the feasibility of the PN-SBR technology for the partial nitritation of ammonium present in landfill leachate, treating a maximum NLR of 1.75 kgN·m^{-3}·d^{-1}. During these studies, proper operational conditions of the reactor were obtained. In addition, two different feeding strategies were analysed in terms of stability and process performance, with the step-feed strategy yielding a much better result. Analysis of the in-cycle dynamics profiles of both feeding strategies allowed identifying the stability of pH as one of the main reasons for the better performance of the step-feed.

The inhibition of AOB by free ammonia and free nitrous acid, as well as possible bicarbonate substrate limitation, were experimentally screened, from which it was concluded that the AOB community presented a high tolerance to elevated FA concentrations ($k_{I,FA}$ = 605.48±87.18 mgN-NH$_3$·L^{-1}). Inhibition and half-saturation constants for FNA and HCO$_3^-$ were also obtained in these experiments, although these were not completely reliable because the same data set was used to determine both effects.

In terms of process assessment, the bicarbonate to ammonium molar ratio was found to be the key factor in controlling the nitrite to ammonium effluent molar ratio. However, taking into account the low biodegradable organic matter content of the leachate, there was a high correlation between the amount of oxygen consumed per day and the nitrite production rate, resulting on a good indicator of process performance.

7.3 Pilot scale

Studies at pilot scale allowed obtaining a stable and suitable influent for feeding an anammox reactor, treating leachate with extremely high ammonium concentrations (up to 5000 mgN-NH$_4^+$·L^{-1}). These experiments also demonstrated the feasibility of removing organic matter by heterotrophic denitrification, with a consequent reduction in the total nitrogen inside the reactor.

The amount of nitrogen denitrified was now very high due to the low biodegradable organic matter content. It was also found that the denitrification process may be negatively affected by the elevated amounts of FNA. This being the case, such a strategy could yield better results when dealing with lower nitrogen concentrations, and/or leachate with a higher biodegradable fraction.

The long-term experience (450 days) confirmed the bicarbonate to ammonium molar ratio and the OC as key factors for controlling effluent speciation and assessing process performance, respectively.

Finally, the microbiological and kinetic study of the biomass enabled a characterisation of the bacterial community. The use of molecular techniques revealed AOB enrichment around 60-70%, with dominance of only one phylotype, *Nitrosomonas* sp. IWT514. This phylotype had a high resistance to FA inhibition but a low affinity to the substrate, characteristics which correspond to an r-strategist organism. With regards to NOB populations, *Nitrobacter* and *Nitrospira* were detected in the system despite the severe operational conditions. These populations were not very active, but a change in the reactor conditions may allow their development.

7.4 Partial nitritation modelling

A mathematical model of the PN-SBR was successfully developed, calibrated and validated using historical data. Therefore, a pre-existing biokinetic model was modified to include hydrolysis and endogenous respiration processes. The hydraulic model was adapted to an SBR, and physical processes, such as ammonia stripping were included. As a result, this model was capable of accurately predicting the main outcomes of the system (ammonium, nitrite, nitrate, inorganic carbon concentrations and pH).

A systematic modelling guideline was upgraded and refined by including an identifiability analysis step to select the kinetic parameters which would be fine tuned during the calibration. The evaluation stage was enhanced by the inclusion of additional statistics for the quantification of the model fitting.

Finally, the model was used in a scenario analysis which aimed to study the influence of different factors (influent ammonium concentration, the bicarbonate to ammonium influent molar ratio and NLR) on long-term effluent speciation. An "applicability map" of the PN-SBR was created, which allowed the operational conditions leading to nitrite or nitrate accumulation to be identified.

Chapter 8.   REFERENCES

Abdul Aziz, H., Adlan, M.N., Zahari, M.S.M. and Alias, S. 2004. Removal of ammoniacal nitrogen (N-NH$_3$) from municipal solid waste leachate by using activated carbon and limestone. *Waste Manage. Res.* **22** (5), 371-375.

Abeling, U. and Seyfried, C. 1992. Anaerobic-aerobic treatment of high-strength ammonium wastewater–nitrogen removal via nitrite. *Water Sci. Technol.* **26**(5-6), 1007–1015.

Abma, W.R., Schultz, C.E., Mulder, J.W., van der Star, W.R.L., Strous, M., Tokutomi, T., van Loosdrecht, M.C.M. 2007a. Full-scale granular sludge Anammox process. *Water Sci. Technol.* **55** (8-9), 27-33.

Abma, W., Schultz, C., Mulder, J.-W., Van Loosdrecht, M., Van Der Star, W., Strous, M. and Tokutomi, T. 2007b. The advance of Anammox. *Water 21*. (FEB.). 36-37.

Ahn Y.H., Hwang I.S. and Min, K.S. 2004. ANAMMOX and partial denitritation in anaerobic nitrogen removal from piggery waste. *Water Sci. Technol.* **49**(5-6), 145-153.

Altinbaş, M., Yangin, C. and Ozturk, I. 2002. Struvite precipitation from anaerobically treated municipal and landfill wastewaters. *Water Sci. Technol.* **46** (9), 271-278.

Altschul, S.F., Gish, W., Miller, W., Myers, E.W. and Lipman, D.J. 1990. Basic local alignment search tool. *J. Mol. Biol*. **215**, 403.410.

Amann, R. I., L. Krumholz, and D. A. Stahl. 1990. Fluorescent-oligonucleotide probing of whole cells for determinative, phylogenetic, and environmental studies in microbiology. *J. Bacteriol*. **172**, 762–770.

Amman, R.I. 1995. Fluorescently labelled, ribosomal-RNA-targeted oligonucleotide probes in the study of microbial ecology. *Mol. Ecol.* **4**(5), 543-553.

Anthonisen, A.C., Loehr, R.C., Prakasam, T.B.S. and Srinath, E.G. 1976. Inhibition of nitrification by ammonia and nitrous acid. *J. Water Pollut. Con. F*. **48** (5), 835-852.

APHA. 2005. Standard Methods for the examination of Water and Wastewater. 19th edn. American Public Health Association/American Water Works Association/Water Environment Federation, Washington DC, USA.

Aslan, S., Miller, L. and Dahab, M. 2009. Ammonium oxidation via nitrite accumulation under limited oxygen concentration in sequencing batch reactors. *Bioresour. Technol.* **100** (2), 659-664.

Bernet, N., Dangcong, P., Delgenès, J.P. and Moletta, R. Nitrification of low oxygen concentration in biofilm reactor. (2001) *J. Envir. Eng*. **127** (3), 266-272.

Blackburne, R., Yuan, Z. and Keller, J. 2008a. Partial nitrification to nitrite using low dissolved oxygen concentration as the main selection factor. *Biodegradation*. **19** (2), 303-312.

Blackburne, R., Yuan, Z. and Keller, J. 2008b. Demonstration of nitrogen removal via nitrite in a sequencing batch reactor treating domestic wastewater. *Water Res.* **42** (8-9), 2166-2176.

Blum, D.J. and Speece, R.E. 1991. A database of chemical toxicity to environmental bacteria and its use in interspecies comparisons and correlations. *Res. J. Water Pollut. C.* **63,** 198–207.

Bohdziewicz, J., Neczaj, E. and Kwarciak, A. 2008. Landfill leachate treatment by means of anaerobic membrane bioreactor. *Desalination*. **221** (1-3), 559-565.

Broda, E. 1977. Two kinds of lithotrophs missing in nature. *Z. Allg. Mikrobiol.* **17** (6), 491-493.

Brun, R., Kühni, M., Siegrist, H., Gujer, W. and Reichert, P. 2002. Practical identifiability of ASM2d parameters-systematic selection and tuning of parameter subsets. *Water Res.*, **36**(16), 4113–4127.

Caffaz, S., Lubello, C., Canziani, R. and Santianni, D. 2006. Autotrophic nitrogen removal from anaerobic supernatant of Florence's WWTP digesters. *Water Sci. Technol.* **53** (12), 129-137.

Calli, B., Mertoglu, B. and Inanc, B. 2005. Landfill leachate management in Istanbul: Applications and alternatives. *Chemosphere*. **59** (6), 819-829.

Campos, J.L., Mosquera-Corral, A., Sánchez, M., Méndez, R. and Lema, J.M. 2002. Nitrification in saline wastewater with high ammonia concentration in an activated sludge unit. *Water Res.* **36** (10), 2555–2560.

Carrera, J., 2001. Eliminación biológica de nitrógeno en un efluente con alta carga. Estudio de los parámetros de proceso y diseño de una depuradora industrial. Ph.D. Thesis, Universitat Autònoma de Barcelona. ISBN: B-37628-2004 / 84-688-7809-X
Available at: http://www.tdx.cat/TESIS_UAB/AVAILABLE/TDX-1027104-162956//jcm1de1.pdf

Castillo, E., Vergara, M. and Moreno, Y. 2007. Landfill leachate treatment using a rotating biological contactor and an upward-flow anaerobic sludge bed reactor. *Waste Manage.* **27** (5), 720-726.

Cema, G., Wiszniowski, J., Zabczyński, S., Zabłocka-Godlewska, E., Raszka, A. and Surmacz-Górska, J. 2007. Biological nitrogen removal from landfill leachate by deammonification assisted by heterotrophic denitrification in a rotating biological contactor (RBC). *Water Sci. Technol.* **55** (8-9), 35-42.

Chamchoi N., Nitisoravut S. and Schmidt J.E. 2008. Inactivation of ANAMMOX communities under concurrent operation of anaerobic ammonium oxidation (ANAMMOX) and denitrification. *Bioresour. Technol.* **99** (9), 3331–3336.

Cheung, K.C., Chu, L.M., Wong, M.H. 1997. Ammonia stripping as a pretreatment for landfill leachate. *Water Air Soil Poll*. **94** (1-2), 209-221.

Christensen, T.H., Kjeldsen, P., Albrechtsen, H. J., Heron, G., Nielsen, P.H., Bjerg, P.L. and Holm, P.E. 1994 Attenuation of landfill leachate pollutants in aquifers. *Crit. Rev. Env. Sci. Tec.* **24**, 119.

Chuang, H.P., Ohashi, A., Imachi, H., Tandukar, M. and Harada, H. 2007. Effective partial nitrification to nitrite by down-flow hanging sponge reactor under limited oxygen condition. *Water Res*. **41** (2), 295-302.

Corominas, Ll. 2006. Control and optimization of an SBR for nitrogen removal: from model calibration to plant operation. Ph.D. Thesis, University of Girona, Girona, Spain. ISBN: Gi-930-2006/84-690-0241-4
Available at: http://www.tdx.cesca.es/TESIS_UdG/AVAILABLE/TDX-0720106-115017//tlct.pdf.

Corominas, Ll., Sin, G., Puig, S., Balaguer, M.D., Vanrolleghem, P.A. and Colprim, J. 2008 Model-based evaluation of the SBR flexibility. *4th Sequencing Batch Reactor Technology conference*. Rome, Italy, April 7-10 (2008).

Dahl, C., Sund, C., Kristensen, G.H. and Vredenbregt, L., 1997. Combined biological nitrification and denitrification of high salinity wastewater. *Water Sci. Technol*. **36** (2–3), 345–352.

Daims, H., Bruhl, A., Amann, R., Schleifer, KH. and Wagner, M. 1999. The domain specific probe EUB338 is insufficient for the detection of all Bacteria: development and evaluation of a more comprehensive probe set. *Syst. Appl. Microbiol*. **22**(3), 434–444.

Daims, H., Nielsen, J.L., Nielsen, P.H., Schleifer, K.H. and Wagner, M. 2001. In situ characterization of Nitrospira-like nitrite oxidizing bacteria active in wastewater treatment plants. *Appl. Environ. Microbiol.* **67**, 5273–5284.

Damasceno, L., Rodrigues, J.A.D., Ratusznei, S.M., Zaiat, M. and Foresti, E. 2007. Effects of feeding time and organic loading in an anaerobic sequencing batch biofilm reactor (ASBBR) treating diluted whey. *J Environ Manage*. 85(4),927–935.

Dangcong, P., Bernet, N., Delgenes, J.P. and Moletta, R. 2000. Effects of oxygen supply methods on the performance of a sequencing batch reactor for high ammonium nitrification. *Water Environ. Res.* **72**(6), 195-200.

Dapena-Mora, A., Campos, J.L., Mosquera-Corral, A. and Méndez, R. 2006. Anammox process for nitrogen removal from anaerobically digested fish canning effluents. *Water Sci. Technol.* **53** (12), 265-274.

Degrange, V. and Bardin, R. 1995. Detection and counting of Nitrobacter populations in soil by PCR. *Appl. Environ. Microbiol.* **61**, 2093-2098.

De Heyder, B., Vanrolleghem, P.A., Van Langenhove, H. and Verstraete, W. 1997. Kinetic characterisation of mass transfer limited degradation of a poorlywater soluble gas in batch experiments. Necessity formultiresponse fitting. *Biotechnol. Bioeng.* **55**, 511–519.

De Pauw, D. and Vanrolleghem, P.A. 2003 Practical aspects of sensitivity analysis for dynamic models. *Proceedings of IMACS 4th MATHMOD Conference.* February 5-7, 2003, Vienna, Austria, pp. 328-336.

Dionisi, H.M., Layton, A.C., Harms, G., Gregory, I.R., Robinson, K.G. and Sayler, G.S. 2002. Quantification of Nitrosomonas oligotropha-like ammonia-oxidizing bacteria and Nitrospira spp. from full-scale wastewater treatment plants by competitive PCR. *Appl. Environ. Microbiol.* **68**, 245-253.

Di Palma, L., Ferrantelli, P., Merli, C. and Petrucci, E. 2002. Treatment of industrial landfill leachate by means of evaporation and reverse osmosis. *Waste Manage.* **22** (8), 951-955.

Dincer, A.R. and Kargi, F. 1999. Salt inhibition of nitrification and denitrification in saline wastewater. *Environ. Technol.* **20**, 1147–1153.

Egli, K., Fanger, U., Alvarez, P.J.J., Siegrist, H., Van der Meer, J.R. and Zehnder, A.J.B. 2001. Enrichment and characterization of an anammox bacterium from a rotating biological contactor treating ammonium-rich leachate. *Arch. Microbiol.* **175** (3), 198-207.

EPA. 2000. *Landfill manuals: landfill side design.* Environmental Protection Agency. Wexford, Ireland.

Frascari, D., Bronzini, F., Giordano, G., Tedioli, G. and Nocentini, M. 2004. Long-term characterization, lagoon treatment and migration potential of landfill leachate: A case study in an active Italian landfill. *Chemosphere.* **54** (3), 335-343.

Fux, C., Böhler, M., Huber, P., Brunner, I. and Siegrist, H. 2002. Biological treatment of ammonium-rich wastewater by partial nitration and subsequent anaerobic ammonium oxidation (anammox) in a pilot plant. *J. Biotechnol.*, **99**(3), 295–306.

Fux, C., Lange, K., Faessler, A., Huber, P., Grueniger, B. and Siegrist, H. 2003. Nitrogen removal from digester supernatant via nitrite: SBR or SHARON? *Water Sci. Technol.,* 48(8),9–18.

Fux, C., Huang, D., Monti, A. and Siegrist, H. 2004. Difficulties in maintaining long-term partial nitritation of ammonium-rich sludge digester liquids in a moving-bed biofilm reactor (MBBR). *Water Sci. Technol.* **49** (11-12), 53-60.

150

Fux, C., Velten, S., Carozzi, V., Solley, D. and Keller, J. 2006. Efficient and stable nitritation and denitritation of ammonium-rich sludge dewatering liquor using an SBR with continuous loading. *Water Res.* 40(4), 2765–2775.

Galí, A., Dosta, J., van Loosdrecht, M.C.M. and Mata-Alvarez, J. 2007. Two ways to achieve an anammox influent from real reject water treatment at lab-scale: Partial SBR nitrification and SHARON process. *Process Biochem.*, **42** (4), 715-720.

Ganigué, R., López, H., Balaguer, M.D. and Colprim, J. 2007. Partial ammonium oxidation to nitrite of high ammonium content urban landfill leachates. *Water Res.* **41**(15), 3317-3326.

Ganigué, R., López, H., Ruscalleda, M., Balaguer, M.D. and Colprim, J. 2008. Operational strategy for a Partial Nitritation-SBR (PN-SBR) treating urban landfill leachate to achieve a stable influent for an anammox reactor. *J. Chem Technol. Biot.* **83** (3), 365-371.

García, P.A. and Fernandez-Polanco, F. 1996. *Parámetros de operación en sistemas de eliminación de Nutrientes (Operational parameters in systems for nutrient removal).* in: Flotats, X. (Ed). Eliminació biològica de nutrients en aigües residuals. 2nd course on Environmental Engineering. Paperkite Editorial, Lleida, Spain.

Garrido, J.M., van Benthum, W.A.J., van Loosdrecht, M.C.M. and Heijnen, J.J. 1997. Influence of dissolved oxygen concentration on nitrite accumulation in a biofilm airlift suspension reactor. *Biotechnol. Bioeng.* **53**,168–178.

Gernaey, K.V., Van Loosdrecht, M.C.M., Henze, M., Lind, M., and Jorgensen, S.B. 2004 Activated sludge wastewater treatment plant modelling and simulation: state of the art. *Environ. Model. Softw.* **19**, 763-783.

Glass, C., Silverstein, J. and Oh, J. 1997. Inhibition of denitrification in activated sludge by nitrite. *Water Environ. Res.* **69**(6),1086–1093.

Grantham, G. and Robinson, H. 1988. Instrumentation and monitoring of a bentonite landfill liner. *Waste Manage. Res.* **6** (2), 125-139.

Guisasola, A., Jubany, I., Baeza, J.A., Carrera, J. and Lafuente, J. 2005. Respirometric estimation of the oxygen affinity constants for biological ammonium and nitrite oxidation. *J. Chem. Technol. Biot.* **80** (4), 388-396.

Guisasola, A., Petzet, S., Baeza, J.A., Carrera, J. and Lafuente, J. 2007. Inorganic carbon limitations on nitrification: Experimental assessment and modelling. *Water Res.* **41**(2), 277-286.

Guo, J.H., Peng, Y.Z., Wang, S.Y., Zheng, Y.N., Huang, H.J. and Ge, S.J. 2009. Effective and robust partial nitrification to nitrite by real-time aeration duration control in an SBR treating domestic wastewater. *Process Biochem.* **44** (9), 979-985

Gut, L., Płaza, E., Trela, J., Hultman, B. and Bosander, J. 2006. Combined partial nitration/Anammox system for treatment of digester supernatant. *Water Sci. Technol.* **53** (12), 149-159.

Haarstad, K. and Mæhlum, T. 1999. Important aspects of long-term production and treatment of municipal solid waste leachate. *Waste Manage. Res.* **17** (6), 470-477.

Hao, X., Heijnen, J.J. and van Loosdrecht, M.C.M. 2002. Sensitivity analysis of a biofilm model describing a one-stage completely autotrophic nitrogen removal (CANON) process. *Biotechnol. Bioeng.* **77**, 266-277.

Haro, E., Sánchez, G. and Colprim, J. 2007. Viability of wastewater treatment with a SBR system in an industry of municipal solid waste treatment. In CLONIC Final Workshop'07, Vol. I, Barcelona; 144–147.

Helgeson, H.C. 1967. Thermodynamics of complex dissociation in aqueous solution at elevated temperatures. *J. Phys. Chem.* **71** (10), 3121-3136.

Hellinga, C., Schellen, A.A.J.C., Mulder, J.W., van Loosdrecht, M.C.M. and Heijnen J.J. 1998. The SHARON process: an innovative method for nitrogen removal from ammonium-rich waste water. *Water Sci. Technol.* **37**(9), 135-142.

Hellinga, C., van Loosdrecht, M.C.M. and Heijnen, J.J. 1999. Model based design of a novel process for nitrogen removal from concentrated flows. *Math. Comp. Model. Dyn.* **5**(4), 351-371.

Helmer, C. and Kunst, S. 1998. Simultaneous nitrification/denitrification in an aerobic biofilm system. *Water Sci. Technol.* **37** (4-5) 183-187.

Helmer, C., Tromm, C., Hippen, A., Rosenwinkel, K.-H., Seyfried, C.F. and Kunst, S. 2001. Single stage biological nitrogen removal by nitrification and anaerobic ammonium oxidation in biofilm systems. *Water Sci. Technol.* **43** (1), 311-320.

Henderson, J.P., Besler, D.A., Atwater, J.A. and Mavinic, D.S. 1997. Treatment of methanogenic landfill leachate to remove ammonia using a rotating biological contactor (RBC) and a sequencing batch reactor (SBR). *Environ. Technol.* **18** (7), 687-698.

Henze, M., Harremoës, P., Jansen, J. and Arvin, E. 1995. *Wastewater Treatment. Biological and Chemical Processes*. Springer-Verlag, Berlin, Germany.

Henze, M., Gujer, W., Mino, T. and van Loosdrecht, M.C.M. 2000. Activated Sludge Models ASM1, ASM2, ASM2d and ASM3. Scientific and Technical Report. IWA Publishing, London, UK, 121p.

Hippen, A., Rosenwinkel, K.-H., Baumgarten, G. and Seyfried, C.F. 1997. Aerobic deammonification: A new experience in the treatment of wastewaters. *Water Sci. Technol.* **35** (10), 111-120.

Hwang, I.S., Min, K.S., Choi, E. and Yun, Z. 2005. Nitrogen removal from piggery waste using the combined SHARON and ANAMMOX process. *Water Sci. Technol.* **52** (10-11), 487-494.

Hwang, I.S., Min, K.S., Choi, E. and Yun Z. 2006. Resource recovery and nitrogen removal from piggery waste using the combined anaerobic processes. *Water Sci. Technol.* **54**(8), 229-236.

Insel, G., Sin, G., Lee, D.S., and Vanrolleghem, P.A. 2006. A calibration methodology and model-based systems analysis for SBR's removing nutrients under limited aeration conditions. *J. Chem. Technol. Biotechnol.*, **81**, 679-687.

Johansen, N.H., Andersen, J.S. and La Cour Jansen, J. 1997. Optimum operation of a small sequencing batch reactor for BOD and nitrogen removal based on online OUR calculation. *Water Sci Technol.* **35**(6), 29–36.

Jones, R. M., Dold, P., Takács, I., Chapman, K., Wett, B., Murthy, S. and O'Shaughnessy, M. 2007. Simulation for operation and control of reject water treatment processes. Proceedings of the. WEFTEC, San Diego, USA.

Joo, S.H., Kim, D.J., Yoo, I.K., Park, K. and Cha, G.C. 2000. Partial nitrification in an upflow biological aerated filter by O limitation. *Biotechnol. Lett.* **22** (11), 937-940.

Kaelin, D., Manser, R., Rieger, L., Eugster, J., Rottermann, K. and Siegrist, H. 2009. Extension of ASM3 for two-step nitrification and denitrification and its calibration and validation with batch tests and pilot scale data. *Water Res.* **43** (6), 1680-1692.

Kalyuzhnyi, S.V. and Gladchenko, M.A. 2004. Sequenced anaerobic-aerobic treatment of high strength, strong nitrogenous landfill leachates. *Water Sci. Technol.* **49** (5-6), 301-308.

Kampschreur, M. J., Picioreanu, C., Tan, N. C. G., Kleerebezem, R., Jetten, M. S. M. and van Loosdrecht, M. C. M. 2007. Unraveling the source of nitric oxide emission during nitrification. *Water Environ. Res.* **79**, 2499–2509.

Kim, D., Lee, D. and Keller, J. 2006. Effect of temperature and free ammonia on nitrification and nitrite accumulation in landfill leachate and analysis of its nitrifying bacterial community by FISH. *Bioresour Technol.* **97**, 459–468.

Kjeldsen, P., Barlaz, M.A., Rooker, A.P., Baun, A., Ledin, A. and Christensen, T.H. 2002. Present and long-term composition of MSW landfill leachate: A review. *Crit. Rev. Env. Sci. Tec.* **32** (4), 297-336.

Knox, K. 1985. Leachate treatment with nitrification of ammonia. *Water Res.* **19** (7), 895-904.

Kowalchuk, G.A., Stephen, J.R., Boer, W.D., Prosser, J.I., Embley, T.M. and Woldendorp, J.W. 1997 Analysis of ammonia-oxidizing bacteria of the beta subdivision of the class Proteobacteria in coastal sand dunes by denaturing gradient gel electrophoresis and sequencing of PCR-amplified 16S ribosomal DNA fragments. *Appl. Environ. Microbiol.* **63**, 1489-1497.

Kruempelbeck, I. and Ehrig, H.J. 1999. Long-term behavior of municipal solid waste landfills in Germany. *Proceedings 7th International Waste Management and Landfill Symposium*, 4-8 October, S. Margherita di Pula, Cagliari, Italy.

Kuai, L. and Verstraete, W. 1998. Ammonium removal by the oxygen-limited autotrophic nitrification-denitrification system. Applied and Environmental Microbiology, **64** (11), 4500-4506.

Kulikowska, D. and Klimiuk, E. 2008. The effect of landfill age on municipal leachate composition. *Bioresour. Technol.* **99** (13), 5981-5985.

Kurniawan, T.A., Lo, W.H. and Chan, G.Y.S., 2006. Physico-chemical treatments for removal of recalcitrant contaminants from landfill leachate. *J. Hazard. Mater.* **129** (1-3), pp. 80-100.

Lai, E., Senkpiel, S., Solley, D. and Keller, J. 2004. Nitrogen removal of high strength wastewater via nitritation/denitritation using a sequencing batch reactor. *Water Sci. Technol.* **50** (10), 27-33.

Li, X.Z. and Zhao, Q.L. 2001. Efficiency of biological treatment affected by high strength of ammonium-nitrogen in leachate and chemical precipitation of ammonium-nitrogen as pre-treatment. *Chemosphere.* **44** (1). 37-43.

Liang, Z. and Liu, J. 2007. Control factors of partial nitrition for landfill leachate treatment. *J. Environ. Sci.-China.* **19** (5), pp. 523-529.

Liang, Z. and Liu, J. 2008. Landfill leachate treatment with a novel process: Anaerobic ammonium oxidation (Anammox) combined with soil infiltration system. *J. Hazard Mater.*, **151** (1), 202-212.

Lin, L.Y. and Sah, J.G. 2002. Nitrogen removal in leachate using carrousel activated sludge treatment process. *J. Environ. Sci. Heal. A.* **37** (9), 1607-1620.

Lochtman, S.F.W. 1995. *Proceskeuze en-optimalisatie van het SHARON process voor slibverwerkingsbedrijf Sluisjesdijk (Process choice and optimization of the SHARON process for the sludge treatment plant Sluisjesdijk).* BODL report. TU Delft.

154

Madigan, M.T., Martinko J.M. and Parker, J. 1997. *Brock biology of microorganisms*. Prentice Hall Iberia, Madrid, Spain.

Magrí, A., Corominas, Ll., López, H., Campos, E., Balaguer, M.D., Colprim, J. and Flotats, X. 2007. A model for the simulation of the SHARON process: pH as a key factor. *Environ. Technol.* **28** (3), 255–265.

Marttinen, S.K, Kettunen, R.H, Sormunen, K.M, Soimasuo, R.M and Rintala, J.A. 2002. Screening of physical-chemical methods for removal of organic material, nitrogen and toxicity from low strength landfill leachates. Chemosphere. **46** (6), 851-858.

Mehmood, M.K., Adetutu, E., Nedwell, D.B. and Ball, A.S. 2009. In situ microbial treatment of landfill leachate using aerated lagoons. *Bioresource Technol.* **100**(10), 2741-2744.

Mobarry, B.K., Wagner, M., Urbain, V., Rittmann, B.E. and Stahl, D.A. 1996 Phylogenetic probes for analyzing abundance and spatial organization of nitrifying bacteria. *Appl. Environ. Microbiol.* **62** (6), pp. 2156-2162.

Molinuevo, B., García, M., Karakashev, D. and Angelidaki, I. (2009) Anammox for ammonia removal from pig manure effluents: Effect of organic matter content on process performance. *Bioresource Technol.* **100**(7), 2171-2175.

Monclús, H., Puig, S., Coma, M., Bosch, A., Balaguer, M.D. and Colprim, J. 2009. Nitrogen removal from landfill leachate using the SBR technology. *Environ. Technol.* **30**(3), 283-290.

Mosquera-Corral, A., González, F., Campos, J.L. and Méndez, R. 2005. Partial nitrification in a SHARON reactor in the presence of salts and organic carbon compounds. *Process Biochem.* **40** (9), 3109-3118.

Moussa, M. S., Hooijmans, C. M., Lubberding, H. J., Gijzen, H. J. and van Loosdrecht, M. C. M. 2005 Modelling nitrification, heterotrophic growth and predation in activated sludge. *Water Res.* **39**, 5080–5098.

Moussa, M.S., Sumanasekera, D.U., Ibrahim, S.H., Lubberding, H.J., Hooijmans, C.M., Gijzen, H.J. and Van Loosdrecht, M.C.M. 2006. Long term effects of salt on activity, population structure and floc characteristics in enriched bacterial cultures of nitrifiers. *Water Res.* **40** (7), 1377-1388.

Mulder, A., Van De Graaf, A.A., Robertson, L.A. and Kuenen, J.G. 1995. Anaerobic ammonium oxidation discovered in a denitrifying fluidized bed reactor. *FEMS Microbiol. Ecol.* **16** (3), 177-184.

Mulder, J.W., Van Loosdrecht, M.C.M., Hellinga, C. and Van Kempen, R. 2001. Full scale application of the Sharon process for treatment of reject water of digested sludge dewatering. *Wat. Sci. Tech.*, **43**(11), 127–134.

Muller, A., Wentzel, M.C., Loewenthal, R.E. and Ekama, G.A. 2003. Heterotroph anoxic yield in anoxic aerobic activated sludge systems treating municipal wastewater. *Water Res.* **37**, 2435-2441.

Neczaj, E., Okoniewska, E. and Kacprzak, M. 2005. Treatment of landfill leachate by sequencing batch reactor. *Desalination.* **185** (2005), 357–362.

Ozturk, I., Altinbas, M., Koyuncu, I., Arikan, O. and Gomec-Yangin, C. 2003. Advanced physico-chemical treatment experiences on young municipal landfill leachates. *Waste Manage.* **23** (5), 441-446.

Pambrun, V., Paul, E. and Spérandio, M. 2006. Modelling the partial nitrification in a Sequencing Batch Reactor for biomass adapted to high ammonia concentrations. *Biotechnol. Bioeng.* **95**(1), 120–131.

Peng, Y., Zhang, S., Zeng, W., Zheng, S., Mino, T. and Satoh, H. 2008. Organic removal by denitritation and methanogenesis and nitrogen removal by nitritation from landfill leachate. *Water Res.* **42** (4-5), 883-892.

Perry, R.H. and Green D.W. 1984. *Perry's chemical engineer's handbook*. McGraw-Hill, 1984.

Picioreanu, C., Van Loosdrecht, M.C.M. and Heijnen, J.J. 1997. Modelling the effect of oxygen concentration on nitrite accumulation in a biofilm airlift suspension reactor. *Water Sci. Technol.* **36** (1), 147-156.

Power, M. 1993. The predictive validation of ecological and environmental models. *Ecol. Model.*, **68**, 33-50.

Puig, S., Vives, M.T., Corominas, LI., Balaguer, M.D. and Colprim, J. 2004. Wastewater nitrogen removal in SBRs applying a step-feed strategy: from lab-scale to pilot plant operation. *Water Sci. Technol.,* **50**(10), 89–96.

Puig, S., Corominas, Ll., Vives, M.T., Balaguer, M.D. and Colprim, J. 2005. Development and Implementation of a Real-Time Control System for Nitrogen Removal Using OUR and ORP as End Points. *Ind. Eng. Chem. Res.* **44**, 3367-3373.

Puig, S., Coma, M., van Loosdrecht, M.C.M., Colprim, J. and Balaguer, M.D. 2007. Biological nutrient removal in a sequencing batch reactor using ethanol as carbon source. *J. Chem. Technol. Biot.* **82** (10), 898-904.

Puig, S. 2008. Operation and control of SBR processes for enhanced biological nutrient removal from wastewater. Ph.D. Thesis, University of Girona, Girona, Spain. ISBN: Gi-208-2008/978-84-691-2388-1.

Available at: http://www.tesisenxarxa.net/TDX/TDX_UdG/TESIS/AVAILABLE/TDX-0211108-130619//tspb.pdf

Pynaert, K., Wyffels, S., Sprengers, R., Boeckx, P., Van Cleemput, O. and Verstraete, W. 2002. Oxygen-limited nitrogen removal in a lab-scale rotating biological contactor treating an ammonium-rich wastewater. *Water Sci. Technol.* **45** (10), 357-363.

Qiao, S., Yamamoto, T., Misaka, M., Isaka, K., Sumino, T., Bhatti, Z. and Furukawa, K. 2009. High-rate nitrogen removal from livestock manure digester liquor by combined partial nitritation-anammox process. *Biodegradation*. In press.

Renou, S., Givaudan, J.G., Poulain, S., Dirassouyan, F. and Moulin, P. 2008. Landfill leachate treatment: Review and opportunity. *J. Hazard Mater.* **150** (3), 468-493

Robinson, H.D. 1995. The technical aspects of controlled waste management. A review of the composition of leachates from domestic wastes in landfill sites. Report for the UK Department of the Environment. Waste Science and Research, Aspinwall & Company, Ltd., London, UK.

Roeleveld, P.J. and Van Loosdrecht, M.C.M. 2002. Experience with guidelines for wastewater characterisation in The Netherlands. *Water. Sci. Technol.* **45** (6), 77-87.

Ruano, M.V., Ribes, J., De Pauw, D.J.W. and Sin, G. 2007. Parameter subset selection for the dynamic calibration of Activated Sludge Models (ASMs): experience versus systems analysis. *Wat. Sci. Technol.*, **56**(8), 107-115.

Ruscalleda M., López H., Ganigué R., Puig S., Balaguer M.D. and Colprim J. 2008. Heterotrophic denitrification on granular anammox SBR treating urban landfill leachate. *Water Sci. Technol.* **58** (9), 1749-1755.

Sander, R. 1999. Compilation of Henry's Law Constants for Inorganic and Organic Species of Potential Importance in Environmental Chemistry.
Available at: http://www.mpch-mainz.mpg.de/~sander/res/henry.html

Seyfried, C.F., Hippen, A., Helmer, C., Kunst, S., Rosenwinkel, K.-H. 2001. One-stage deammonification: Nitrogen elimination at low costs. *Water Sci. Technol.: Water Supply.* **1** (1), 71-80.

Siegrist, H., Reithaar, S. and Lais, P. 1998. Nitrogen loss in a nitrifying rotating contactor treating ammonium rich leachate without organic carbon. *Water Sci. Technol.* **37** (4-5), 589-591.

Sin, G. and Vanrolleghem, P. A. 2006. Evolution of an ASM2d-like model structure due to operational changes of an SBR process. *Water Sci. Technol.* **53**(12), 237–245.

Sin, G., Kaelin, D., Kampschreur, M.J., Takács, I., Wett, B., Gernaey, K., Rieger, L., Siegrist, H. and van Loosdrecht, M.C.M. 2008. Modelling nitrite in wastewater treatment systems: a discussion of different modelling concepts. *Water Sci. Technol.* **58**(6), 1155-1171.

Skinner, F. and Walker, N. 1961. Growth of Nitrosomonas in batch and continuous culture. *Arch. Mikrobiol.* **38**, 339.

Sliekers, A.O., Derwort, N., Gomez, J.L.C., Strous, M., Kuenen, J.G. and Jetten, M.S.M. 2002. Completely autotrophic nitrogen removal over nitrite in one single reactor. *Water Res.* **36** (10), 2475-2482.

Sliekers, A.O., Third, K.A., Abma, W., Kuenen, J.G. and Jetten, M.S.M. 2003. CANON and Anammox in a gas-lift reactor. *FEMS Microbiol. Lett.* **218** (2), 339-344.

Smith, S. A. and Chen, S. 2006. Activity corrections for ionization constants in defined media. *Water Sci. Technol.*, **54**(4), 21–29.

Spagni, A., Marsili-Libelli, S. and Lavagnolo, M.C. 2008. Optimisation of sanitary landfill leachate treatment in a sequencing batch reactor. *Water Sci. Technol.* **58** (2), 337-343.

Spagni, A. and Marsili-Libelli, S. 2009. Nitrogen removal via nitrite in a sequencing batch reactor treating sanitary landfill leachate. *Bioresource Technol.* **100**, 609-614.

Strous, M., Van Gerven, E., Kuenen, J.G. and Jetten, M. 1997. Effects of aerobic and microaerobic conditions on anaerobic ammonium-oxidizing (anammox) sludge. *Appl. Environ. Microb.* **63** (6), 2446-2448.

Strous, M., Heijnen, J.J., Kuenen, J.G. and Jetten, M.S.M. 1998. The sequencing batch reactor as a powerful tool for the study of slowly growing anaerobic ammonium-oxidizing microorganisms. *Appl. Microbiol. Biotechnol.* **50**, 589–596.

Strous, M., Kuenen, J.G. and Jetten, M.S.M. 1999. Key physiology of anaerobic ammonium oxidation. *Appl. Environ. Microb.* **65** (7), 3248-3250.

Strous, M. 2000. Microbiology of anaerobic ammonium oxidation. PhD Thesis. Technical University of Delft, Delft, The Netherlands.

Stumm, W. and Morgan, J.J. 1996. *Aquatic chemistry*. Environmental science and technology. Wiley-Interscience.

Sundberg, C., Tonderski, K. and Lindgren, P.E. 2007. Potential nitrification and denitrification and the corresponding composition of the bacterial communities in a compact constructed wetland treating landfill leachates. *Water Sci. Technol.* **56** (3), 159-166.

Suzuki, I., Dular, U. and Kwok, S.C. 1974. Ammonia or ammonium ion as substrate for oxidation by Nitrosomonas europaea cells and extracts. *J. Bacteriol.* **120** (1), 556-558.

Tchobanoglous, G., Burton, F.B., Stensel, H.D., 2003. *Wastewater Engineering Treatment and Reuse*, fourth ed. Metcalf and Eddy, Inc., USA.

Third, K.A., Sliekers, A.O., Kuenen, J.G. and Jetten, M.S.M. 2001. The CANON system (completely autotrophic nitrogen-removal over nitrite) under ammonium limitation: Interaction and competition between three groups of bacteria. *Syst. Appl. Microbiol.* **24** (4), 588-596.

Turk, O. and Mavinic, D.S. 1989. Maintaining nitrite build-up in a system acclimated to free ammonia. *Water Res.* **23** (11), 1383-1388.

Uygur, A. and Kargi, F. 2004. Biological nutrient removal from pre-treated landfill leachate in a sequencing batch reactor. *Environ. Manag.* **71**, 9–14.

Vadivelu, V.M., Keller, J. and Yuan, Z., 2007. Free ammonia and free nitrous acid inhibition on the anabolic and catabolic processes of Nitrosomonas and Nitrobacter. *Water Sci. Technol.* **56** (7), 89-97.

van der Lans, R., 2000. *Advanced course on environmental biotechnology.* Chapter 21: Gas-liquid interphase transport. Syllabus. Biotechnological sciences, Delft, Leiden, 2000.

van der Star, W.R.L., Abma, W.R., Blommers, D., Mulder, J.-W., Tokutomi, T., Strous, M., Picioreanu, C., and van Loosdrecht, M.C.M. 2007. Startup of reactors for anoxic ammonium oxidation: Experiences from the first full-scale anammox reactor in Rotterdam. *Water Res.* **41** (18), 4149-4163.

van Dongen, L.G.J.M., Jetten, M.S.M. and van Loosdrecht, M.C.M. 2001. The Combined Sharon/Anammox process. A Sustainable Method for N-Removal from Sludge Water. STOWA, IWA Publishing. London.

Van Hulle, S.W.H. 2005. Modelling, simulation and optimization of autotrophic nitrogen removal processes. PhD thesis, Ghent University, Ghent, Belgium, 228p. ISBN: 90-5989-050-7
Available at: http://biomath.rug.ac.be/publications/download/vanhullestijn_phd.pdf

Van Hulle, S.W.H., Van Den Broeck, S., Maertens, J., Villez, K., Donckels, B.M.R., Schelstraete, G., Volcke, E.I.P. and Vanrolleghem, P.A. 2005. Construction, start-up and operation of a continuously aerated laboratory-scale SHARON reactor in view of coupling with an Anammox reactor. *Water SA.* **31** (3), 327-334.

van Hulle, S.W.H., Volcke, E.I.P., López-Teruel, J., Donckels, B., van Loosdrecht, M.C.M. and Vanrolleghem, P.A. 2007. Influence of temperature and pH on the kinetics of the SHARON nitritation process. *J. Chem. Technol. Biotechnol.* **82**(5),471-480.

Vanrolleghem, P.A., Insel, G., Petersen, B., Sin, G., De Pauw, D., Nopens, I., Dovermann, H., Weijers, S. and Gernaey, K. (2003) A comprehensive model calibration procedure for activated sludge models. *Proceedings 76th Annual WEF Conference and Exposition*. Los Angeles, USA, October 11-15, 2003.

Vanrolleghem, P.A., Sin, G. and Gernaey, K.V. 2004. Transient response of aerobic and anoxic activated sludge activities to sudden substrate concentration changes. *Biotechnol. Bioeng.* **88**(3), 277–290.

Vilar, A., Kennes, C. and Veiga, M.C. 2007. Full-scale biological treatment of landfill leachate from urban solid wastes. *Proceeding s of the CLONIC Final Workshop'07, 156-158.* 19-20 April 2007, Barcelona, Spain.

Villaverde, S., Fdz-Polanco, F. and García, P.A. 2000. Nitrifying biofilm acclimation to free ammonia in submerged biofilters. Start-up influence. *Water Res.* **34** (2), 602-610.

Vlaeminck, S.E., Terada, A., Smets, B.F., Van Der Linden, D., Boon, N., Verstraete, W. and Carballa, M. 2009. Nitrogen removal from digested black water by one-stage partial nitritation and anammox. *Environmental Sci. Technol.* **43** (13), 5035-5041

Volcke, E.I.P., Hellinga, C., Van Den Broeck, S., van Loosdrecht, M.C.M. and Vanrolleghem, P.A. 2002. Modelling the SHARON process in view of coupling with Anammox. *Proceedings 1st IFAC International Scientific and Technical Conference on Technology, Automation and Control of Wastewater and Drinking Water Systems (TiASWiK'02).* Gdansk-Sobieszewo, Poland, June 19–21 2002, 65–72.

Volcke E.I.P. 2006a. Modelling, analysis and control of partial nitritation in a SHARON reactor. PhD thesis, Ghent University, Ghent, Belgium, 300p. ISBN: 90-5989-108-2
Available at: http://biomath.ugent.be/publications/download/VolckeEveline_PhD.pdf

Volcke, E.I.P., van Loosdrecht, M.C.M. and Vanrolleghem, P.A. 2006b. Continuity-based model interfacing for plant-wide simulation: A general approach. *Water Res.* **40** (15), 2817-2828.

Vredenbregt, L.H.J., Nielsen, K., Potma, A.A., Kristensen, G. H., and Sund, C. 1997. Fluid bed biological nitrification and denitrification in high salinity wastewater. *Water Sci. Technol.* **36**, 93–100.

Wagner, M., Rath, G., Koops, H.P., Flood, J. and Amann, R. 1996. In situ analysis of nitrifying bacteria in sewage treatment plants. *Water Sci. Technol.* **34**, 237–244.

Waki, M., Tokutomi, T., Yokoyama H. and Tanaka, Y. 2007. Nitrogen removal from animal waste treatment water by anammox enrichment. *Bioresource Technol.* **98** (14), 2775-2780.

Wett, B. and Rauch, W. 2003. The role of inorganic carbon limitation in biological nitrogen removal of extremely ammonia concentrated wastewater. *Water Res.* **37** (5), 1100–1110.

160

Wett, B. 2006. Solved upscaling problems for implementing deammonification of rejection water. *Water Sci. Technol.* **53** (12), 121-128.

Wett, B. 2007. Development and implementation of a robust deammonification process. *Water Sci. Technol.* **56** (7), 81-88.

Wiesmann, U. 1994. *Advances in biochemical engineering/biotechnology*, volume 51. Springer-Verlag, Berlin, Germany, pp. 113-154.

Windey, K., De Bo, I. and Verstraete, W. 2005. Oxygen-limited autotrophic nitrification-denitrification (OLAND) in a rotating biological contactor treating high-salinity wastewater. *Water Res.* **39** (18), 4512-4520.

Wiszniowski, J., Robert, D., Surmacz-Gorska, J., Miksch, K. and Weber, J.V. 2006. Landfill leachate treatment methods: A review. *Environ. Chem. Lett.* **4** (1), 51-61.

Wu, G., Guan, Y. and Zhan, X. 2008. Effect of salinity on the activity, settling and microbial community of activated sludge in sequencing batch reactors treating synthetic saline wastewater. *Water Sci. Technol.* **58** (2), 351-358.

Wyffels, S., Boeckx, P., Pynaert, K., Verstraete, W. and Van Cleemput, O. 2003. Sustained nitrite accumulation in a membrane-assisted bioreactor (MBR) for the treatment of ammonium-rich wastewater. *J. Chem. Technol. Biot.* **78** (4), 412-419.

Yamamoto, T., Takaki, K., Koyama, T. and Furukawa, K. 2008. Long-term stability of partial nitritation of swine wastewater digester liquor and its subsequent treatment by Anammox. *Bioresource Technol.* **99** (14), 6419-6425.

Yang, Q., Peng, Y., Liu, X., Zeng, W., Mino, T. and Satoh, H. 2007. Nitrogen removal via nitrite from municipal wastewater at low temperatures using real-time control to optimize nitrifying communities. *Environmental Sci. Technol.* **41** (23), 8159-8164.

Yilmaz, G. and Öztürk, I. 2001. Biological ammonia removal from anaerobically pre-treated landfill leachate in sequencing batch reactors (SBR), *Water Sci. Technol.* **43,** 307–314.

Yuan, Z., Oehmen, A., Peng, Y., Ma, Y. and Keller, J. 2008. Sludge population optimisation in biological nutrient removal wastewater treatment systems through on-line process control: A re/view. *Re-views in Environmental Science and Biotechnology*. **7** (3), 243-254.

Zhang, T., Ding, L. and Ren, H. 2009. Pretreatment of ammonium removal from landfill leachate by chemical precipitation. *J. Hazard Mater*. **166** (2-3), 911-915.